APPENDIX E

Hydrodynamic Modeling Report

for:
Weston Solutions

Alabama Department of Conservation & Natural Resources

Hydrodynamic Modeling Report

Restoration of Hydrology of Mobile Bay Causeway, Alabama

{CIAP AL-12}

Bret M. Webb, Ph.D., P.E.
Scott Douglass, Ph.D., P.E., D.CE
Beau Buhring, Chris Blackwood

Report Date | October 7, 2014

SOUTH COAST ENGINEERS | PO Box 72 | Fairhope, AL 36533

EXECUTIVE SUMMARY

This report, prepared by Dr. Bret Webb of South Coast Engineers (SCE), describes the hydrodynamic modeling activities completed as part of the CIAP AL-12 project aimed at investigating hypothetical restoration strategies for the Mobile Bay Causeway in Alabama. The report documents the steps taken to develop and validate a tidal circulation model for the study area, including field data collection and model hindcasting of the data collection period. The results of fourteen (14) unique model simulations of the hypothetical restoration alternatives, their forcing conditions and parameters, and their pertinent results, are described in this report. Simulation results are presented in a manner that addresses project goals, objectives, and performance measures identified in the project plan formulation.

The primary goal of this hydrodynamic model study is to evaluate the effects of constructed openings through the Mobile Causeway on tidal exchange between Mobile Bay and water bodies north of the Causeway. The hypothetical scenarios include openings through the Causeway at Choccolatta Bay, Justin's Bay, and Shellbank River, herein referred to as "Pass Choccolatta," "Pass Justin," and "Shellbank Cut." Specific areas of interest include Choccolatta Bay, Justin's Bay, Sardine Pass, John's Bend, Ducker Bay, and Shellbank River. Four specific objectives are used to frame simulation results and include assessments of: 1) increased tidal communication; 2) increased tidal prisms; 3) decreased tidal phase lags with Mobile Bay; and 4) increased flushing within each system. Specific performance measures for each objective are used to quantify the degree to which an objective is met.

Field data collection was completed over the period March 27, 2014 to April 9, 2014, with ship-based surveys of velocity and bathymetry conducted on April 3, 2014. Data collection included the measurement of water levels (i.e., tides) in Choccolatta Bay, Ducker Bay, and Sardine Pass over the two-week period; as well as mapping of velocity, discharge, bathymetry, and standard water characteristics (e.g., temperature and salinity) at I-10 Cut, the box culverts, Pass Picada, Apalachee River, Sardine Pass, Duck Skiff Pass, and Blakeley River. These data were used to develop the unstructured mesh for the hydrodynamic model and to validate the model through comparisons of predicted and measured water levels and velocities.

The Advanced Circulation (ADCIRC) model was applied to a hindcast simulation of the period March 27, 2014 to April 4, 2014. Forcing included predicted tides, observed discharge for the Mobile and Tensaw Rivers, and observed meteorology (i.e., winds and pressure). Model-data comparisons were generally good within the study area, capturing the range and phase of tides as well as the magnitudes and directions of flows. Predictive errors for water levels were 20% (~10 cm) or less over the entire simulation. Predictive velocity errors were 30% (~5 cm/s) or less over the entire simulation.

The ADCIRC model was used to simulate unique restoration alternative scenarios under representative tidal forcing and river discharge for present and future sea levels. Five restoration scenarios were simulated with typical summer (July) river discharge (~470 m^3/s) on present-day sea levels. Those same forcing conditions were used to simulate the five restoration scenarios with an elevated sea level that was 30 cm higher than present-day levels. The restoration alternative with openings at Choccolatta Bay, Justin's Bay and Shellbank River was simulated with high (wet season) river discharge (~1950 m^3/s) on

present-day sea levels. A corresponding simulation of existing conditions within the study area (i.e., no openings) was performed for each of the three forcing conditions, resulting in fourteen (14) total model simulations.

Restoration scenario results are generally expressed in terms of changes, increases or decreases, relative to existing conditions. A summary of the major conclusions, relative to the objectives stated above, are listed below:

- The restoration scenarios at Choccolatta and Justin's Bay would measurably increase all aspects of tidal communication between those bays and Mobile Bay
- Model predictions suggest that the proposed restoration alternatives would, overall, experience an 80% increase in tidal exchange (volume of water entering the water body) for Choccolatta Bay, and a 120% increase for Justin's Bay.
- Constructed openings would generally eliminate all existing tidal phase lags in Choccolatta and Justin's Bays. In other words, the high tide would occur at the same time as it does in northern Mobile Bay.
- Tidal prisms in Choccolatta and Justin's Bays would increase by 8% and 64%, respectively.
- Flushing of Choccolatta and Justin's Bays would be improved under the restoration alternatives considered.
- The existing man-made tidal channels that were built north of the Causeway (Pass Picada and the I-10 Cut) that govern the tidal exchange of Choccolatta Bay under existing conditions would experience 90% reductions in tidal exchange as a result of the constructed openings evaluated here as restoration alternatives. Optimizing the size of the hypothetical opening through the Causeway could moderate such reductions.
- Reductions in tidal exchange in Pass Picada, I-10 Cut, and Sardine Pass may alter the characteristics of those systems, including changes to water quality and possible sediment deposition over time. These uncertainties could be addressed in future studies.
- The restoration alternatives mostly act independent of one another with only small changes (<1%) noted between scenarios.
- Tidal exchange would be reduced at higher river discharge due to a general reduction of tidal forcing.
- Most effects of the constructed openings evaluated as restoration alternatives would be within the immediate vicinity of the Causeway, Choccolatta Bay, Justin's Bay, and Shellbank River.
- The effects of these hypothetical openings on wave action in Choccolatta and Justin's Bays was not considered here, but could be evaluated in future studies.

Table of Contents

List of Tables

List of Figures

List of Abbreviations

Abbreviation	Description	Explanation or Units
5RDRC	Five Rivers Delta Resource Center	
ADCIRC	Advanced Circulation Model	
ADCP	Acoustic Doppler Current Profiler	
DEM	Digital Elevation Model	
Dep	Potential Deposition	(+1: Deposition; 0: No Deposition)
Dep'	Potential Deposition Change	(+1: More; 0: No change; -1.0: Less)
LAPS	Lap's on the Causeway	
LMTRD	Lower Mobile Tensaw River Delta	
LPTM	Lagrangian Particle Tracking Model	
MSP	Meaher State Park	
NAVD88	North American Vertical Datum, 1988	
NOAA	National Oceanic and Atmospheric Admin.	
Qb	Bedload Transport Rate	($m^3/s/m^2$)
Qb'	Bedload Transport Rate Change	($m^3/s/m^2$)
Qr	Resuspension Rate	($m^3/s/m^2$)
Qr'	Resuspension Rate Change	($m^3/s/m^2$)
Tr	Residence Time	(days)
Tr'	Residence Time Change	(days)
USGS	United States Geological Survey	
<V>	Subtidal Velocity	(m/s) or (cm/s)

Abbreviation	Description	Explanation or Units
<V'>	Subtidal Velocity Difference	(cm/s)
Vmax	Maximum Velocity	(m/s)
Vmax'	Maximum Velocity Change	(m/s)
WSEmax	Maximum Water Surface Elevation	(m)
WSEmax'	Max. Water Surface El. Change	(m)

Introduction

This report, prepared by Dr. Bret Webb of South Coast Engineers (SCE), describes the hydrodynamic modeling activities completed as part of the CIAP AL-12 project aimed at investigating hypothetical restoration strategies for the Mobile Bay Causeway in Alabama. The report documents the steps taken to develop and validate a tidal circulation model for the study area, including field data collection and model hindcasting of the data collection period. The report also provides an overview of the five restoration alternative scenarios simulated, their forcing conditions and parameters, and their pertinent results. Simulation results are presented in a manner that addresses project goals, objectives, and performance measures identified in the project plan formulation. These are restated in the Goals, Objectives portion of this section.

Background

The Mobile Bay Causeway (US Highway 90/98), constructed in 1927, serves as a secondary transportation link between Baldwin and Mobile Counties. Completion of this roadway was achieved by converting large areas of open water and habitat to the roadway base through dredge and fill. Many areas adjacent to the Causeway were dredged to depths far greater than the ambient depths of 1 m to 3 m (~3 ft to 10 ft). While bridges were used to span the large conveyance channels of the Blakeley, Apalachee, and Tensaw/Spanish Rivers, the roadway embankment effectively impounded some water bodies and relic channels. These include Choccolatta Bay, Justin's Bay, Sardine Pass, and Shellbank River. The Alabama Department of Transportation later installed box culverts to improve flushing between northern Mobile Bay and Choccolatta Bay.

The purpose of this CIAP (AL-12) project entitled *Investigation of Restoration of Hydrology on Mobile Bay Causeway* is to assess the effects of potential restoration alternatives on the hydrology and hydrodynamics surrounding the Mobile Bay Causeway. The overall project includes 1) a synthesis of literature and knowledge related to construction of the Causeway and its subsequent impacts; 2) investigation of sediment characteristics and quality; and 3) hydrodynamic modeling to describe existing conditions as well as five potential restoration scenarios. For the purposes of this study, the restoration scenarios are assumed to be open channels.

This report describes the hydrodynamic model used to simulate tidal circulation, water levels, and river discharge in Mobile Bay, Alabama. The hydrodynamic model is focused on resolving flows and water levels within the northern portions of Mobile Bay closest to the Causeway, as well as north of the Causeway in the Lower Mobile-Tensaw River Delta (LMTRD). The report 1) provides an overview of the field data collection performed as part of the hydrodynamic modeling task; 2) describes the hydrodynamic model validation process and pertinent results; 3) describes the restoration alternative simulation characteristics and model setup; 4) hydrodynamic characteristics of proposed alternatives for typical summer river discharge; 5) hydrodynamic characteristics of a proposed alternative under high river discharge; and 6) hydrodynamic characteristics of proposed alternatives for typical river discharge with an elevated sea level corresponding to the year 2100.

Study Area

The study area for this project is shown in Figure 1, which provides names of relevant roadways, rivers, water bodies, tributaries, and creeks. Specific points of interest include the I-10 Cut; Choccolatta Bay; the existing box culverts under the Causeway; Pass Picada; Justin's Bay; Sardine Pass; John's Bend; Ducker Bay; and Shellbank River. The study area for the hydrodynamic modeling is focused on the features shown on this map, but the model domain is much more comprehensive.

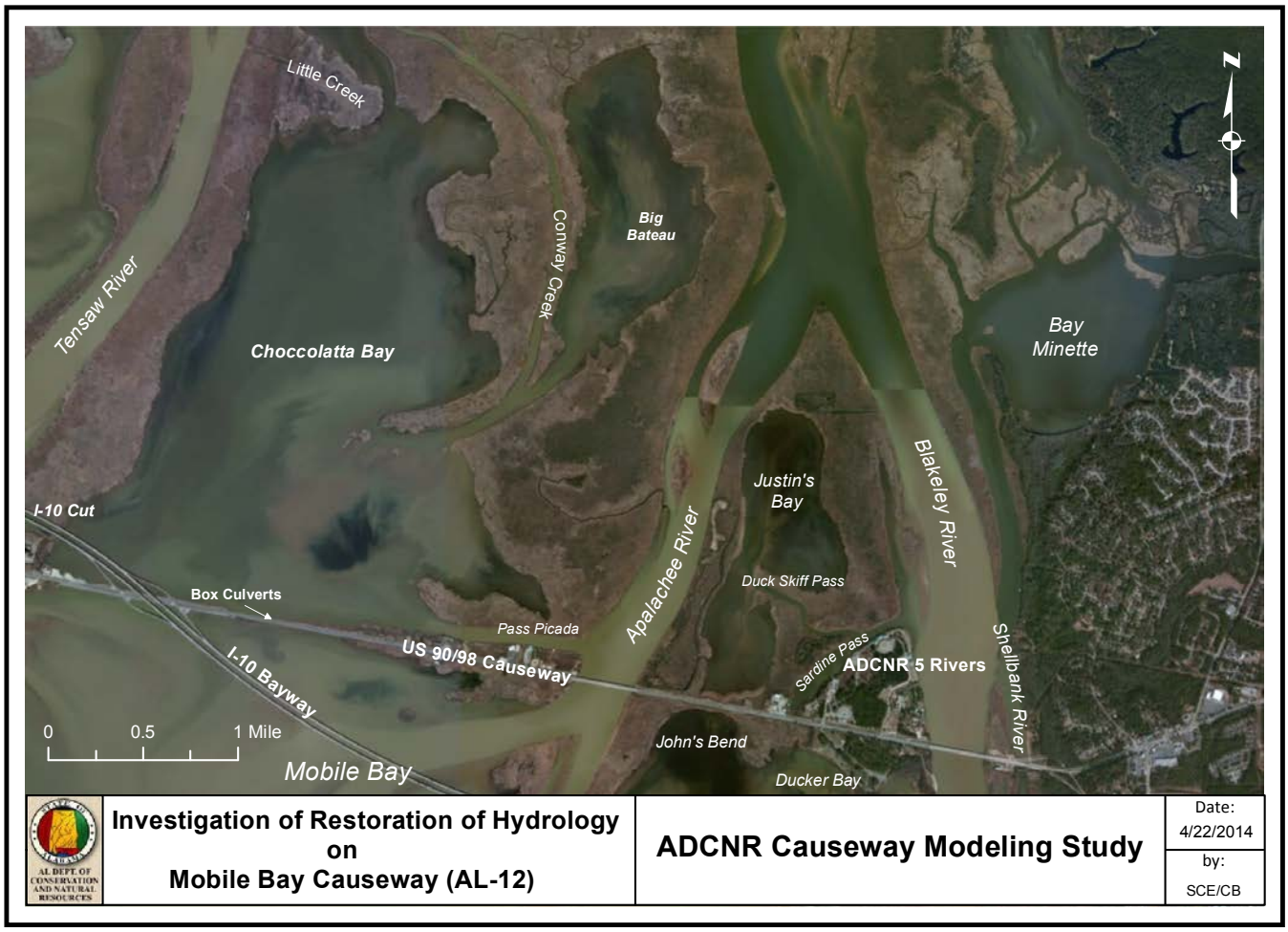

Figure 1. Study area map showing major roadways, river names, water bodies, and features mentioned elsewhere in the model study.

Goals, Objectives & Performance Measures

As stated in the final project plan formulation, the primary goal of the overarching study is to evaluate Mobile Bay Causeway breach alternatives for restoration of tidal exchange and improved water quality at Choccolatta Bay, Justin's Bay, Sardine Pass, and Shellbank River. There are four specific objectives related to the overarching project goal, and a corresponding suite of performance measures used to

quantify the effectiveness of each objective. The objectives and hydrodynamic modeling performance measures (only) are as follows:

Objective 1: Increase the tidal communication between Mobile Bay and areas north of the Causeway.

- Estimate the volume flux of water per tidal cycle and compare to existing conditions
- Estimate the subtidal exchange flows and rates and compare to existing conditions
- Estimate tidal current velocity in the study area and compare to existing conditions
- Estimate and identify the potential for sediment resuspension, transport rates, and depositional areas relative to existing conditions

Objective 2: Increase the tidal prism in water bodies north of the Causeway.

- Estimate water levels in the study area and compare to existing conditions
- Estimate the tide range in the affected water bodies and compare to existing conditions
- Estimate the tidal prism of affected water bodies and compare to existing conditions

Objective 3: Decrease the tidal phase lag between Mobile Bay and areas north of the Causeway.

- Estimate the tidal stage inside and outside of the study area and compare to existing conditions
- Estimate the tidal phase lag in affected water bodies and compare to existing conditions

Objective 4: Increase the flushing of water bodies north of the Causeway.

- Estimate the residence (flushing) times of affected water bodies and compare to existing conditions
- Estimate the improvement of residence time, per tidal day, in affected water bodies relative to existing conditions

The performance measures stated above are used to frame the hydrodynamic modeling results in a manner that compares the predicted effects of restoration to existing conditions for relevant hydrodynamic criteria. For all but one model scenario, the restoration alternative simulation results will be compared to existing conditions in the study area under a "typical" summer river discharge scenario. This includes simulations of the proposed alternatives under present day and future sea levels.

Two model scenarios with a much higher river discharge value were also completed: one under existing site conditions and a second representing one of the five proposed restoration alternatives (all sites open). The results of those two "high flow" scenarios will be compared against one another so that the potential restoration effects can be segregated from the influence of river discharge.

Specific details regarding the hydrodynamic model setup and descriptions of the forcing conditions, sea levels, and restoration alternative simulations are provided in the sections that follow.

Field Data Collection

Limited field data were collected as part of the hydrodynamic modeling task (Task 4.1) over the period March 27, 2014 to April 9, 2014. The sections that follow describe the objectives of the field data collection, sampling locations, conditions during the sampling period, measured water levels and velocities, and bathymetric sampling. South Coast Engineers and the University of South Alabama's Civil Engineering department collected the field data.

Objectives

The specific objectives of the field data collection were to a) measure bathymetry for use in updating and refining the hydrodynamic model mesh; and b) measure water levels and velocities for the purpose of model validation and/or calibration. The data collection objectives were achieved through the deployment of three tide gages within the study area on March 27, 2014, as well as underway ship sampling of bathymetry and currents on April 3, 2014.

Sampling Locations

Temporary tide gages were installed and surveyed to a known vertical datum (NAVD88) at three locations within the study area. One tide gage was installed in the southwest corner of Choccolatta Bay at Lap's on the Causeway. Another was installed on the Ducker Bay fishing pier at Meaher State Park, which is on the south side of the Causeway. A third tide gage was installed on the boat docks behind Five Rivers Delta Resource Center in Sardine Pass. An atmospheric pressure gage was installed below an adjacent building at Five Rivers to correct the tide gage measurements for changes in barometric pressure. The locations of these gages are shown on a map labeled as Figure 2.

Underway ship sampling of bathymetry was conducted at areas needed to update and refine the hydrodynamic model mesh (depths). Underway sampling of currents was conducted in areas used to validate the hydrodynamic model predictions (velocity, discharge). Velocity profiling was conducted along a transect perpendicular to the I-10 Cut below the elevated I-10 Bayway spans; along an east-west transect north of the box culverts in Choccolatta Bay; at the east end of Pass Picada along a transect perpendicular to the channel; along an east-west transect north of the US HWY 90/98 Apalachee River bridge; at the Blakeley River side of Sardine Pass; and along an east-west transect north of the US HWY 90/98 Blakeley River bridge. Bathymetric sampling was conducted at all of those locations, with additional detailed sampling performed along the I-10 Cut; near the box culverts; along Pass Picada; in Sardine Pass; and in Duck Skiff Pass. The locations of underway ship sampling (i.e., the transects) are shown on a map labeled as Figure 3.

Conditions

Field data were collected over the dates March 27, 2014 to April 9, 2014. The tide gage deployment captured portions of a neap (or equatorial) tidal cycle and portions of a spring (or tropic) tidal cycle. The

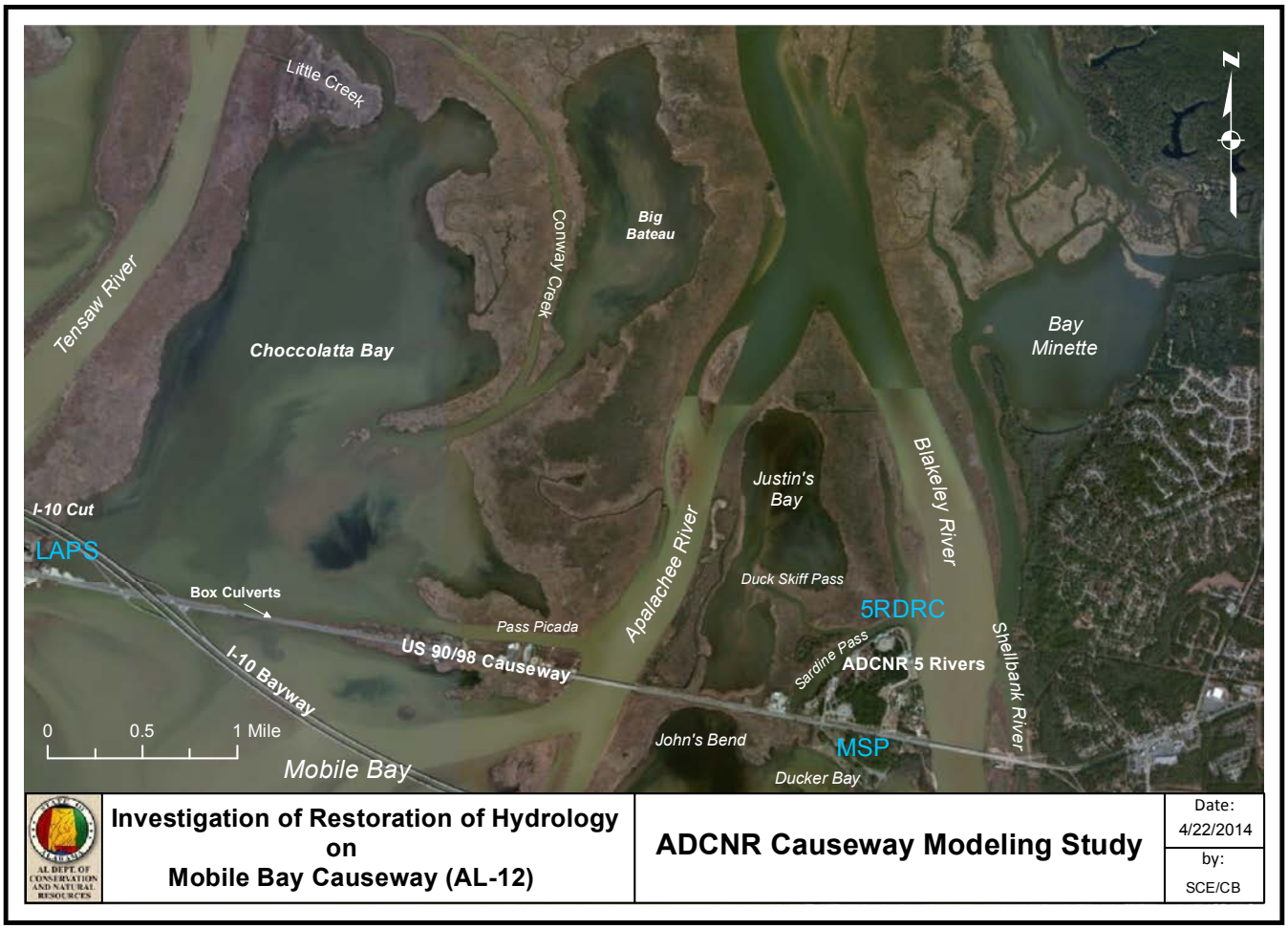

Figure 2. Study area map showing the locations of temporary tide gages installed at Lap's on the Causeway (LAPS), Meaher State Park (MSP), and Five Rivers Delta Resource Center (5RDRC).

observed tides deviated from their predicted (NOAA) stage due to the influence of high river discharge and stronger than normal winds during the observation period.

A sample of predicted and observed water levels at Mobile State Docks (NOAA CO-OPS station 8737048) for the period March 30, 2014 to April 4, 2014 is shown in Figure 4. Observed water levels were below their predicted stage through early on March 31, 2014, after which time the observed water levels were consistently higher than their predicted stage. This behavior was likely reinforced by the local winds, which were strongly out of the north through mid-day on March 31, 2014, then strongly out of the south on the following days. Observed meteorological data at Coast Guard Sector Mobile (NOAA CO-OPS station 8736897), located in northern Mobile Bay, is shown in Figure 5 for reference.

Observed river discharge was, on most days, higher than the two-year daily average statistic during the data collection period. Some discharge values were 50% greater than their daily average. Discharge measurements from USGS gages on the Tensaw and Mobile Rivers, located just upstream from the study area, are shown in Figure 6 and Figure 7, respectively. These large discharge values likely contributed to the observed increased tidal stages in the northern portion of Mobile Bay.

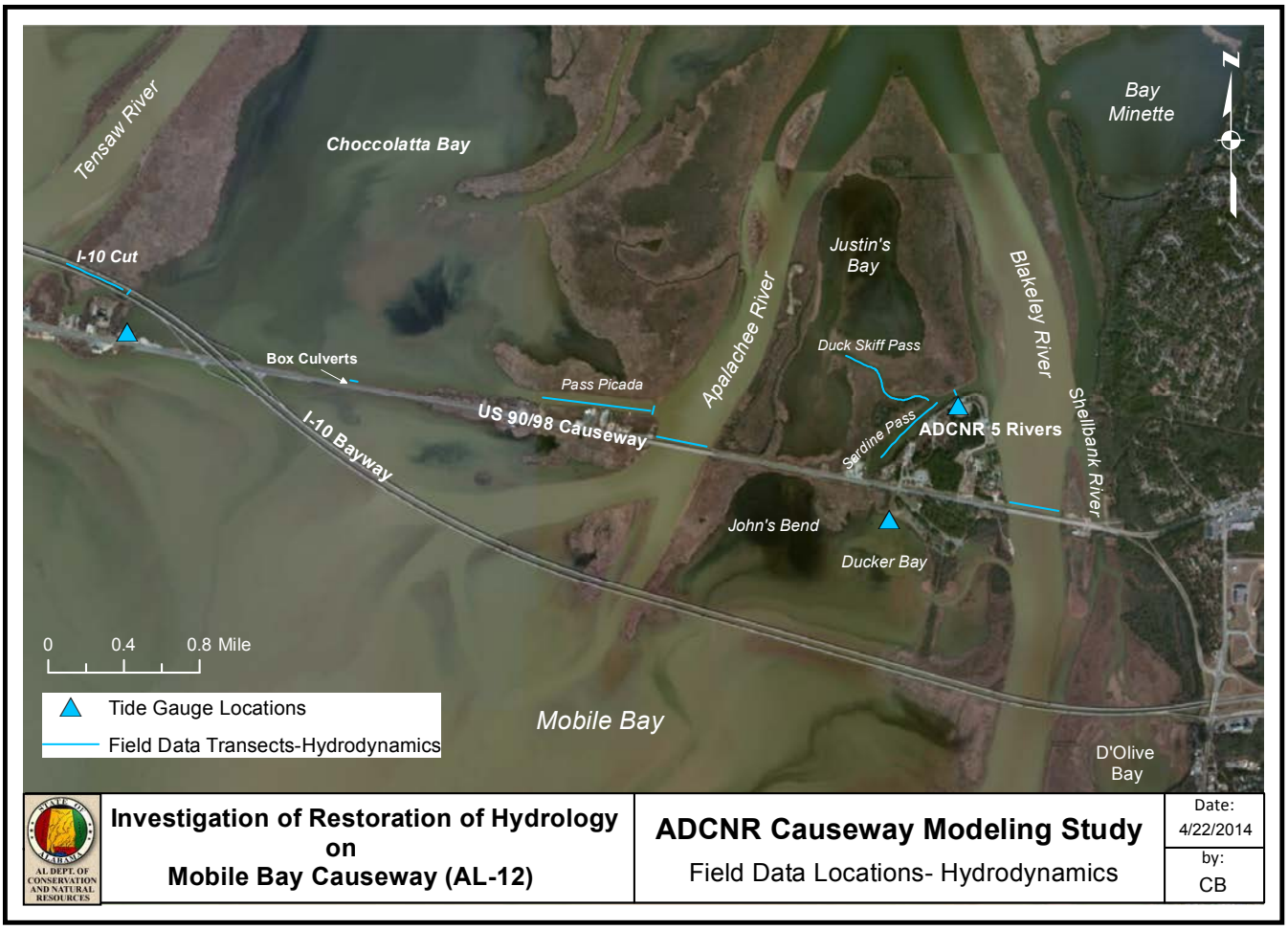

Figure 3. Study area map showing the locations of underway ship sampling of bathymetry and currents, and also the locations of temporary tide gages.

Salinity within the study area was < 0.1 PSU as measured by casts of conductivity and temperature over depth (CTD) at the times of tide gage deployment and retrieval, and also by a Dauphin Island Sea Lab monitoring station located at the end of the Meaher State Park fishing pier in Ducker Bay. Water temperature within the study area ranged from 16 ^{o}C to 20 ^{o}C. The low salinity and water temperatures were consistent with the higher than average river discharge that occurred during the study period.

Tides & Water Levels

Water levels within the study area were measured continuously over the period March 27, 2014 to April 9, 2014 at three locations in the study area (see Figure 2). The temporary tide gages were surveyed to a known vertical datum (NAVD88) to provide a consistent vertical reference for the measurement and comparison of water levels in different water bodies. While the NOAA CO-OPS program maintains a number of tide gages throughout Mobile Bay, only a few of them provide water levels measured relative to a static vertical datum. One of the stations, at Mobile State Docks, is relatively close to the study area, but it is located in a completely different part of the LMTRD. Another, located on Dauphin Island, provides an excellent long-term record of tidal elevations and sea level statistics, but again is far removed from the study area.

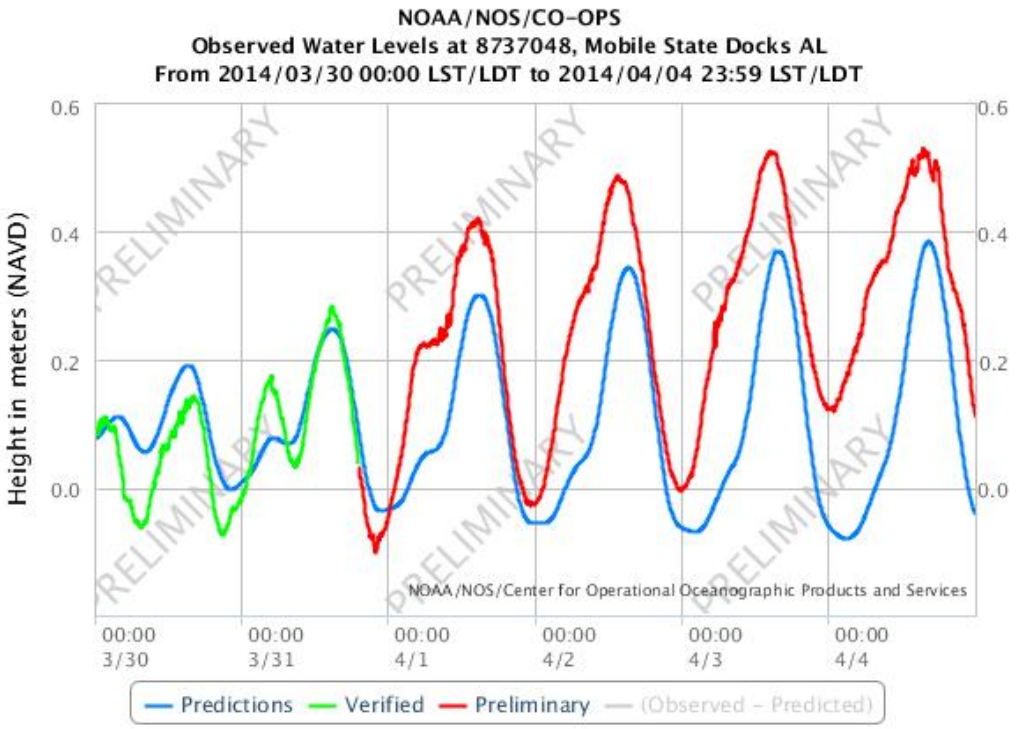

Figure 4. Predicted and observed water levels at Mobile State Docks for the period March 30, 2014 to April 4, 2014.

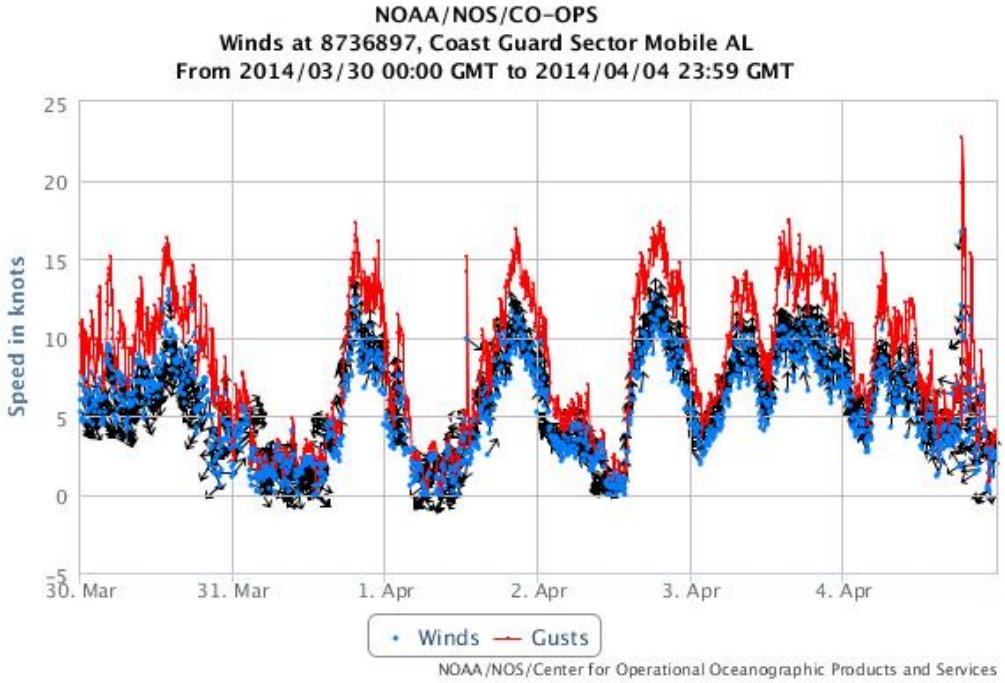

Figure 5. Observed wind speeds, wind gusts, and directions at Coast Guard Sector Mobile for the period March 30, 2014 to April 4, 2014.

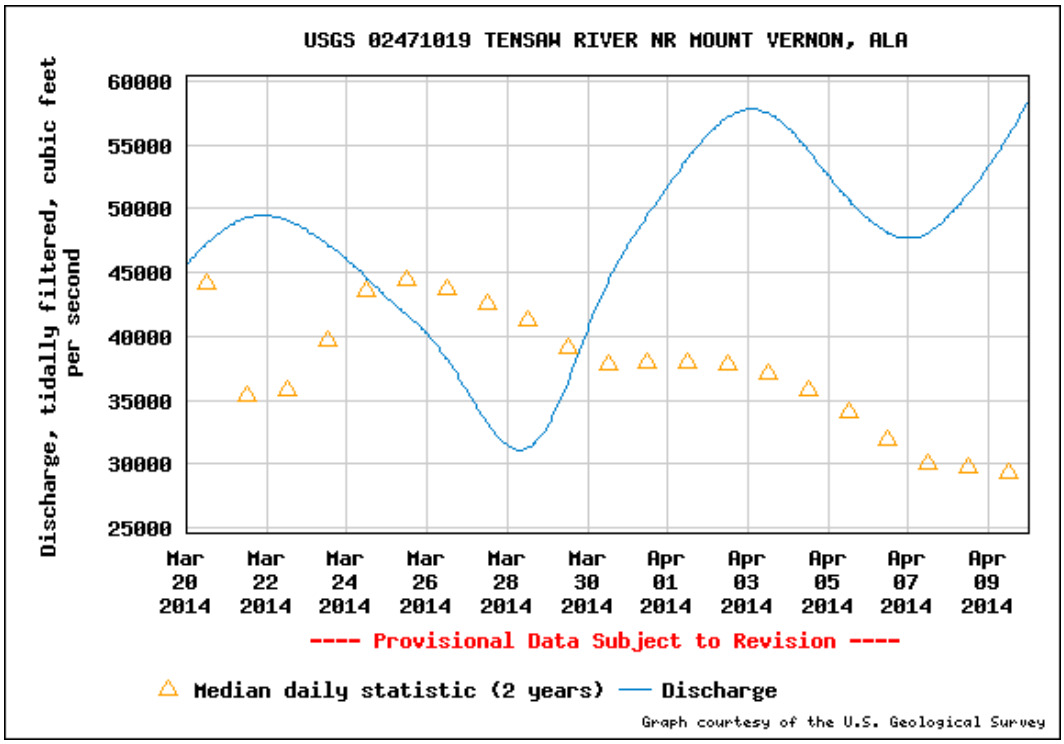

Figure 6. Tidally filtered discharge measurements on the Tensaw River near Mount Vernon, Alabama at USGS gage 02471019.

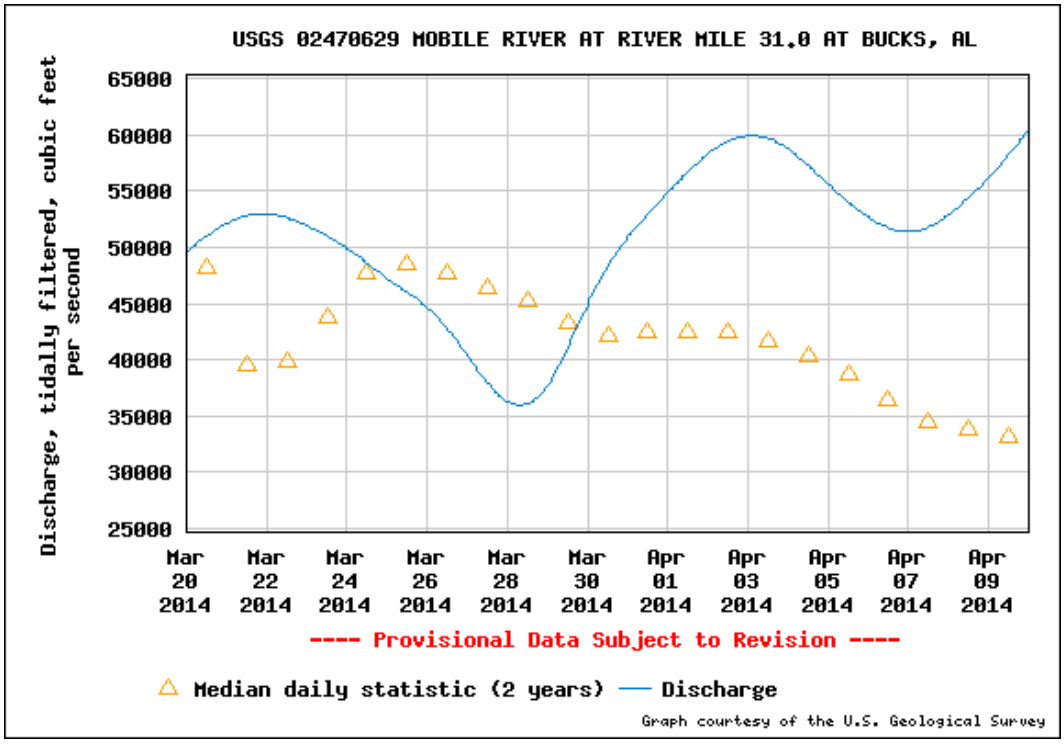

Figure 7. Tidally filtered discharge measurements on the Mobile River near Bucks, Alabama at USGS gage 02470629.

Measured water levels are shown in Figure 8 for each of the three temporary tide gage locations. The NOAA CO-OPS measurements at Mobile State Docks and Dauphin Island are also shown for reference. Water levels measured at these five locations were used to validate the hydrodynamic model within the study area.

The elevated tidal stage in the northern portion of Mobile Bay is evident in this figure, where the observed water levels at Dauphin Island were consistently lower than other locations. Furthermore, tide gages located north of the Causeway (5RDRC, LAPS) show consistently higher stages than the gage located south of the Causeway (MSP).

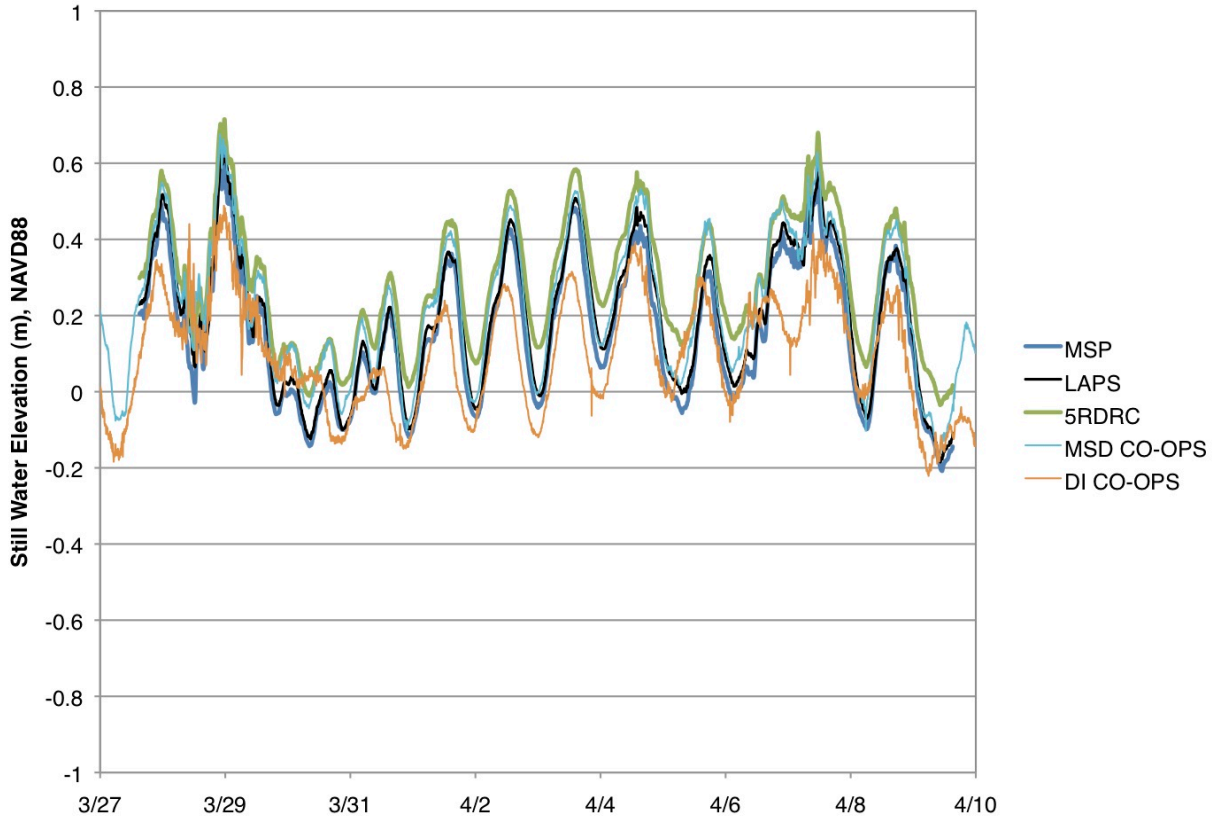

Figure 8. Measured water levels at the three temporary tide gage locations within the study area (MSP, LAPS, 5RDRC), as well as the NOAA CO-OPS stations at Mobile State Docks (MSD CO-OPS) and Dauphin Island (DI CO-OPS).

Velocity & Discharge

Underway velocity data were collected using the University of South Alabama's Jag Ski mapping system. Velocity profiles were measured with a SonTek M9 acoustic Doppler current profiler (ADCP). The ADCP provided measurements of water velocity in an east-north-up coordinate system that was geo-referenced using an onboard differential global positioning system (GPS). Measurements of water velocity were corrected to account for vessel course over ground and speed over ground using a combination of GPS data and a measurement method known as bottom tracking, where the instrument

"tracks" its position relative to the seafloor. The ADCP returned measurements of water velocity along the vessel track, and in increments of 1 cm to 10 cm over the water depth, every one second. The average operating speed of the vessel was 1 m/s to 2 m/s, resulting in a typical point spacing of 1 m to 2 m along the profiling transect.

Velocity and discharge data were collected between 0700 HRS and 1600 HRS on April 3, 2014. The tide was flooding during that time, reaching high water shortly after 1400 HRS. Repeated underway profiling of water velocity was performed along transects oriented perpendicular to primary flow directions at five locations in the study area. The locations, shown in Figure 3, included I-10 Cut (3 repetitions), the north side of the box culverts (4 repetitions), Pass Picada (4 repetitions), Apalachee River (4 repetitions), and Blakeley River (2 repetitions). Additional profiling was performed across Sardine Pass and Duck Skiff Pass, but these locations were only sampled once during the day. All locations were sampled to ensure that flow magnitude and direction were consistent between the field and model predictions.

Typical underway velocity profiling results are provided in Figure 9 and Figure 10 for the Apalachee and Blakeley Rivers, respectively. These figures show bathymetry, or water depth, along the profiling transect; the vessel tracks; and contouring of northing velocity (+, flows to the north; -, flows to the south) over distance and depth. Synthesized velocity data collected from the field are presented in the Model Validation section of this report.

Bathymetric Mapping

Limited mapping of bathymetry was performed within the study area as part of the ship-based data collection effort on April 3, 2014. The purpose of this mapping was to update and refine some depth measurements for the hydrodynamic model mesh. The underlying mesh bathymetry and shoreline position were extracted from a high-resolution (10 m) digital elevation model (DEM) of Mobile Bay. However, some tidal channels within the study area were not well resolved even by this high-resolution elevation data.

Bathymetric mapping efforts were focused on the I-10 Cut, areas north of the box culverts, Pass Picada, Duck Skiff Pass, and Sardine Pass. An overview of those sampling locations and the spacing of measurements are shown in Figure 11. Representative bathymetric measurements obtained during data collection are shown in Figure 12 for Sardine Pass. A composite figure showing bathymetric measurements in Duck Skiff Pass and Sardine Pass is shown in Figure 13. These data, and data from other sampling locations, were interpolated to an improved high-resolution hydrodynamic model mesh to ensure the most accurate representation of the study area as practical. More details about the hydrodynamic model mesh and characteristics are provided in the sections that follow.

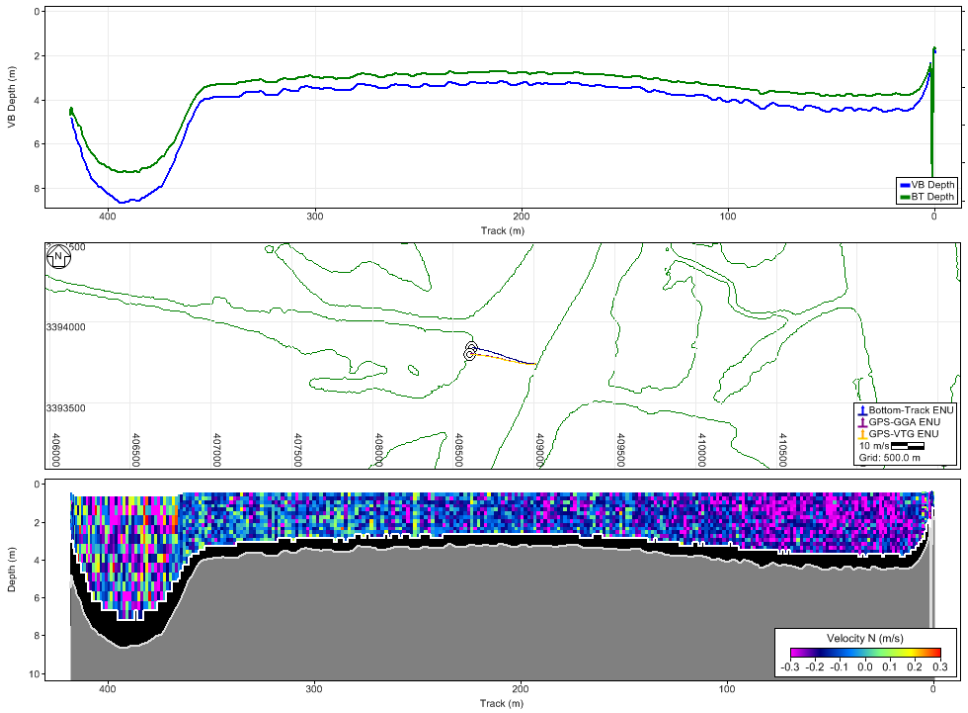

Figure 9. Typical underway velocity sampling data for Apalachee River. The top panel shows the depth along the transect. The middle panel shows the transect location relative to an approximate shoreline. The lower panel shows contours of northing velocity (positive = water moving north). The orientation of the top and bottom panels is that of an observer looking to the north.

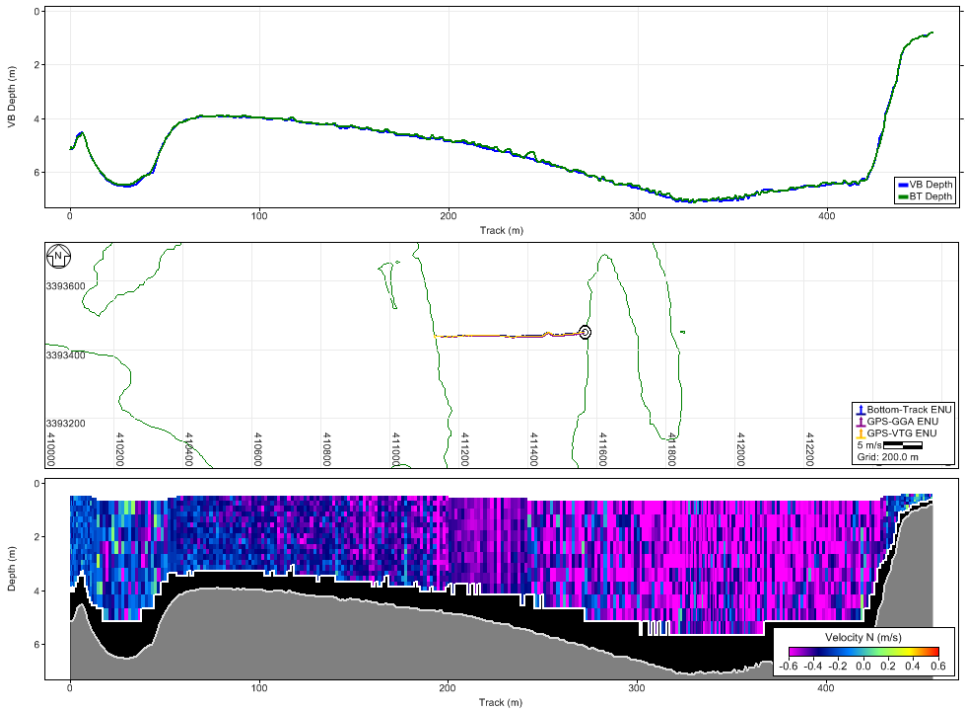

Figure 10. Typical underway velocity sampling data for Blakeley River. The top panel shows the depth along the transect. The middle panel shows the transect location relative to an approximate shoreline. The lower panel shows contours of northing velocity (positive = water moving north). The orientation of the top and bottom panels is that of an observer looking to the north.

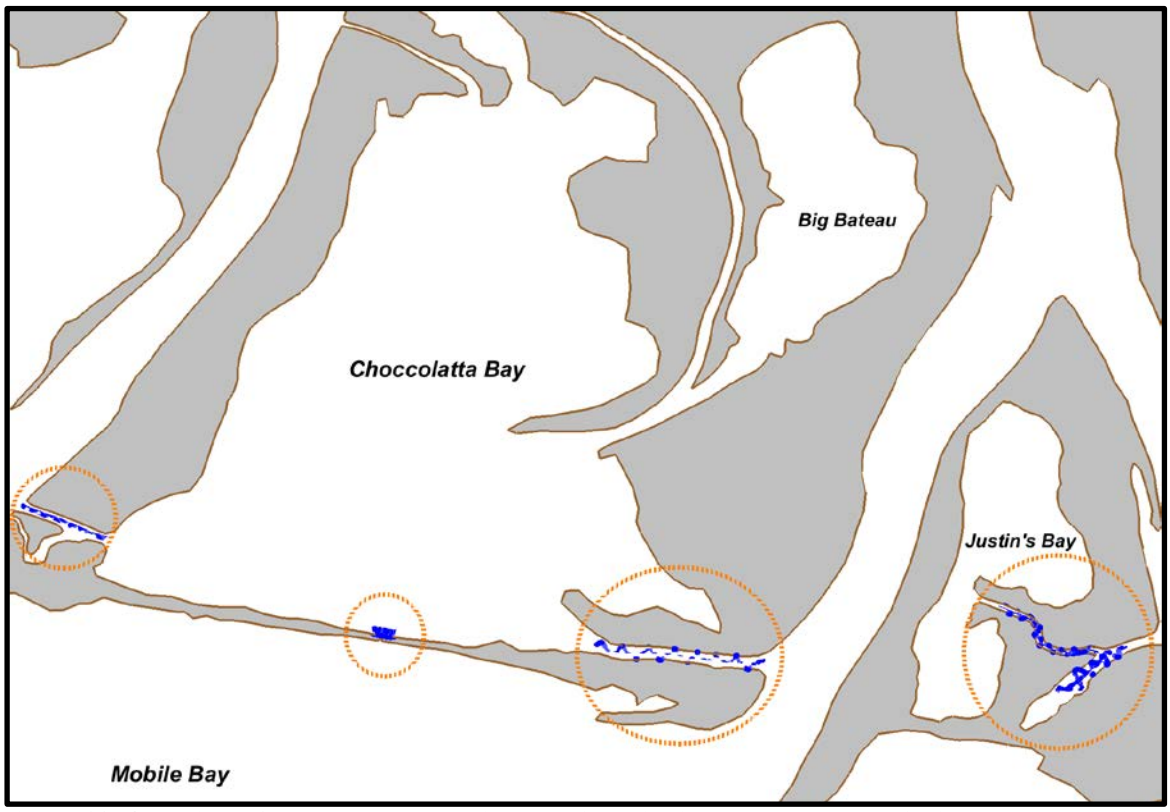

Figure 11. Overview of bathymetry sampling locations, indicated by blue dots inside the orange circled areas, within the study area.

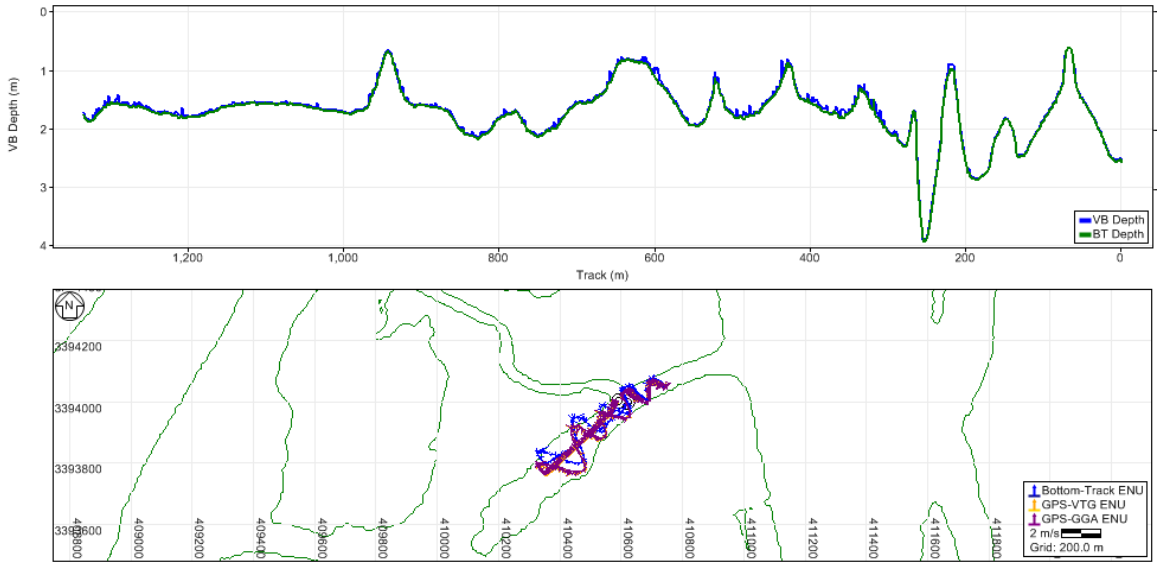

Figure 12. Typical measurements collected during bathymetric mapping in Sardine Pass. The top panel shows the recorded depth along the vessel track. The lower panel shows the vessel track and the approximate shoreline location.

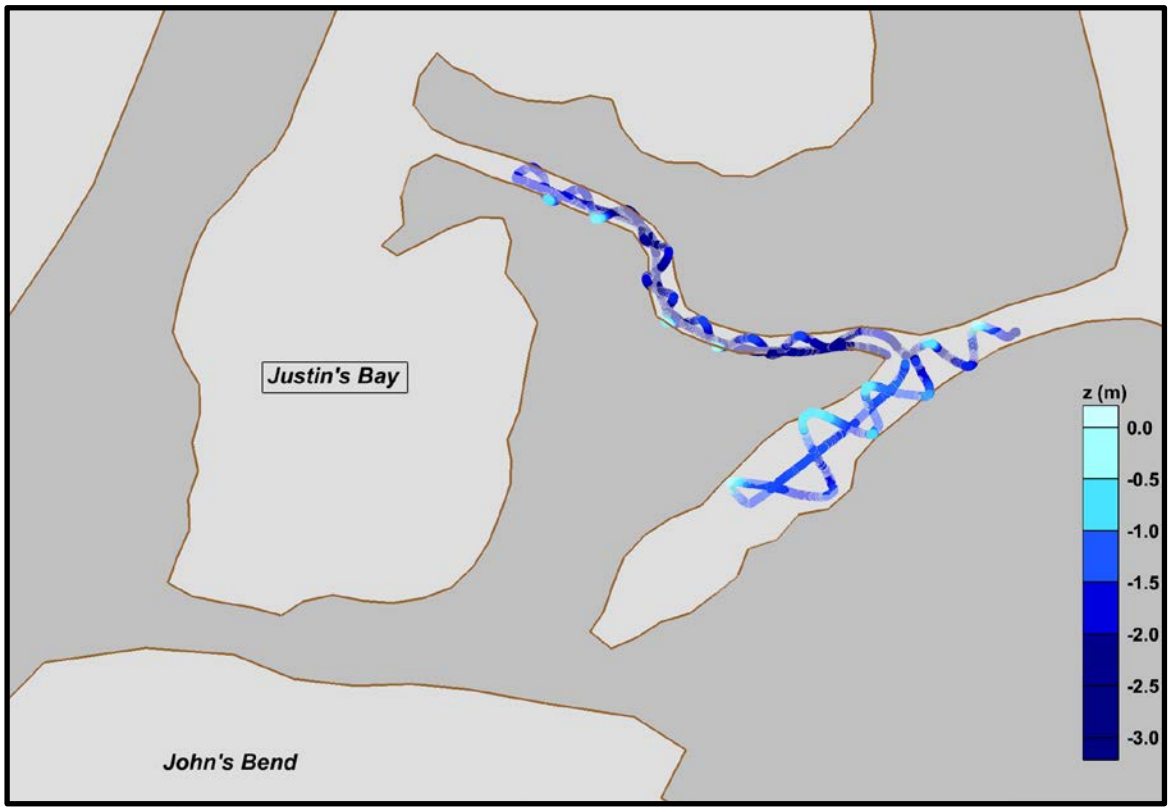

Figure 13. Sample bathymetric mapping in Duck Skiff Pass and Sardine Pass. The bed elevation of each measurement corresponds to the provided color scale.

Model Validation

This section of the report describes the hydrodynamic model used to simulate circulation, flows and water levels within the study area. A summary of the model validation conditions and results is provided and makes use of measured water levels and the underway velocity profiling described in the previous section.

Model Description

The ADvanced CIRCulation (ADCIRC) model, described in Luettich et. al (1992) and Westerink et al. (1994), was selected for use in this hydrodynamic model investigation of hypothetical restoration alternatives along the Mobile Bay Causeway. The ADCIRC model is actually a suite of hydrodynamic models used for simulating tidal circulation and water levels in estuaries and open seas. The ADCIRC model has been successfully applied to a variety of studies ranging from larval transport to storm surge. It is used exclusively by FEMA for mapping flood risk in coastal areas and is often used by other federal agencies like NOAA, the US Army Corps of Engineers, and the US Geological Survey.

ADCIRC is a two-dimensional depth-integrated model that solves the nonlinear shallow water equations. The model is capable of performing three-dimensional simulations, but is rarely applied in such a fashion owing to computational requirements and the complexity of performing such simulations.

The model is typically forced by representative tidal constituents along an open ocean boundary, as is the case in this study. The implementation of ADCIRC considered for this study also includes non-periodic inflow boundary conditions to simulate riverine flows upstream of the study area. These locations roughly correspond to Bucks, Alabama on the Mobile River, and Mount Vernon, Alabama on the Tensaw River. USGS monitoring stations near these locations provide the discharge measurements required to specify the boundary conditions. Note that in this two-dimensional implementation of the ADCIRC model the water is assumed to be completely mixed and homogeneous in nature.

Model Mesh

The underlying structure of the hydrodynamic model is the mesh (grid) of information that is referenced when performing numerical calculations of flows through space and time. The ADCIRC model is a finite element model built upon an unstructured mesh consisting of triangular elements. A distinct advantage of an unstructured mesh consisting of triangular elements is its ability to resolve complex shoreline geometries by alternatively shrinking or expanding the size of each element as needed.

The triangular elements of the ADCIRC mesh consist of three neighboring "nodes" or points in space. The spacing of nodes defines the resolution of the mesh and serves as the limiting factor for accurate resolution of complex shoreline geometries, channels, tributaries, or upland terrain features. Each node is defined by at least two essential attributes: its coordinates in the horizontal plane, and the corresponding depth at that location. For the purposes of this study, the ADCIRC mesh nodes are defined in the geographic coordinate system of latitude and longitude. Nodal "elevations" in the mesh are specified as positive values when below the zero elevation (bathymetry), and as negative values

when above the zero elevation (topography). This convention is used for convenience in the model computations.

The basic geometry of the ADCIRC mesh used for this study was adapted from a mesh developed by SCE for a previous hydrodynamic study in southwest Mobile Bay. The essential nodal attributes were updated using a 2011 NOAA 1/3rd arc-second DEM of Mobile Bay. The nodal elevations were referenced to the North American Vertical Datum of 1988 (NAVD88). Refinement of the underlying mesh was performed throughout much of the study area using recent aerial imagery and the bathymetric data collected in April 2014. Specific areas of refinement included the I-10 Cut, Choccolatta Bay, Big Bateau, Pass Picada, Justin's Bay, Duck Skiff Pass, Sardine Pass, and Shellbank River.

The completed ADCIRC mesh consists of 45,294 nodes and 84,225 elements. The spatial extents of the mesh cover an area approximately 40 km south of Mobile Pass to over 20 km north of the Causeway. The mesh extents, triangular elements, and corresponding nodal elevations (depths) are shown in Figure 14. Nodal spacing ranges from 1000s of meters along the tidal forcing boundary in the Gulf of Mexico to as little as 5 m in complex areas, like the box culverts. Typical nodal spacing throughout the study area varies from 10 m to 150 m. The increased resolution of the mesh in the study area is demonstrated in Figure 15.

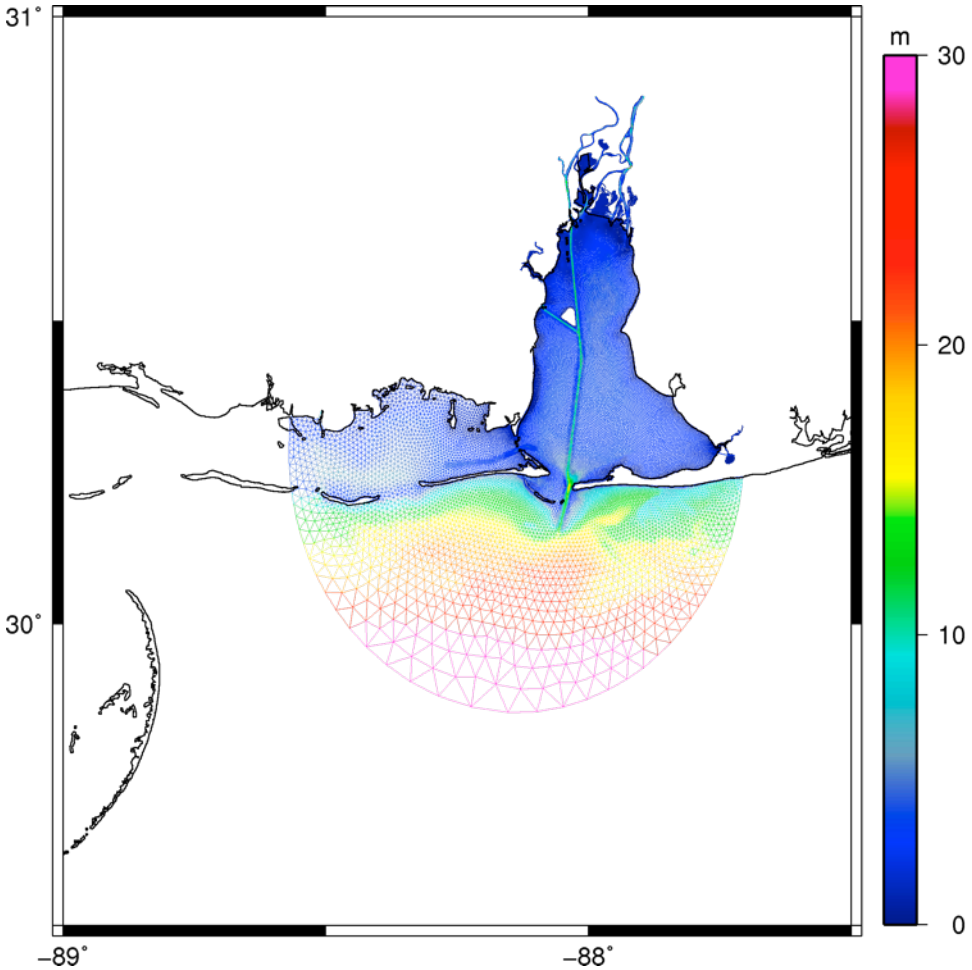

Figure 14. Spatial extents of the ADCIRC mesh showing the distribution and size of triangular mesh elements, and their corresponding nodal elevation (depth) relative to the color scale. Depths are in meters below NAVD88.

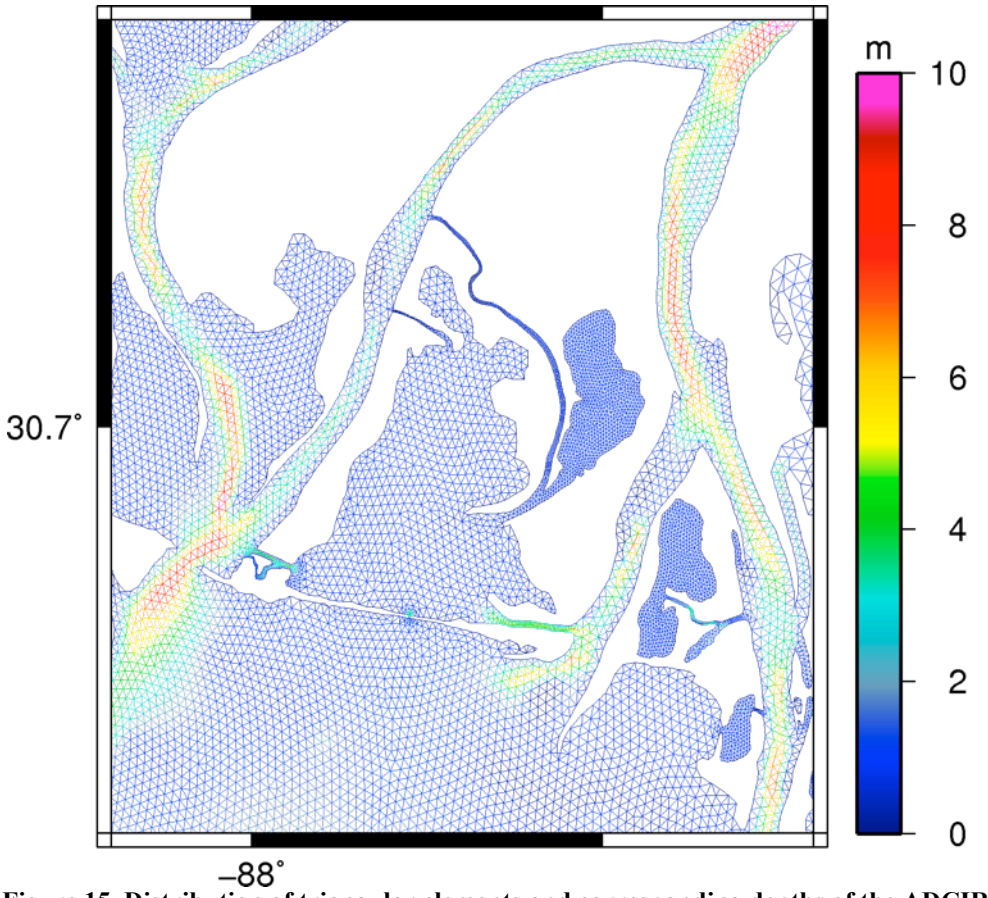

Figure 15. Distribution of triangular elements and corresponding depths of the ADCIRC mesh within the study area. Depths correspond to the color scale and are in meters below NAVD88.

Mesh Boundary Conditions

In addition to the essential nodal attributes of the unstructured finite element mesh, the ADCIRC model requires specified boundary conditions for forcing and numerical calculations. This model mesh consists of a tidal forcing boundary condition in the Gulf of Mexico, non-periodic inflow boundary conditions on the Mobile and Tensaw Rivers, and a combination of mainland and island boundary conditions that define the shorelines. The locations of these boundary conditions are shown in Figure 16.

Tidal and inflow boundary conditions constitute the applied forcing for ADCIRC simulations. Tidal forcing was specified along the tidal forcing boundary using the dominant tidal constituents for Mobile Bay, as determined by analysis of harmonic constituents at the NOAA Dauphin Island CO-OPS station: K1, O1, P1, Q1, M2, N2, and S2. The constituent amplitudes, phases, frequencies, and equilibrium (time) arguments were extracted from an ADCIRC tidal database. The inflow boundary conditions were specified as discharge per unit width at each node defining that inflow boundary string. Discharge values for the model periods (validation and alternative simulations) were obtained from USGS gage records on the Mobile and Tensaw Rivers located upstream of the corresponding mesh boundaries.

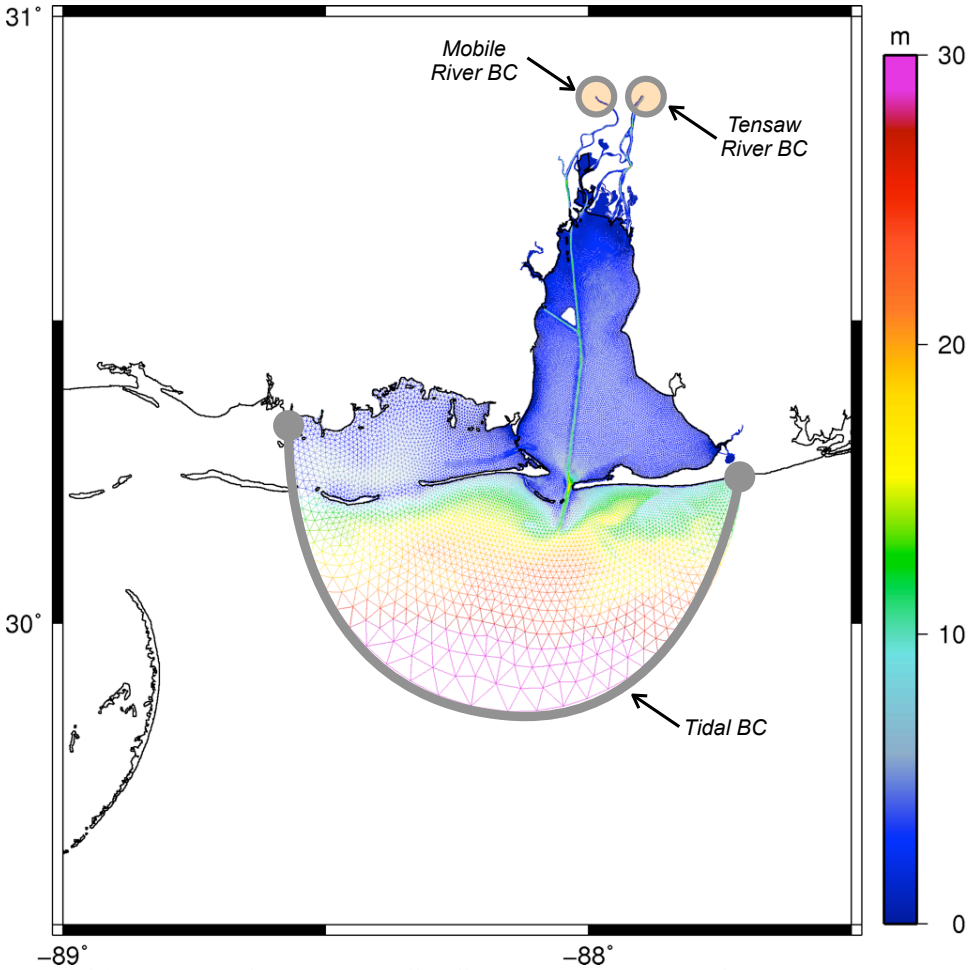

Figure 16. Location of essential ADCIRC boundary conditions for model simulations in Mobile Bay.

Validation Period & Conditions

The hydrodynamic model of the study area was validated by simulating conditions during the field data collection period of March 27, 2014 to April 9, 2014. This process is called "hindcasting" as the process involves recreating, or re-simulating, the conditions as they existed at a previous time. By supplying representative tide, river, and wind forcing for the hindcast period, the model predictions of water levels and velocities can then be compared to physical measurements.

The field data collection period captured nearly two weeks of tidal elevations. Velocity sampling was performed over an eight-hour period on a single day in that two-week period. The specific hindcast period for model validation was March 30, 2014 to April 5, 2014. This period was selected to allow the model predictions to stabilize over a three-day period prior to the day on which velocity sampling was conducted. This period allowed the water levels and velocities to adjust to the tidal, river, and wind forcing.

In addition to the tidal constituent and river discharge forcing supplied over the hindcast period, meteorological forcing was supplied to the ADCIRC model using observed wind speed, direction and

atmospheric pressure at 16 locations throughout the north central Gulf Coast (Figure 17). The observations were extracted from NOAA National Data Buoy Center station records having six- or thirty-minute recording intervals. All observations were interpolated to a consistent six-minute interval in time, and to a rectangular grid of 0.25-degree spacing covering the extents of the ADCIRC mesh. The ADCIRC model then interpolated those wind and pressure measurements to match the model time step (~5 s) and to each node location in the mesh.

Validation Results

The model validation results corresponding to the hindcast simulation period of March 30, 2014 to April 5, 2014 are provided in the following sections. Model validation consists of direct comparisons between model predictions of water levels and velocities and measurements of water levels and velocities obtained during that same period. The validation comparisons will mostly focus on water levels and velocities within the study area.

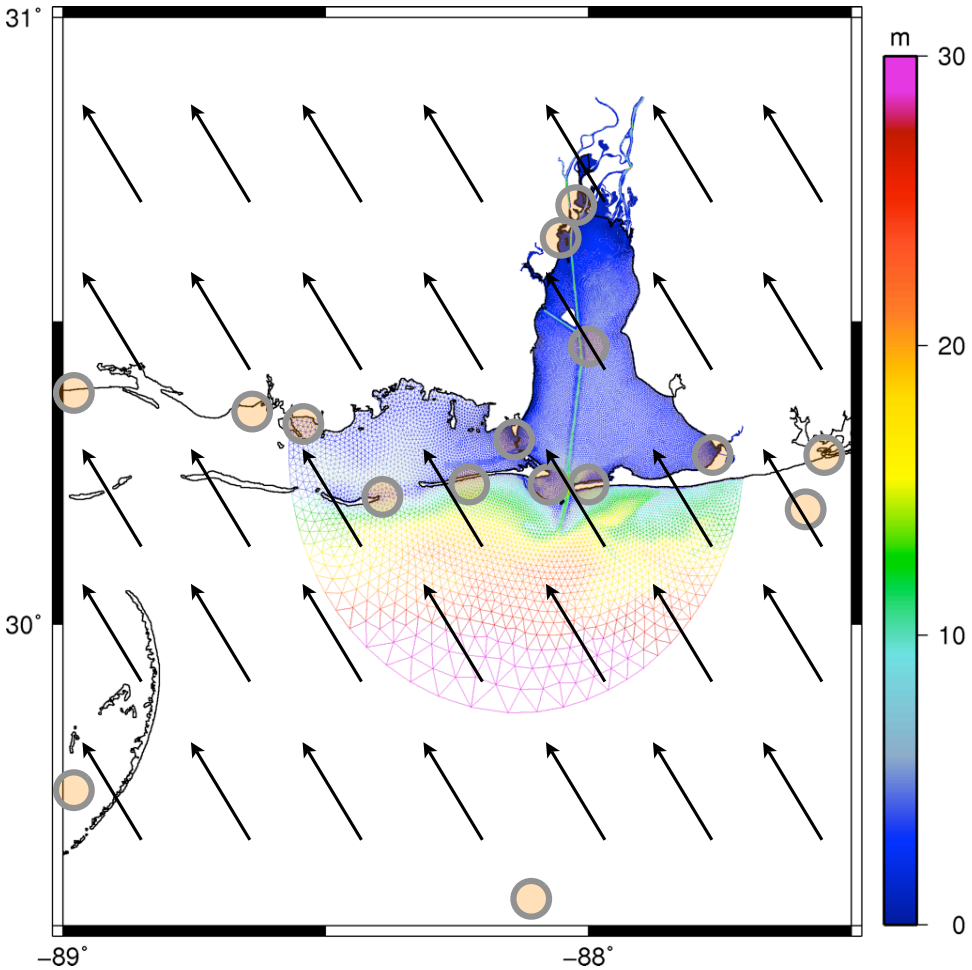

Figure 17. Locations of NOAA NDBC meteorological forcing observations and schematic of regularly spaced wind forcing relative to the ADCIRC mesh.

Water Levels

Hindcast water level predictions were compared against measured water levels at Dauphin Island, Mobile State Docks, Lap's on the Causeway, Meaher State Park, and Five Rivers Delta Resource Center. The water level time-series comparisons for each location are shown in Figure 18 (Dauphin Island), Figure 19 (Mobile State Docks), Figure 20 (Lap's), Figure 21 (Meaher), and Figure 22 (Five Rivers). The ADCIRC model was able to reasonably predict the phase, range, and high water levels during the hindcast period. The model predictions also demonstrated the increase in mean tidal position over the hindcast period, at the northern locations, due to the increased river discharge during that time. This increased staging of water levels in the northern portion of Mobile Bay was captured by the temporary tide gages, too.

A quantitative assessment of model-data error was developed for each tide gage over the hindcast period April 1, 2014 to April 5, 2014. Errors associated with predicted water levels were 20% or less within the study area. Errors were calculated by considering the square root of the mean square difference (RMS difference) between measurements and predictions. The resulting "mean" errors are presented in Table 1 as heights and as a percentage of the tide range at the corresponding tide gage.

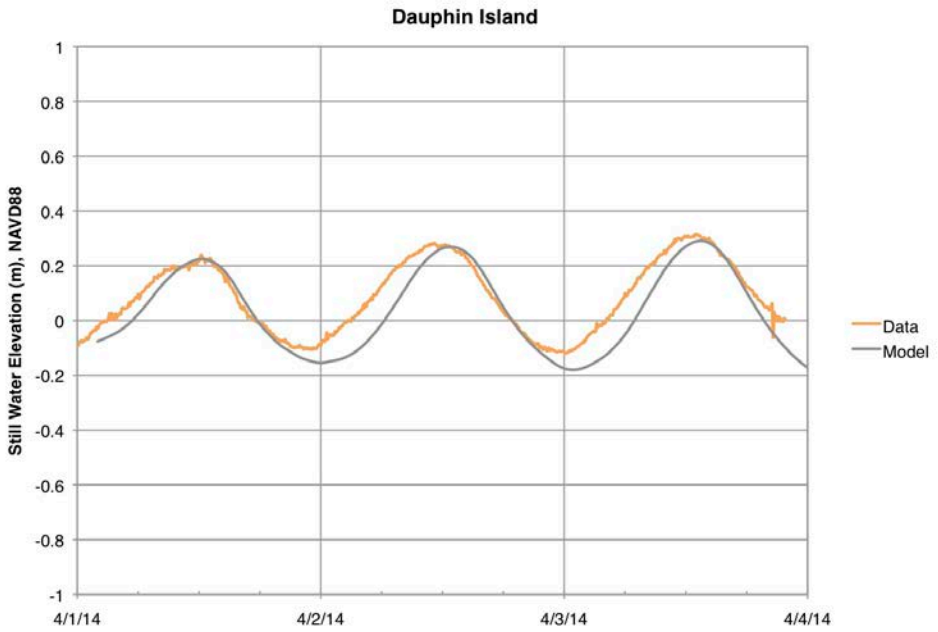

Figure 18. Comparison of measured (Data) and predicted (Model) water levels at Dauphin Island (NOAA CO-OPS 8735180) for the hindcast validation period.

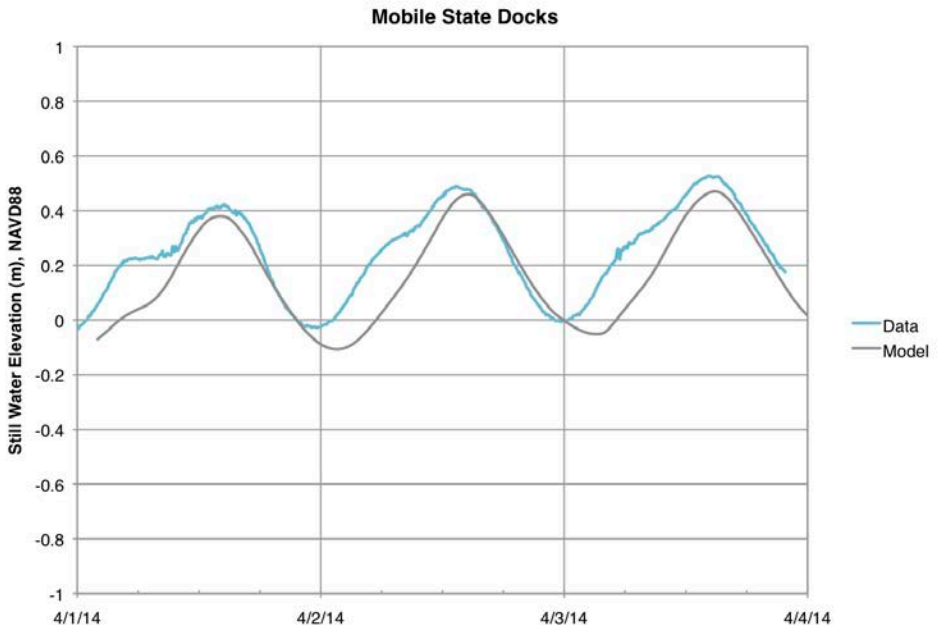

Figure 19. Comparison of measured (Data) and predicted (Model) water levels at Mobile State Docks (NOAA CO-OPS 8737048) for the hindcast validation period.

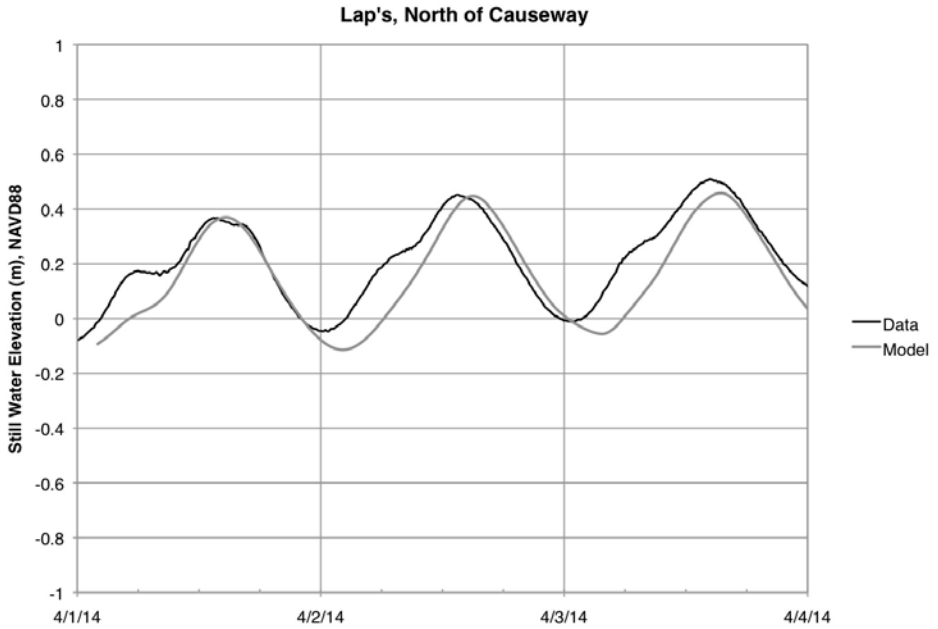

Figure 20. Comparison of measured (Data) and predicted (Model) water levels at the temporary tide gage in Choccolatta Bay for the hindcast validation period.

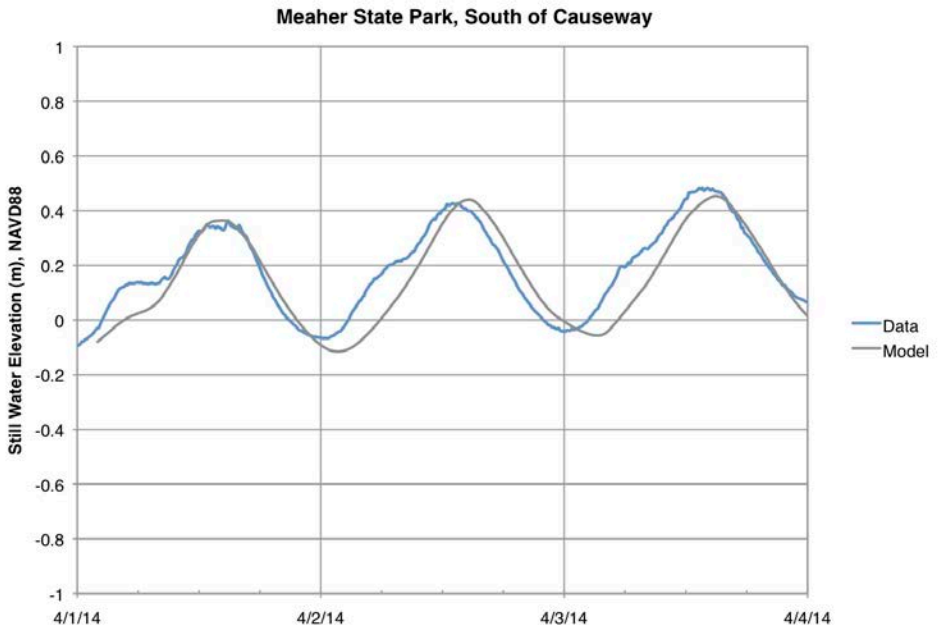

Figure 21. Comparison of measured (Data) and predicted (Model) water levels at the temporary tide gage in Ducker Bay at Meaher State Park for the hindcast validation period.

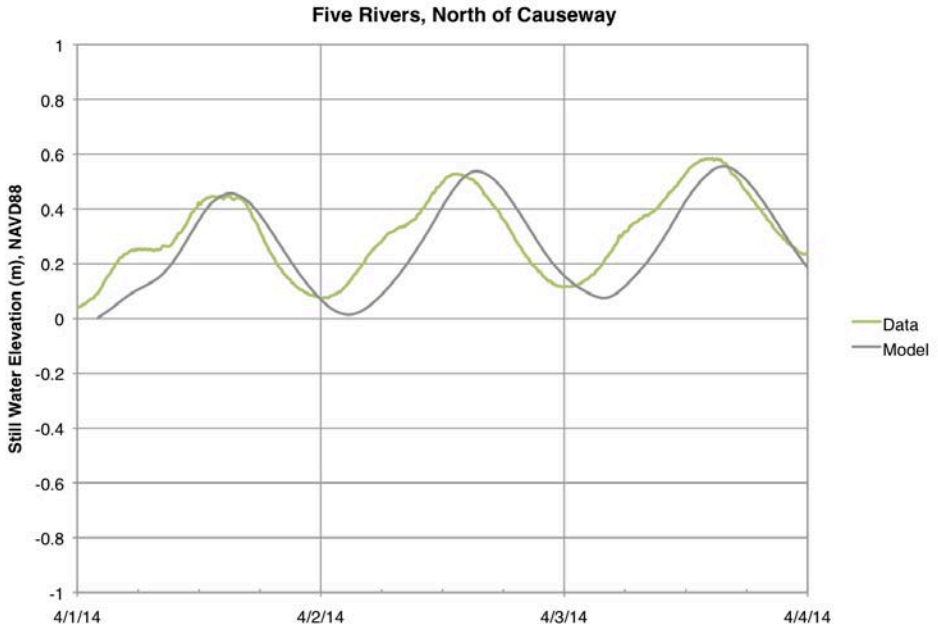

Figure 22. Comparison of measured (Data) and predicted (Model) water levels at the temporary tide gage in Sardine Pass behind Five Rivers Delta Resource Center for the hindcast validation period.

Table 1. Root mean square difference (error) assessment for predicted and measured water levels at five tide gages.

Location	Mean Height Error (cm)	% of Tide Range
Dauphin Island	7.3	17.0
Mobile State Docks	11.6	21.0
Choccolatta Bay (Lap's)	9.7	17.8
Ducker Bay (Meaher)	9.0	16.4
Sardine Pass (5 Rivers)	10.3	20.0

Velocity

Hindcast water velocity predictions were compared against measured water velocities at the I-10 Cut, box culverts, Pass Picada, Apalachee River, and Blakeley River. The water velocity time-series comparisons for each location are shown in Figure 23 (I-10 Cut), Figure 24 (box culverts), Figure 25 (Pass Picada), Figure 26 (Apalachee River), and Figure 27 (Blakeley River). Since the ADCIRC model predicts depth-averaged water velocity, the measured velocities were averaged over depth for the purpose of model-data comparisons. The model was able to faithfully reproduce the flow direction and magnitude at most locations.

A quantitative assessment of model-data error for direct comparisons of predicted and measured water velocity is provided in Table 2. As was done with water levels, the mean difference between predicted and measured water velocity was determined and is reported as an average error velocity and also as a percentage of the average velocity measured over the data collection period. With the exception of flow through the I-10 Cut, the velocity errors were less than 5 cm/s or 30% of measured values. The model overestimated the magnitude of water velocity early in the data collection period, likely due to a slight phase lead in the tidal stage as compared to observed values. The model predictions and measured data at I-10 Cut come into better agreement later in the day.

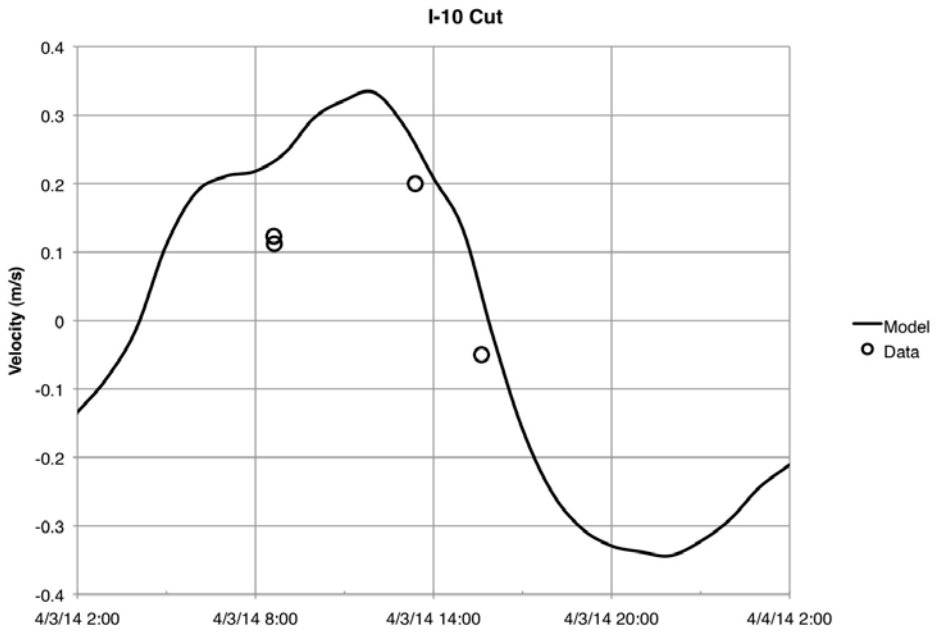

Figure 23. Comparison of measured (Data) and predicted (Model) depth-averaged water velocity along the channel centerline at I-10 Cut.

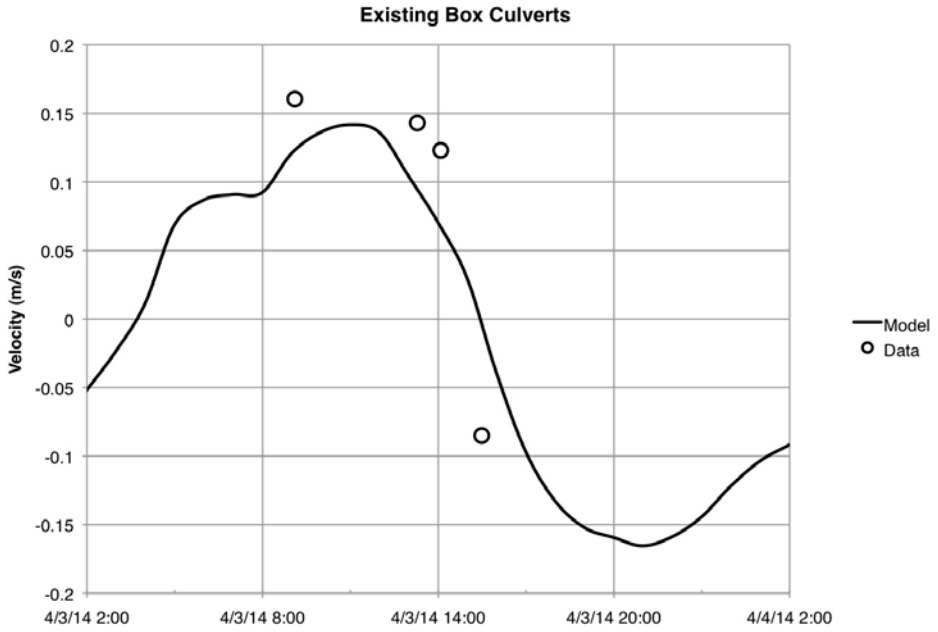

Figure 24. Comparison of measured (Data) and predicted (Model) depth-averaged water velocity immediately north of the existing box culverts in Choccolatta Bay.

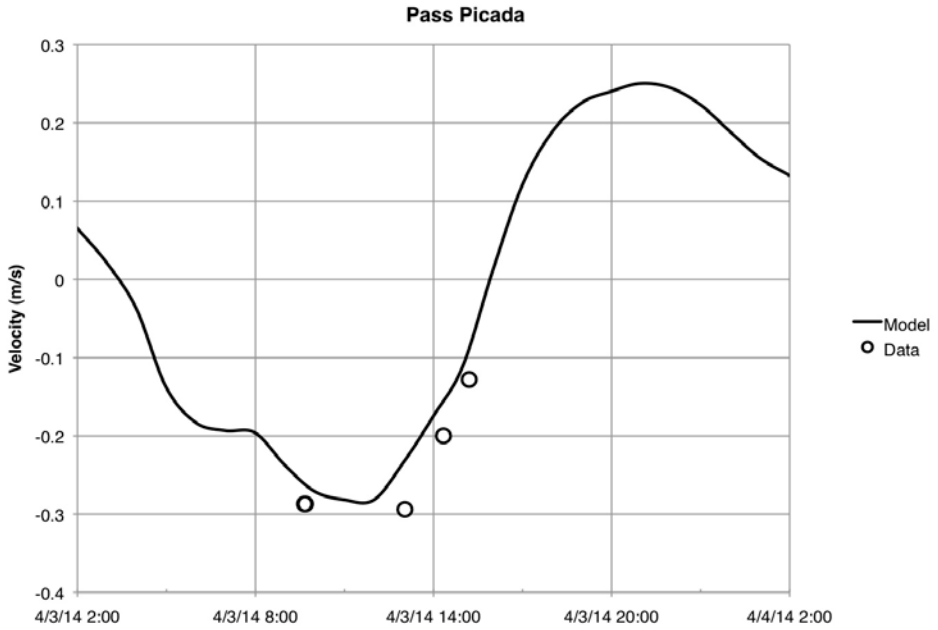

Figure 25. Comparison of measured (Data) and predicted (Model) depth-averaged water velocity along the channel centerline at the east end of Pass Picada.

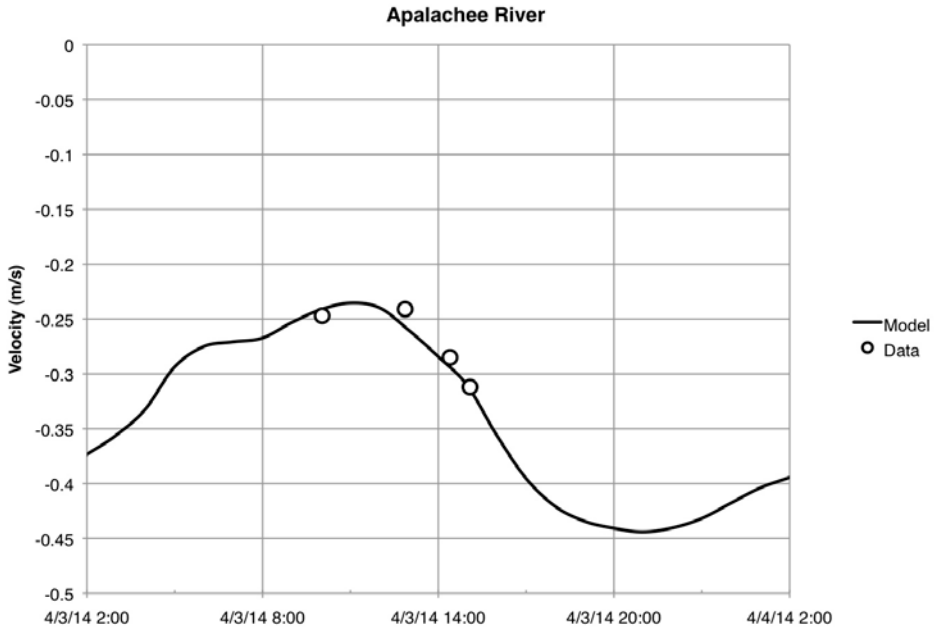

Figure 26. Comparison of measured (Data) and predicted (Model) depth-averaged water velocity along the channel centerline at Apalachee River.

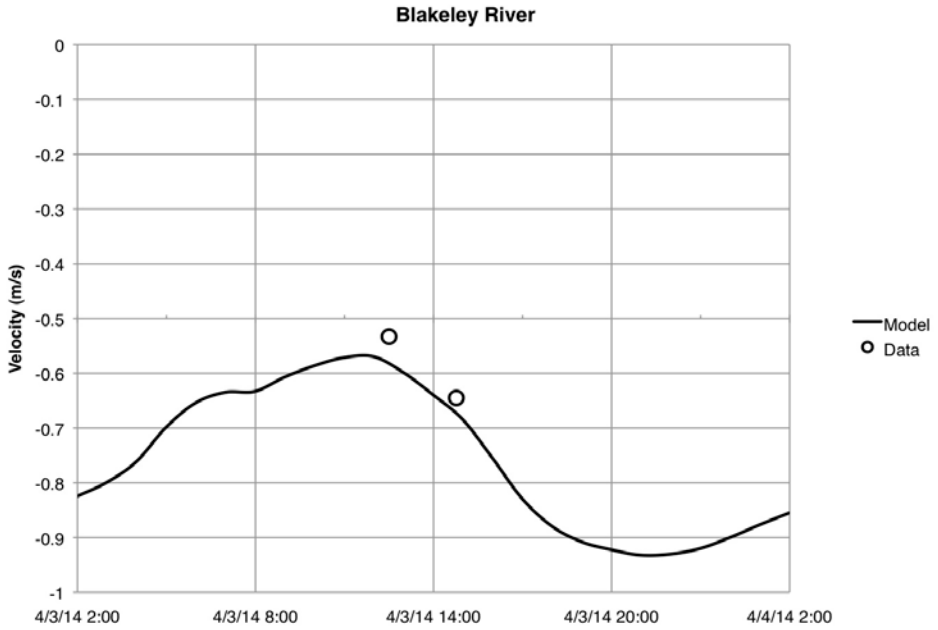

Figure 27. Comparison of measured (Data) and predicted (Model) depth-averaged water velocity along the channel centerline at Blakeley River.

Table 2. Assessment of model-data errors for depth-averaged water velocity during the data collection period.

Location	Velocity Error (cm/s)	% of Average Velocity
I-10 Cut	5.8	60.1
Box Culverts	4.4	30.7
Pass Picada	4.2	17.4
Apalachee River	0.6	2.2
Blakeley River	3.4	5.8

Restoration Alternative Model Setup

This section of the report addresses application of the ADCIRC model to assess the hydrodynamic characteristics of five restoration alternative scenarios under various conditions. A brief overview of the restoration alternatives is followed by a description of the naming conventions used to identify each simulation, as well as information about the model characteristics and forcing conditions. This section concludes with a description of the analysis methodology applied to address the performance measures described previously.

Overview

The ADCIRC model was used to evaluate five (5) hypothetical restoration alternative scenarios for constructed openings along the Mobile Bay Causeway. Simulations were performed under: 1) representative tidal and flow forcing for present day sea levels; 2) representative tidal and high flow forcing for present day sea levels; and 3) representative tidal and flow forcing for future, higher sea levels (year 2100). Additional details regarding forcing conditions are provided in the following sections. In addition to the five restoration alternative simulations, a corresponding simulation of the existing site conditions was performed for the purpose of comparative analysis.

The original number of possible restoration sites was reduced from four to three in earlier project meetings. Ducker Bay was eliminated as a possible restoration site due to potential easement/ownership issues. The remaining restoration locations included Choccolatta Bay, Justin's Bay, and Shellbank River. Each of these restoration alternatives was simulated in isolation (3 scenarios), with all of them open simultaneously (1 scenario), and with only Choccolatta and Justin's Bay open (1 scenario) for a total of five possible restoration alternative scenarios.

For the purposes of this hydrodynamic model study, the hypothetical restoration alternatives were assumed to be openings through the Causeway having depths equal to surrounding conditions. Culverts were not explicitly included in the hydrodynamic model.

Naming Conventions

Each scenario has a three-digit identifier. The first digit (0, 1, 2, 3, 4, 5) represents the scenario considered, where 0 corresponds to existing conditions and numbers 1 - 5 correspond to each of the five hypothetical restoration scenarios considered. The second digit (0, 1) represents the sea level scenario, with "0" corresponding to present-day levels and "1" representing the future sea level condition. The third digit (2, 3) corresponds to the river forcing where "2" represents the average July (low) flows, and "3" corresponds to the average wet season (high) flows. The naming convention and general characteristics of all hydrodynamic model simulations performed for this study is provided in Table 3. These conventions will be used throughout the remaining sections of the report.

Model Setup

The ADCIRC model parameters and characteristics were held constant across all restoration alternative simulations. For a particular forcing condition and sea level scenario, the only thing altered was the unstructured mesh. Additional nodes and elements were added or subtracted, as needed, to incorporate each of the hypothetical openings. Mesh properties are listed in Table 4. Images of the existing and altered meshes are provided in Figure 28.

Table 3. Naming convention and general conditions for all simulated restoration alternative scenarios.

Name	Restoration Scenario	Flow Conditions	Sea Level
Case 002	Existing Conditions	Average Summer	Present Day
Case 102	Choccolatta Bay		
Case 202	Justin's Bay		
Case 302	Shellbank River		
Case 402	All Open		
Case 502	Choccolatta + Justin's		
Case 003	Existing Conditions	Average Wet Season	
Case 403	All Open		
Case 012	Existing Conditions	Average Summer	Year 2100
Case 112	Choccolatta Bay		
Case 212	Justin's Bay		
Case 312	Shellbank River		
Case 412	All Open		
Case 512	Choccolatta + Justin's		

Table 4. Existing and altered mesh properties.

Case Name	Number of Nodes	Number of Elements
002, 003, 012	45294	84225
102, 112	45239	84151
202, 212	45320	84286
302, 312	45304	84242
402, 403, 412	45275	84229
502, 512	45265	84212

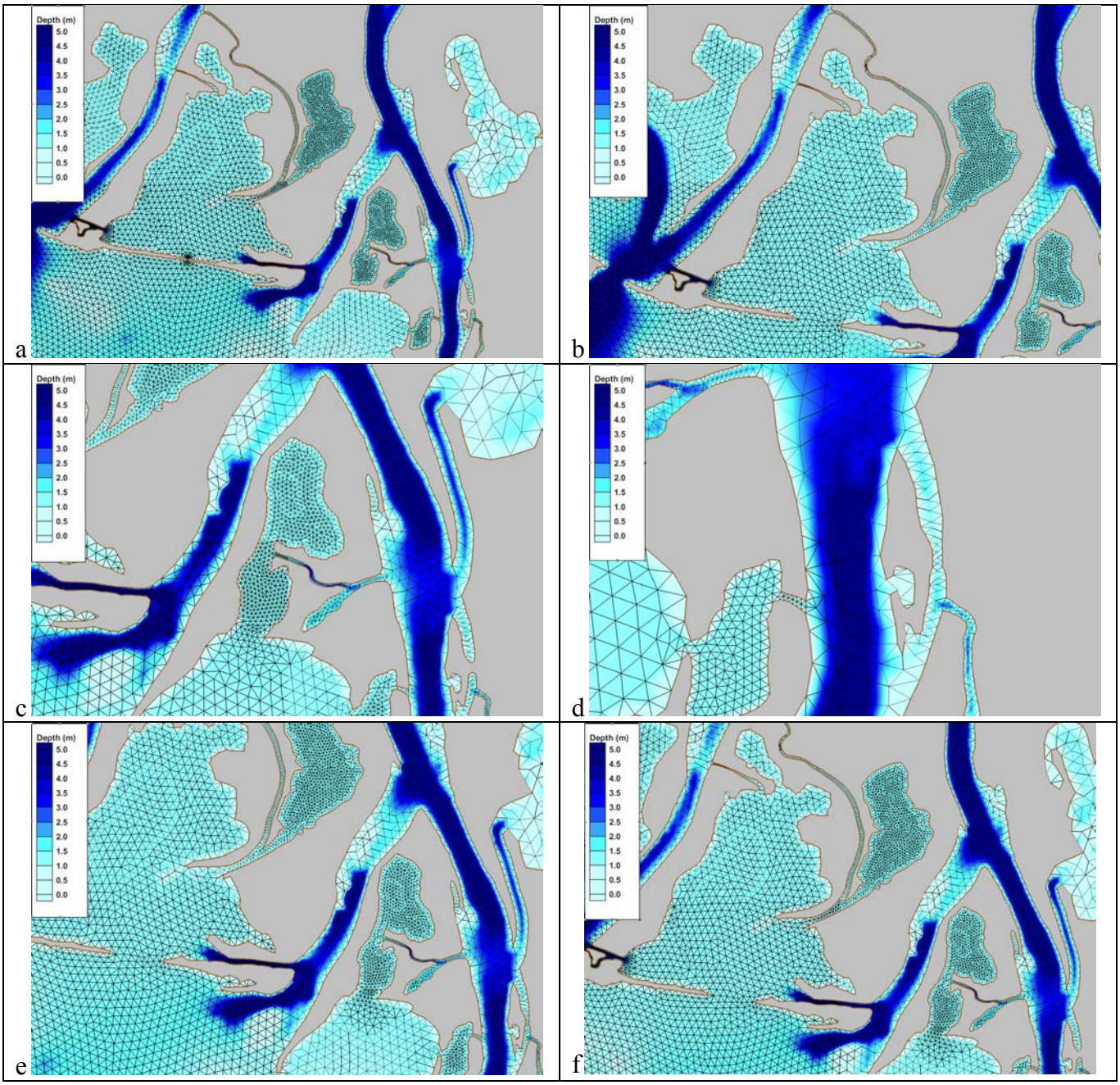

Figure 28. Images of the ADCIRC mesh for a) existing conditions, b) Choccolatta Bay opening, c) Justin's Bay opening, d) Shellbank River opening, e) all sites open, and f) Choccolatta + Justin's Bay openings. The distribution of triangular elements is shown and the colors correspond to depths in meters below NAVD88.

Simulation Conditions

Each of the restoration alternative simulations included tidal and flow forcing representative of the study area. All model simulations covered a period of ten days beginning July 16, 2014. In this case, the date is only relevant for determining the stage and phase of the tide. The period of time simulated included the end of a neap (equatorial) tide cycle and most of the seven-day spring (tropic) tidal cycle.

For the initial set of restoration alternative simulations, discharge values supplied to the Mobile and Tensaw River boundaries were assumed to be representative of average inflow conditions for the month of July over the years 2008 to 2012. Discharge statistics were computed from measured flows at USGS gages located on the Mobile and Tensaw Rivers upstream of the mesh boundaries. Those values are shown in Figure 29 and Figure 30.

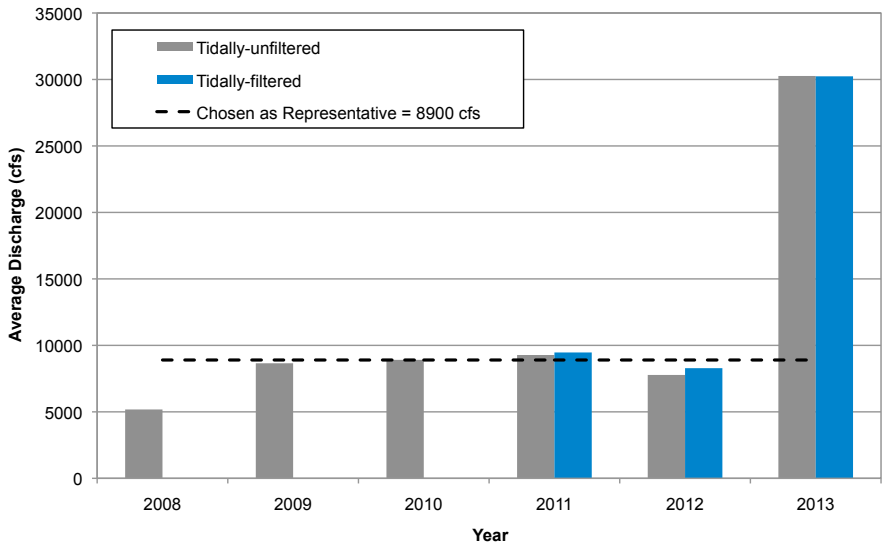

Figure 29. Average discharge at Mobile River near Bucks, AL for the month of July (USGS 02470629).

Two additional simulations (Case 003 and Case 403) were conducted to determine the effects of high river discharge on sediment transport potential within the study area. The discharge values for those simulations were determined by considering an average "wet season" value for the months December through May over the years 2010 to 2014. The discharge values were obtained from the same USGS gages on the Mobile and Tensaw Rivers. Those values are shown in Figure 31 and Figure 32.

The final suite of restoration alternative simulations were conducted to determine the effects of elevated future sea levels on hydrodynamic characteristics within the study area. These simulations were prepared by incorporating an additional nodal attribute to account for the sea level offset relative to the existing nodal elevations.

The future sea level offset was estimated using the NOAA relative sea level trend statistics at Dauphin Island. That rate is currently 2.98 mm/yr and was determined by considering a linear change, without acceleration, in relative sea level position at that location. A target year of 2100 was selected for the purposes of modeling and a nominal 0.3 m rise in the relative sea level position was incorporated into the hydrodynamic model. This value was applied as a water level offset to simulate the effects of sea level rise on hydrodynamics in the study area. Technically, the projected linear increase in relative sea

level in the year 2100 would be 0.256 m higher than the 2014 sea level position (2.98 mm * 86 years = 256 mm), but the model bathymetry is not accurate within 0.01 m, so the value was rounded up to 0.3 m for the purposes of modeling.

For reference, the tidal, flow, and sea level parameters used for each model simulation are summarized in Table 5.

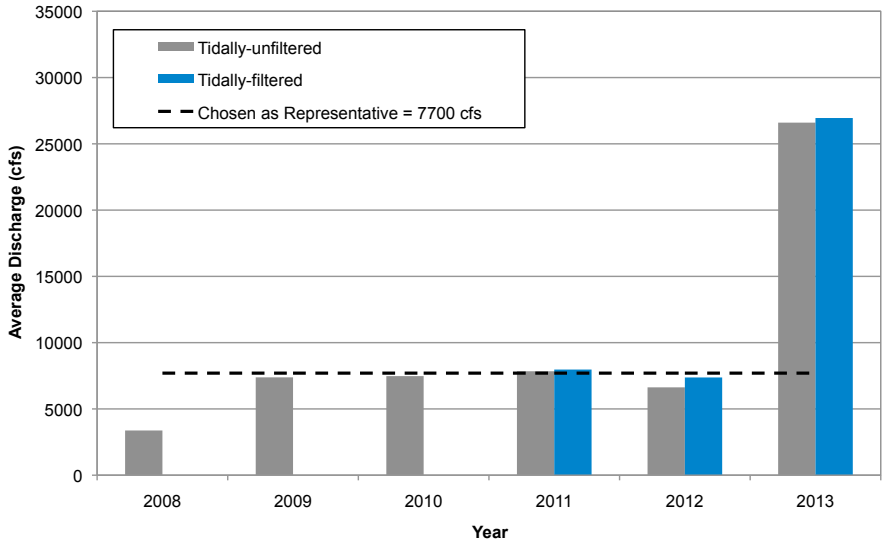

Figure 30. Average discharge at Tensaw River near Mount Vernon, AL for the month of July (USGS 02471019).

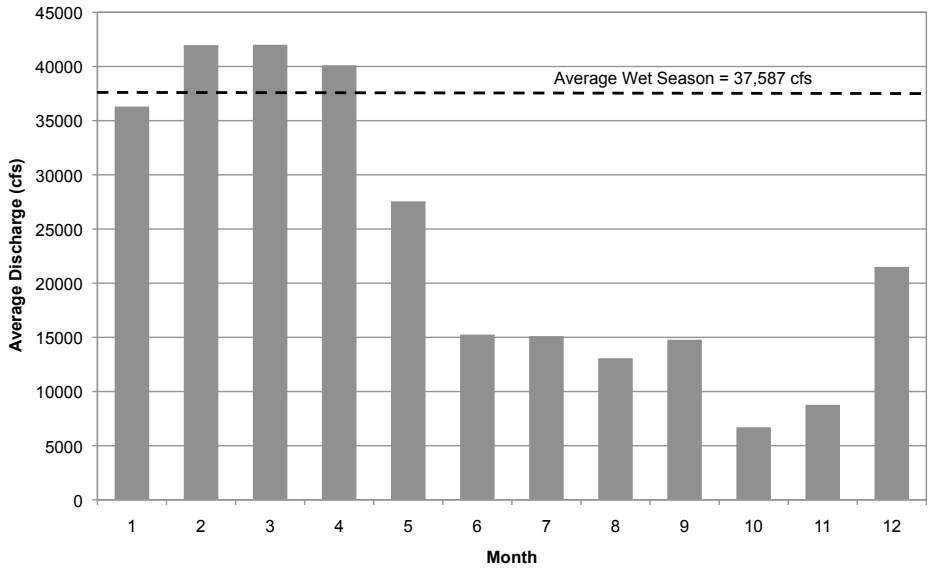

Figure 31. Average monthly discharge at Mobile River for the years 2010 to 2014 (USGS 02470629).

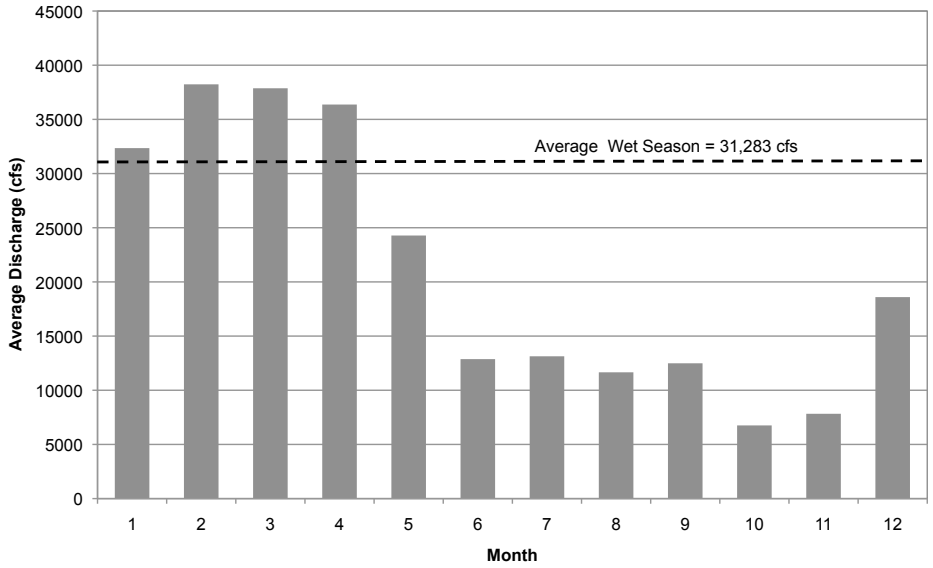

Figure 32. Average monthly discharge at Tensaw River for the years 2010 to 2014 (USGS 02471019).

Table 5. Summary of tidal, flow, and sea level characteristics applied to each ADCIRC simulation.

Name	Tidal Constituents	Average Discharge (cfs)		Sea Level Offset (m)
		Mobile River	Tensaw River	
Case 002	K1, O1, P1, Q1, M2, S2, N2	8900	7700	+0.0
Case 102				
Case 202				
Case 302				
Case 402				
Case 502				
Case 003		37587	31283	
Case 403				
Case 012		8900	7700	+0.3
Case 202				
Case 302				
Case 402				
Case 502				

Analysis Methodology

The restoration alternative simulation results were analyzed to specifically address hydrodynamic performance measures tied to the four study objectives mentioned previously. Generally speaking, the analysis of each simulation required an assessment of tide ranges; tidal prisms and volume fluxes; tidal phase lags; residence times; subtidal[1] velocities; and sediment transport potential.

Tide ranges were determined by considering the range between high and low water throughout the study area. Tidal prisms and volume fluxes were calculated by considering the cumulative discharge across defined transects between subsequent high and low water conditions throughout the study area. Tidal phase lags were determined by considering the time of high water inside and immediately outside of affected water bodies. Residence times were calculated using a Lagrangian Particle Tracking Model (LPTM) to simulate the removal of passive particles from defined water bodies in the study area (see Dietrich et al., 2012 and Marr, 2013). Subtidal velocities were calculated by averaging all predicted tidal velocities over the simulation period.

The LPTM analysis of residence times was accomplished by passing the predicted water velocities to an ADCIRC sub-model that tracks the movement of passive particles from their initial position. Particle displacements were controlled by the predicted water velocity without dispersion. The LPTM results were used to determine how long it took for a specific particle to exit a water body of interest for the first time. This corresponds to the most widely accepted definition of the residence time.

A total of 1677 passive particles were initialized in the Choccolatta Bay system, which includes Big Bateau, Little Creek, and Conway Creek. A total of 579 passive particles were initialized in the Justin's Bay system, which also includes Duck Skiff Pass and Sardine Pass. A figure showing the distribution and initial positions of passive particles is provided in Figure 33. These particles were tracked over the last nine days of the ADCIRC simulations and the results summarized in terms of residence times, exposure times, and percentage of particles removed under each scenario. The exposure time is defined as the total amount of time a particle spends within a region of interest, recognizing that tidal action may return a particle to a water body escaped on a previous tide.

Since only Choccolatta Bay and Justin's Bay are nearly enclosed with defined exit boundaries, they were considered in the LPTM analysis and Shellbank River was excluded. The exit boundaries for Choccolatta Bay were assumed to be I-10 Cut, Pass Picada, Little Creek, Conway Creek, and either the existing culverts or the hypothetical opening, depending on the alternative considered. The exit boundaries for Justin's Bay were assumed to be Sardine Pass and the hypothetical opening, depending on the scenario.

Sediment transport, resuspension, and deposition potential were determined using established models available in the published literature. Namely, bedload sediment transport rates and sediment resuspension rates were calculated using the methods of Meyer-Peter & Muller (1948) and van Rijn (1984). These methods and their application to hydrodynamic modeling are more fully described in Webb (2008), Webb & Slinn (2006), Webb & Slinn (2008), and Zedler & Street (2001). Application of these equations to coastal sediment transport is also described in Nielsen (1992).

[1] Subtidal refers to the non-periodic component of circulation, which could be a combination of river forcing and/or non-linear tidal forcing within the study area.

These methods are based on exceedance of a critical sediment stress (e.g., Shields' stress), which is a function of sediment diameter and specific gravity (van Rijn, 1993). The fluid stress is a function of the square of the ADCIRC predicted water velocity at each nodal location, the density of fluid (1000 kg/m^3), and a typical friction coefficient (0.0025). The transport and resuspension rates have dimensions of volume rate of bed material exchange per unit area (e.g., $m^3/s/m^2$).

Sediment characteristics were obtained from the Calscience sediment analysis reports (No. 14-05-1270; No. 14-05-1271_s1; No. 14-05-1383) provided by Weston Solutions as part of the Task 2 deliverables. These data reports provided average particle diameters and gradation characteristics for each sediment core collected in the study area. These particle diameters were then mapped to the hydrodynamic model mesh nodes using inverse distance weighted interpolation.

Sediment deposition potential was modeled by considering the balance between horizontal momentum imparted by the predicted water velocity, the gravitational force acting on the particle, and the vertical momentum due to the particle's mass and fall velocity (van Rijn, 1984). Once the particle had fallen a distance equivalent to the surrounding water depths it was assumed to settle on the bed. These areas were flagged during the simulations as depositional.

It should be stressed that sediment transport modeling is an inherently inaccurate process. All sediment transport modeling should be evaluated through a lens of conservatism and changes in magnitudes should be considered in a relative, or comparative, sense. Therefore, the qualitative changes in sediment transport and resuspension rates between scenarios should be weighed more heavily than any specific quantity predicted by the sediment transport models.

In all cases, the potential effects of a restoration alternative scenario on a parameter of interest were evaluated by subtracting the parameter value under existing conditions from the parameter value in the alternative condition. In other words, the effects of a restoration alternative are evaluated as the difference between its characteristics and those of the existing conditions. Comparing results in this manner provides a very easy way of qualitatively assessing restoration effects on a particular parameter of interest: positive values indicate an increase in that parameter from its value under existing conditions, while negative values suggest a decrease in that parameter from its value under existing conditions.

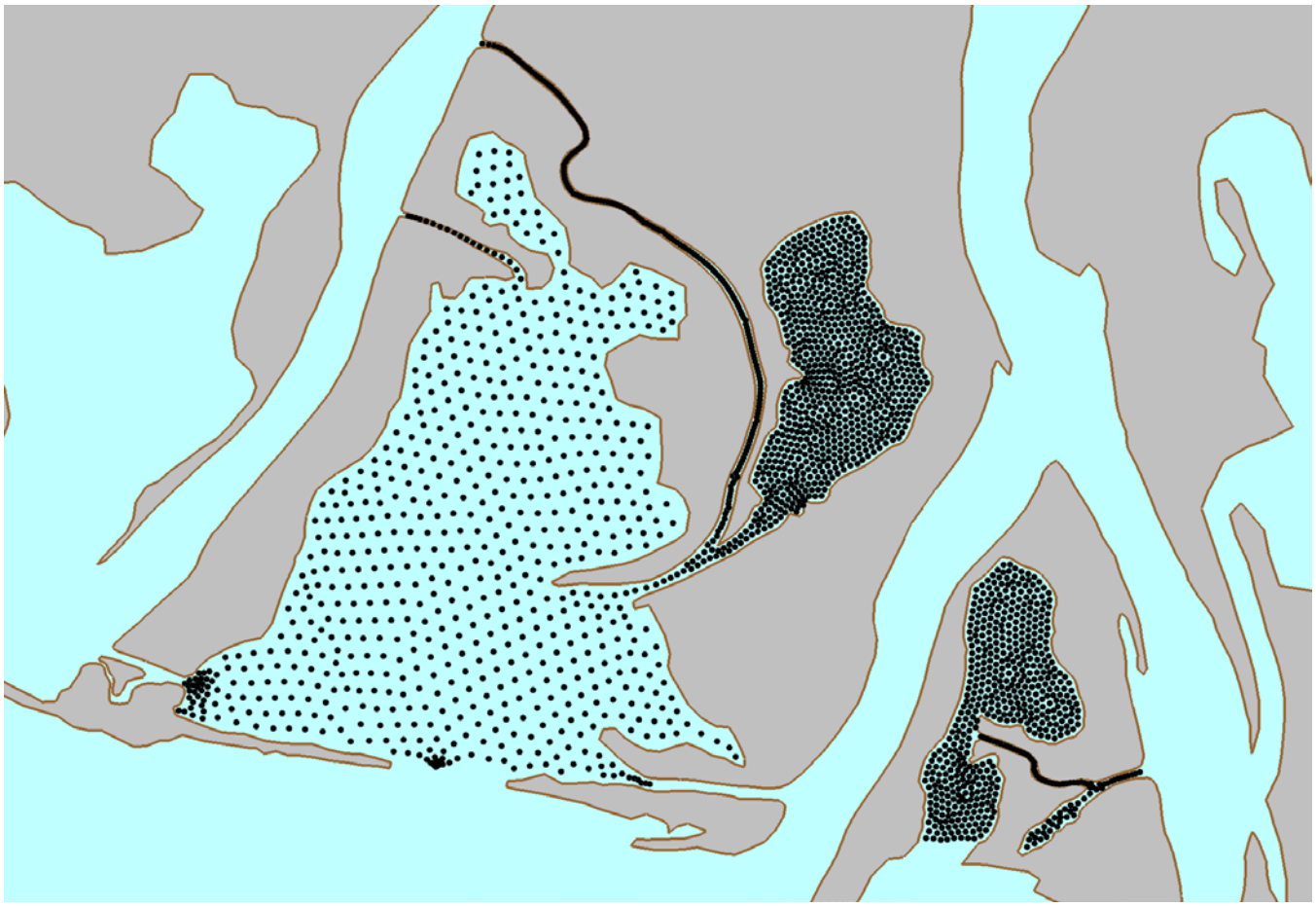

Figure 33. Distribution and initial position of passive particles used in LPTM simulations (black dots). The distribution and initial position of particles was the same for each simulation. The mesh corresponding to Case 412 (all open) is shown for reference.

Simulation Results | Typical Conditions

This section describes the potential effects of restoration alternatives on hydrodynamic characteristics under representative tidal and flow conditions for present-day sea levels. Existing conditions throughout the study area are described first, and then the potential effects of restoration alternatives are described as changes (increases, decreases, etc.) relative to those existing conditions.

Existing Conditions - Case 002

These simulation results reflect predictions of the existing hydrodynamic conditions within the study area. The forcing conditions consist of representative tides and average summer river discharge under present day sea levels.

Water Levels

The predicted maximum water levels in Choccolatta Bay were approximately 2 cm to 4 cm lower than areas south of the Causeway, while maximum water levels in Justin's Bay were 10 cm lower than other areas. Due to their highly constricted nature, these systems experience substantially less tidal forcing as compared to other parts of Mobile Bay. These results are shown in Figure 34 and are reinforced by the predicted maximum tide ranges listed in Table 6. Predicted tide ranges in Choccolatta and Justin's Bays were 6% and 40%, respectively, less than the tide range at a location immediately south of the Causeway in Mobile Bay.

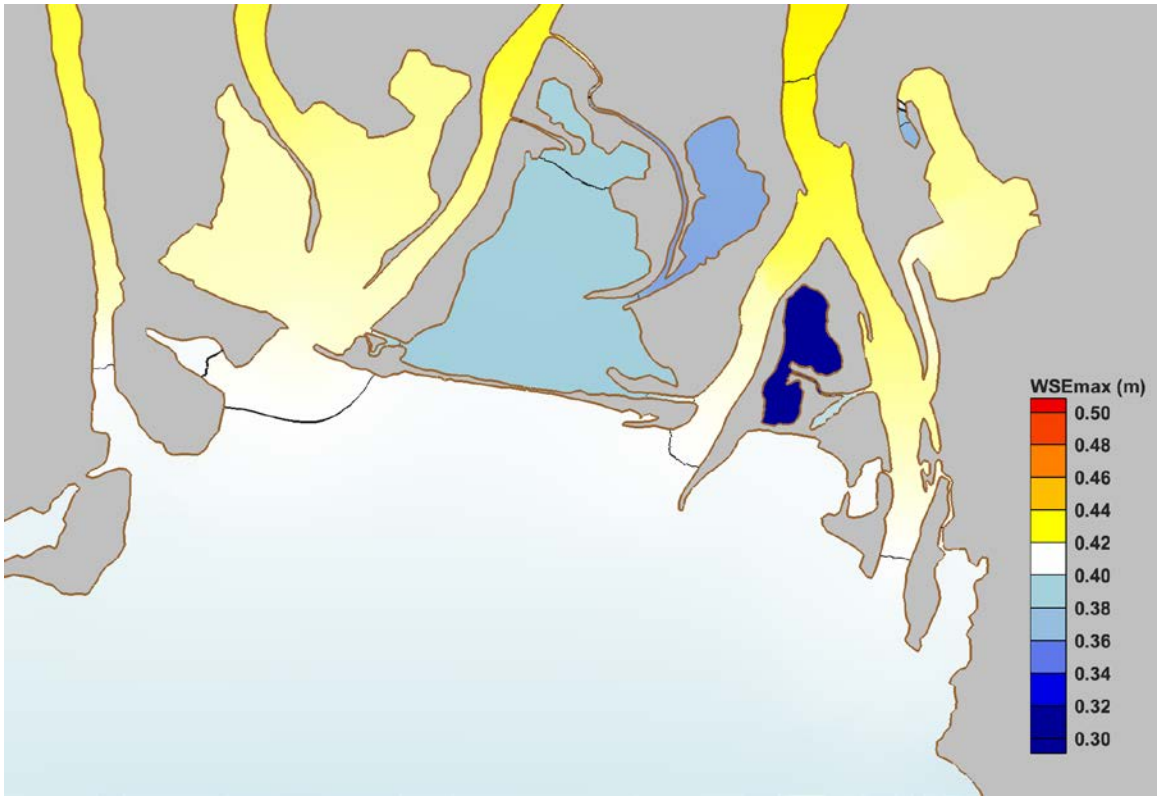

Figure 34. Distribution of maximum water levels (meters relative to NAVD88) for Case 002.

Table 6. Tide range at selected locations within the study area for Case 002.

Location	Tide Range (m)
Choccolatta Bay	0.675
North Mobile Bay	0.720
Justin's Bay	0.441
Ducker Bay	0.718
Shellbank River North	0.721
Shellbank River South	0.719

Flows

The largest velocity values were predicted to occur in the rivers, tributaries, and some constricted tidal channels. For example, note the large values at the confluence of Conway Creek and the channel from Big Bateau, in I-10 Cut, and also in Pass Picada for Choccolatta Bay. The discharge magnitude going through these channels is high relative to their area, resulting in high velocities. The magnitude of maximum depth-averaged water velocities throughout the study area is shown in Figure 35.

Because of their poor flushing and limited tidal communication with Mobile Bay, Choccolatta Bay, Big Bateau, Justin's Bay, and Shellbank River experience very little subtidal flow. Subtidal velocities were calculated as the average of velocities at each node over the last nine days of model simulation. The subtidal velocity magnitude and direction are shown in Figure 36.

In Choccolatta Bay, a majority of the tidal volume exchanged with Mobile Bay enters through I-10 Cut (40%), Pass Picada (41%), and the existing box culverts (17%); and exits through Little Creek and Conway Creek. Pass Picada and I-10 Cut served as the primary conduits of tidal communication under existing conditions (~80% of total exchange). The distributions and directions of tidal volume exchange under existing conditions are shown graphically for Choccolatta Bay in Figure 37.

For Justin's Bay, 100% of the tidal exchange occurred through Sardine Pass (and Duck Skiff Pass), as it was the only opening for the system under existing conditions. Tidal exchange was calculated from model results by tracking the cumulative discharge across specific transects between successive low and high water events for the maximum flood tide. The cumulative tidal exchange volumes for Choccolatta Bay and Justin's Bay are provided in Table 7.

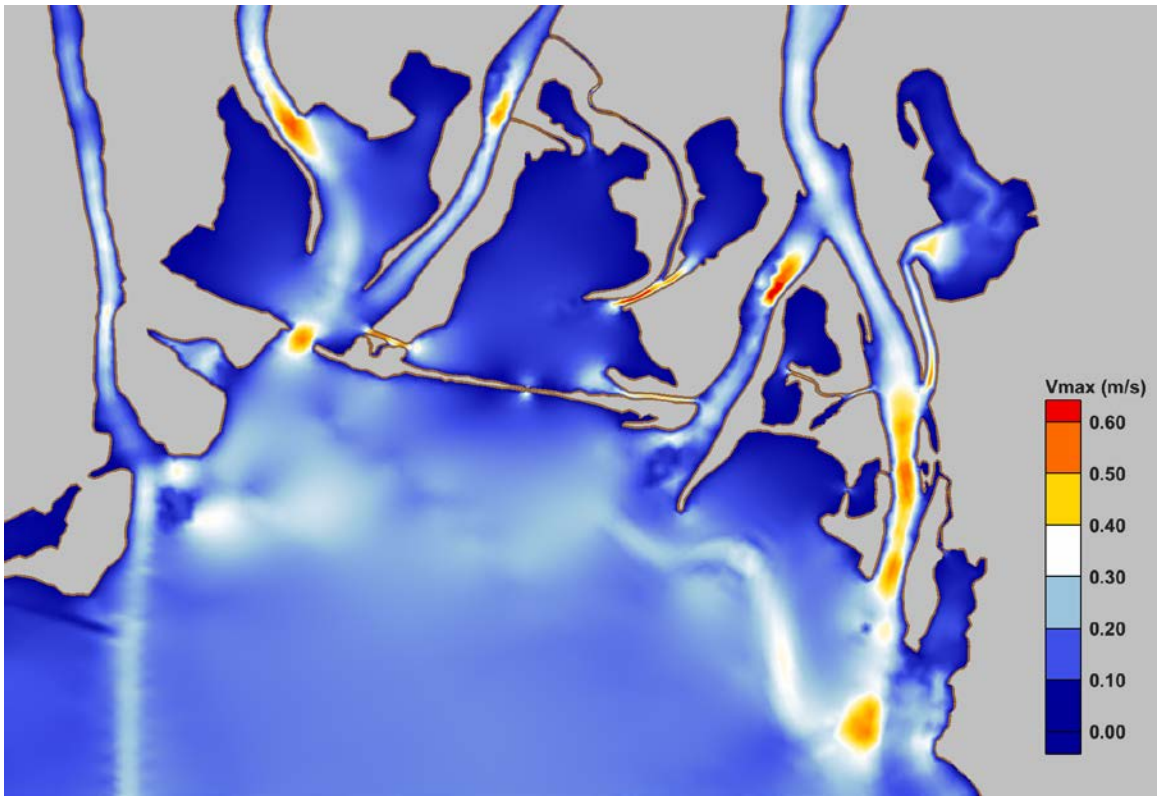

Figure 35. Magnitude of maximum depth-averaged velocity (meters per second) for Case 002.

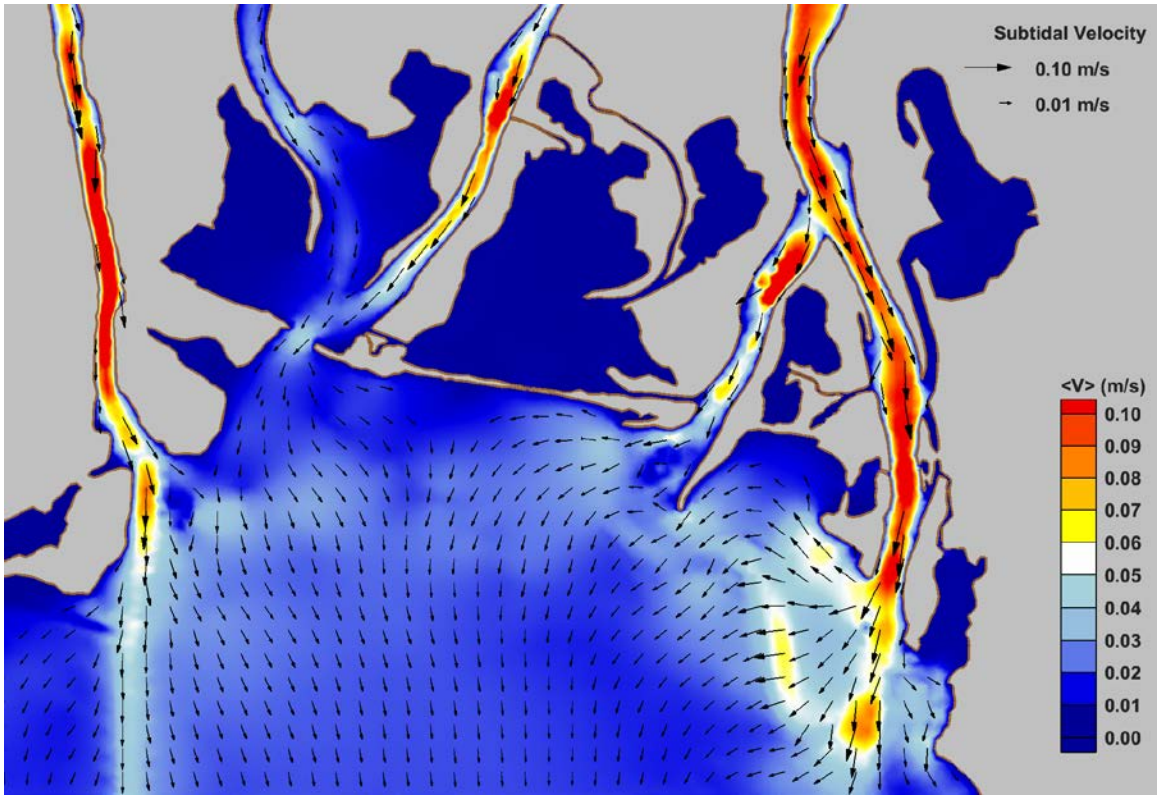

Figure 36. Subtidal velocity magnitude (colors) and direction (vectors) for Case 002.

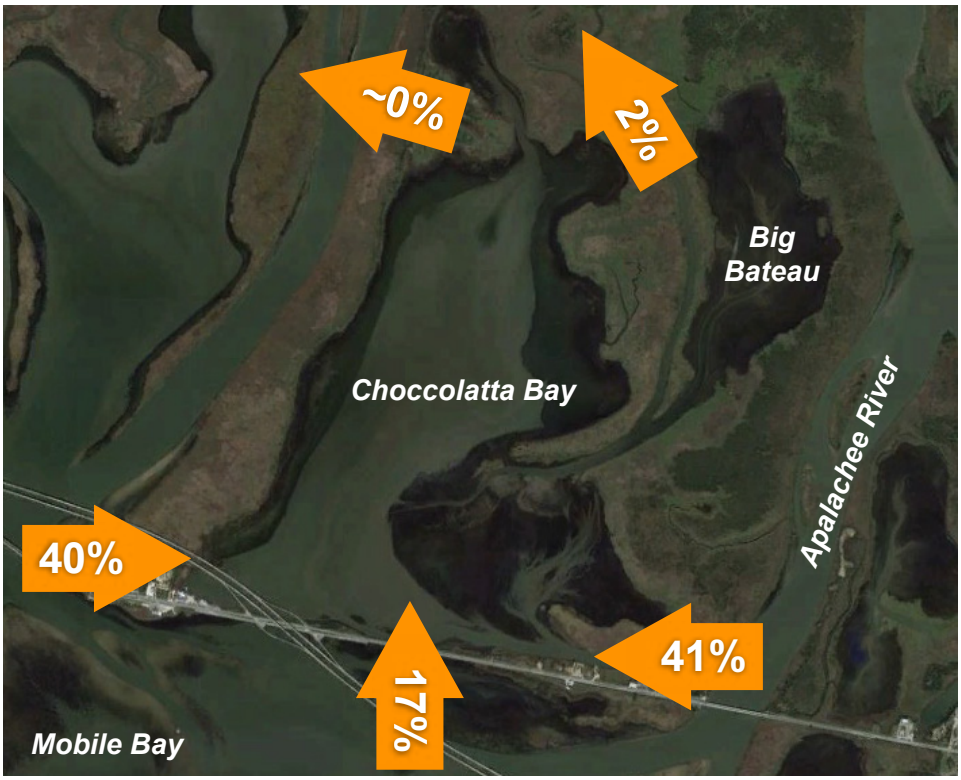

Figure 37. Distribution and direction of tidal exchange volumes for Choccolatta Bay under existing conditions (Case 002). Values are shown as percentages of the total volume of water exchanged.

Table 7. Maximum tidal volume exchanged (in cubic meters) between successive low and high water on a maximum flooding tide for Case 002.

Location		Tidal Volume Exchange (m^3)
Choccolatta Bay	I-10 Cut	2,204,867 (in)
	Little Creek	6,543 (out)
	Conway Creek	927,292 (out)
	Culverts	85,586 (in)
	Pass Picada	2,270,914 (in)
	Total (net)	**3,627,533 (in)**
Justin's Bay	Sardine Pass	411,800 (in)

Sediment Transport Potential

The locations of the largest bedload and resuspension sediment transport rates corresponded to locations having the largest velocities throughout the study area. These areas included constricted tidal channels having high velocities, and also reaches within the Apalachee and Blakeley Rivers. Areas experiencing bedload transport also exhibited sediment resuspension. These potential bedload and resuspension sediment transport rates are shown in Figure 38 and Figure 39, respectively. The rates, expressed as the volume rate of bed material exchange per unit area, are potential transport rates averaged over the last

nine days of model simulation time. As such, there are times when rates were higher and times when rates were lower than the values shown.

The predicted patterns of potential deposition throughout the study area are reflective of the characteristics and behavior of the system. For example, the depositional areas within Justin's Bay somewhat mimic the bathymetry of the Bay. Furthermore, the noted deposition in North Shellbank River is representative of long-term shoaling (i.e., sediment deposition) that has occurred there. Potential sediment depositional areas within the study region were determined as described previously. These areas were flagged (1 = deposition, 0 = no deposition) and then averaged over the final nine days of the model simulation.

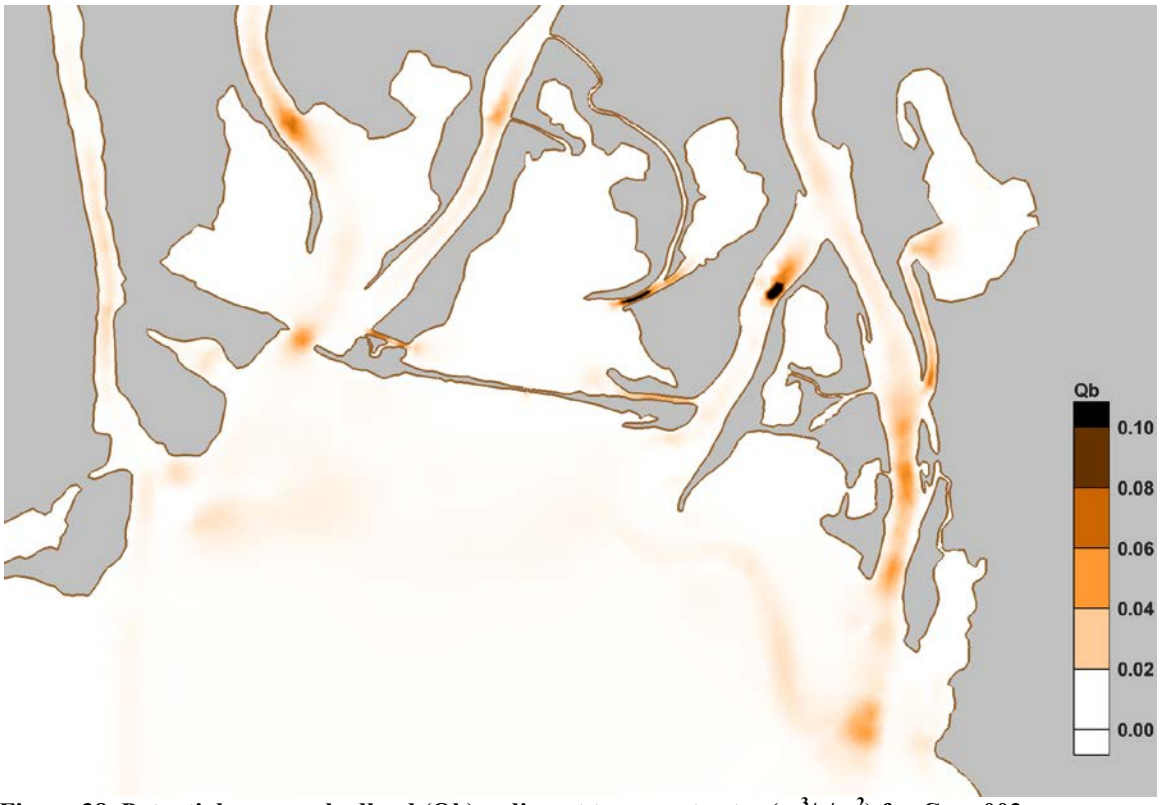

Figure 38. Potential average bedload (Qb) sediment transport rates ($m^3/s/m^2$) for Case 002.

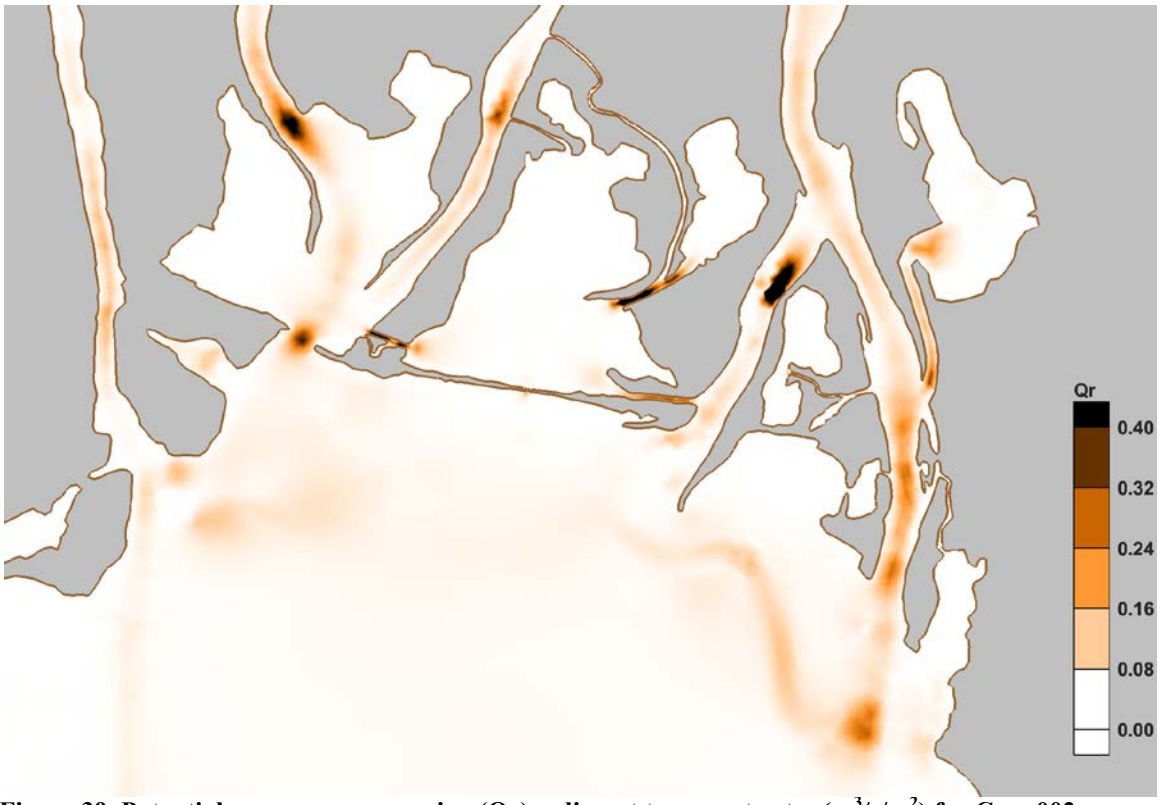

Figure 39. Potential average resuspension (Qr) sediment transport rates ($m^3/s/m^2$) for Case 002.

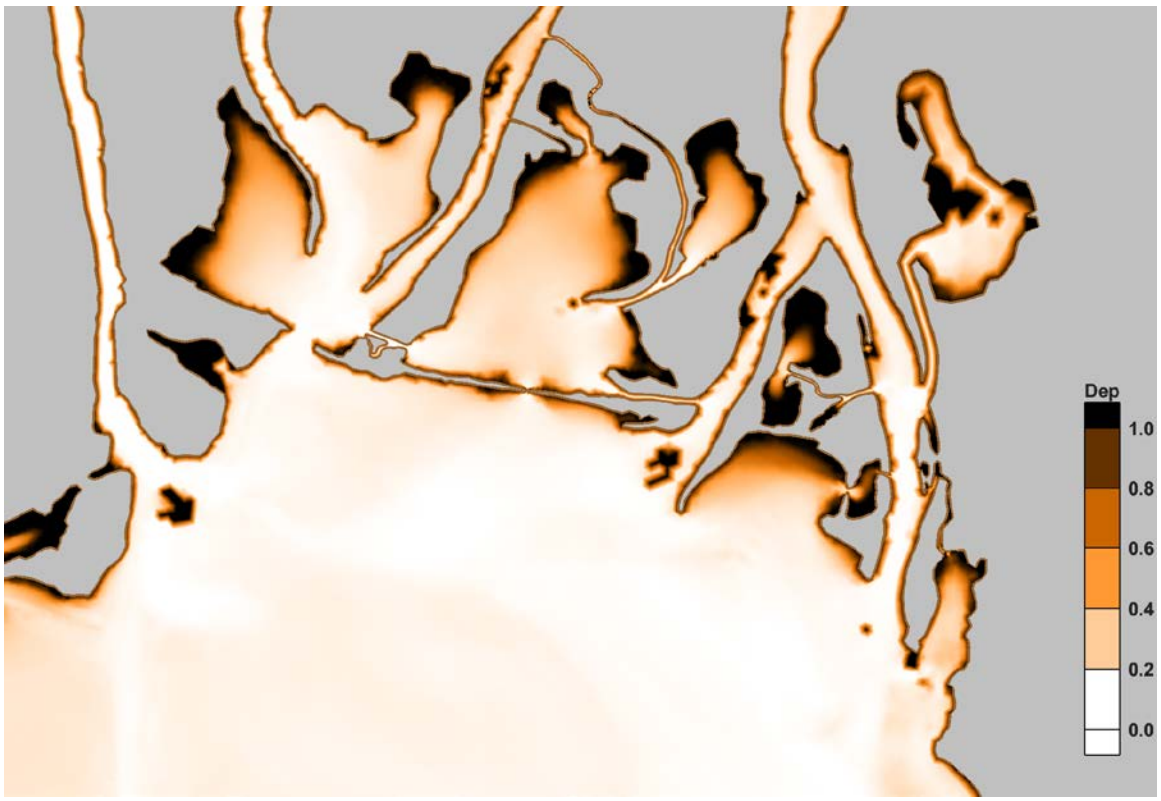

Figure 40. Sediment deposition potential for Case 002. Areas that are strongly depositional have a value of 1.0. Areas that are unlikely to experience deposition have a value of 0.0.

Flushing

The flushing potential of Choccolatta and Justin's Bays were evaluated by passing the hydrodynamic model output to the Lagrangian Particle Tracking Model as described previously. Particles were tracked over the last nine days of the model simulation to estimate residence times, exposure times, and percentage of particle removed from each water body. These characteristics were evaluated on a particle-by-particle basis as well as considering system-wide averages, which unfortunately are not completely representative of the nature of these systems.

Under existing conditions, the LPTM results indicated that just over 20% of particles would be flushed from Choccolatta Bay, while only 7% of particles would be flushed from Justin's Bay. For Choccolatta Bay, 41% of the escaping particles left through I-10 Cut, 36% left through the culverts, and 19% left through Pass Picada, with the remaining (<5%) exiting through Little and Conway Creeks. Under existing conditions, 100% of escaping particles left Justin's Bay through Sardine Pass. The residence times of particles within the systems, relative to their initial positions, are shown in Figure 41 under existing conditions. Note that the residence times are lower (<1 day) near system openings. The system-wide LPTM averages are provided in Table 8.

Since many of the particles do not leave either system, the reported system-wide averages for residence and exposure time are somewhat biased. Remember that the simulation results were analyzed over only nine days. Particles not leaving the system were assigned a value of nine days, when in reality their values are unknown at present. The simulations need to be performed for a much longer duration in order to capture their true residence times.

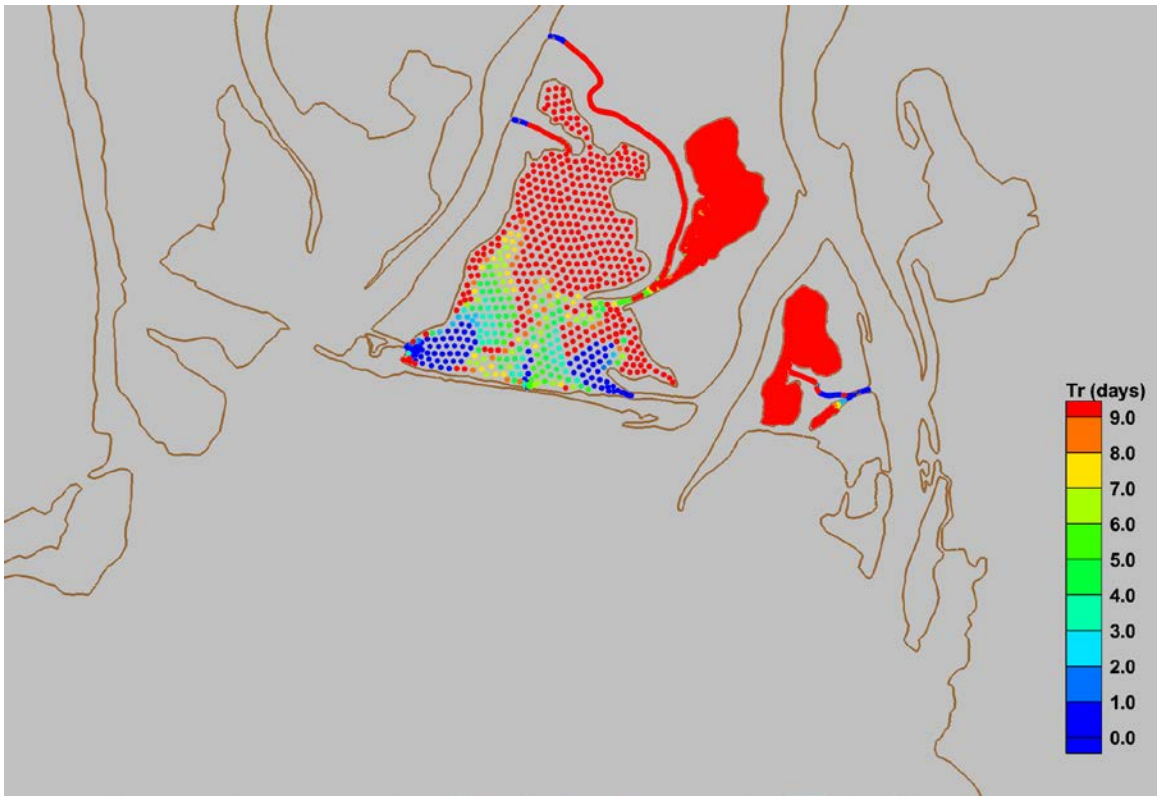

Figure 41. Residence times (Tr) in days of passive particles, relative to initial position, for Case 002.

Table 8. Flushing characteristics for Choccolatta and Justin's Bays in Case 002.

Value	Choccolatta Bay	Justin's Bay
Average Residence Time (days)	7.9	8.4
Average Exposure Time (days)	8.4	8.6
Percentage of Particles Removed	20.2	7.1

Choccolatta Bay - Case 102

This alternative restoration scenario considers a constructed opening through the Causeway at Choccolatta Bay only. The forcing conditions consist of representative tides and average summer river discharge under present day sea levels. Simulation results presented for Case 102 are shown as differences relative to existing conditions (Case 002).

Water Levels

The results indicate that the constructed opening resulted in maximum water levels that were approximately 3 cm higher than existing conditions. These results are shown in Figure 42. The figure shows the difference in maximum water levels between the two scenarios, calculated as the water levels for the modified scenario minus the water levels under existing conditions. Therefore, positive values represent increases in maximum water levels, while negative values indicate decreases in maximum water levels, relative to existing conditions.

When compared to a location just south of the constructed opening, the modified condition (Case 102) completely removed the existing one-hour phase lag in tide stage inside and outside of Choccolatta Bay (see Figure 43). Model results suggested that the constructed opening in Choccolatta Bay also affected the tidal range. A time-series of water levels in Choccolatta Bay for Case 002 and Case 102 is shown in Figure 44. The increase in high and low water is evident, as is the earlier arrival of low and high tides.

With the constructed opening in place, the model predicted an increase of 8% in Choccolatta Bay's tide range with negligible effects (<1%) noted elsewhere in the study area. Therefore, any potential restoration for Choccolatta Bay, by itself, isn't likely to have a measurable effect on tide range in other parts of the study area. The tide ranges at various locations in the study area are provided in Table 9.

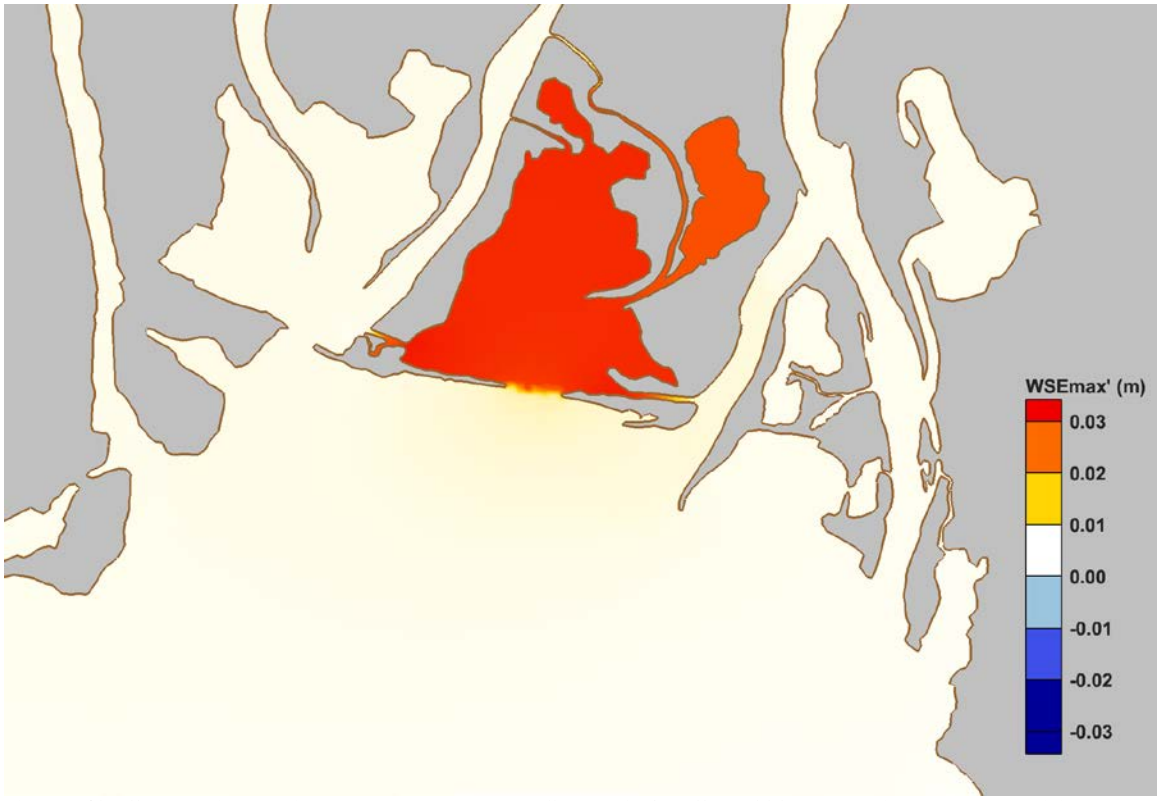

Figure 42. Change in maximum water levels (WSEmax') for Case 102, shown in meters. Positive values show increases relative to existing conditions and negative values show decreases.

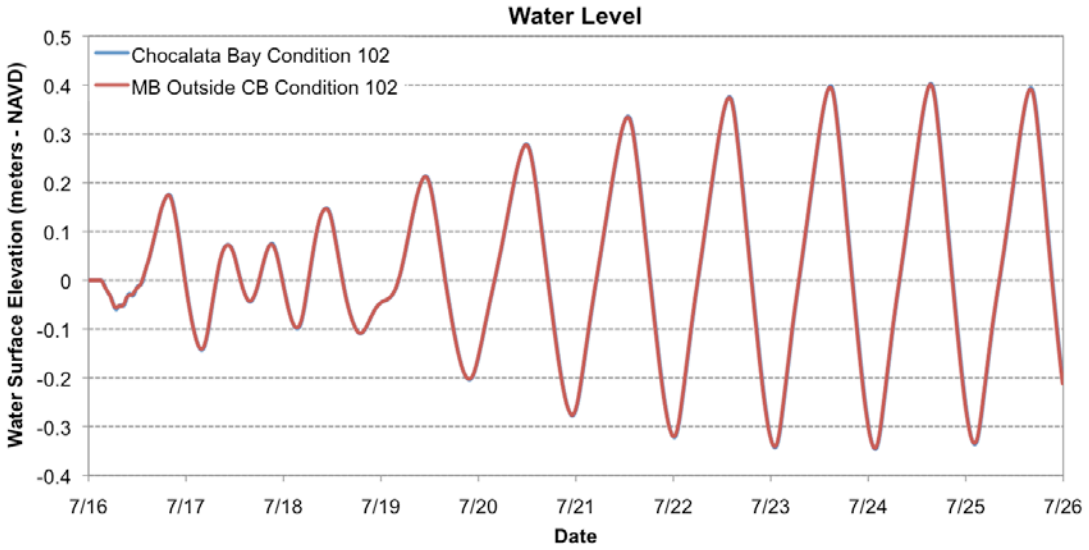

Figure 43. Comparison of predicted water level time series inside and outside of Choccolatta Bay for Case 102.

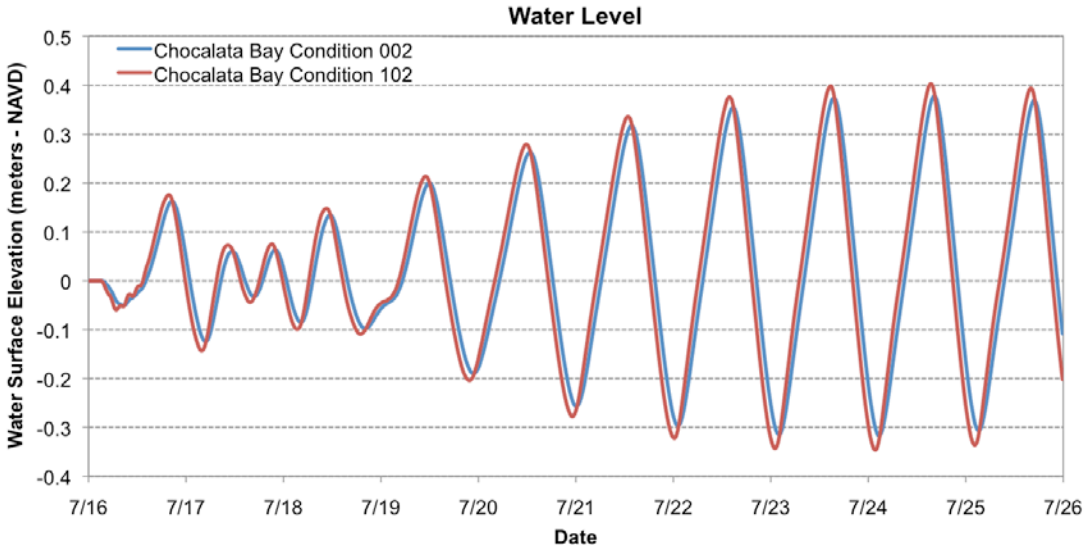

Figure 44. Comparison of water levels in Choccolatta Bay for Case 002 and Case 102.

Table 9. Tide range at selected locations for Case 102 and the corresponding change relative to Case 002.

Location	Tide Range (m)	% Change, 002
Choccolatta Bay	0.729	+8
North Mobile Bay	0.724	<+1
Justin's Bay	0.442	<+1
Ducker Bay	0.720	<+1
Shellbank River North	0.723	<+1
Shellbank River South	0.721	<+1

Flows

The constructed opening at Choccolatta Bay, "Pass Choccolatta," relieved head differences between Choccolatta Bay and surrounding water bodies, thereby reducing velocities through existing relief channels like I-10 Cut and Pass Picada. These decreases were substantial in magnitude (30 cm/s). There were increases in maximum velocity of a similar magnitude in "Pass Choccolatta," immediately south of the opening in Mobile Bay, and also in the lower portion of Conway Creek. These results are shown in Figure 45 as changes, positive or negative, relative to existing conditions.

The model results suggest that Choccolatta Bay would have a measurable subtidal velocity that would export water from the system. The results, shown in Figure 46, suggest that there would be an increase in subtidal flow to the south through "Pass Choccolatta," an increase in subtidal inflow through Pass Picada, and a decrease in subtidal inflow through I-10 Cut.

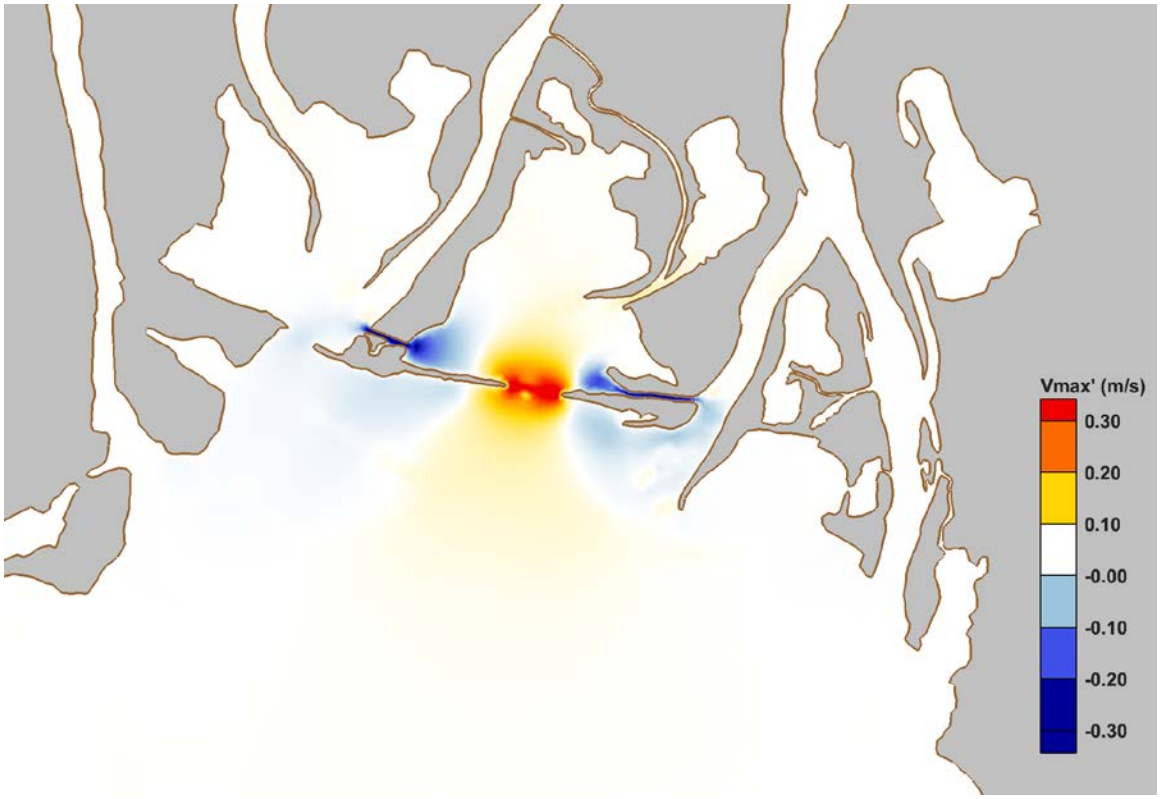

Figure 45. Change in maximum depth-averaged velocity between Case 102 and Case 002.

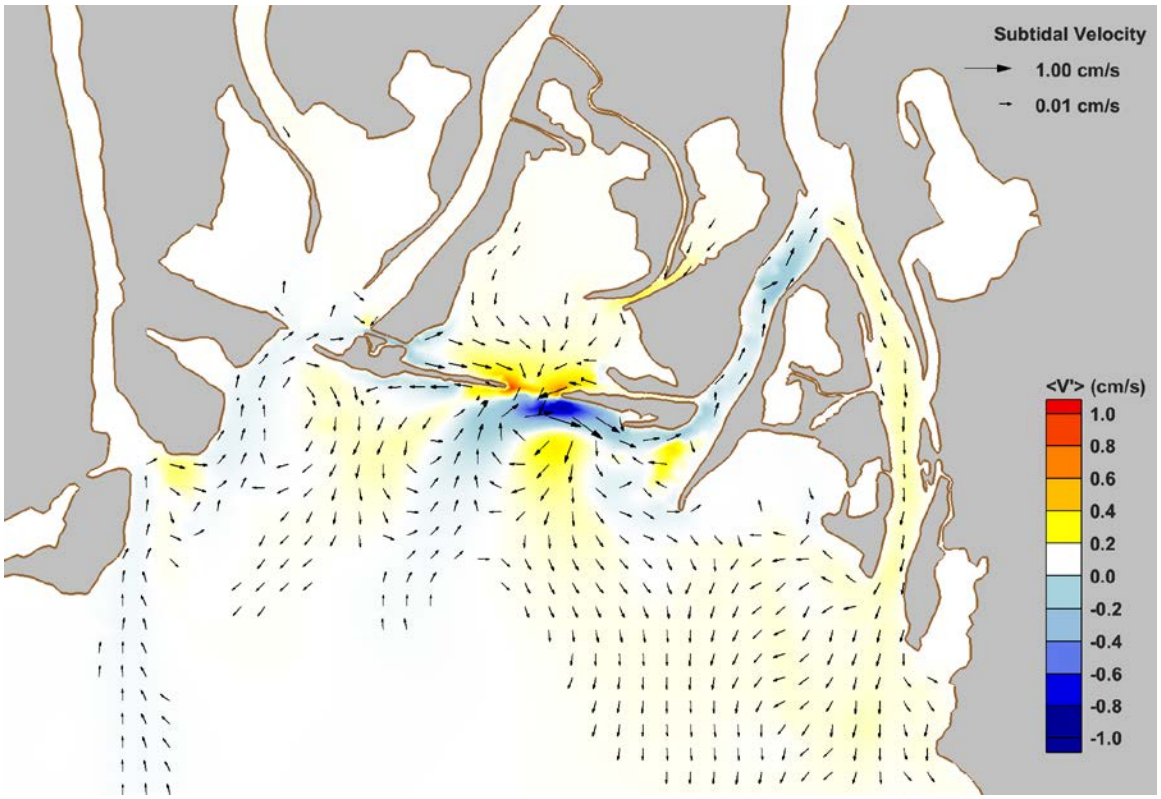

Figure 46. Change in subtidal velocity between Case 102 and Case 002.

Changes in the predicted velocities through each of Choccolatta Bay's connections produced substantial changes in volume discharge through those openings. For example, the effects of the new constructed opening on discharge through I-10 Cut and Pass Picada are shown in Figure 47 and Figure 48, respectively. Ignoring the first day of the time-series, which has oscillations attributed to model spinup, the discharge through each opening decreased by an order of magnitude when compared to existing conditions.

While the constructed opening had no effect on tidal exchange at Justin's Bay, there was an 82.1% increase in the volume of water exchanged for Choccolatta Bay relative to existing conditions. The model predicted 90% reductions in tidal exchange through I-10 Cut and Pass Picada, and a more than 8000% increase in tidal exchange through "Pass Choccolatta," as compared to the culverts. The tidal exchange volumes associated with the maximum flood tide range for Case 102 are summarized in Table 10.

The substantial reductions in tidal exchange in I-10 Cut and Pass Picada could lead to changes in water quality over time. The extent to which water characteristics might change in these areas could be considered in future studies.

In terms of the percentage of total volume of water exchanged in the system, "Pass Choccolatta" was responsible for 84% of tidal exchange, with the I-10 Cut and Pass Picada exchanging only 1.4% and 2.6% of the total volume, respectively. This distribution is shown graphically in Figure 49.

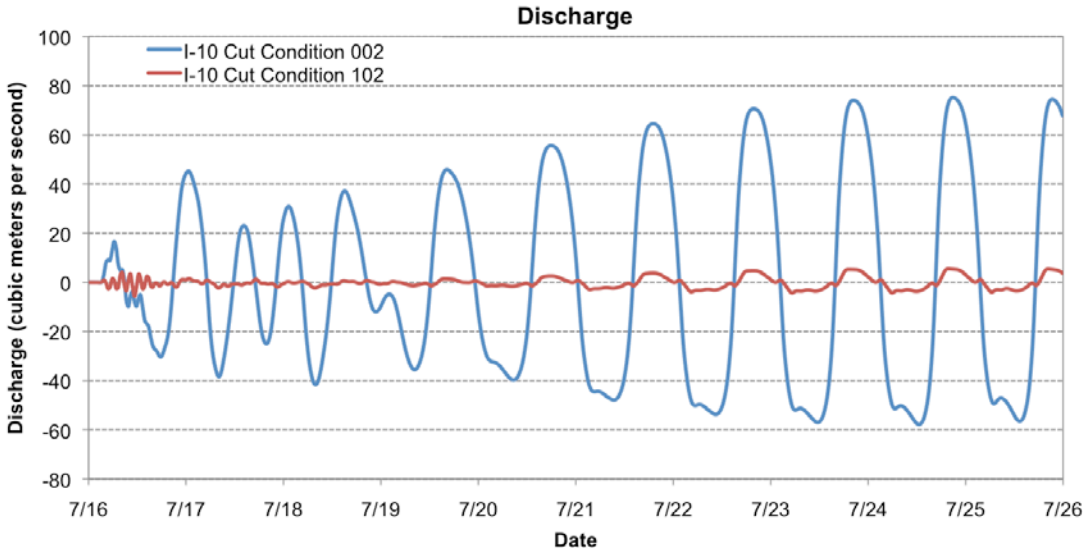

Figure 47. Time-series of discharge through I-10 Cut for Case 102 and Case 002.

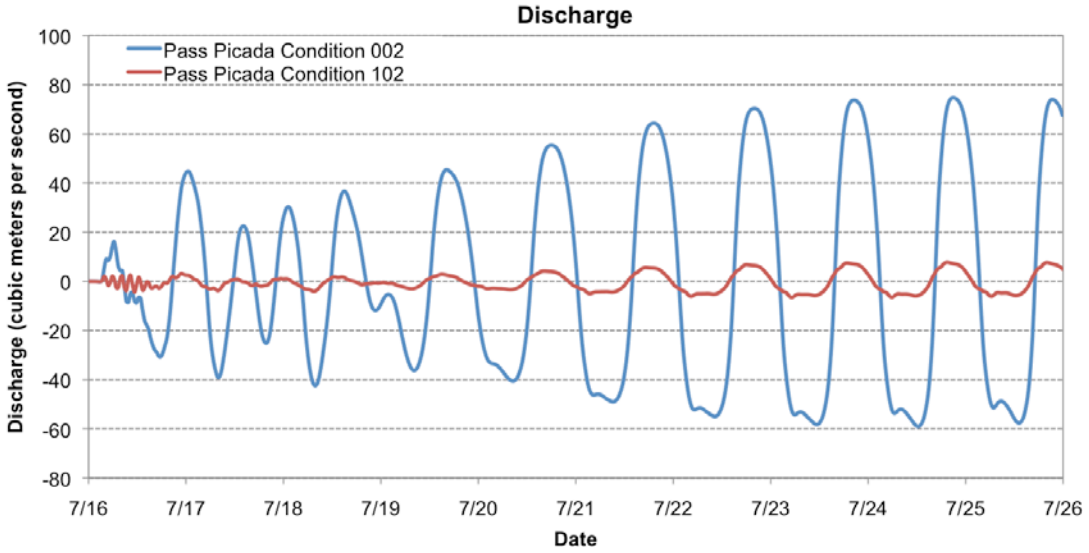

Figure 48. Time-series of discharge through Pass Picada for Case 102 and Case 002.

Table 10. Maximum tidal volume exchanged (in cubic meters) between successive low and high water on a flooding tide for Case 102, and the percent change relative to existing conditions (Case 002).

Location		Tidal Volume Exchange (m^3)	% Change, 002
Choccolatta Bay	I-10 Cut	121,073 (in)	-94.5
	Little Creek	11,770 (out)	+79.9
	Conway Creek	996,890 (out)	+7.5
	"Pass Choccolatta"	7,269,809 (in)	+8394.1
	Pass Picada	221,881 (in)	-90.2
	Total (net)	**6,604,103 (in)**	**+82.1**
Justin's Bay	Sardine Pass	413,050 (in)	<+1

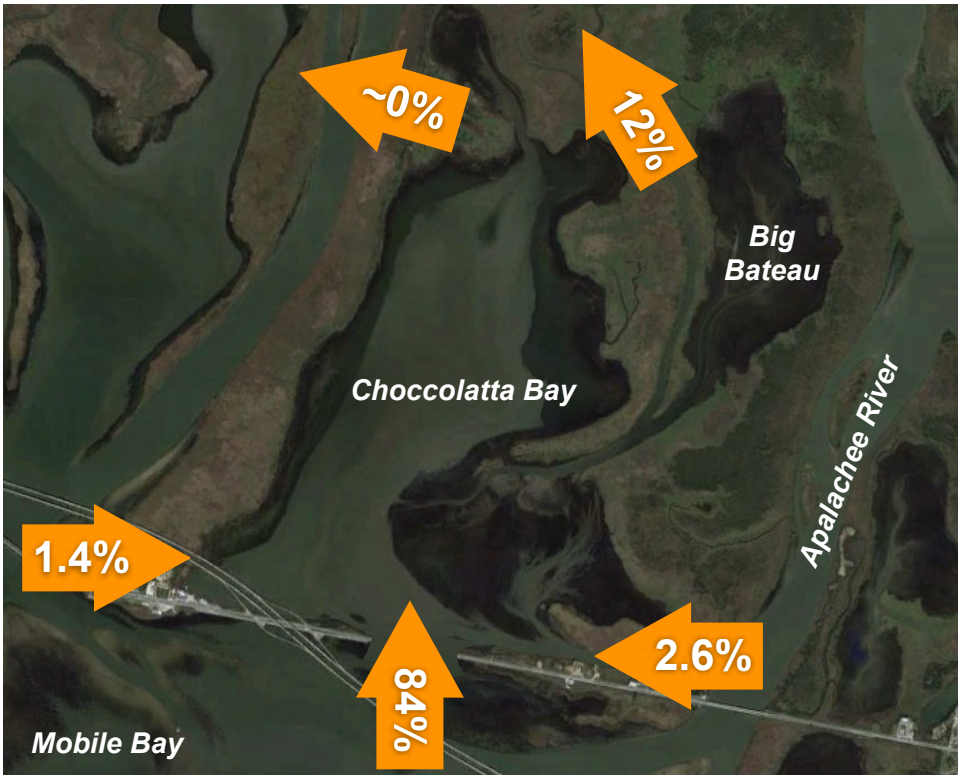

Figure 49. Distribution and directions of tidal exchange volumes, expressed as percentages of the total volume, for Choccolatta Bay in the modified scenario.

Sediment Transport Potential

Predicted changes in velocity for the constructed opening result in decreased sediment transport through I-10 Cut and Pass Picada, with increased sediment transport likely in lower Conway Creek and "Pass Choccolatta." The magnitude of the changes is generally 25% to 50%, positive and negative, relative to sediment transport under existing conditions. As in previous comparisons, positive values indicate increases relative to existing conditions while negative values indicate decreases relative to existing conditions. These potential changes in sediment transport characteristics, including bedload transport, resuspension rates, and depositional patterns, are presented in Figure 50, Figure 51, and Figure 52, respectively.

The decreased velocities and tidal exchange through I-10 Cut and Pass Picada increased the potential for sediment deposition in those areas. Areas in and near "Pass Choccolatta," as well as in the upper portions of Choccolatta Bay, showed a tendency of becoming less depositional in this scenario. The potential changes in depositional areas and patterns are shown in Figure 52. Here, a value of +1.0 indicates an area that becomes depositional as a result of the modification; a value of 0.0 indicates no change in depositional patterns between the scenarios; and a value of -1.0 indicates that an area that was depositional under existing conditions is no longer.

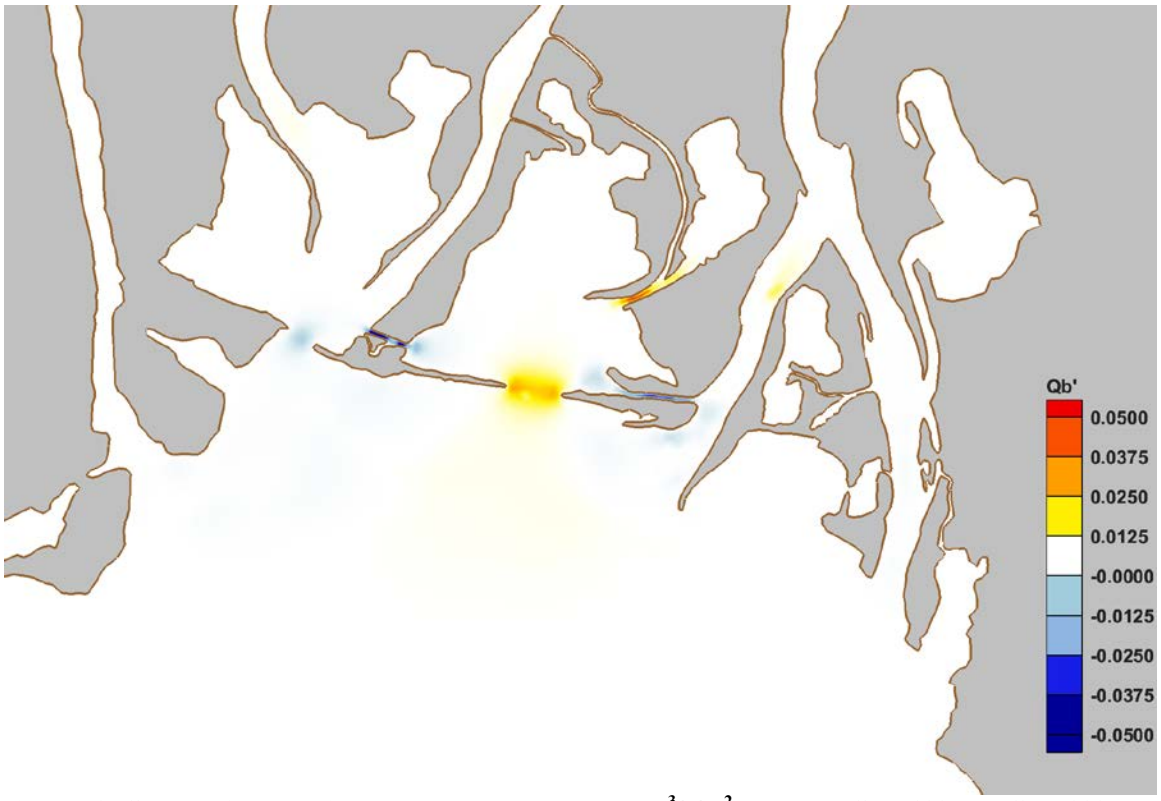

Figure 50. Changes in potential bedload transport rates ($m^3/s/m^2$) between Case 102 and Case 002.

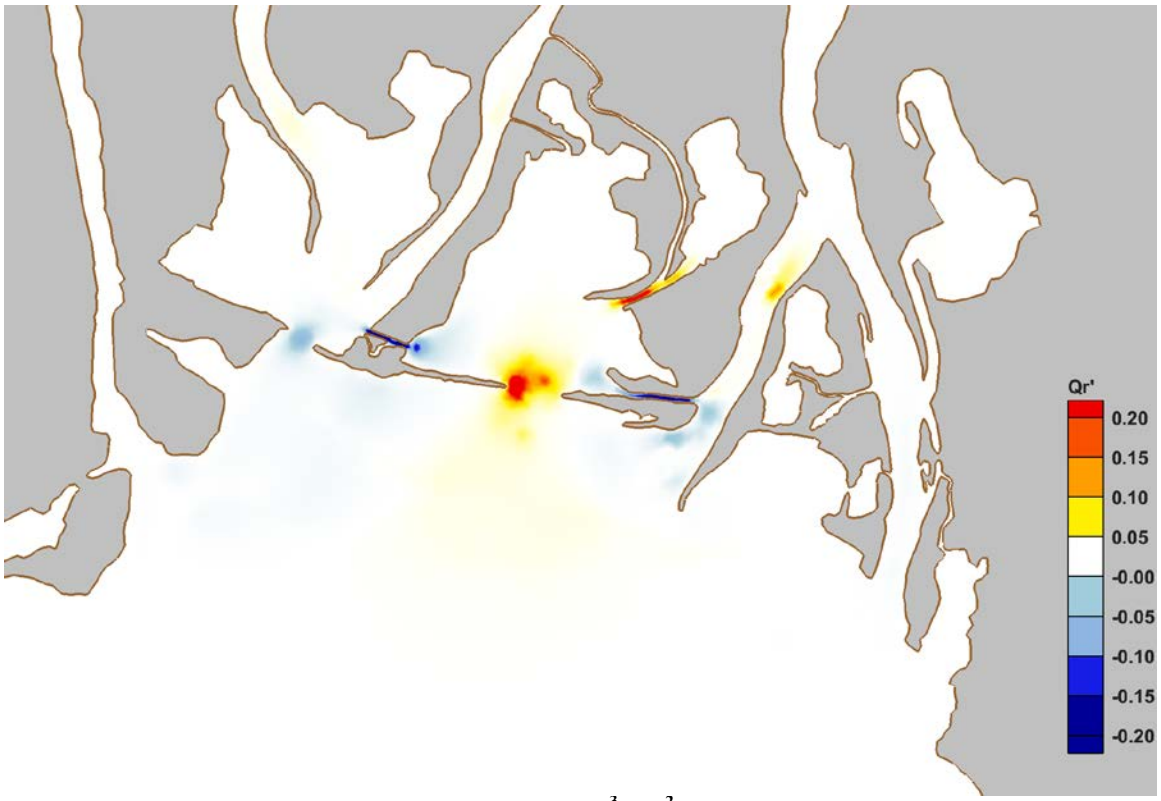

Figure 51. Changes in potential resuspension rates ($m^3/s/m^2$) between Case 102 and Case 002.

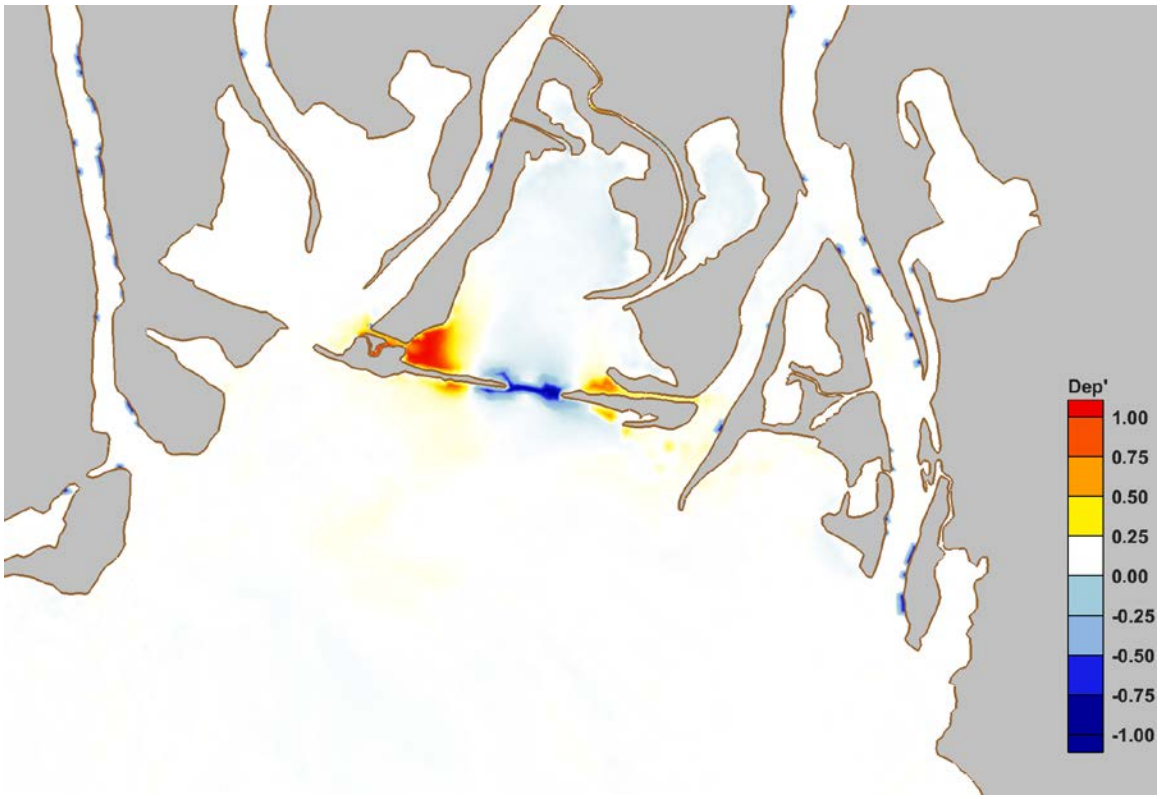

Figure 52. Changes in potential sediment deposition patterns (+1.0, more deposition; 0.0 no change; -1.0 no longer depositional).

Flushing

Increases in particle residence time were predicted near I-10 Cut and Pass Picada, whereas a decrease in residence time by more than 3 days extended far into Choccolatta Bay from the constructed opening. Therefore, some areas of the system saw improved flushing while other areas experienced decreased flushing. The potential effects of a constructed opening for Choccolatta Bay on its flushing characteristics are shown in Figure 53. The changes in residence time are presented as the difference between Case 102 and Case 002 ($Tr' = Tr_{102} - Tr_{002}$).

The simulation of "Pass Choccolatta" improved flushing of particles from the system by nearly 10% compared to existing conditions. Approximately 97% of the particles escaped through "Pass Choccolatta," with no particles exiting through I-10 Cut or Pass Picada. The system-wide averages for residence and exposure time, as well as the percent of particles removed from the system, are listed in Table 11. While the changes are modest, reductions in residence and exposure time are evident as is the increased number of particles removed from the system.

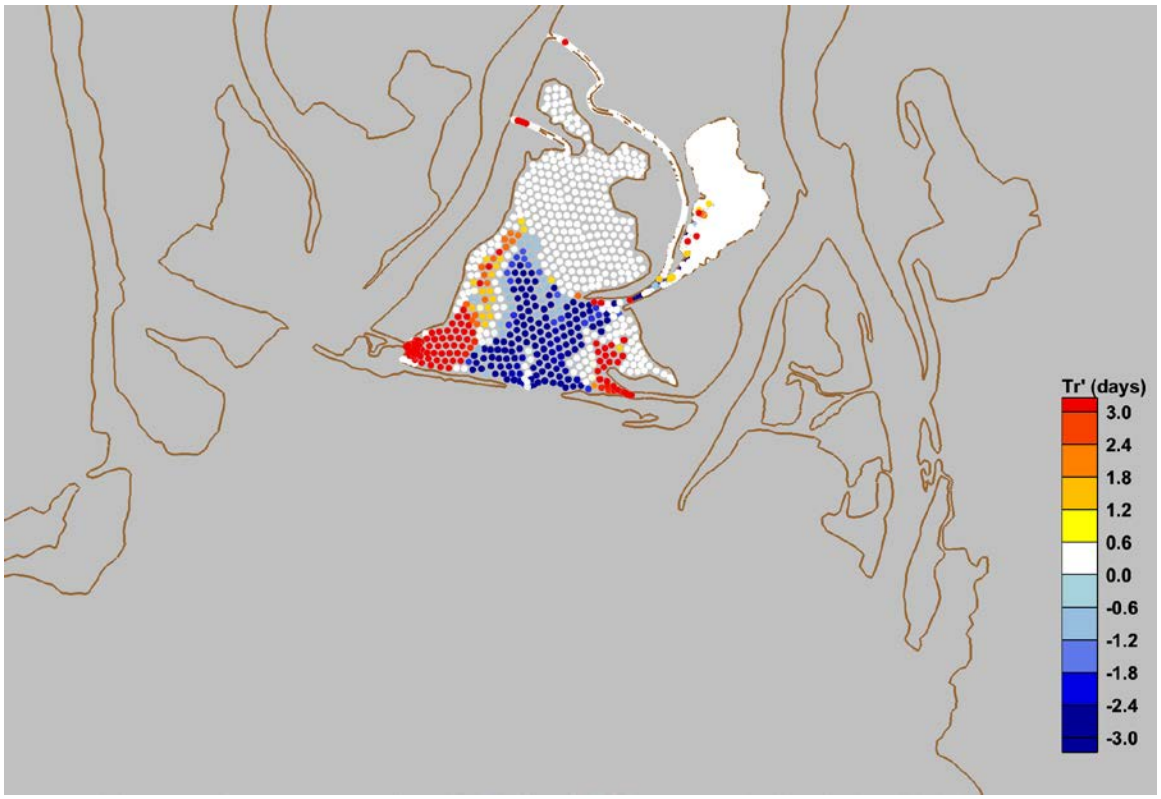

Figure 53. Change in particle residence time (Tr') as a function of initial position for Case 102.

Table 11. Changes in average residence and exposure times, and percentage of particles removed, for Case 102.

Location	Avg. Residence Time (days)		Avg. Exposure Time (days)		% Particles Removed	
	Case 002	Case 102	Case 002	Case 102	Case 002	Case 102
Choccolatta Bay	7.9	7.8	8.4	8.3	20.2	21.6
Justin's Bay	8.4	N/A	8.6	N/A	7.1	N/A

Justin's Bay - Case 202

This alternative restoration scenario considers a hypothetical opening, "Pass Justin," through the Causeway at Justin's Bay only. The forcing conditions consist of representative tides and average summer river discharge under present day sea levels. Simulation results for Case 202 are presented as differences relative to existing conditions (Case 002).

Water Levels

The constructed opening of "Pass Justin" resulted in a more than 10 cm increase in maximum water levels within Justin's Bay, and an increase of approximately 5 cm in Sardine Pass. Model predictions revealed negligible changes in maximum water levels elsewhere in the study area. These changes are shown in Figure 54.

The model predicted a 63.7% increase in the tide range of Justin's Bay while completely removing the exiting three-hour tidal phase lag with Mobile Bay (Figure 55). The opening did not have a measurable

effect on tide range elsewhere in the system. A comparison of water levels in time under existing and modified conditions for Justin's Bay is shown in Figure 56, and a summary of tide ranges is listed in Table 12.

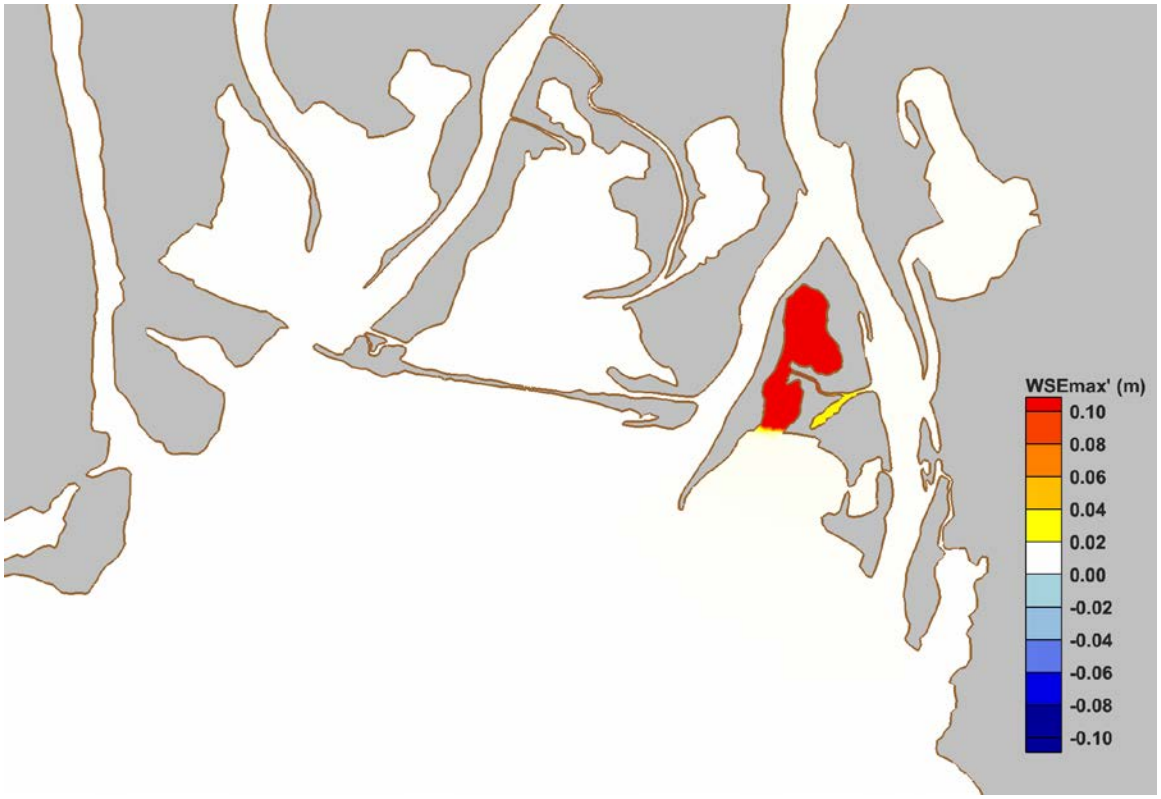

Figure 54. Changes in maximum predicted water levels (WSEmax') between Case 202 and Case 002.

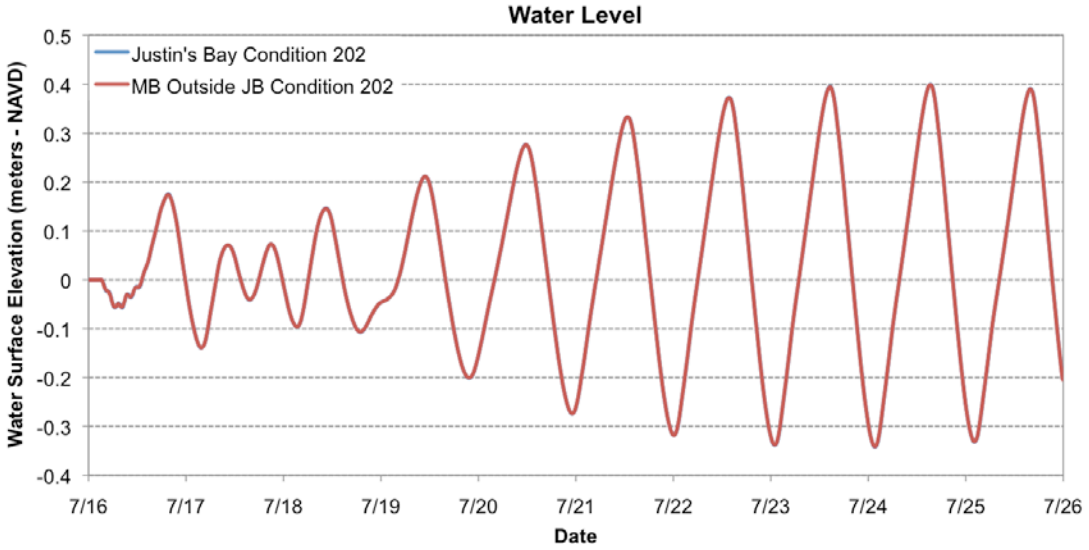

Figure 55. Comparison of predicted water levels in Justin's Bay and a point in John's Bend for Case 202.

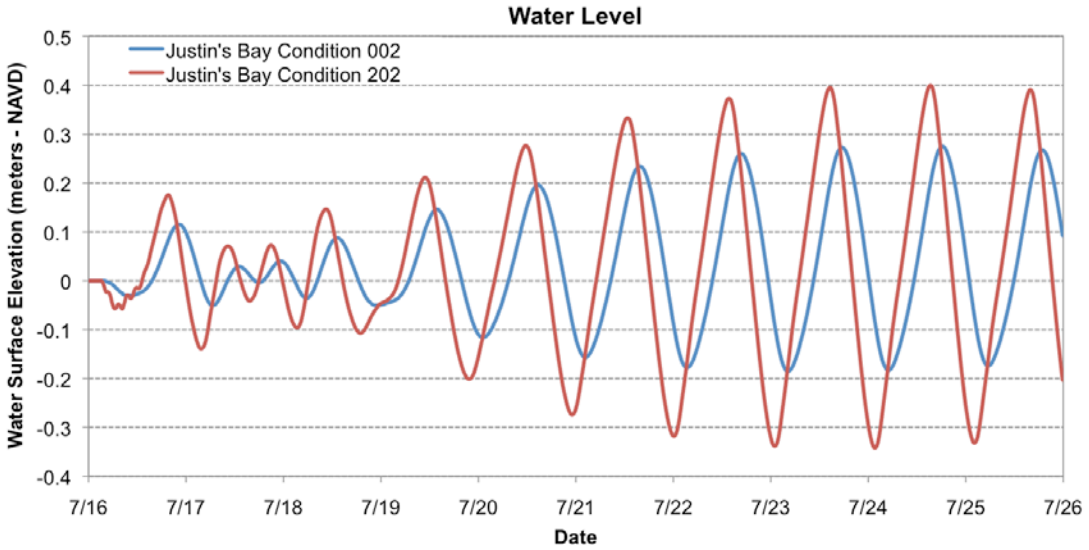

Figure 56. Time-series of water levels in Justin's Bay for Case 202 and Case 002.

Table 12. Maximum tide ranges for Case 202 and changes relative to existing conditions in the study area.

Location	Tide Range (m)	% Change, 002
Choccolatta Bay	0.676	<+1
North Mobile Bay	0.720	NC
Justin's Bay	0.722	+63.7
Ducker Bay	0.720	<+1
Shellbank River North	0.723	<+1
Shellbank River South	0.721	<+1

Flows

The predicted change in maximum depth-averaged water velocity relative to existing conditions is shown in Figure 57. The model predicted an increase in maximum velocity on the order of 10 to 15 cm/s throughout much of Justin's Bay, with increases on the order of 5 to 10 cm/s in Ducker Bay and John's Bend. A substantial decrease in maximum velocity through Duck Skiff Pass and Sardine Pass was also predicted and is attributed to decreased hydraulic efficiency due to the constructed opening.

The model predicted an increase in subtidal flow to the west in Sardine and Duck Skiff Pass, and increased subtidal flow to the south in Justin's Bay. Modest changes were also evident in the lower Apalachee and Blakeley Rivers. The magnitude of predicted subtidal velocity differences were on the order of ±1 cm/s and extended beyond Justin's Bay. Changes in subtidal velocity, relative to existing conditions, are shown in Figure 58 for the constructed opening at Justin's Bay.

While a goal of the constructed opening for Justin's Bay is to increase tidal communication with Mobile Bay, model results indicate that other portions of the existing system may be impacted. For example, consider the time-series of discharge through Sardine Pass under existing and modified conditions

shown in Figure 59. Under existing conditions Sardine Pass experienced a balanced discharge of ±15 m^3/s, whereas under modified conditions the discharge magnitude decreased to ~2 m^3/s and was directed into the system on average.

When compared to the volume exchanges under existing conditions (Case 002), the total volume exchange between Justin's Bay and adjacent water bodies increased by over 122% in spite of a more than 87% reduction in tidal volume exchange through Sardine Pass. As in the existing channels of Choccolatta Bay, the substantial reductions in tidal exchange and water velocities through Sardine Pass could affect water quality over time. This should be considered in future studies.

The effect of "Pass Justin" on volume exchange elsewhere in the study area was calculated as much less than 1%. The volume exchange through Pass Justin and Sardine Pass, as well as elsewhere in the system, is summarized in Table 13. As in previous comparisons, the volume exchange was computed as the cumulative discharge through an existing or proposed opening between successive low and high water stages for the maximum flood tide.

In terms of the total volume of water exchanged, "Pass Justin" was responsible for 94% of the tidal exchange with Sardine Pass contributing only 6% of the exchange volume. A graphical representation of this tidal exchange distribution is shown in Figure 60.

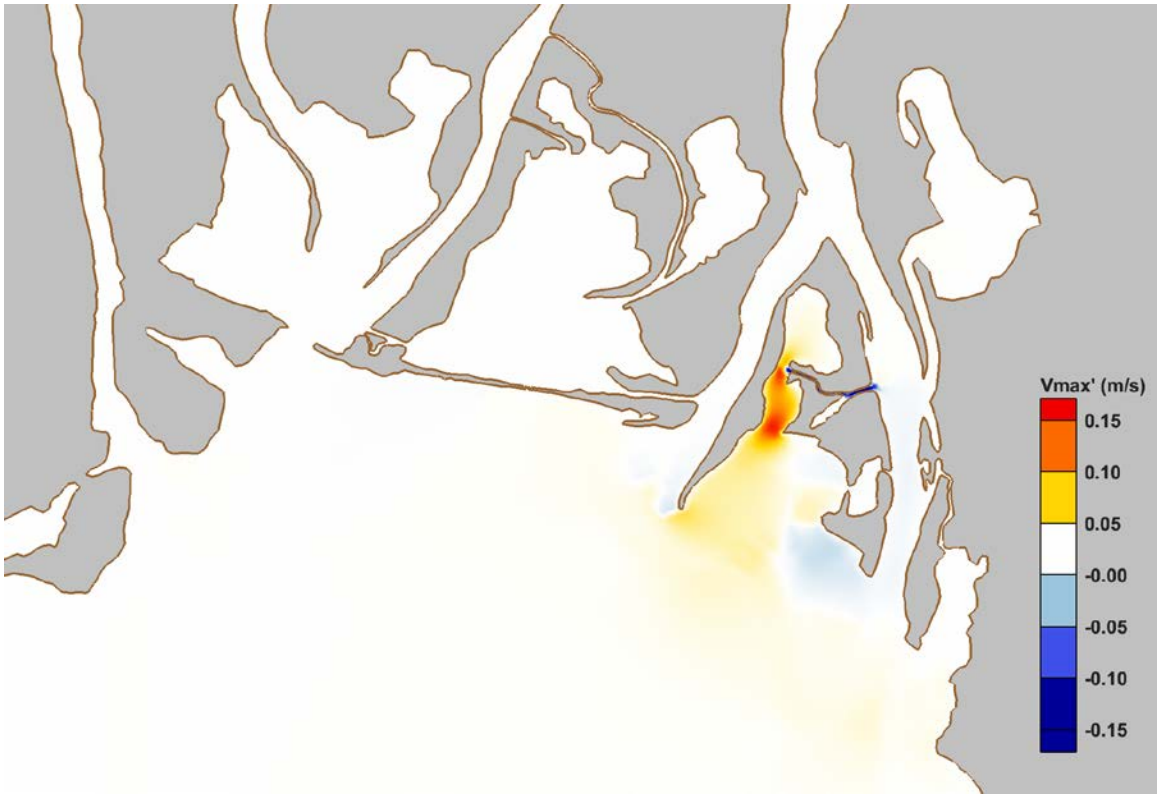

Figure 57. Predicted change in maximum depth-averaged velocity (Vmax') between Case 202 and Case 002.

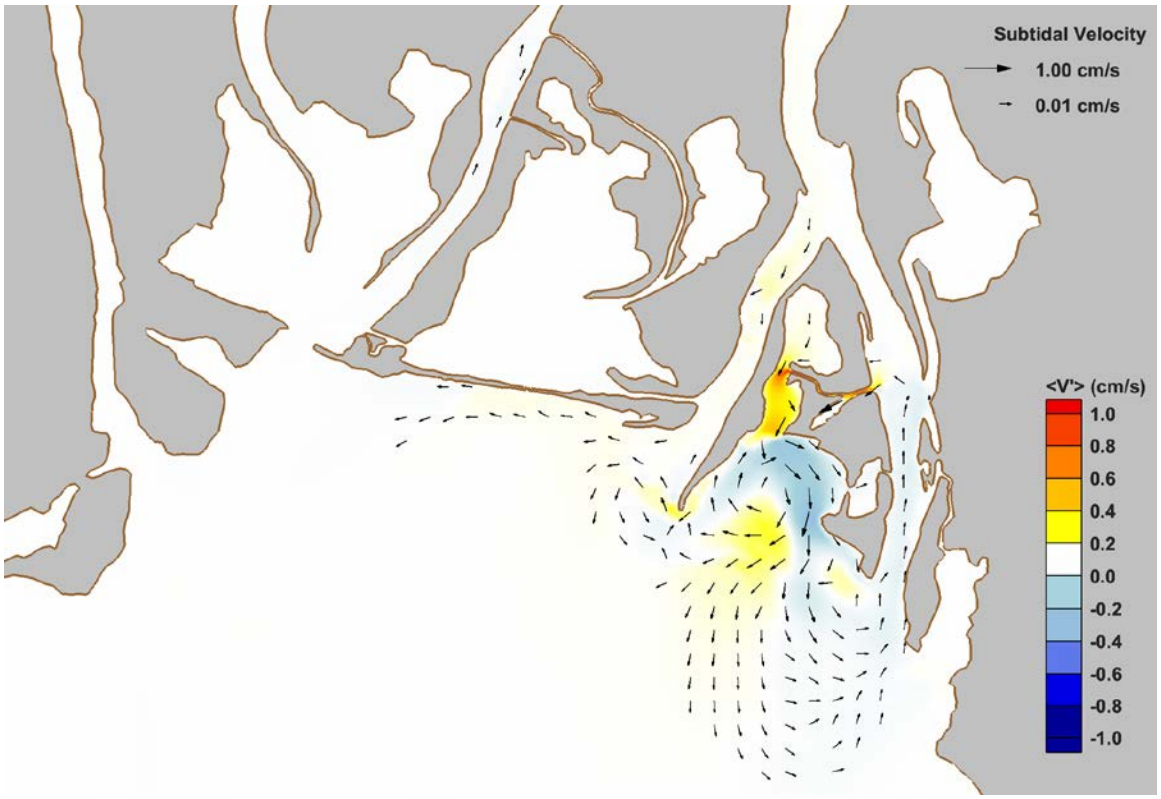

Figure 58. Predicted change in subtidal velocity (<V'>) between Case 202 and Case 002.

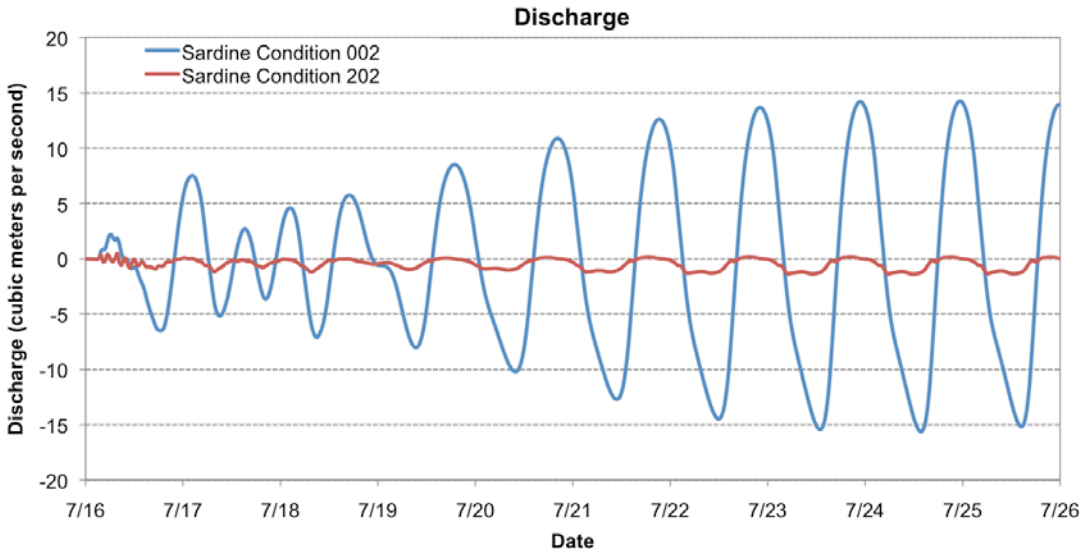

Figure 59. Time-series discharge through Sardine Pass for Case 202 and Case 002.

Table 13. Maximum tidal volume exchanged (in cubic meters) between successive low and high water on a flooding tide for Case 202, and the percent change relative to existing conditions (Case 002).

Location		Tidal Volume Exchange (m^3)	% Change, 002
Choccolatta Bay	I-10 Cut	2,218,129 (in)	<+1
	Little Creek	6,696 (out)	+2.3
	Conway Creek	946,084 (out)	+2
	Culverts	86,418 (in)	+1
	Pass Picada	2,281,426 (in)	<+1
	Total (net)	**3,633,194 (in)**	**<<+1**
Justin's Bay	Sardine Pass	52,063 (in)	-87.4
	"Pass Justin"	862,391 (in)	N/A
	Total (net)	**914,454 (in)**	**+122.1**

Figure 60. Distribution and direction of tidal exchange volumes in Justin's Bay for Case 202, expressed as percentages of the total volume of water exchanged.

Sediment Transport Potential

Changes in potential transport rates correspond to predicted changes of velocity increase and/or decrease throughout the system. For example, predicted increases in velocity throughout Justin's Bay yielded higher transport rates in those areas, whereas decreased velocity in Duck Skiff and Sardine Pass resulted in reductions in transport rates in those water bodies. The magnitude of bedload transport and resuspension rate changes, relative to existing conditions, was on the order of 5% and 25%, respectively.

The predicted changes in potential bedload transport and resuspension rates, relative to rates under existing conditions, are shown in Figure 61 and Figure 62, respectively.

As a result of "Pass Justin," most of Justin's Bay was predicted to become less depositional, whereas increased deposition was predicted to occur in Sardine Pass and some isolated portions of Ducker Bay. Predicted changes in sediment deposition patterns are shown in Figure 63.

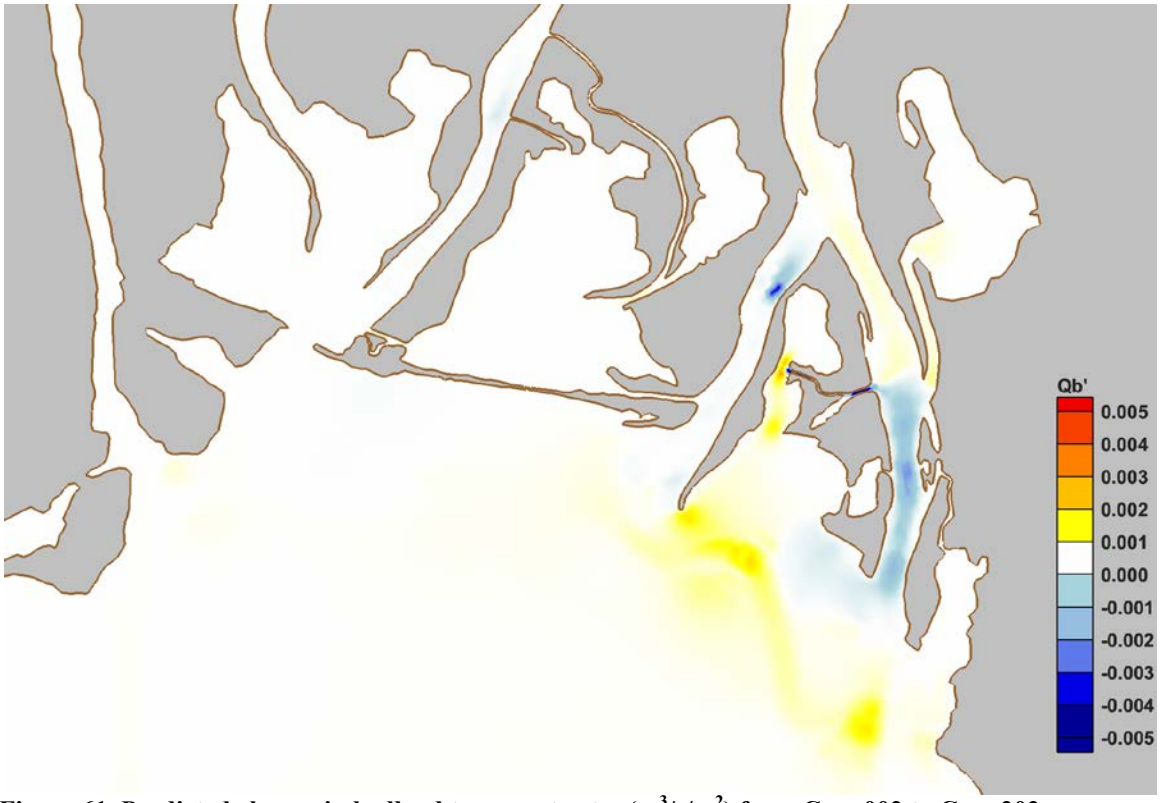

Figure 61. Predicted change in bedload transport rates ($m^3/s/m^2$) from Case 002 to Case 202.

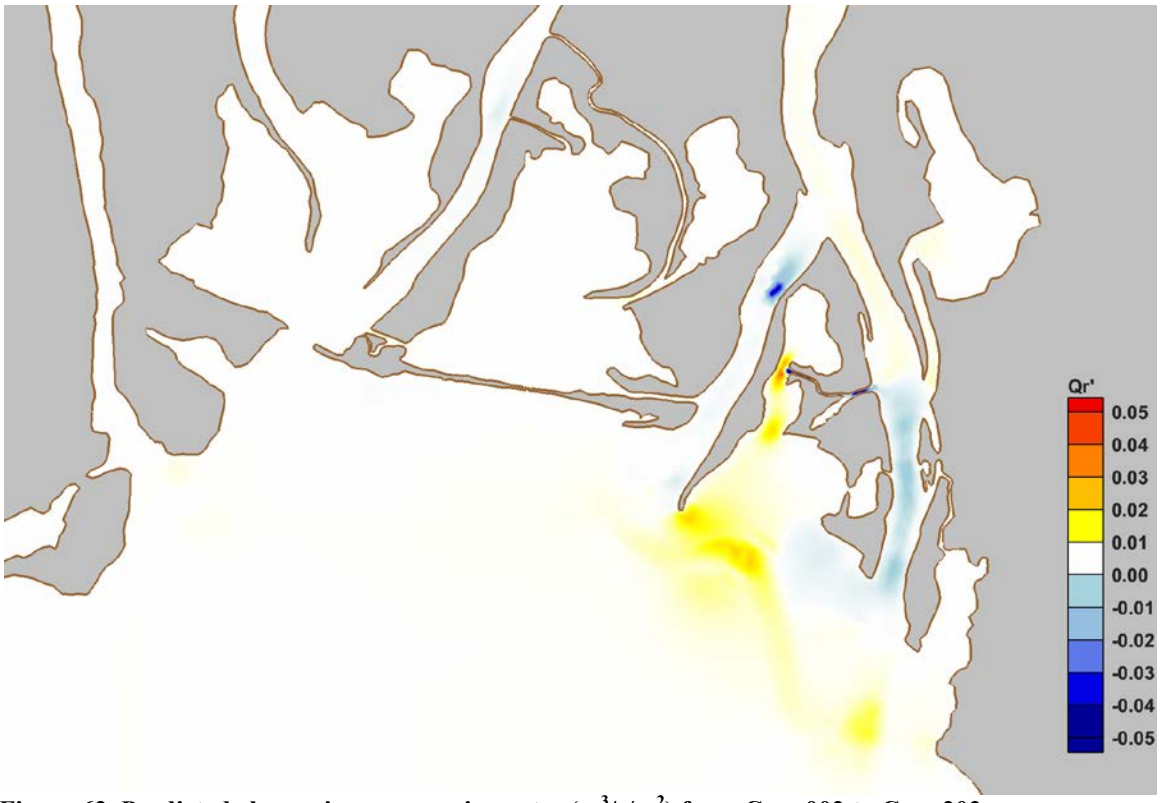

Figure 62. Predicted change in resuspension rates ($m^3/s/m^2$) from Case 002 to Case 202.

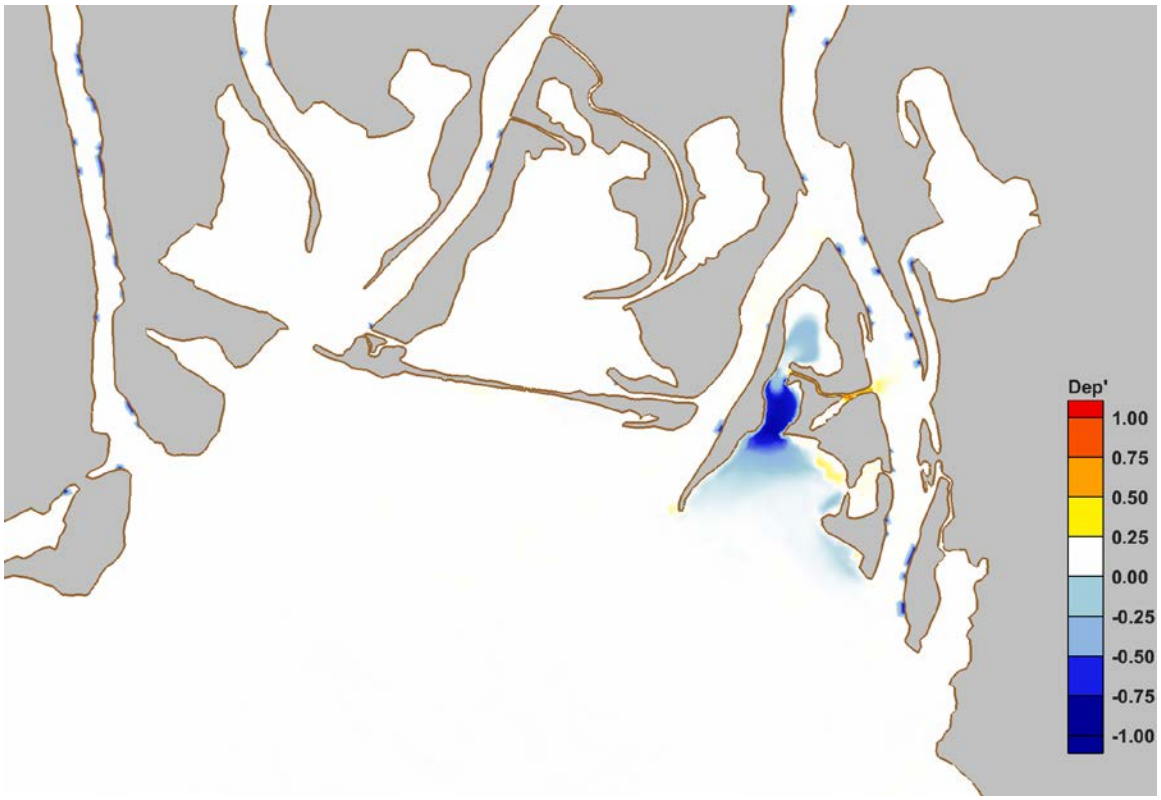

Figure 63. Potential change in sediment depositional areas from Case 002 to Case 202, where 1.0 indicates new deposition, 0.0 indicates no change, and -1.0 indicates the area is no longer depositional.

Flushing

The LPTM analysis predicted a substantial reduction in residence times throughout much of Justin's Bay, but a substantial increase in residence times for particles in Sardine Pass. On average, residence and exposure times were predicted to decrease by 15% and the total number of particles removed from the system increased from 7.1% to 35.6%. That is a 500-fold increase in the number of particles flushed from the Justin's Bay system. The predicted effects of "Pass Justin," on the flushing characteristics of Justin's Bay and Sardine Pass are shown in Figure 64 and are summarized in Table 14.

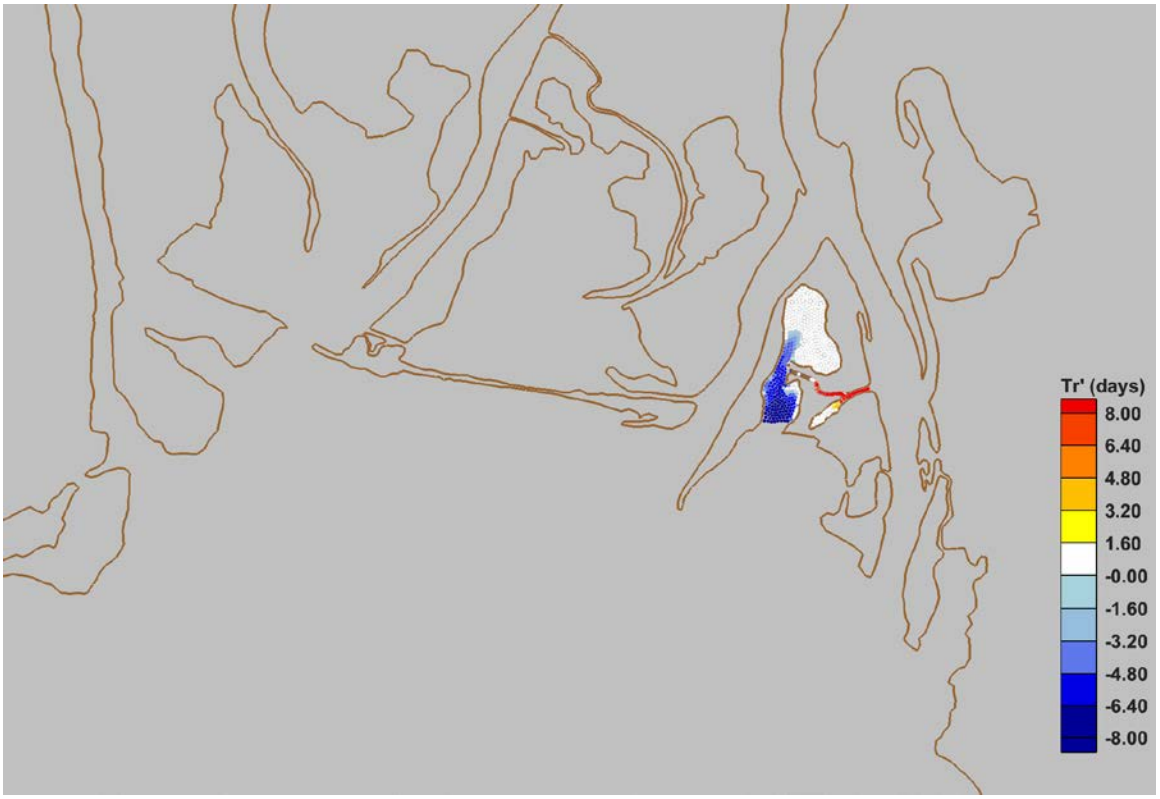

Figure 64. Predicted change in residence time (Tr') from Case 002 to Case 202 as a function of particle initial position.

Table 14. Changes in average residence and exposure times, and percentage of particles removed, for Case 202.

Location	Avg. Residence Time (days)		Avg. Exposure Time (days)		% Particles Removed	
	Case 002	Case 202	Case 002	Case 202	Case 002	Case 202
Choccolatta Bay	7.9	N/A	8.4	N/A	20.2	N/A
Justin's Bay	8.4	6.8	8.6	7.4	7.1	35.6

Shellbank River - Case 302

This alternative restoration scenario considers a hypothetical opening, "Shellbank Cut," through the Causeway at Shellbank River only. The forcing conditions consist of representative tides and average

summer river discharge under present day sea levels. Simulation results for Case 302 are presented as differences relative to existing conditions (Case 002).

Water Levels

The model predicted a very small, and very local, increase in maximum water levels (<1 cm) below "Shellbank Cut." The predicted changes are limited to areas south of the Causeway in Shellbank River and also the tidal creek connecting to D'Olive Bay. These results are shown in Figure 65. The constructed opening at Shellbank River had a negligible effect on tide ranges elsewhere in the study area, as shown in Table 15.

Figure 65. Predicted change in maximum water elevation (WSEmax') from Case 002 to Case 302.

Table 15. Maximum tide ranges for Case 302 and relative changes from Case 002.

Location	Tide Range (m)	% Change, 002
Choccolatta Bay	0.675	NC
North Mobile Bay	0.720	NC
Justin's Bay	0.441	NC
Ducker Bay	0.718	NC
Shellbank River North	0.721	NC
Shellbank River South	0.720	<+1

Flows

Model predictions suggested an increase in maximum depth-averaged velocity, on the order of 4 to 8 cm/s, through Shellbank River as a result of the opening. Although difficult to see in the color scale, there are very minor changes to velocity in Sardine Pass and Duck Skiff Pass, which are discussed further below. The predicted changes in maximum depth-averaged velocity are shown in Figure 66.

The opening in Shellbank River may increase the subtidal flow to the south by 1 cm/s or more, with additional southward flow through the adjacent tidal creek and D'Olive Bay. These effects are demonstrated by Figure 67. The light blue colors and northward-pointing arrows in Blakeley River indicate a corresponding decrease in southward flow in that portion of the river. This reduction is due to Shellbank River acting as a supplemental flow path for Blakeley River flows.

The predicted discharge magnitude through Shellbank River was predicted to be ~1 m^3/s and was seaward directed on average. Due to river forcing, the model predicted very little northward flow in Shellbank River, but it did increase in magnitude as the tide range grew. A time-series comparison of discharge through Shellbank River under existing conditions (i.e., no flow) and with the proposed opening is shown in Figure 68.

As in other simulations, the volume exchanges for Choccolatta Bay and Justin's Bay were calculated as the cumulative discharge during successive low and high water events during the maximum flood tide. The results are provided in Table 16. The model predicts that an opening in Shellbank River would have a negligible (<<1% change from existing conditions) effect on volume exchange for Choccolatta Bay. However, the proposed opening would have a measurable, but small, effect on the volume exchange for Justin's Bay (~2% decrease from existing conditions). Therefore, an opening at Shellbank River may have a measurable and unintended impact on a separate water body of concern within the study area. This was not the case in the previous simulations where proposed openings at Choccolatta Bay and Justin's Bay were predicted to act in complete isolation, not having measurable impacts at other restoration sites.

Figure 66. Predicted change in maximum water velocity (Vmax') from Case 002 to Case 302.

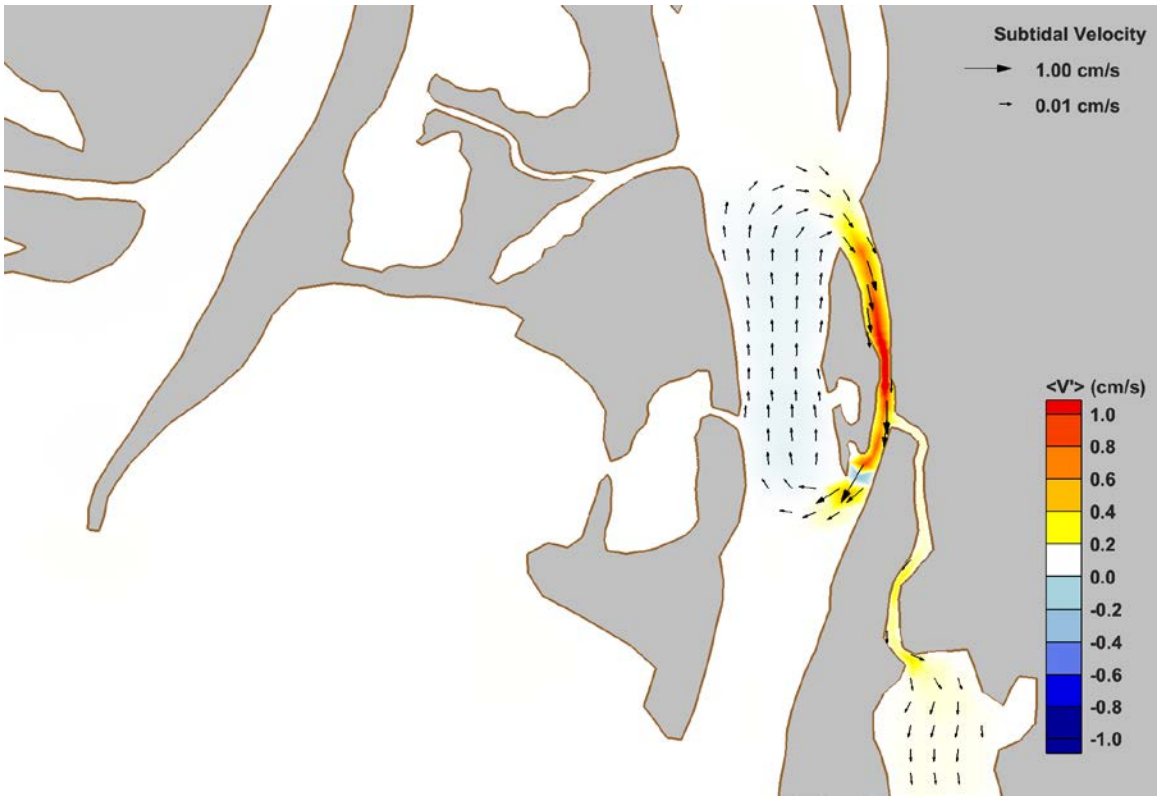

Figure 67. Predicted change in subtidal velocity (<V'>) from Case 002 to Case 302.

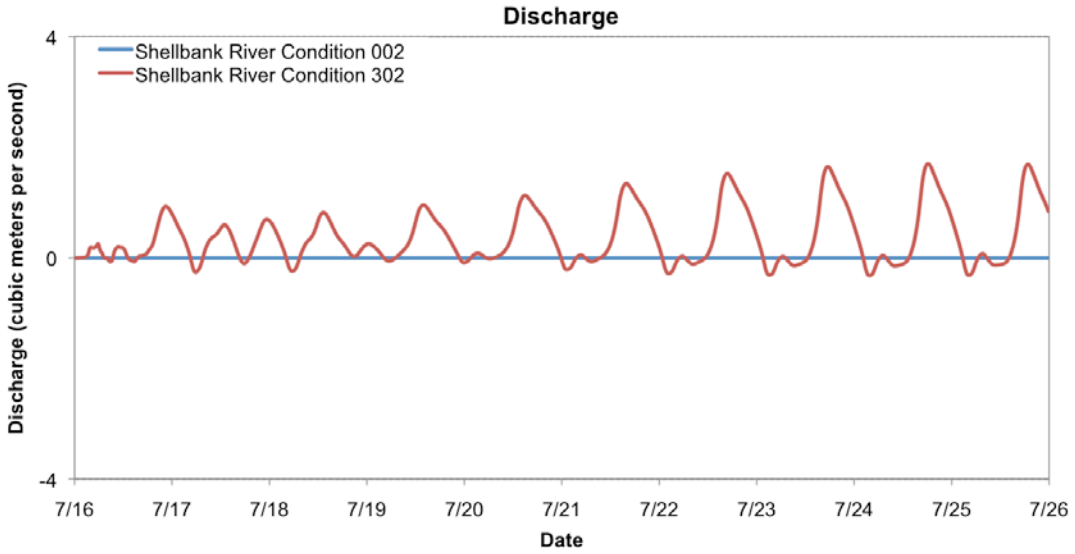

Figure 68. Time-series comparison of discharge through Shellbank River for Case 002 and Case 302.

Table 16. Maximum tidal volume exchanged (in cubic meters) between successive low and high water on a flooding tide for Case 302, and the percent change relative to existing conditions (Case 002).

Location		Tidal Volume Exchange (m^3)	% Change, 002
Choccolatta Bay	I-10 Cut	2,217,002 (in)	<+1
	Little Creek	6,696 (out)	+2.3
	Conway Creek	946,355 (out)	+2.1
	Culverts	86,398 (in)	+1
	Pass Picada	2,280,440 (in)	<+1
	Total (net)	**3,630,789 (in)**	**<<+1**
Justin's Bay	Sardine Pass	403,378 (in)	-2.1

Sediment Transport Potential

The opening of "Shellbank Cut" produced minor changes in sediment transport behavior. The potential change in bedload transport rates vary by less than 5%, with modest increases along Shellbank River and decreases along the Blakeley River immediately to the west. Predicted changes in resuspension rates varied from decreases of 1% along the Blakeley River to increases of <1% along Shellbank River and portions of lower Blakeley River. These potential changes in bedload sediment transport and resuspension rates are shown in Figure 69 and Figure 70, respectively, and are small relative to values under existing conditions. Note the compressed contour scale of these figures.

Predicted changes in sediment deposition potential are shown in Figure 71 for the proposed opening along Shellbank River. There was a slight increase in deposition potential at the northern confluence of Blakeley and Shellbank Rivers. Elsewhere in Shellbank River, the effect of the proposed opening would be to decrease sediment deposition in those areas, and some areas extending south into D'Olive Bay.

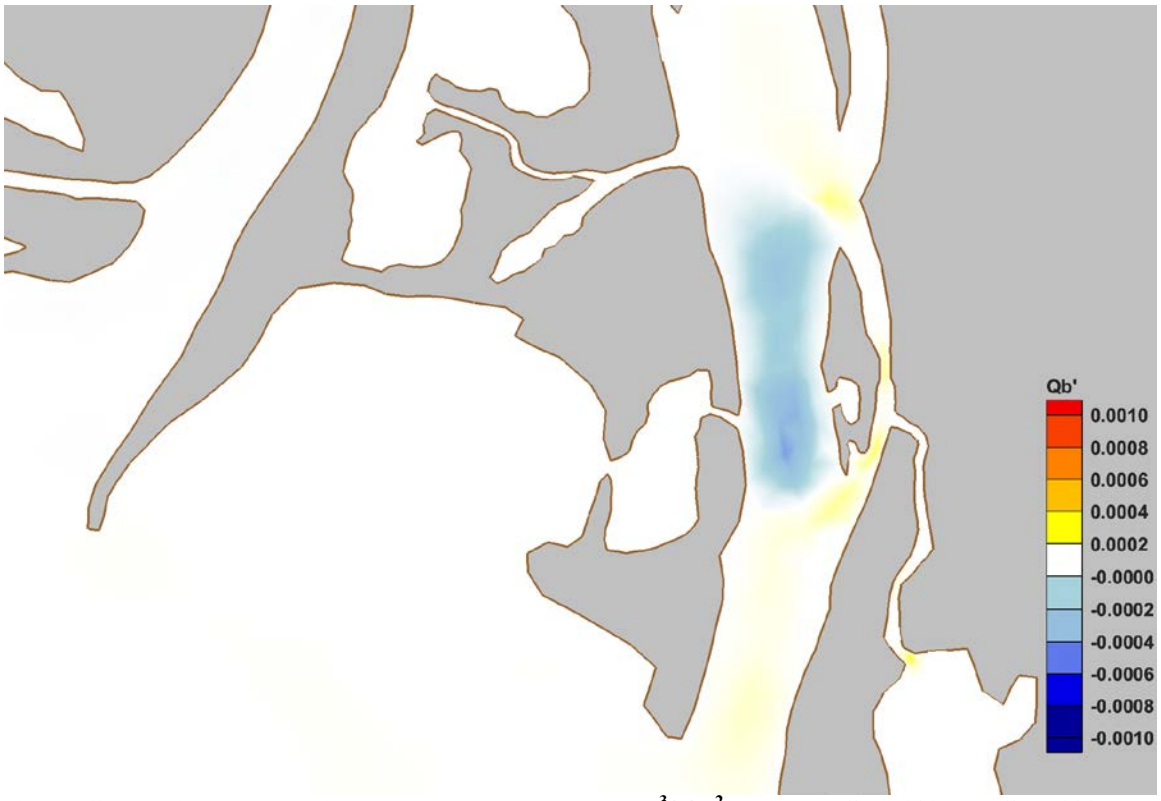

Figure 69. Predicted change in bedload transport rates ($m^3/s/m^2$) between Case 302 and Case 002.

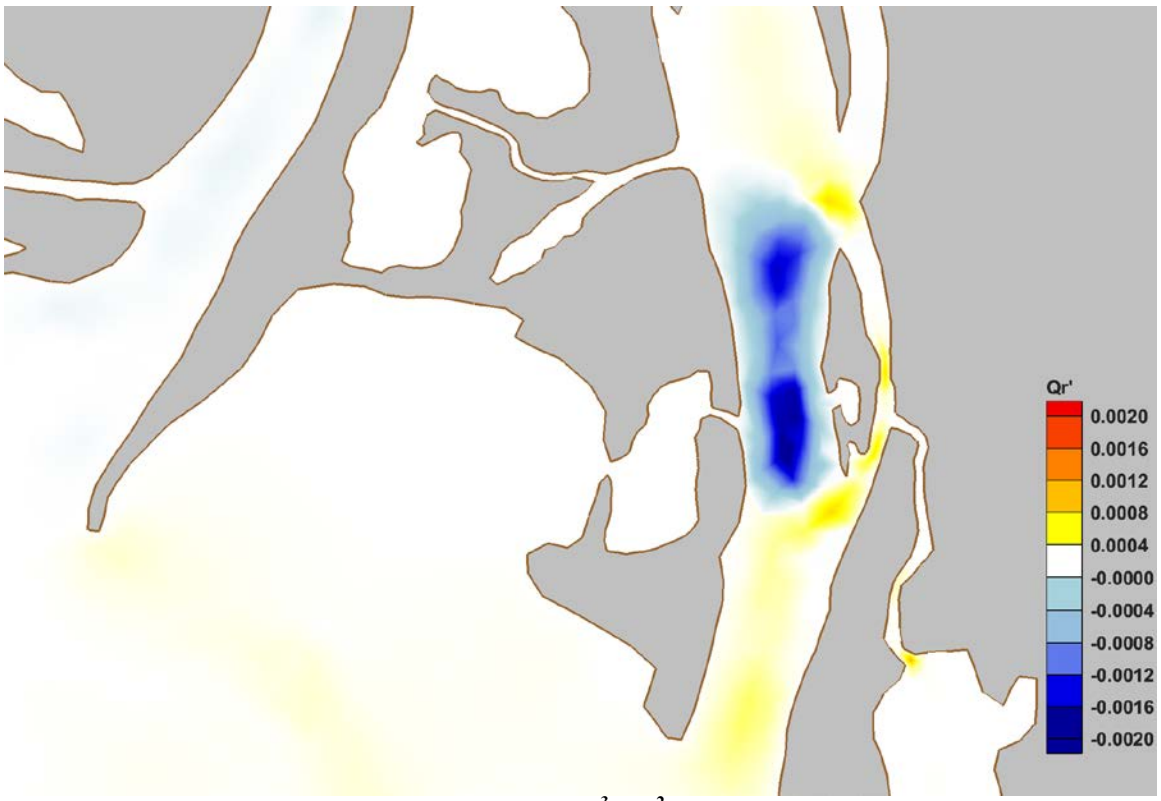

Figure 70. Predicted change in resuspension rates ($m^3/s/m^2$) from Case 002 to Case 302.

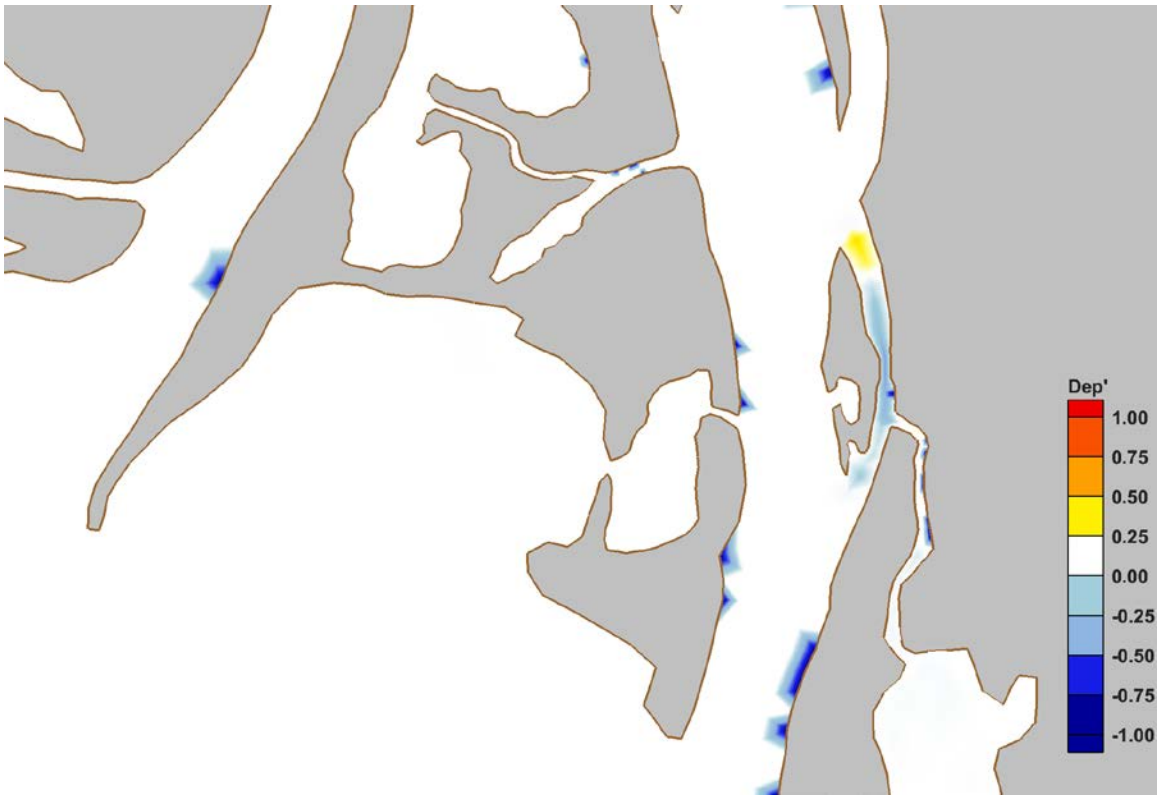

Figure 71. Potential changes in sediment depositional areas from Case 002 to Case 302. A value of +1.0 indicates an area that becomes depositional, a value of 0.0 indicates no change, and a value of -1.0 represents an area that is no longer depositional.

All Open - Case 402

This hypothetical restoration scenario considers all constructed openings through the Causeway acting simultaneously. The forcing conditions consist of representative tides and average summer river discharge under present day sea levels. Simulation results for Case 402 are presented as differences relative to existing conditions (Case 002).

Water Levels

The model predicted an increase in maximum water levels by 3 to 7 cm in Choccolatta Bay and Sardine Pass, while Justin's Bay exhibited increases of more than 10 cm. Changes in maximum water levels, relative to existing conditions (Case 002), were negligible elsewhere in the study area. These predictions are shown in Figure 72. The figure shows almost identical behavior between this case (all open simultaneously) and each case considered individually (see Figure 42, Figure 54, Figure 65).

Similar to Case 102, the tide range in Choccolatta Bay increased by 8% from existing conditions, while Justin's Bay experienced a nearly 64% increase in tide range. Changes to the tide range were negligible elsewhere in the study area. Tidal phase lags between Choccolatta Bay and Mobile Bay, and between Justin's Bay and Mobile Bay, were completed relieved by their constructed openings. Predicted maximum tide ranges at locations throughout the study area are listed in Table 17.

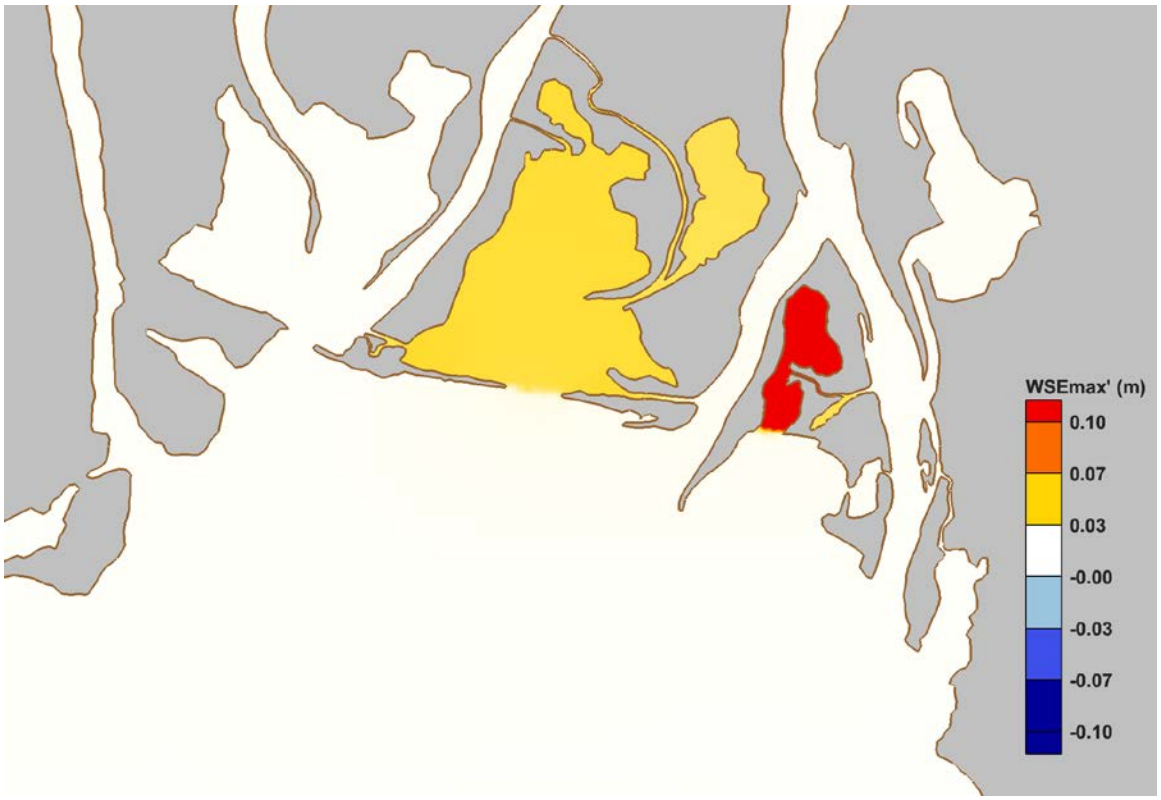

Figure 72. Predicted change in maximum water levels (WSEmax') from Case 002 to Case 402.

Table 17. Maximum tide range at selected locations during Case 402 and their relative changes from Case 002.

Location	Tide Range (m)	% Change, 002
Choccolatta Bay	0.729	+8
North Mobile Bay	0.724	<+1
Justin's Bay	0.722	+63.7
Ducker Bay	0.723	<+1
Shellbank River North	0.685	<+1
Shellbank River South	0.723	<+1

Flows

For Case 402, with all constructed openings acting simultaneously, the predicted changes in maximum depth-averaged water velocity were ±30 cm/s throughout the study area, as shown in Figure 73. The most notable changes occurred within the constructed openings and their surrounding areas, and within existing tidal channels like the I-10 Cut, Pass Picada, and Sardine Pass, which all see substantial reductions in maximum water velocity due to their corresponding decrease in hydraulic efficiency. Note that a secondary effect of the openings was to increase maximum velocities by as much as 25%, relative to existing conditions, over broad areas of northern Mobile Bay.

The potential effects of the constructed openings on predicted subtidal velocities are shown in Figure 74, where magnitudes are generally ±1 cm/s. An increase in seaward-directed flow was predicted in Choccolatta Bay, Justin's Bay and Shellbank River, with some decreases in seaward directed subtidal flow in the Apalachee and lower Blakeley Rivers.

The tidal exchange for Choccolatta Bay increased by 78.6% relative to existing conditions, whereas Justin's Bay experienced a 121.1% increase in tidal exchange with all constructed openings in place. It is interesting to note that these changes are actually slightly less than the calculated change for each opening acting alone (see Table 10, Table 13). While the differences are modest, no more than 5% in either case, it suggests that the constructed openings have some influence on each other when opened simultaneously. An evaluation of tidal exchange volumes for Choccolatta Bay and Justin's Bay under this restoration scenario (Case 402) is provided in Table 18.

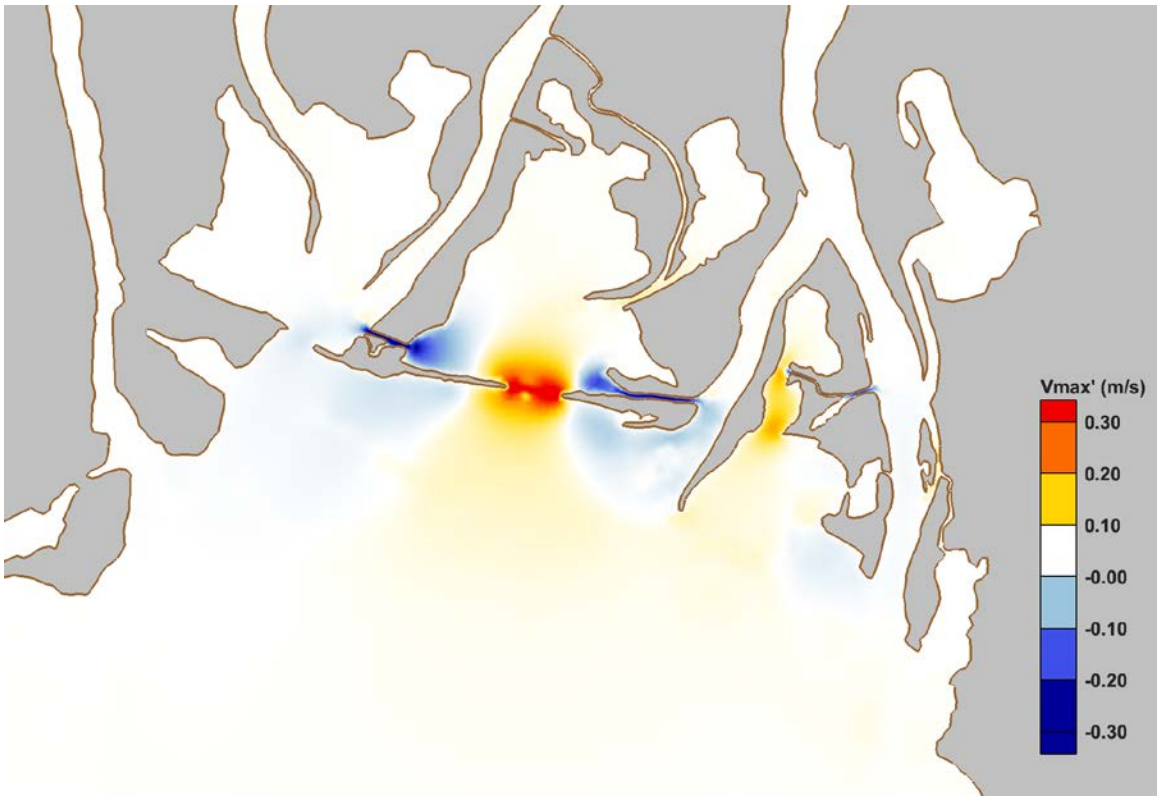

Figure 73. Predicted change in maximum depth-averaged velocity (Vmax') from Case 002 to Case 402.

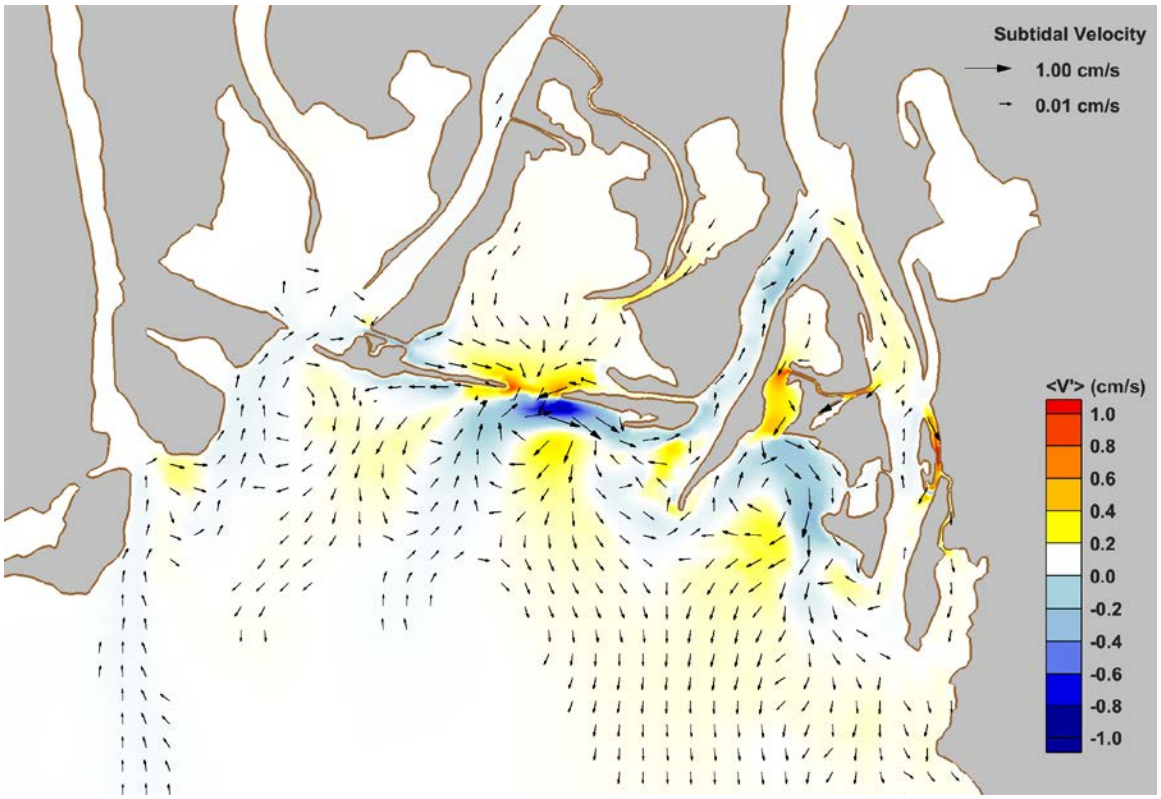

Figure 74. Predicted change in subtidal velocity (<V'>) from Case 002 to Case 402.

Table 18. Maximum tidal volume exchanged (in cubic meters) between successive low and high water on a flooding tide for Case 402, and the percent change relative to existing conditions (Case 002).

Location		Tidal Volume Exchange (m^3)	% Change, 002
Choccolatta Bay	I-10 Cut	122,976 (in)	-94.4
	Little Creek	11,770 (out)	+79.9
	Conway Creek	1,126,255 (out)	+21.5
	"Pass Choccolatta"	7,271,341 (in)	+8395.9
	Pass Picada	222,593 (in)	-90.2
	Total (net)	**6,478,886 (in)**	**+78.6**
Justin's Bay	Sardine Pass	45,967 (in)	-88.8
	"Pass Justin"	864,599 (in)	N/A
	Total (net)	**910,566 (in)**	**+121.1**

Sediment Transport Potential

As in the previous restoration scenarios, the model predicted increased bedload transport in and near the constructed openings on the order of 0.01 $m^3/s/m^2$, or generally 25% to 50% greater than rates under existing conditions. Decreased bedload transport rates were predicted to occur in I-10 Cut, Pass Picada, Sardine Pass, and the lower portions of the Spanish/Tensaw, Apalachee, and Blakeley Rivers. Predicted changes in potential bedload sediment transport and resuspension rates, relative to existing conditions, for this restoration alternative are demonstrated in Figure 75 and Figure 76, respectively.

In terms of resuspension rates, increases and decreases on the order of 25% above/below existing conditions were predicted. Changes in resuspension rates relative to existing conditions were on the order of ±0.1 $m^3/s/m^2$. The largest increases were found within the constructed openings and in lower Conway Creek. Substantial reductions were noted in I-10 Cut, Pass Picada, Sardine Pass, and the lower reaches of each river within the study area.

As in previous scenarios, reductions in sediment deposition (-1.0) were noted within the constructed openings and throughout broad areas of Choccolatta Bay, Big Bateau, Justin's Bay, John's Bend, and Ducker Bay, and in much of Shellbank River. Notable increases in sediment deposition (+1.0) were predicted to occur in the southwest and southeast portions of Choccolatta Bay, I-10 Cut, Pass Picada, and Sardine Pass. Potential changes in sediment depositional areas and patterns, relative to existing conditions (Case 002), are shown in Figure 77 for this restoration scenario of all openings acting simultaneously.

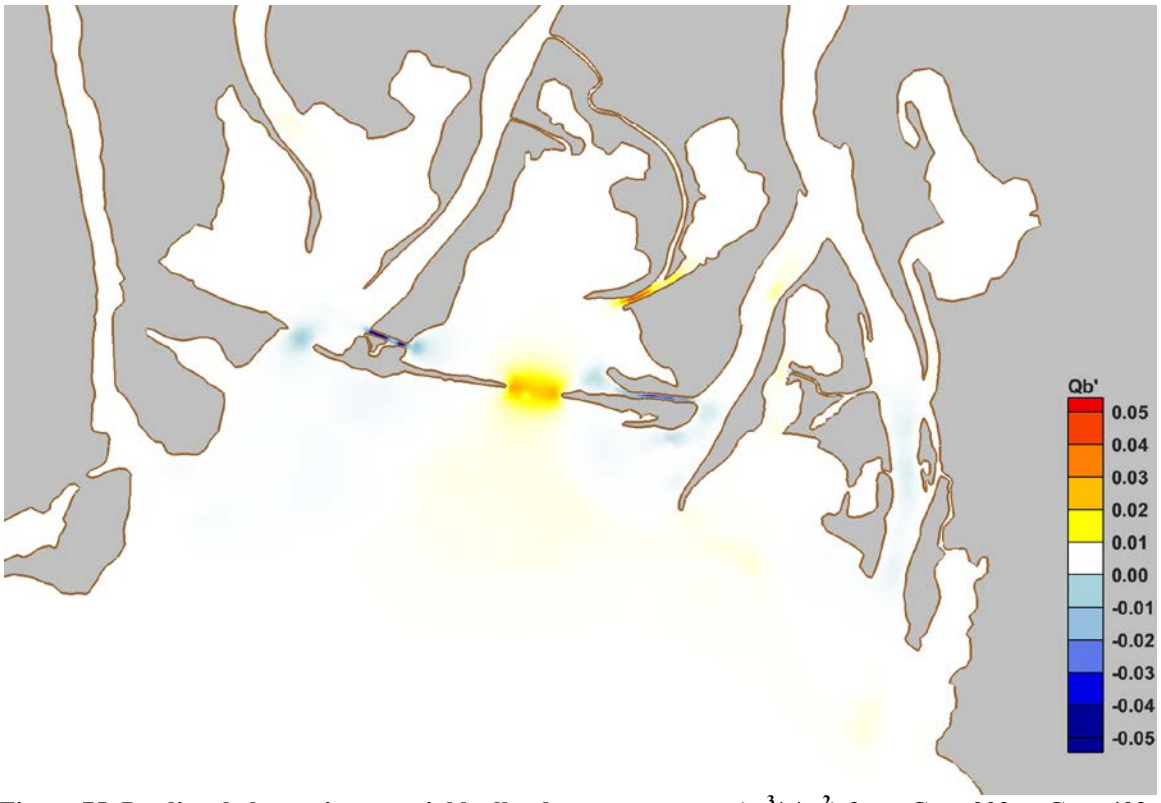

Figure 75. Predicted change in potential bedload transport rates ($m^3/s/m^2$) from Case 002 to Case 402.

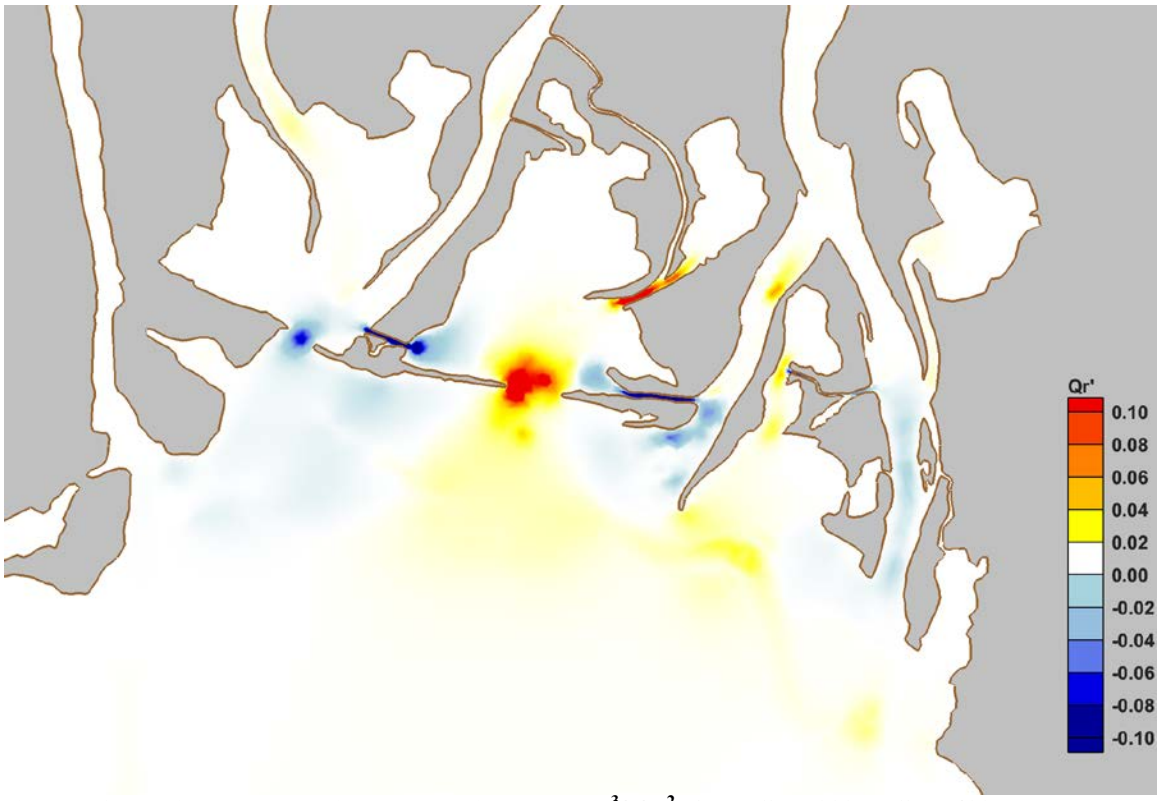

Figure 76. Predicted changes in resuspension rates ($m^3/s/m^2$) from Case 002 to Case 402.

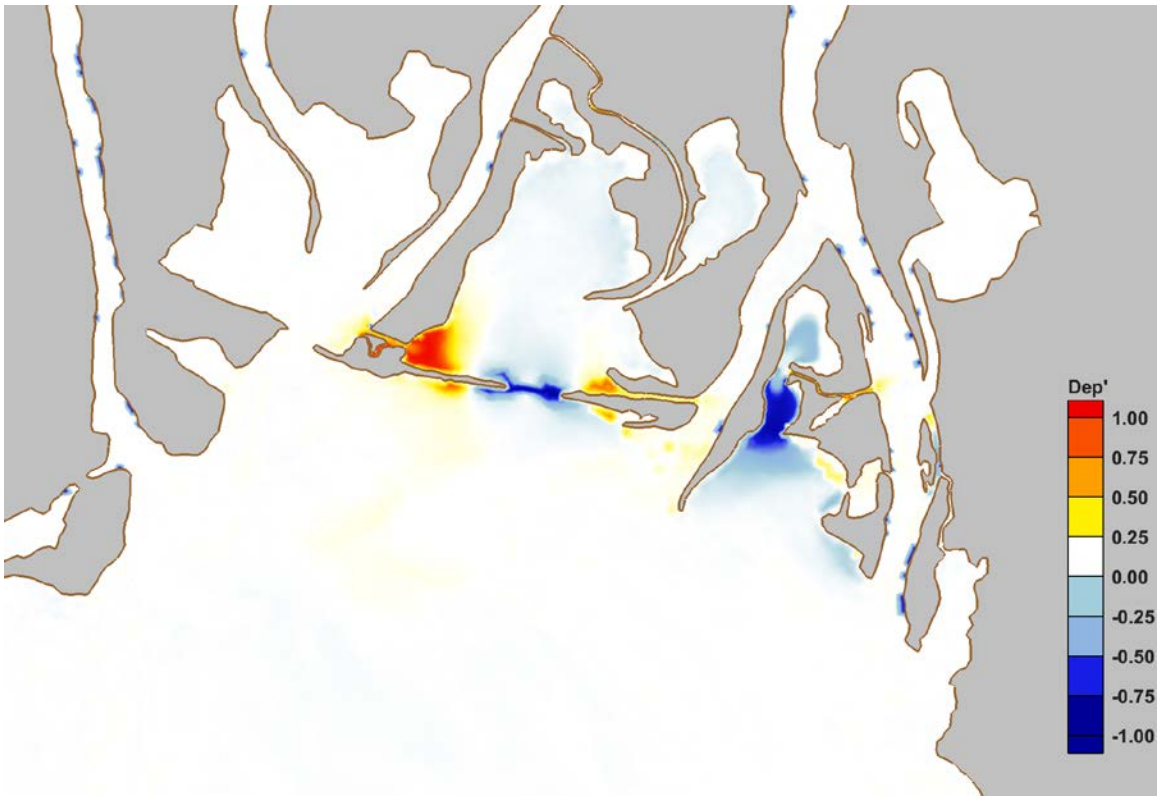

Figure 77. Potential changes in sediment deposition patterns between Case 402 and Case 002 (+1: new deposition; 0: no change; -1: no longer depositional).

Flushing

The LPTM analysis results for this scenario (Case 403) look similar to those of Case 102 (see Figure 53) and Case 202 (see Figure 64). The model results show that the constructed openings lowered residence times considerably in areas close to them, but they increased in and near the existing tidal channels of each system. For example, residence times near the I-10 Cut, Pass Picada, and Sardine Pass increased by more than 5 days. Predicted changes in residence times for Choccolatta Bay and Justin's Bay are shown in Figure 78. The figure shows the change in residence time, in days relative to existing conditions, for the restoration scenario having all openings acting simultaneously.

The flushing of Choccolatta Bay and Justin's Bay improved by 10% and 500%, respectively, with the constructed openings in place. Justin's Bay showed the most substantial reductions in residence and exposure times accompanied by a corresponding increase in the number of particles removed from the Bay as a result of the constructed opening. System-wide average residence and exposure times, and percent of particles removed, for Case 002 and Case 402 are listed in Table 19.

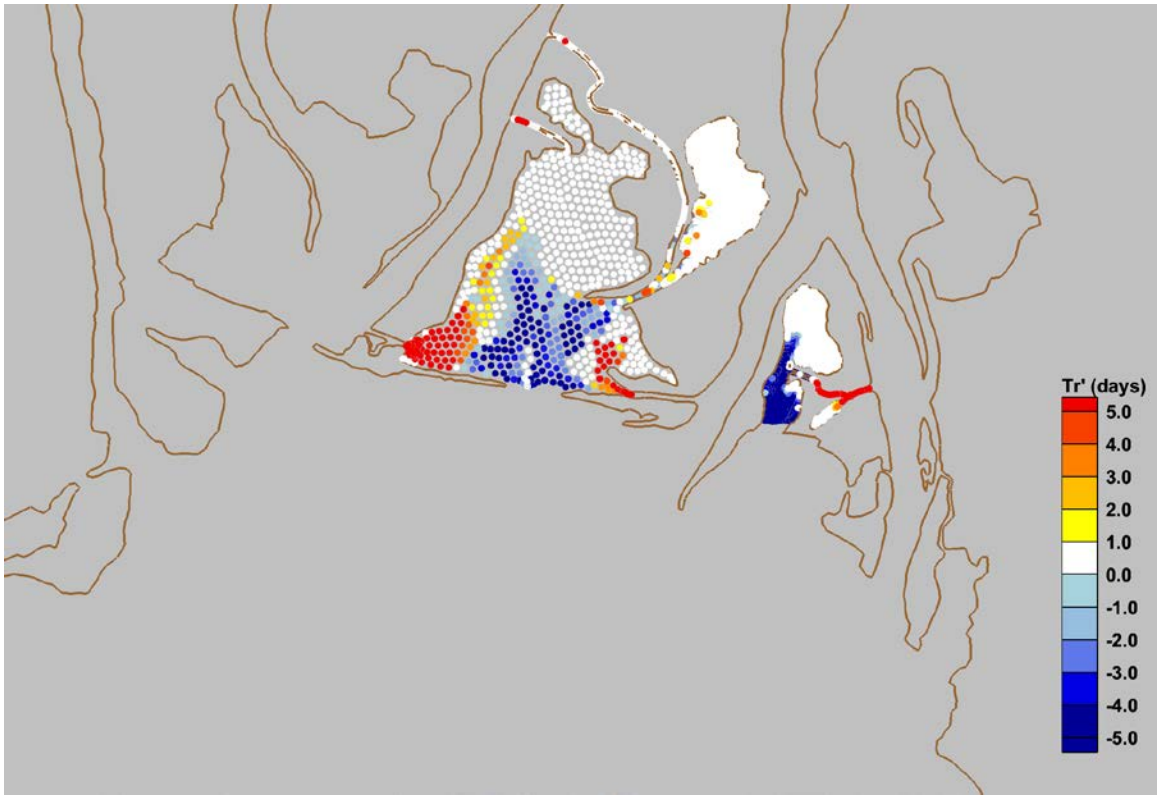

Figure 78. Potential changes in particle residence times from Case 002 to Case 402, relative to particle initial position.

Table 19. System-wide averages of residence and exposure time and the percent of particles removed for Case 402.

Location	Avg. Residence Time (days)		Avg. Exposure Time (days)		% Particles Removed	
	Case 002	Case 402	Case 002	Case 402	Case 002	Case 402
Choccolatta Bay	7.9	7.8	8.4	8.3	20.2	22.3
Justin's Bay	8.4	6.8	8.6	7.3	7.1	36.4

Choccolatta + Justin's - Case 502

This hypothetical restoration scenario considers constructed openings through the Causeway at Choccolatta Bay and Justin's Bay acting simultaneously. The forcing conditions consist of representative tides and average summer river discharge under present day sea levels. Simulation results for Case 502 are presented as differences relative to existing conditions (Case 002).

Water Levels

The predicted changes are nearly identical to those of Case 102 for Choccolatta Bay (Figure 42), Case 202 for Justin's Bay (Figure 54), and Case 402 for both combined (Figure 72). These predicted changes are shown in Figure 79. Closer examination of the predicted maximum tide range at locations within the study area, provided in Table 20, suggests that the tide range in Justin's Bay was slightly larger (~0.5%) than in Case 402 when Shellbank River was also open, but the magnitude of the difference was less than 0.5 cm.

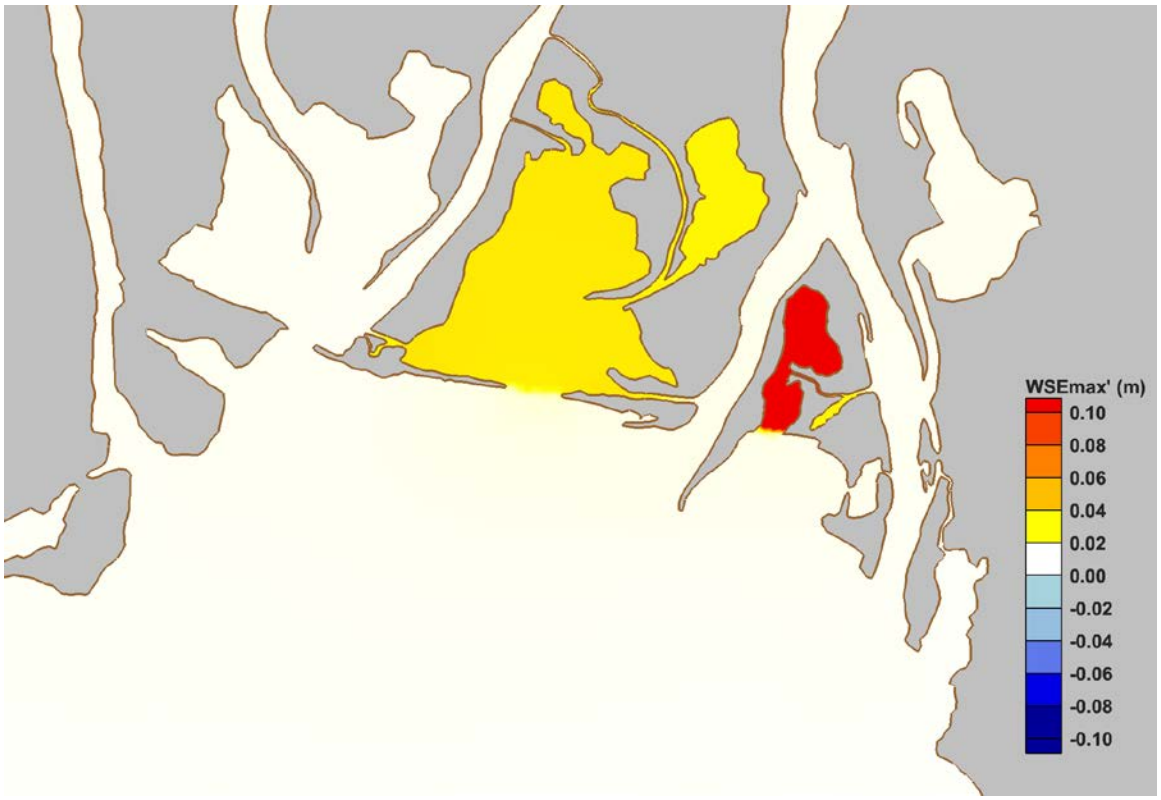

Figure 79. Predicted change in maximum water levels from Case 002 to Case 502.

Table 20. Maximum tide ranges at selected locations for Case 502 and their relative change from Case 002.

Location	Tide Range (m)	% Change, 002
Choccolatta Bay	0.729	+8
North Mobile Bay	0.724	<+1
Justin's Bay	0.724	+64.2
Ducker Bay	0.723	<+1
Shellbank River North	0.726	<+1
Shellbank River South	0.722	<+1

Flows

Model predictions of changes in maximum depth-averaged water velocity for the scenario of constructed openings at Choccolatta and Justin's Bays are shown in Figure 80. The magnitude and pattern of changes are similar to cases presented previously: Case 102, Case 202, and Case 402. The predicted changes in subtidal velocity magnitude and direction, as demonstrated in Figure 81, were also similar to those of previous restoration alternative scenarios. Moreover, estimates of tidal volume exchange in Choccolatta Bay and Justin's Bay were similar to previous cases where each opening was considered alone (Case 102 and Case 202) and also in a combined fashion (Case 402). These values are provided in Table 21. Under this proposed scenario, the tidal volume exchange in Choccolatta Bay and Justin's Bay were predicted to increase by over 80% and 120%, respectively, relative to existing conditions.

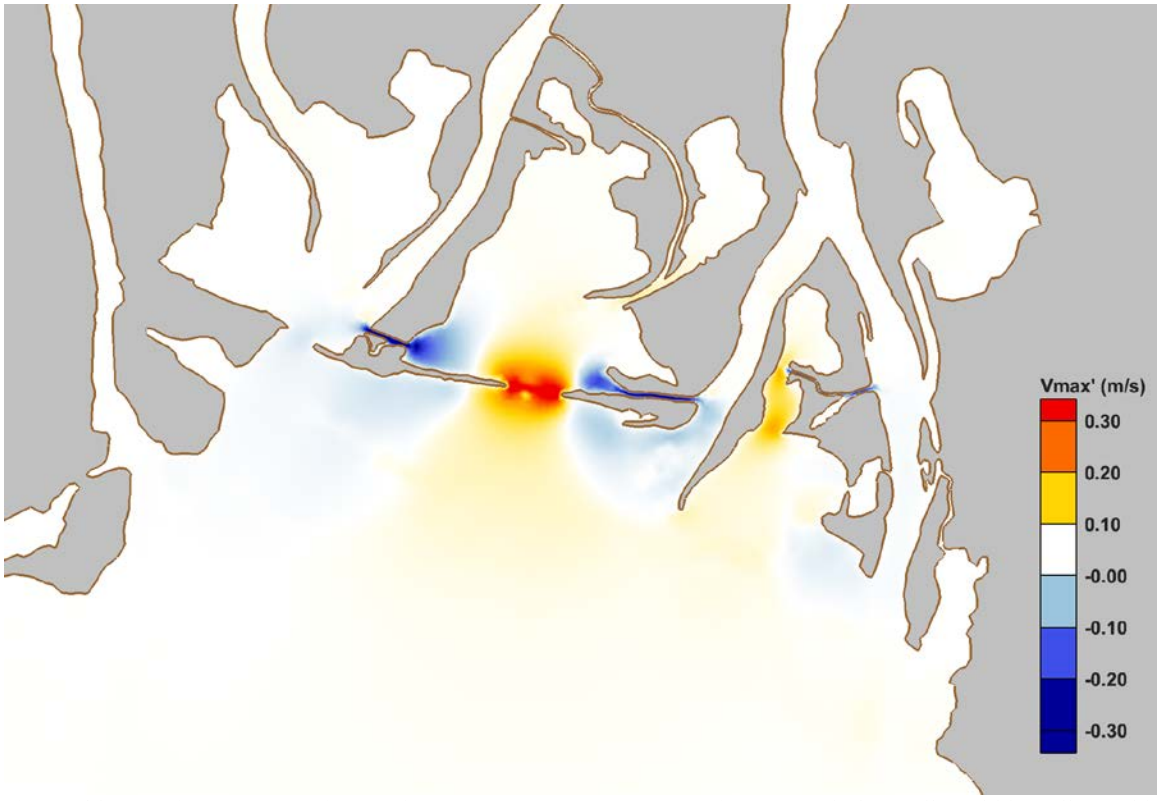

Figure 80. Predicted change in maximum depth-averaged velocity (Vmax') from Case 002 to Case 502.

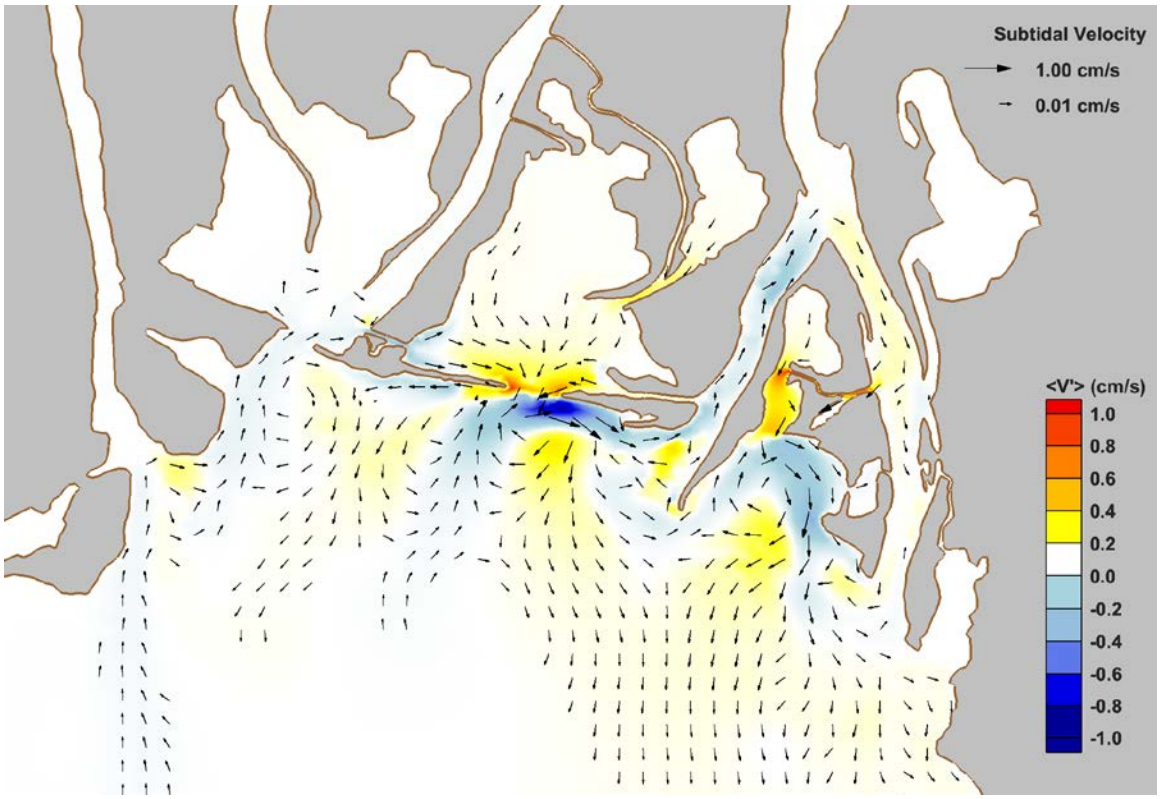

Figure 81. Predicted change in subtidal velocity (<V'>) from Case 002 to Case 502.

Table 21. Maximum tidal volume exchanged (in cubic meters) between successive low and high water on a flooding tide for Case 502, and the percent change relative to existing conditions (Case 002).

Location		Tidal Volume Exchange (m^3)	% Change, 002
Choccolatta Bay	I-10 Cut	122,969 (in)	-94.4
	Little Creek	11,770 (out)	+79.9
	Conway Creek	1,021,468 (out)	+10.2
	"Pass Choccolatta"	7,217,345 (in)	+8395.9
	Pass Picada	222,604 (in)	-90.2
	Total (net)	**6,583,680 (in)**	**+81.5**
Justin's Bay	Sardine Pass	51,273 (in)	-87.6
	"Pass Justin"	863,897 (in)	N/A
	Total (net)	**915,170 (in)**	**+122.2**

Sediment Transport Potential

Model predictions of potential bedload transport and resuspension rates, as well as depositional tendencies, are shown in Figure 82, Figure 83, and Figure 84, respectively. The magnitudes, locations, and patterns of these changes were similar to those found in restoration alternatives Case 102 and Case 202, with very little influence in areas surrounding Shellbank and Blakeley Rivers.

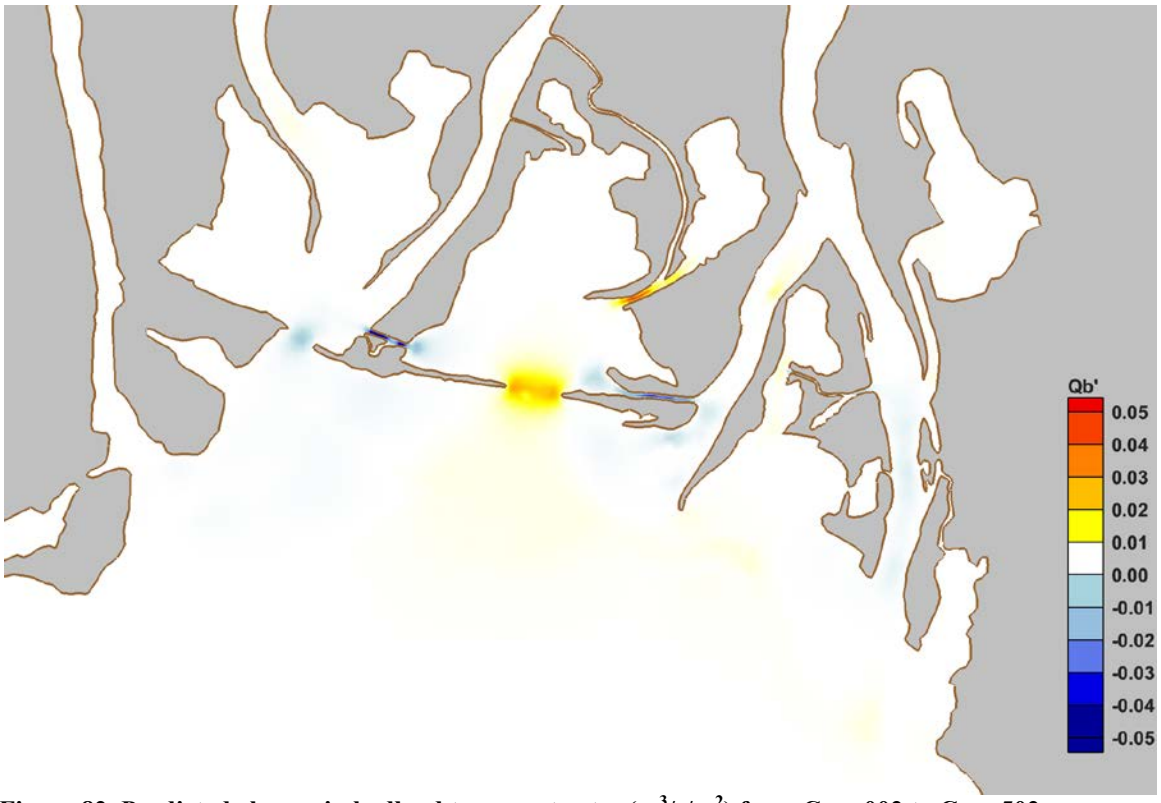

Figure 82. Predicted change in bedload transport rates ($m^3/s/m^2$) from Case 002 to Case 502.

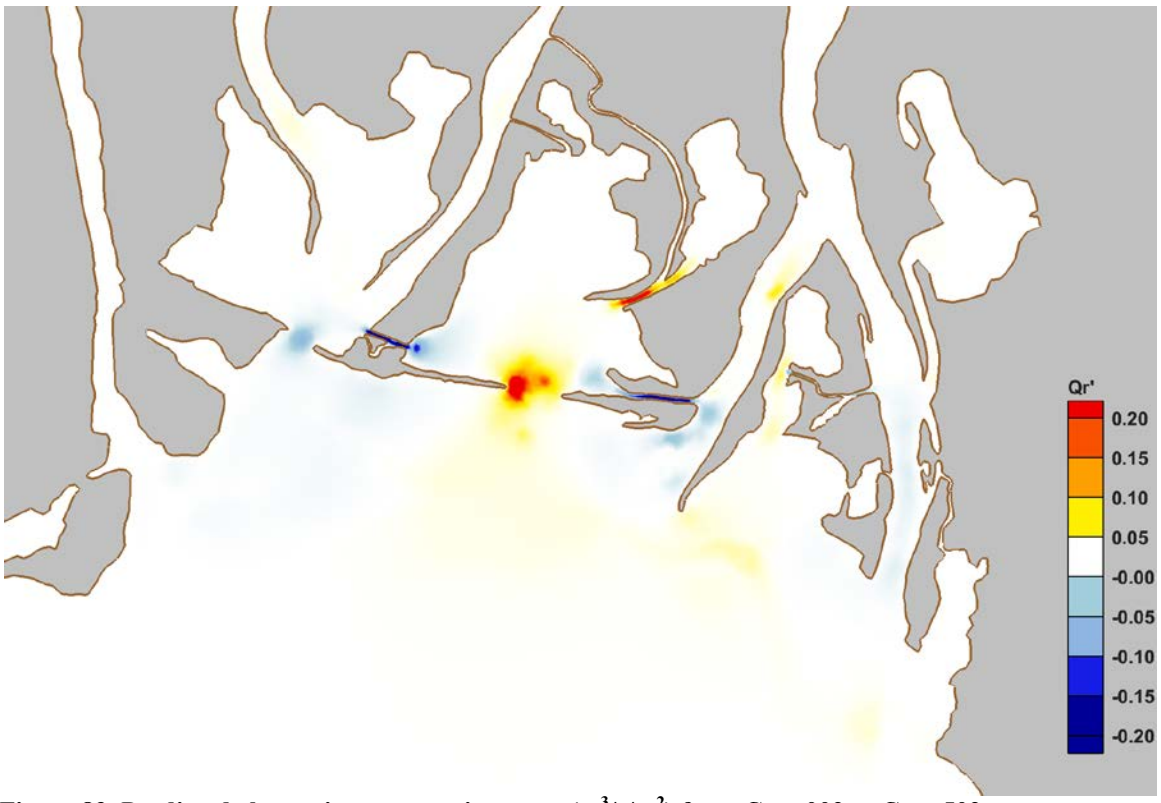

Figure 83. Predicted change in resuspension rates ($m^3/s/m^2$) from Case 002 to Case 502.

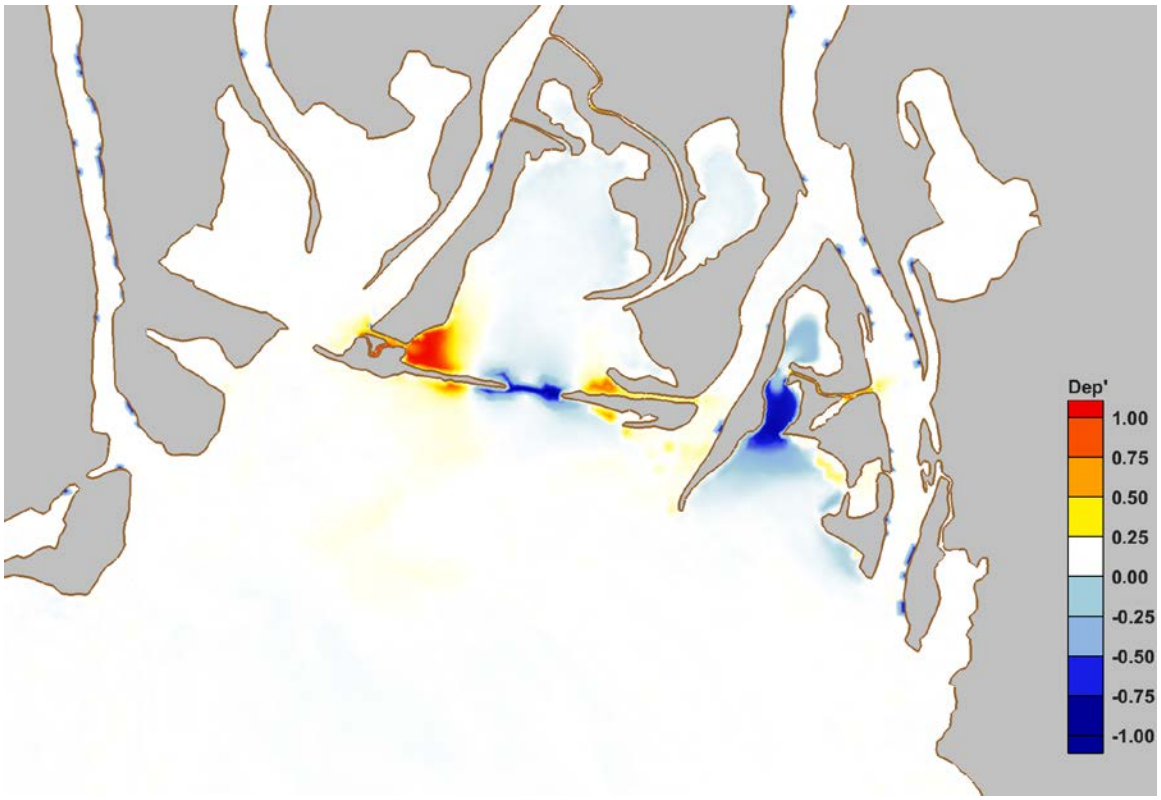

Figure 84. Potential changes in sediment deposition from Case 002 to Case 502 (+1: new deposition; 0: no change; -1: no longer depositional).

Flushing

The flushing characteristics of this restoration scenario are not substantially different than those from the scenarios where each Bay was considered alone, and when all of the openings were acting simultaneously. Predicted changes in particle residence times, relative to initial position under existing conditions, are shown in Figure 85. Reductions in residence time up to 5 days were found near the constructed openings, where similar increases in residence times were predicted near I-10 Cut, Pass Picada, and Sardine Pass. The system-wide averages presented in Table 22 are similar to those presented for earlier Cases 102, 202 and 402. Of the particles that left these Bays, about 98% left Choccolatta Bay and 100% left Justin's Bay through their constructed openings.

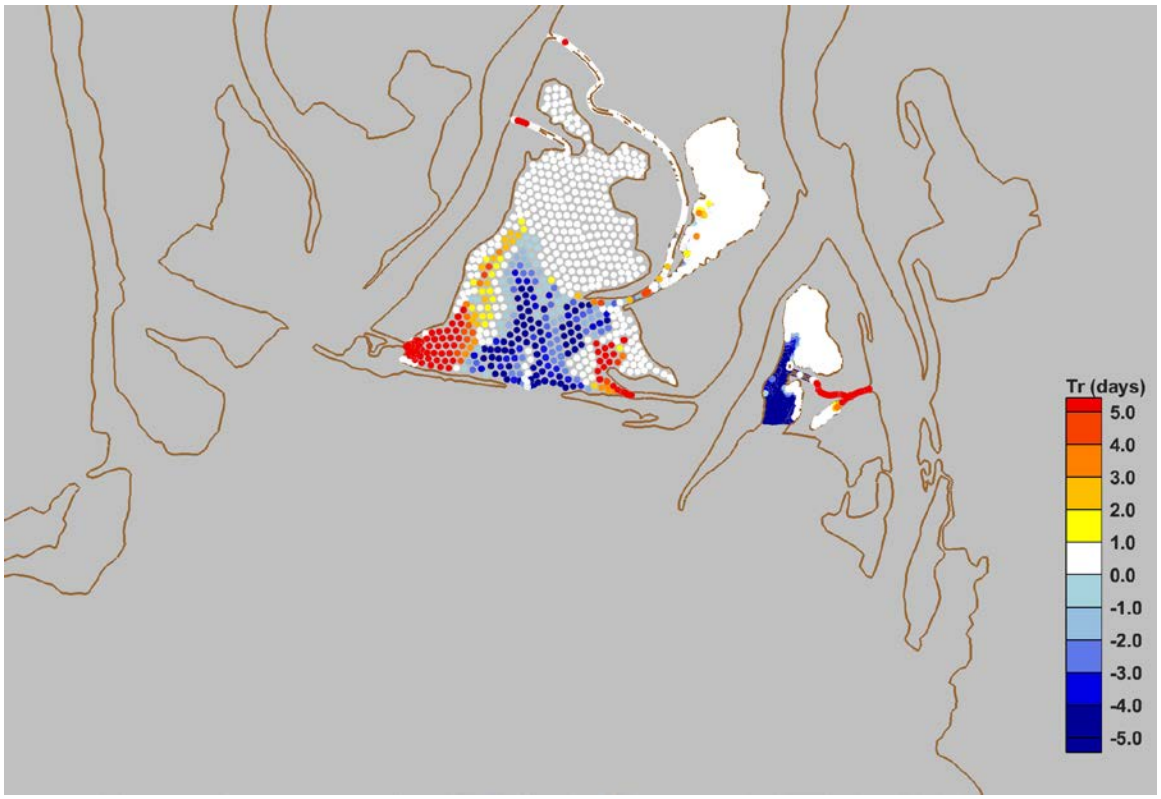

Figure 85. Predicted change in particle residence time, relative to initial position, from Case 002 to Case 502.

Table 22. System-wide average residence and exposure times and the percent of particles removed from the system for Case 502.

Location	Avg. Residence Time (days)		Avg. Exposure Time (days)		% Particles Removed	
	Case 002	Case 502	Case 002	Case 502	Case 002	Case 502
Choccolatta Bay	7.9	7.8	8.4	8.3	20.2	21.3
Justin's Bay	8.4	6.8	8.6	7.4	7.1	35.2

Alternative Simulation Results | High Flows

This section describes the potential effects of hypothetical restoration alternatives on hydrodynamic characteristics under tidal and high flow conditions for present-day sea levels. The magnitude of river discharge considered in these simulations is over four times (4x) larger than the typical flows considered in Cases 002, 102, 202, 302, 402, and 502. Existing conditions throughout the study area are described first, and then the potential effects of a single restoration alternative are described as changes (increases, decreases, etc.) relative to existing conditions under a high flow scenario.

Existing Conditions - Case 003

These simulation results reflect predictions of the existing hydrodynamic conditions within the study area. The forcing conditions consist of representative tides and high (wet season average) river discharge under present day sea levels.

Water Levels

Maximum water levels were predicted to be 2 to 4 cm lower in Choccolatta Bay as compared to Mobile Bay, and 10 to 12 cm lower in Justin's Bay relative to Mobile Bay. These results, shown in Figure 86, are similar to those presented earlier for Case 002. However, the maximum predicted tide ranges at selected locations in the study area, listed in Table 23, were less than those for the case of lower river discharge. These results indicate a reduction in tidal forcing as river discharge grows.

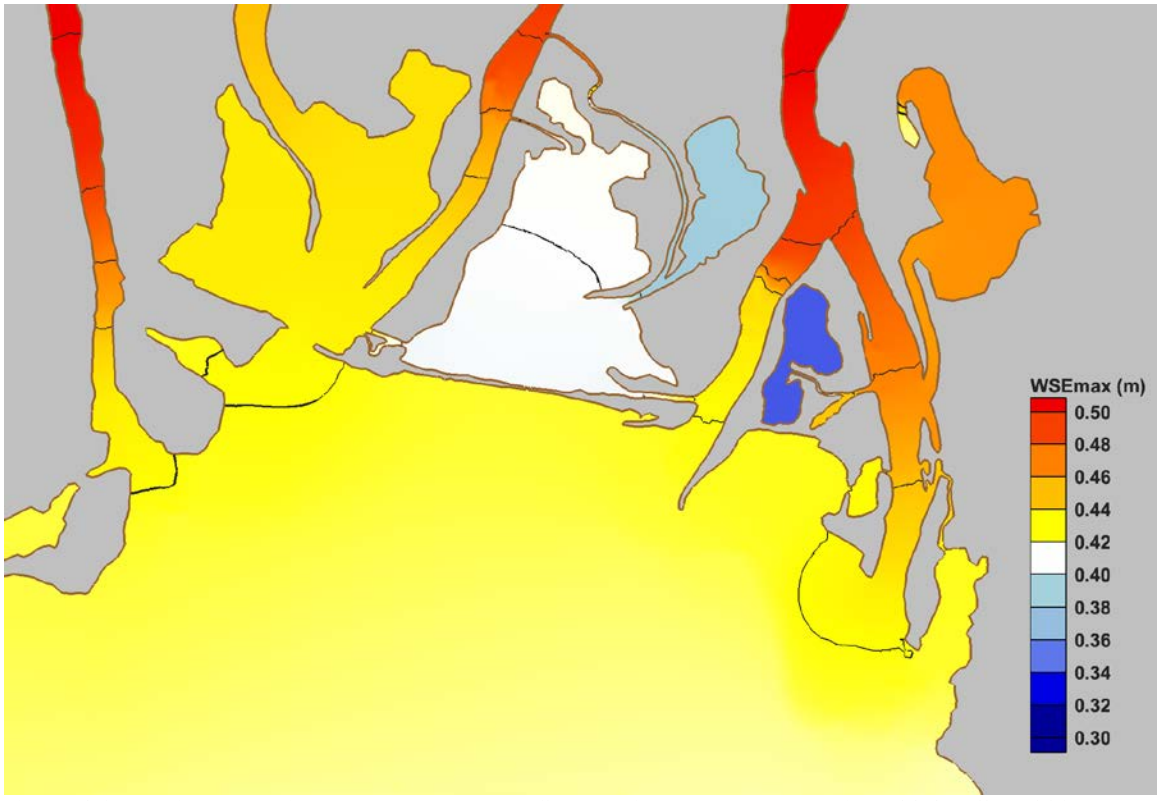

Figure 86. Predicted maximum water levels (WSEmax) in meters above NAVD88 for Case 003.

Table 23. Maximum predicted tide range at locations in the study area for Case 003.

Location	Tide Range (m)
Choccolatta Bay	0.659
North Mobile Bay	0.705
Justin's Bay	0.418
Ducker Bay	0.699
Shellbank River North	0.678
Shellbank River South	0.683

Flows

Depth-averaged velocities well over 0.6 m/s were predicted to occur in the rivers and some of the smaller tributaries and tidal creeks within the study area. Maximum predicted depth-averaged water velocity (Vmax) throughout the study area is shown in Figure 87.

The predicted subtidal velocity magnitudes and directions under existing conditions and high river discharge are shown in Figure 88. Similar to Case 002, there was little to no subtidal flow in Choccolatta Bay, Big Bateau, Justin's Bay, or Shellbank River. The general nature of the subtidal flow patterns under these conditions showed that seaward directed flows from the Spanish, Tensaw, Apalachee, and Blakeley Rivers all tended to approach the central axis of the Bay and move seaward with a velocity of approximately 5 to 10 cm/s.

There were no substantial changes in the magnitude of discharge moving through the culverts even though the river discharge was four times larger in Case 003 as compared to Case 002. This result reinforces what is known regarding the behavior of culverts: they have a maximum hydraulic capacity that cannot be overcome, which typically leads to an increase in upstream water levels. A comparison of discharge magnitude and direction through the existing box culverts for Case 002 and Case 003 is demonstrated in Figure 89.

Calculated tidal volume exchanges between successive low and high water events for the maximum flood tide are provided in Table 24. Exchange volumes were calculated as the cumulative discharge into or out of the system during the flood tide. Although not shown in this table, the cumulative exchange volumes in Choccolatta Bay for the high flow conditions were 2% less than those of the lower flow scenario (Case 002). The exchange volumes for Justin's Bay were nearly 8% less than those of the lower flow scenario. These results demonstrate the reduction in tidal forcing and exchange that occur in the northern portions of Mobile Bay as the system moves toward a river-dominated environment.

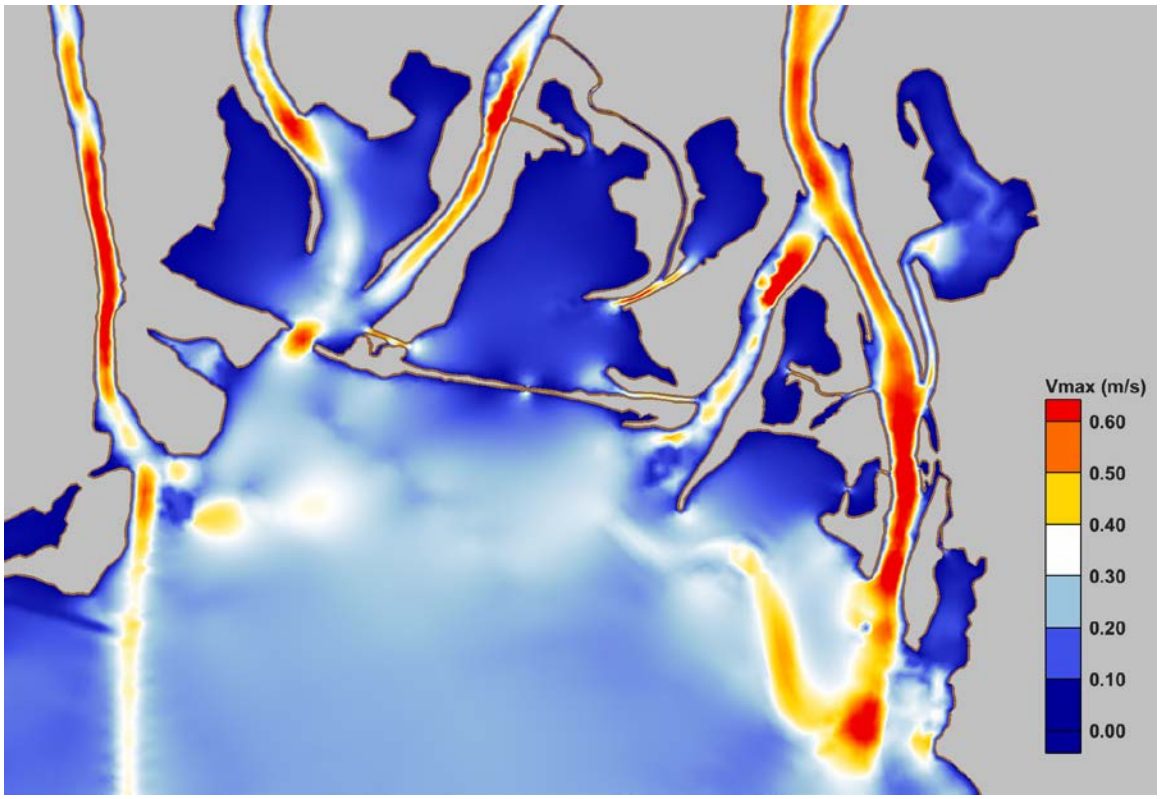

Figure 87. Predicted maximum depth-averaged velocity (Vmax) for Case 003.

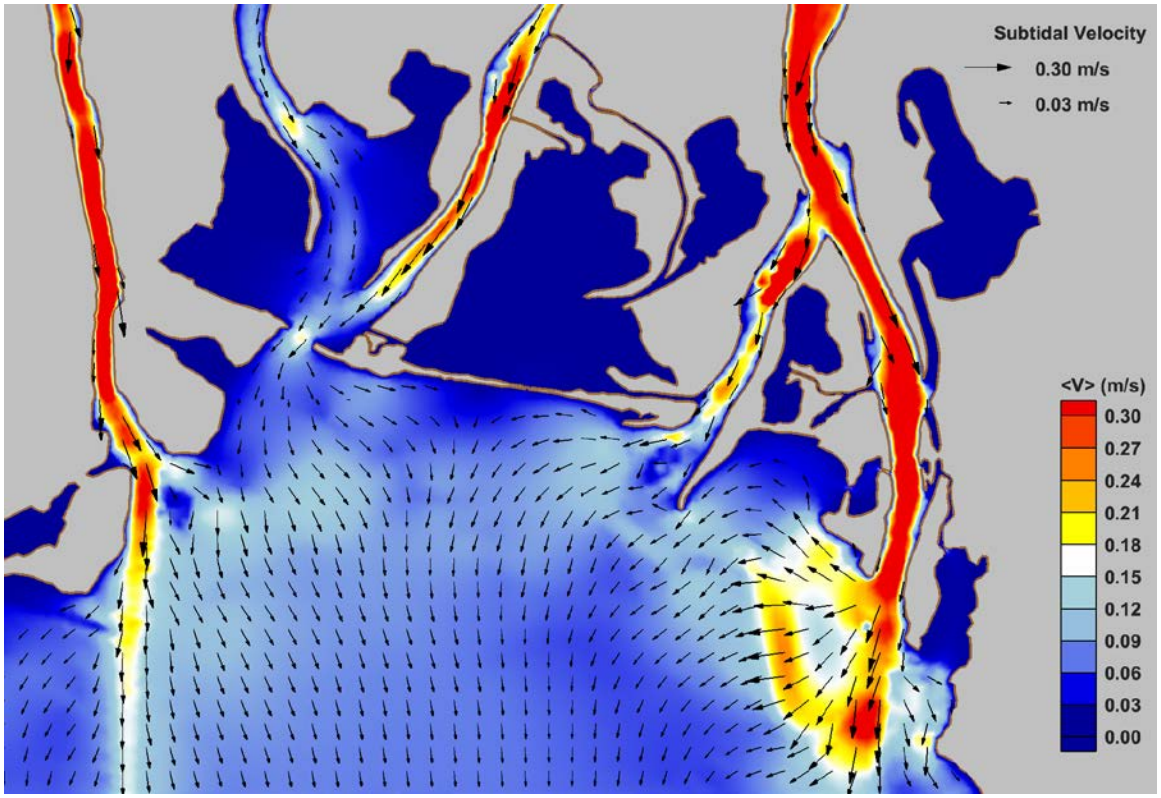

Figure 88. Predicted subtidal velocity magnitude and direction for Case 003.

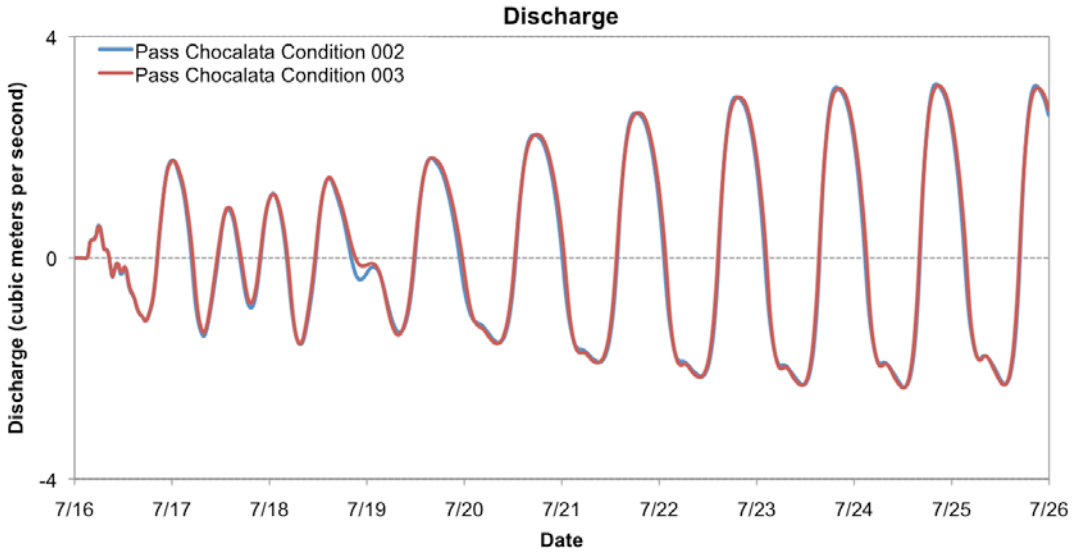

Figure 89. Time-series comparison of discharge through the existing box culverts for Case 002 and Case 003.

Table 24. Maximum tidal volume exchanged (in cubic meters) between successive low and high water on a flooding tide for Case 003.

Location		Tidal Volume Exchange (m^3)
Choccolatta Bay	I-10 Cut	2,172,512 (in)
	Little Creek	5,204 (out)
	Conway Creek	944,829 (out)
	Culverts	81,968 (in)
	Pass Picada	2,248,501 (in)
	Total (net)	**3,552,948 (in)**
Justin's Bay	Sardine Pass	379,336 (in)

Sediment Transport Potential

Sediment transport rates and characteristics within Choccolatta Bay, Justin's Bay and Shellbank River for this scenario are similar to those under the low-flow scenario since these water bodies lack efficient hydraulic connections to adjacent rivers. The model results do suggest increases in bedload transport and resuspension rates within the river systems due to the higher flow, as might be expected. Predicted bedload sediment transport and resuspension rates for this high flow scenario (existing conditions) are shown in Figure 90 and Figure 91, respectively.

Sediment deposition potential for the high flow scenario under existing conditions is shown in Figure 92. Again, the results are not substantially different from those presented in Case 002 (low flow). Notable exceptions include modest reductions in deposition potential in areas influenced by the higher river discharge. These areas are confined to the northern portions of Mobile Bay and within the rivers themselves.

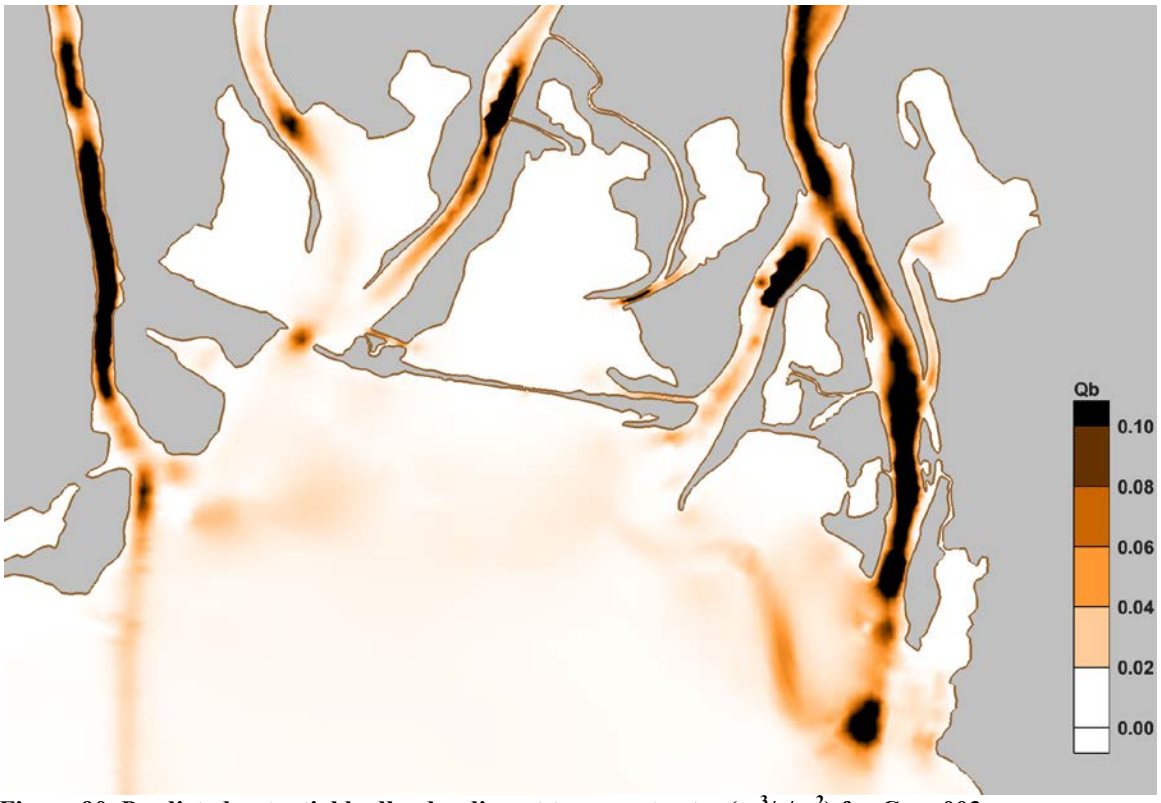

Figure 90. Predicted potential bedload sediment transport rates ($m^3/s/m^2$) for Case 003.

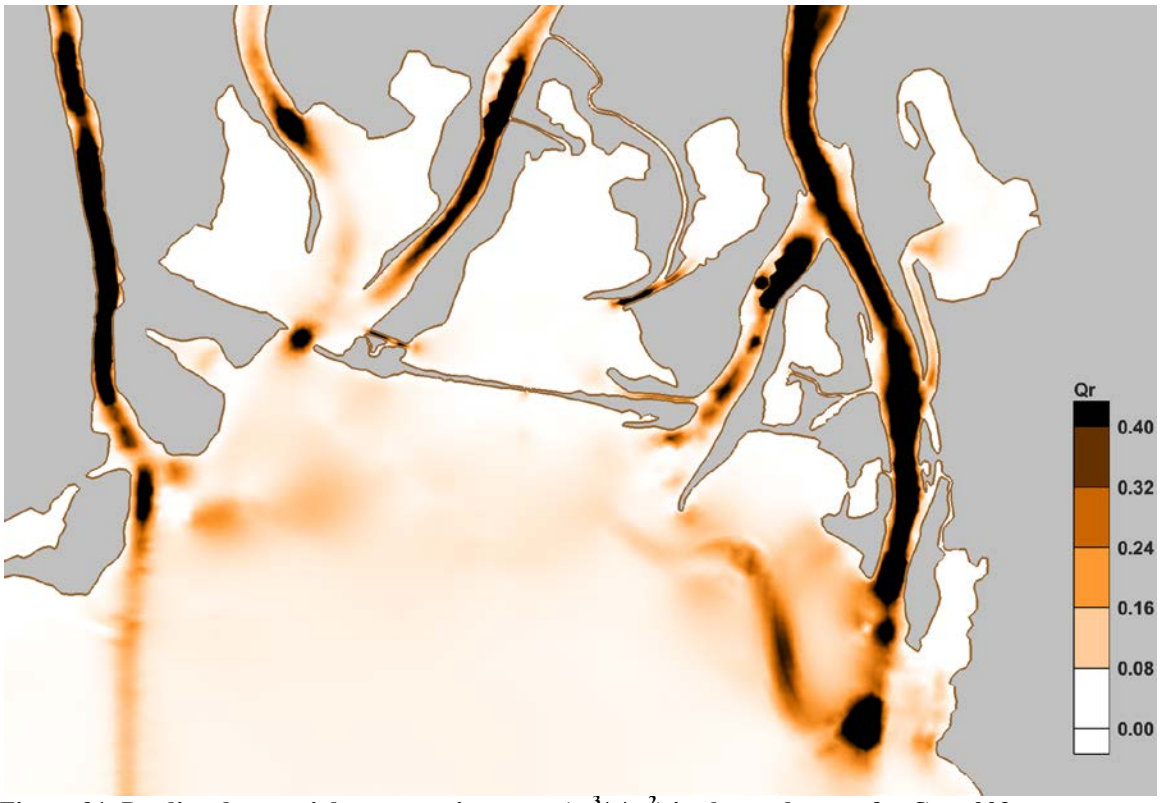

Figure 91. Predicted potential resuspension rates ($m^3/s/m^2$) in the study area for Case 003.

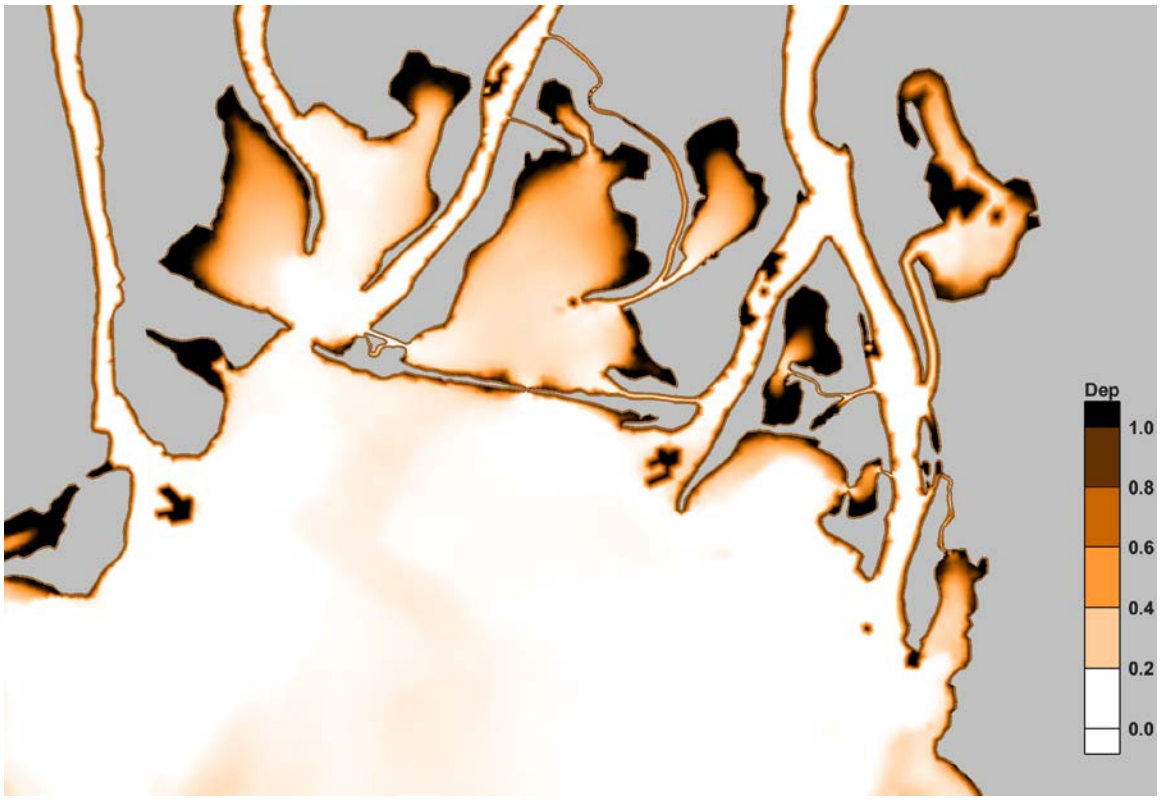

Figure 92. Potential patterns of sediment deposition for Case 003 (1.0: strongly depositional; 0.0 no deposition).

Flushing

Predicted particle residence times, as a function of initial position, are shown in Figure 93. The few particles that escaped Choccolatta Bay, those closest to the culverts, I-10 Cut, and Pass Picada, had residence times of 8 days or less. Particles shown having residence times of 9 days or more (red) did not leave the system. Few particles in Big Bateau escaped during the simulation. For Justin's Bay, only particles initialized in Duck Skiff Pass and Sardine Pass were able to escape into Blakeley River, having predicted residence times of 3 days or less.

Under existing conditions, the model predicted that about 20% of particles would leave Choccolatta Bay and only about 7% would leave the Justin's Bay systems. These values are not substantially different from those calculated for Case 002 with the low river flow. Of the particles that escaped Choccolatta Bay, about 40% exited through I-10 Cut, 20% exited through Pass Picada, and the remaining 40% left through the culverts. System-wide averages of particle residence and exposure time for Choccolatta and Justin's Bay are summarized in Table 25. Again, these system-wide values are somewhat biased by the short duration (9 days) of the LPTM simulations, which would have to be extended for many months to likely capture true residence times within these systems.

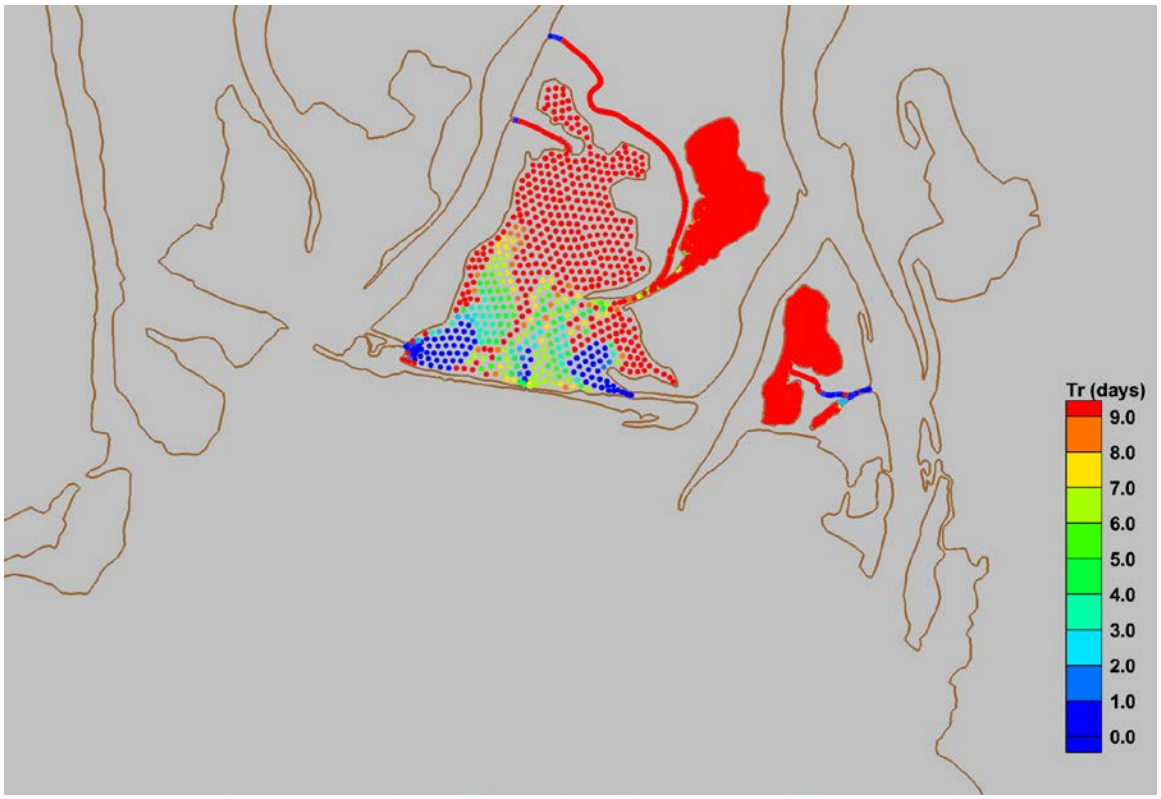

Figure 93. Predicted particle residence times (Tr) in days relative to particle initial position for Case 003.

Table 25. System-wide average residence and exposure times and percent of particles removed from Choccolatta and Justin's Bays for Case 003.

Value	Choccolatta Bay	Justin's Bay
Average Residence Time (days)	7.9	8.4
Average Exposure Time (days)	8.4	8.4
Percentage of Particles Removed	20.5	6.9

All Open - Case 403

This hypothetical restoration scenario considers constructed openings through the Causeway at Choccolatta Bay, Justin's Bay, and Shellbank River acting simultaneously. Since the combination or restoration alternatives did not yield substantially unique results under low-flow conditions, this scenario was chosen as a representative case study to described the potential effects of restoration activities under high flow conditions. The forcing conditions consist of representative tides and average wet season (high) river discharge under present day sea levels. Simulation results presented for Case 403 are shown as differences relative to existing conditions with high flows (Case 003). As such, the differences may be attributed to the constructed openings only, instead of a combination of restoration activities and unique forcing conditions.

Water Levels

The predicted increase in maximum water levels in Choccolatta Bay (2 to 4 cm), Justin's Bay (+10 cm), and Shellbank River (2 to 4 cm), shown in Figure 94, were similar to those predicted for Case 402 under the lower flow conditions. With the openings in place, the tide range in Choccolatta Bay increased by 8%, the tide range in Justin's Bay increased by 68%, and the tide range in Shellbank River increased by a marginal 1%. Changes in the tide range at other locations were negligible, as demonstrated in Table 26.

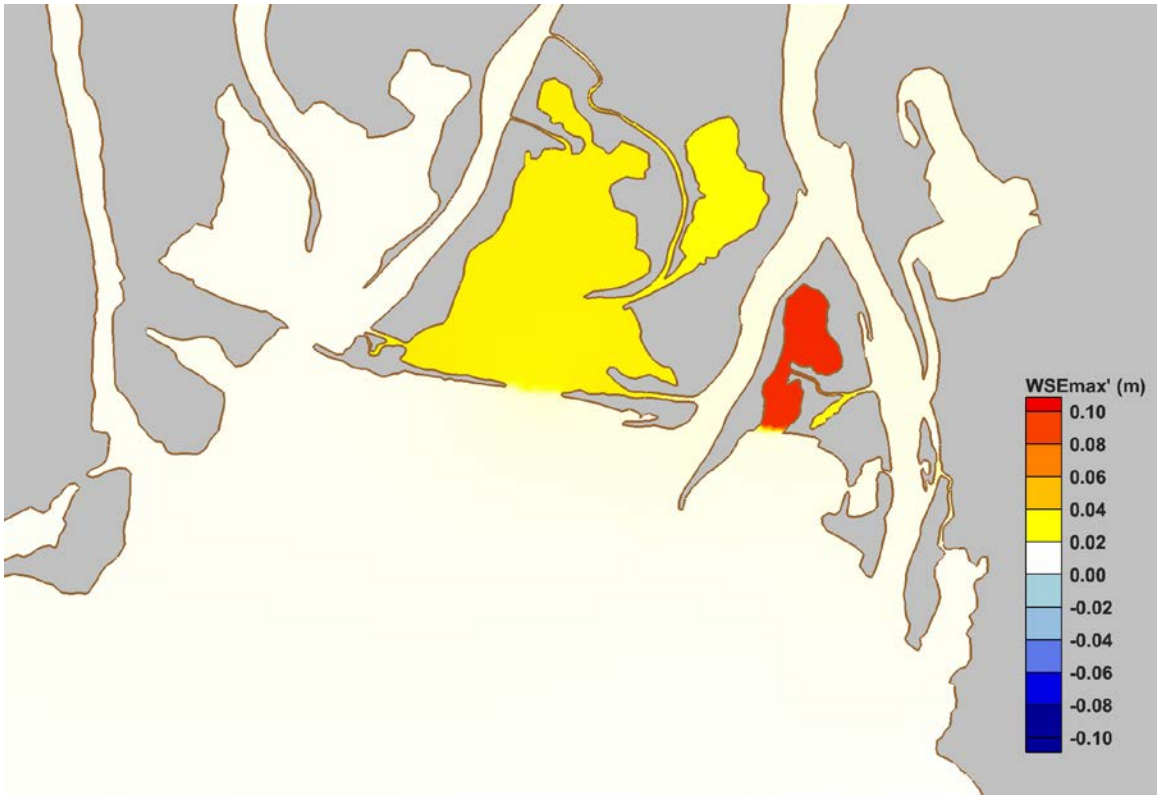

Figure 94. Predicted changes in maximum water levels (WSEmax') for the study area from Case 003 to Case 403.

Table 26. Predicted maximum tide range at selected locations for Case 403 and the relative change from Case 003.

Location	Tide Range (m)	% Change, 003
Choccolatta Bay	0.713	+8.2
North Mobile Bay	0.709	<+1
Justin's Bay	0.704	+68.4
Ducker Bay	0.702	<+1
Shellbank River North	0.685	+1
Shellbank River South	0.687	<+1

Flows

Model predictions of changes in maximum depth-averaged velocity within the study area are shown in Figure 95. The predicted magnitude of change was on the order of ±30 cm/s, with increases found in and adjacent to the constructed openings, and corresponding decreases in the lower portions of the rivers and existing tidal channels. These changes are similar to predicted changes in subtidal velocity magnitude and direction shown in Figure 96, where increased seaward directed subtidal flow having a magnitude of 2 cm/s acts to flush Choccolatta and Justin's Bay.

The hypothetical openings increased tidal volume exchange by 82% and nearly 135% in Choccolatta Bay and Justin's Bay, respectively, when compared to existing conditions under the high flow scenario. Calculated tidal volume exchanges in Choccolatta and Justin's Bays are listed in Table 27.

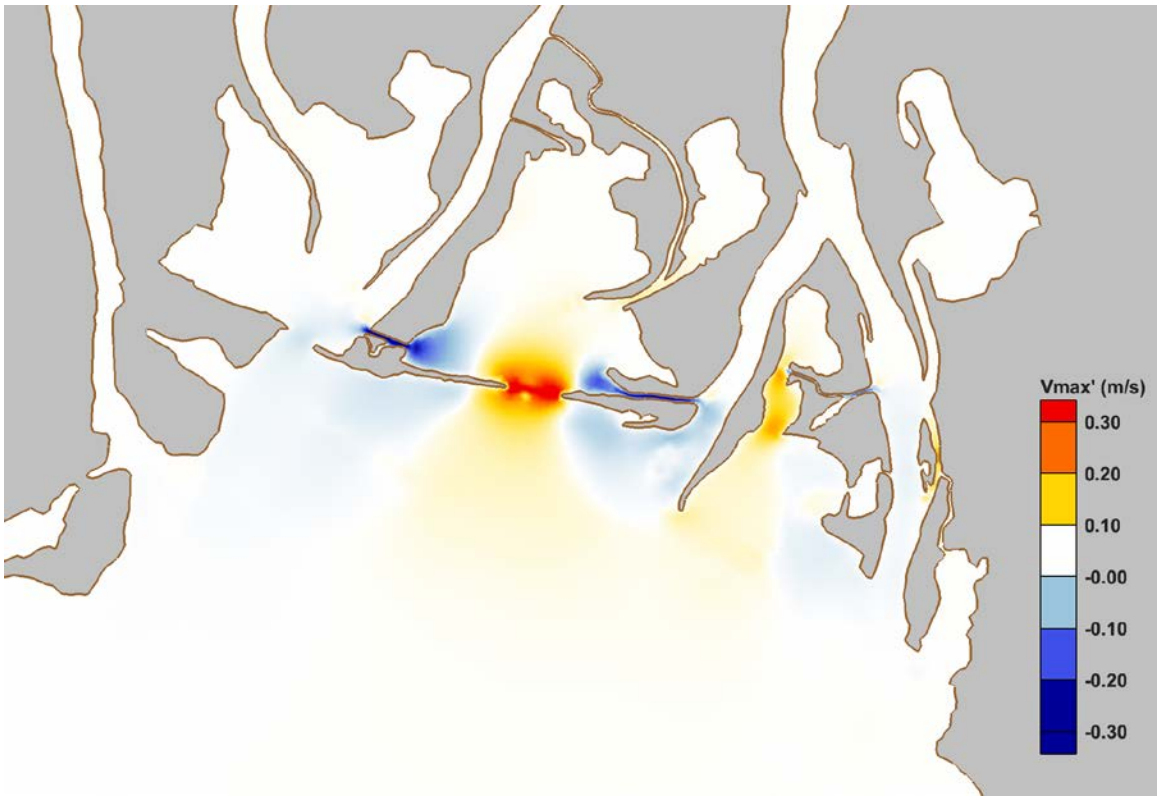

Figure 95. Predicted change in maximum depth-averaged velocity (Vmax') from Case 003 to Case 403.

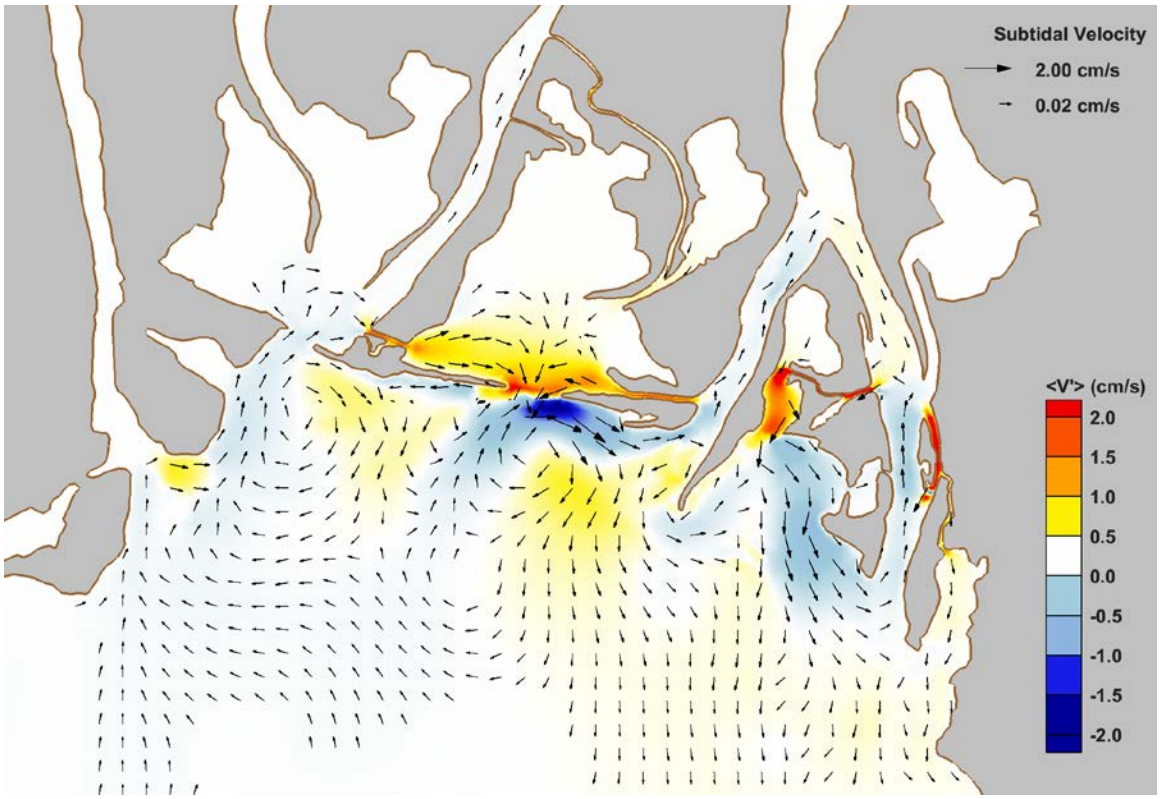

Figure 96. Predicted change in subtidal velocity (<V'>) from Case 003 to Case 403.

Table 27. Maximum tidal volume exchanged (in cubic meters) between successive low and high water on a flooding tide for Case 403, and the percent change relative to existing conditions (Case 003).

Location		Tidal Volume Exchange (m^3)	% Change, 003
Choccolatta Bay	I-10 Cut	183,920 (in)	-91.5
	Little Creek	10,337 (out)	+98.7
	Conway Creek	1,133,282 (out)	+20
	"Pass Choccolatta"	7,119,846 (in)	+8586.1
	Pass Picada	314,852 (in)	-86.0
	Total (net)	**6,475,000 (in)**	**+82.2**
Justin's Bay	Sardine Pass	102,717 (in)	-72.9
	"Pass Justin"	788,324 (in)	N/A
	Total (net)	**891,041 (in)**	**+134.9**

Sediment Transport Potential

Similar to the model simulation results of other restoration scenarios, increases in sediment transport and resuspension are generally confined to areas near the constructed openings while decreases are found in many of the existing tidal channels that serve as the primary tidal connections of those water bodies under existing conditions. The magnitude of predicted changes in simulation-averaged bedload transport rates was ±0.03 $m^3/s/m^2$, or about 30% of the magnitude under existing conditions. Changes in simulation-averaged resuspension rates were ±0.1 $m^3/s/m^2$, or about 25% of the magnitude under

existing conditions. These changes in bedload sediment transport and resuspension rates, relative to Case 003, are shown in Figure 97 and Figure 98, respectively.

The model predictions show that portions of Choccolatta Bay, Justin's Bay, Shellbank River, and John's Bend become much less depositional in nature (-1.0) with the openings in place. However, I-10 Cut and Pass Picada, and areas adjacent to them in Choccolatta Bay, become much more depositional (+1.0) as a result of the constructed openings. The depositional nature of Duck Skiff Pass and Sardine Pass was predicted to increase as well. These changes in sediment depositional patterns and areas, relative to existing conditions, are shown in Figure 99 for Case 403.

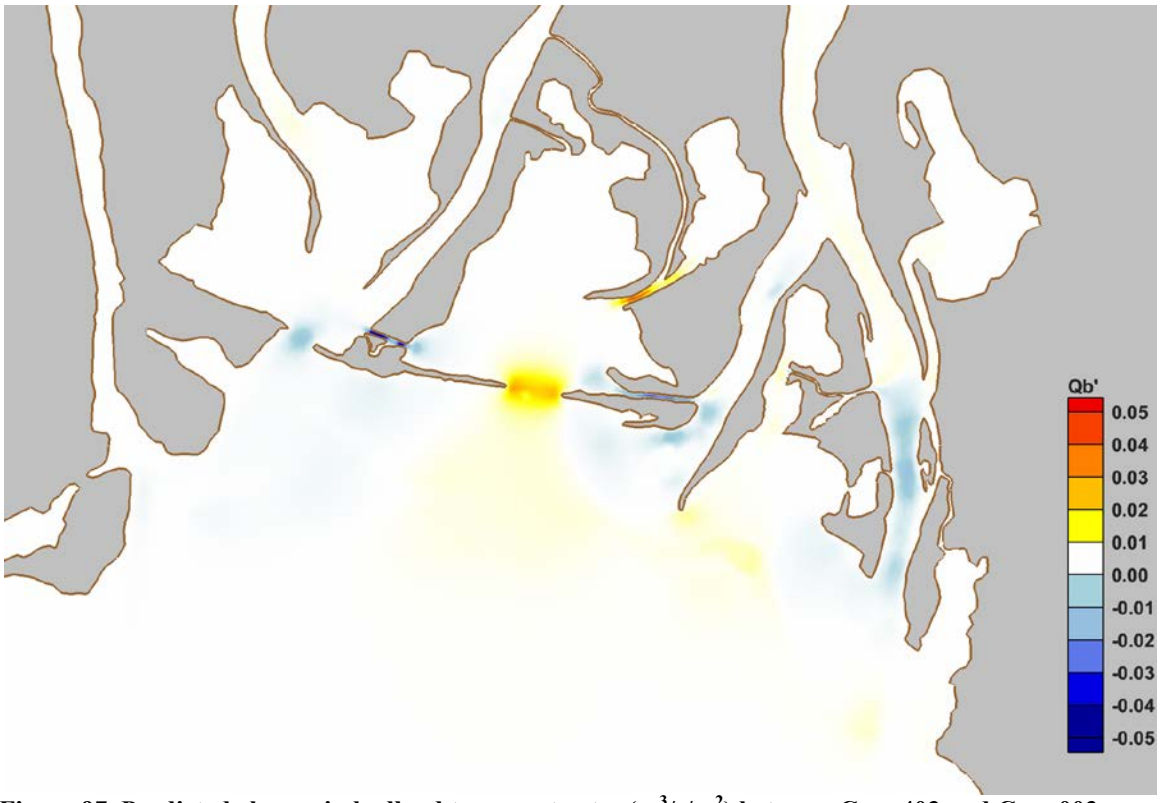

Figure 97. Predicted change in bedload transport rates ($m^3/s/m^2$) between Case 403 and Case 003.

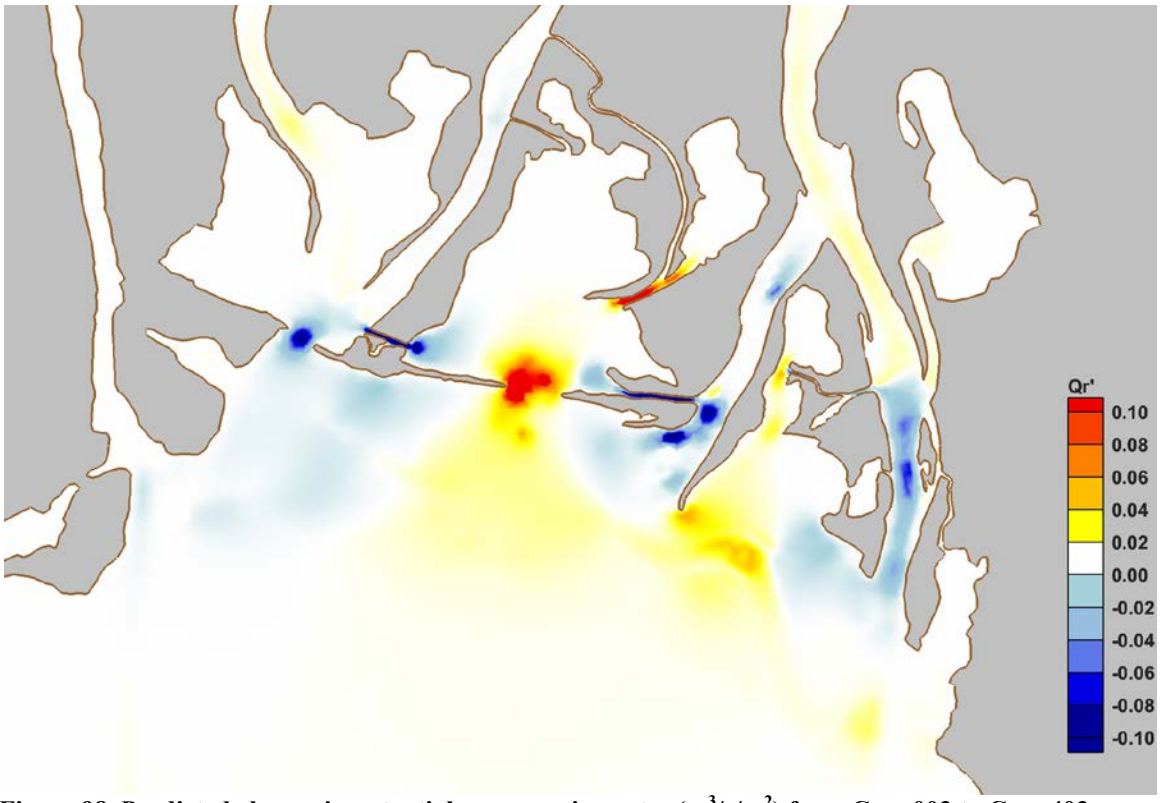

Figure 98. Predicted change in potential resuspension rates ($m^3/s/m^2$) from Case 003 to Case 403.

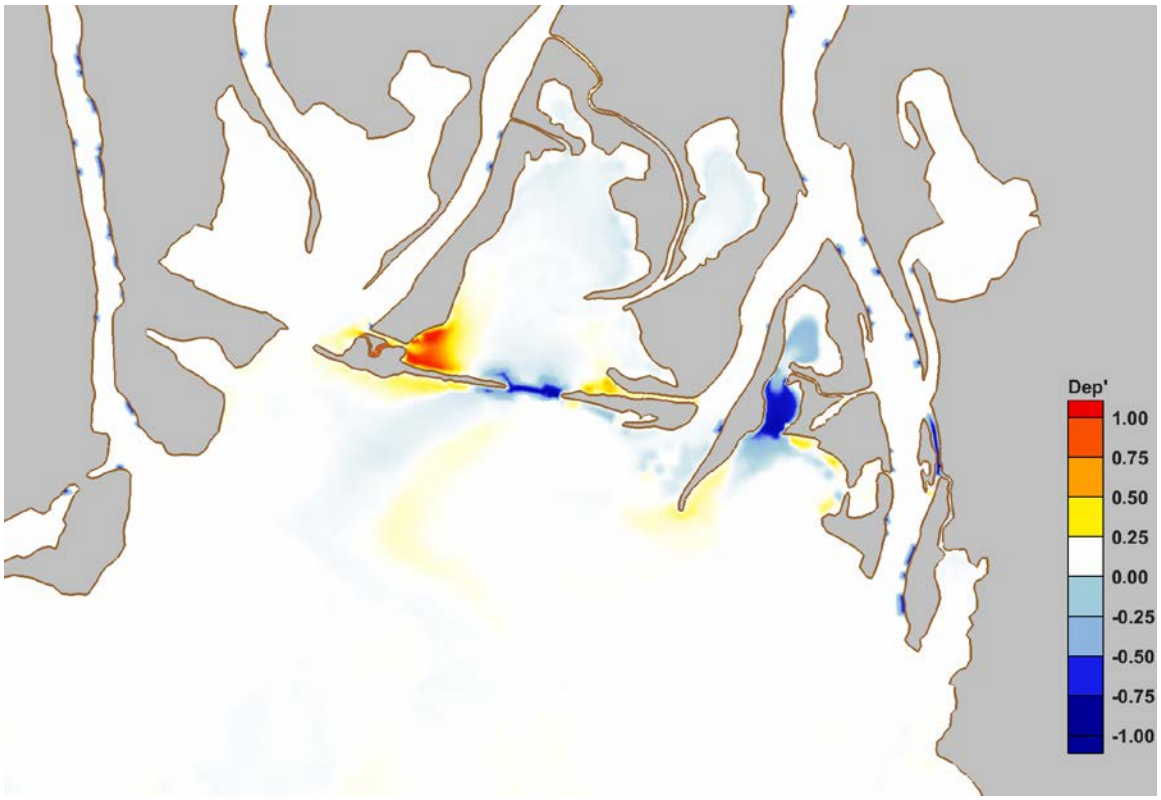

Figure 99. Predicted change in depositional patterns throughout the study area from Case 003 to Case 403 (+1: new depositional area; 0: no change; -1: no longer depositional).

Flushing

Relative to existing conditions, the constructed opening in Choccolatta Bay increased flushing by 35%. In Justin's Bay, the percentage of particles flushed from the system increased from nearly 7% to over 40%. In each case, almost all of the particles that escaped the systems did so through their constructed openings.

The model predicted substantial reductions in residence time through much of lower and central Choccolatta Bay, and much of Justin's Bay. Increased residence times, and decreased flushing capacity, were predicted to occur near I-10 Cut and Pass Picada, for Choccolatta Bay, and in Sardine Pass for Justin's Bay. Predicted changes in particle residence times (Tr'), in days relative to existing conditions, are shown in Figure 100. System-wide average residence and exposure times for Choccolatta and Justin's Bays are provided in Table 28.

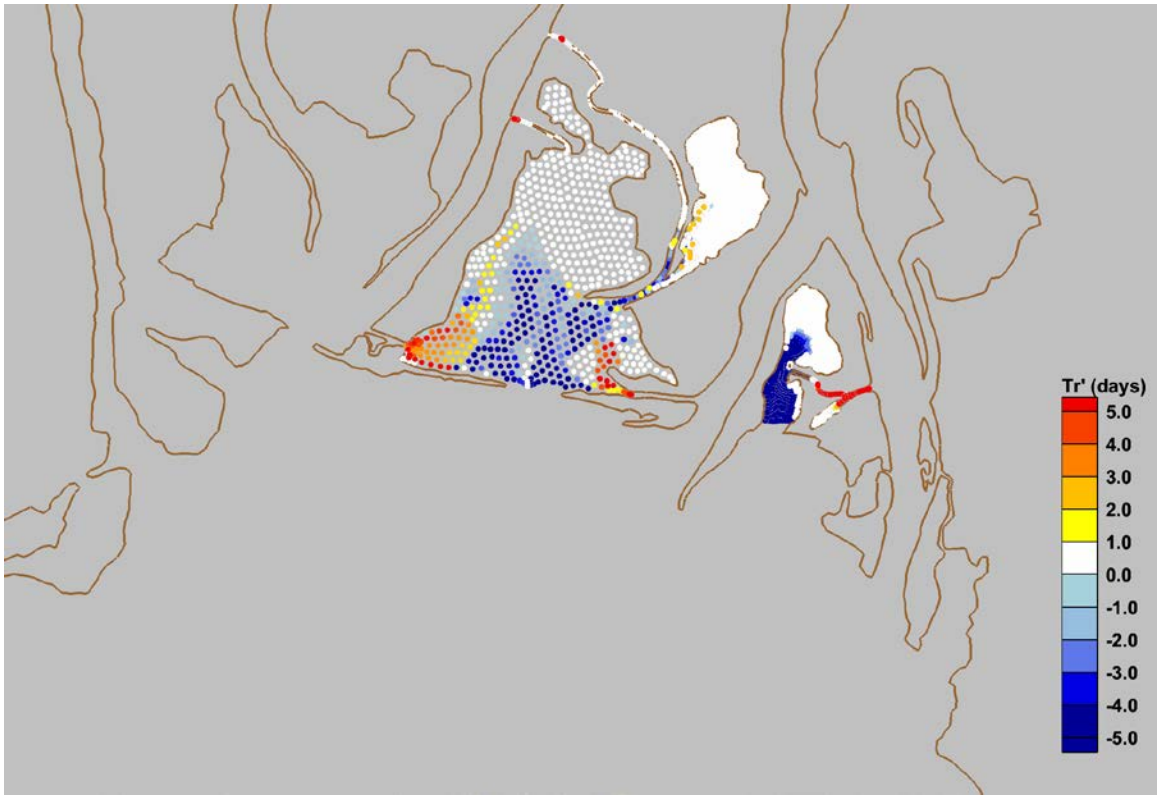

Figure 100. Predicted change in particle residence times (Tr') as a function of initial position from Case 003 to Case 403.

Table 28. System-wide average residence and exposure times and percent of particles removed for Case 403.

Location	Avg. Residence Time (days)		Avg. Exposure Time (days)		% Particles Removed	
	Case 003	Case 403	Case 003	Case 403	Case 003	Case 403
Choccolatta Bay	7.9	7.5	8.4	7.7	20.5	27.3
Justin's Bay	8.4	6.0	8.4	6.1	6.9	41.1

Alternative Simulation Results | Sea Level Rise Scenario

This section describes the potential effects of hypothetical restoration alternatives on hydrodynamic characteristics under representative tidal and flow conditions for an estimated sea level in the year 2100. The sea level offset considered in these scenarios is +0.3 m (about +1 ft higher than present day). The magnitude of river discharge considered in these simulations is representative of the average summer (July) flows. Existing conditions throughout the study area are described first, and then the potential effects of a single restoration alternative are described as changes (increases, decreases, etc.) relative to existing conditions under typical conditions for present day sea levels. These comparisons are made in order to demonstrate the effects of both sea level rise and the restoration alternative on hydrodynamic conditions in the study area.

Existing Conditions - Case 012

These simulation results reflect predictions of the hydrodynamic conditions within the study area, without modification, for an elevated sea level in the year 2100. The forcing conditions consist of representative tides and average summer river discharge with future, higher sea levels. The results of this scenario, when compared to those of Case 002, provide an opportunity to evaluate the effects of sea level rise, alone, on the hydrodynamic behavior of the system. As such, the results of Case 012 will be presented as changes relative to existing conditions with present day sea levels (Case 002).

Water Levels

Predicted changes in maximum water levels for Case 012 are presented in Figure 101, which shows the increase in maximum water levels relative to Case 002. Note that the increases in maximum water levels in Choccolatta Bay, Justin's Bay, and other portions of Mobile Bay were larger than the corresponding sea level offset of +0.3 m, indicating an amplification of water levels. This amplification due to sea level rise is demonstrated in Figure 102. The amplification (Aslr) is calculated as the difference in maximum water levels divided by the sea level offset. Therefore, maximum water levels in Choccolatta Bay were amplified by about 1.25 times greater than the sea level offset, whereas maximum water levels in Justin's Bay and some portions of Shellbank River were amplified by more than 1.5 times the sea level offset.

While the tide range was predicted to increase by 6% and 40% in Choccolatta and Justin's Bays, respectively, there were notable decreases in tide range near Ducker Bay and along Shellbank River. The maximum predicted tide ranges at selected locations in the study area are listed in Table 29, as are their corresponding changes relative to Case 002. Tidal phase lags (not shown) in Choccolatta and Justin's Bays were moderately less than those under present-day sea levels.

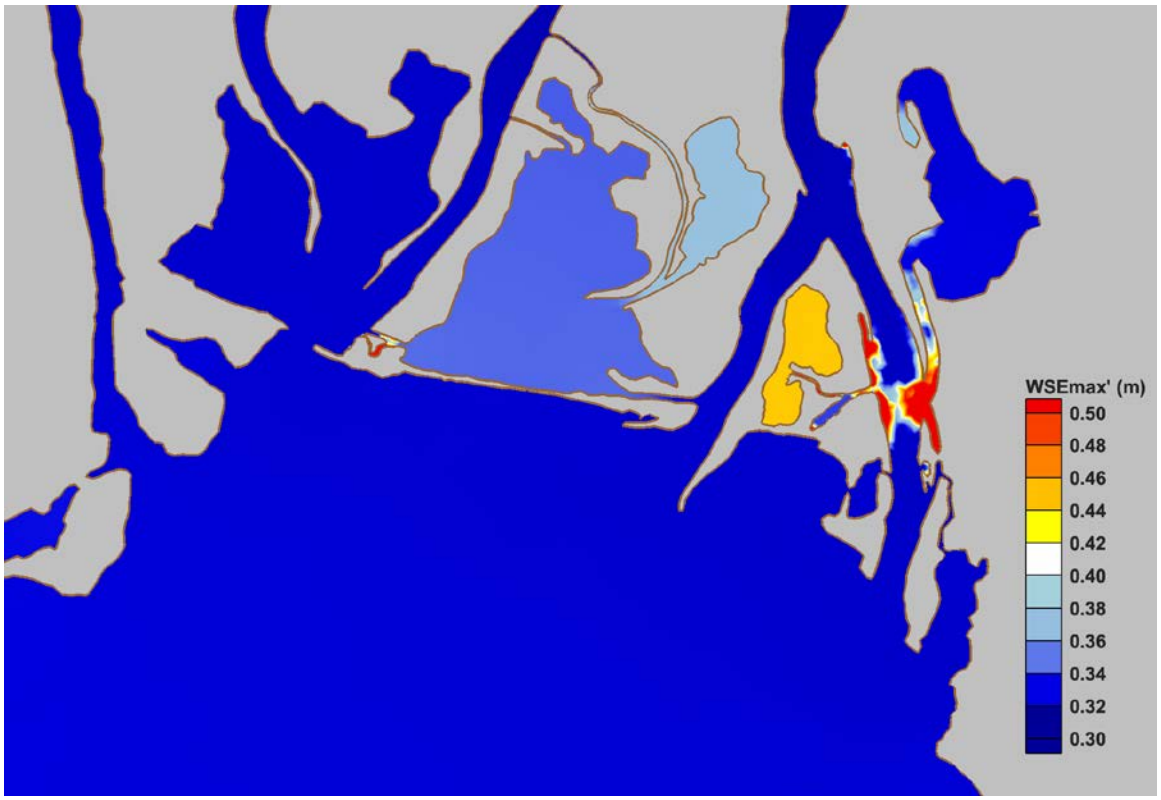

Figure 101. Predicted change in maximum water levels (WSEmax) in the study area from Case 002 to Case 012.

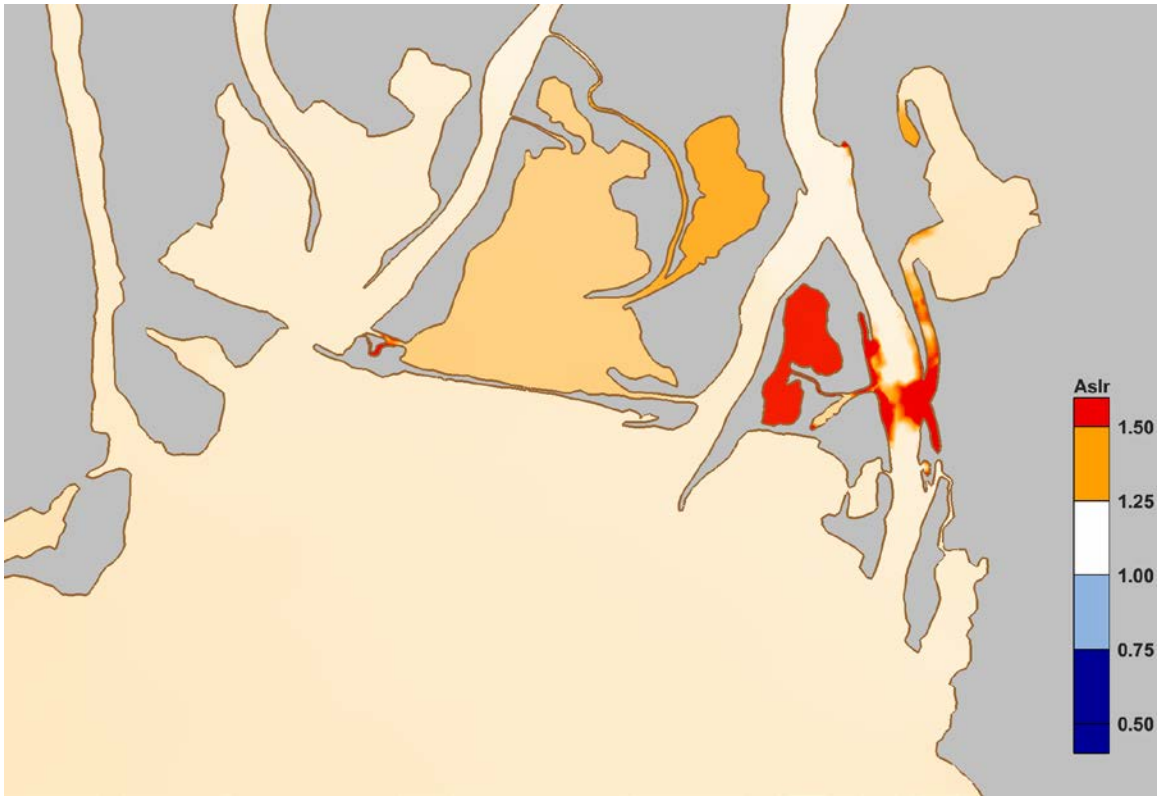

Figure 102. Predicted amplification of maximum water levels due to sea level rise for Case 002 and Case 012.

Table 29. Predicted maximum tide range at selected locations for Case 012 and their relative change from Case 002.

Location	Tide Range (m)	% Change, 002
Choccolatta Bay	0.718	+6.4
North Mobile Bay	0.720	NC
Justin's Bay	0.623	+41.3
Ducker Bay	0.707	-1.5
Shellbank River North	0.697	-3.3
Shellbank River South	0.648	-9.9

Flows

Due to reductions in the frictional nature of the system, the maximum velocities were predicted to change by ±1 m/s. With the exception of a reduction in maximum velocity through lower Conway Creek, most areas of the system exhibited a substantial increase in velocity due to the decreased friction. These predicted changes in maximum depth-averaged water velocity for Case 012, relative to Case 002, are shown in Figure 103.

With the amplification of water levels in Choccolatta Bay and Justin's Bay being higher than surrounding water bodies and rivers, a head difference was established that generated more subtidal flow through these mostly enclosed systems. Changes in the subtidal velocity magnitude were on the order of ±3 cm/s. These changes in subtidal behavior are shown in Figure 104.

Under these existing conditions, the effects of sea level rise reduced the tidal volume exchange in Choccolatta Bay by nearly 68% compared to Case 002, and in Justin's Bay by nearly 74% compared to Case 002. Predicted tidal exchange volumes, calculated as the cumulative discharge (m^3) between successive low and high waters on the largest tide, are listed in Table 30.

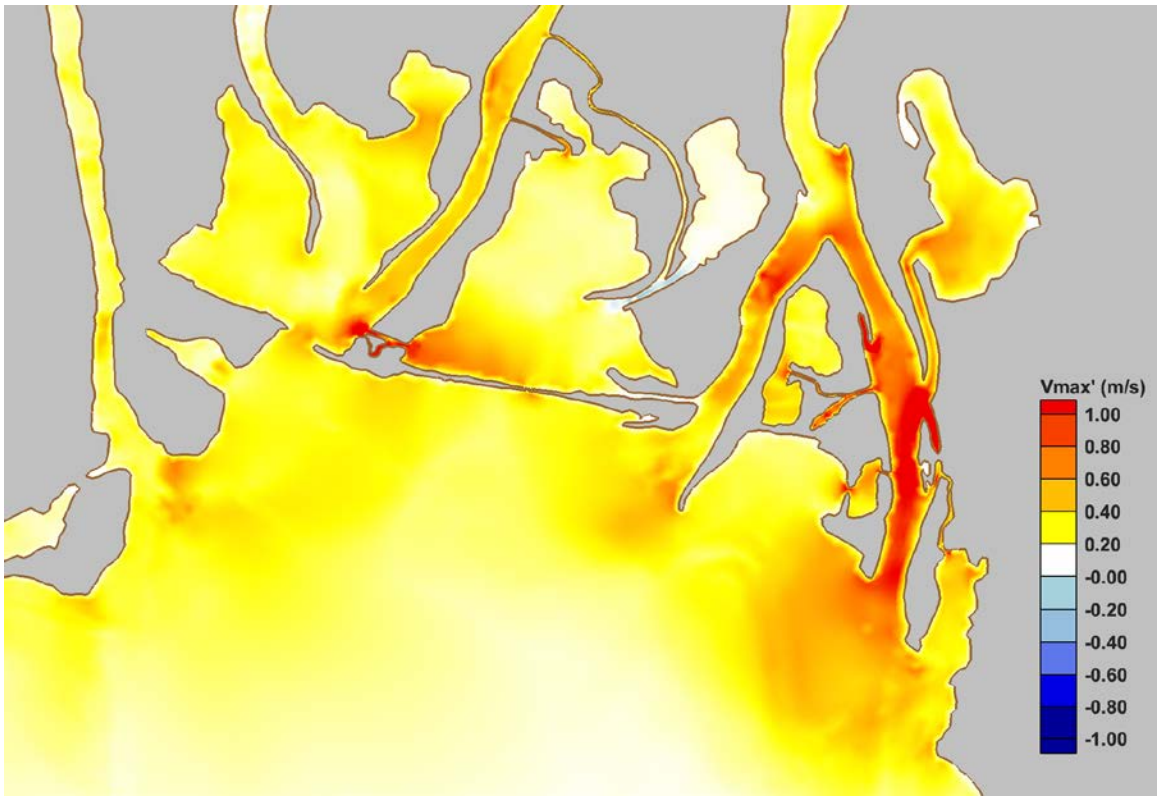

Figure 103. Predicted change in maximum depth-averaged velocity from Case 002 to Case 012.

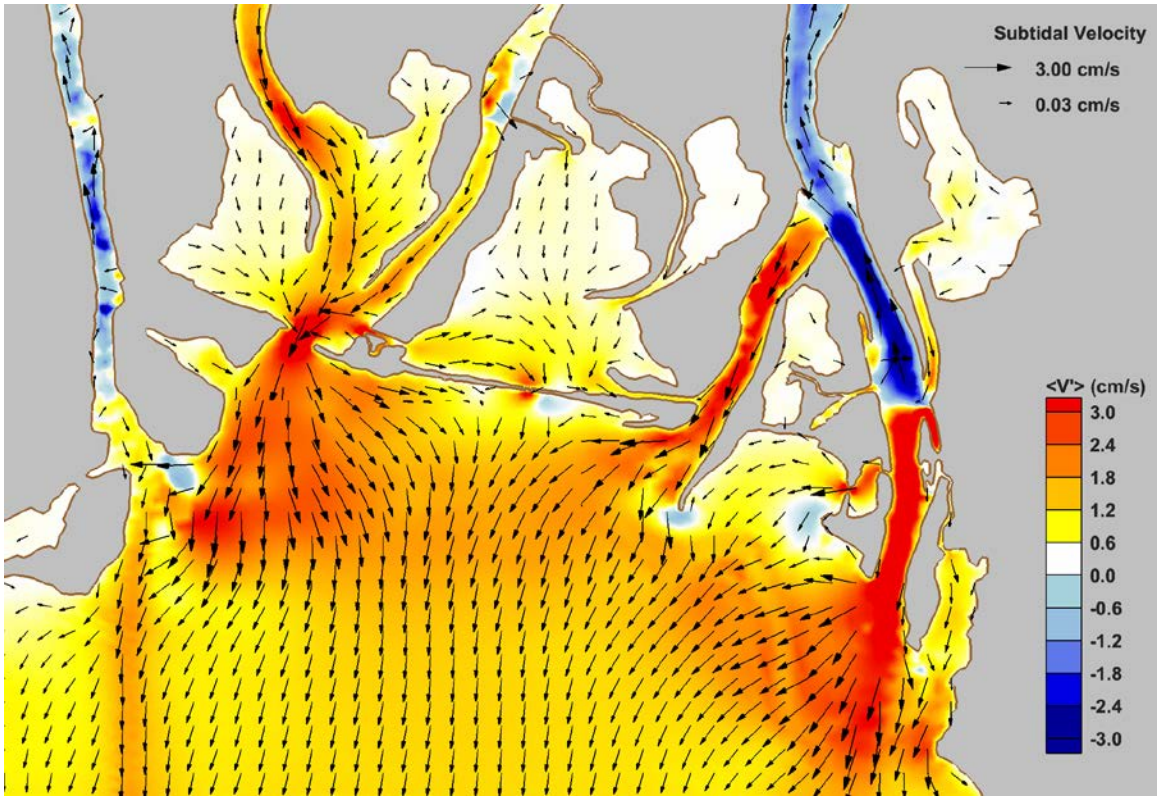

Figure 104. Potential changes in subtidal velocity as a result of sea level rise in the year 2100.

Table 30. Maximum tidal volume exchanged (in cubic meters) between successive low and high water of a maximum tide for Case 012.

Location		Tidal Volume Exchange (m^3)	% Change, 002
Choccolatta Bay	I-10 Cut	919,597	-58.3
	Little Creek	9,938	+51.9
	Conway Creek	595,760	-35.8
	Culverts	28,503	-66.7
	Pass Picada	829,453	-63.5
	Total (net)	**1,171,854**	**-67.7**
Justin's Bay	Sardine Pass	108,137	-73.7

Sediment Transport Potential

The predicted magnitudes of bedload sediment transport and resuspension rates were on the order of ±0.05 $m^3/s/m^2$ and ±0.10 $m^3/s/m^2$, respectively, under existing conditions with sea level rise. These values represent changes on the order of 25% to 50% with respect to existing conditions and present day sea levels. In some areas, the transport and resuspension rates increased due to higher velocities. Some reductions in these rates were noted in areas that were less hydraulically efficient under elevated sea levels. These changes are shown in Figure 105 and Figure 106.

Only modest changes in the depositional tendencies within the study area were noted under elevated sea levels, but their spatial coverage was more comprehensive. Larger interior portions of Choccolatta Bay, for example, were identified as being more depositional in this scenario. However, the behavior of Justin's Bay was predicted to have less potential for deposition under elevated sea levels. Predicted changes in the depositional nature of these systems are shown in Figure 107.

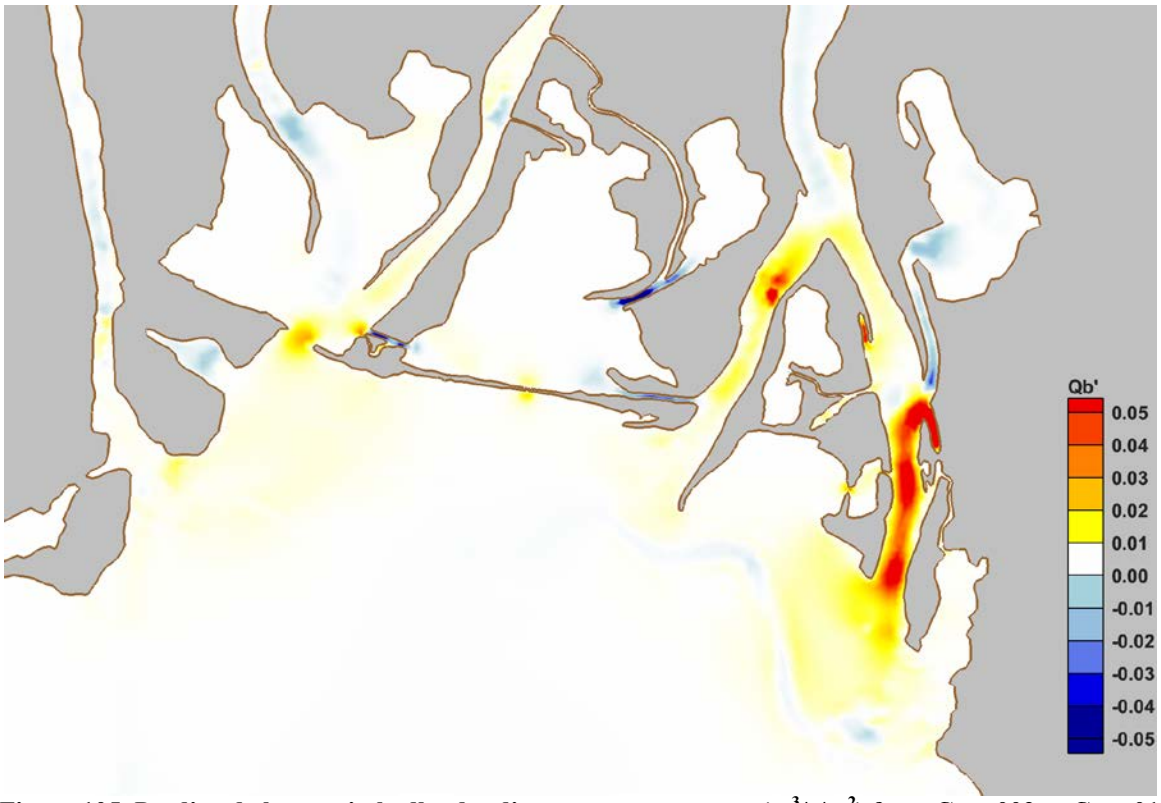

Figure 105. Predicted changes in bedload sediment transport rates ($m^3/s/m^2$) from Case 002 to Case 012.

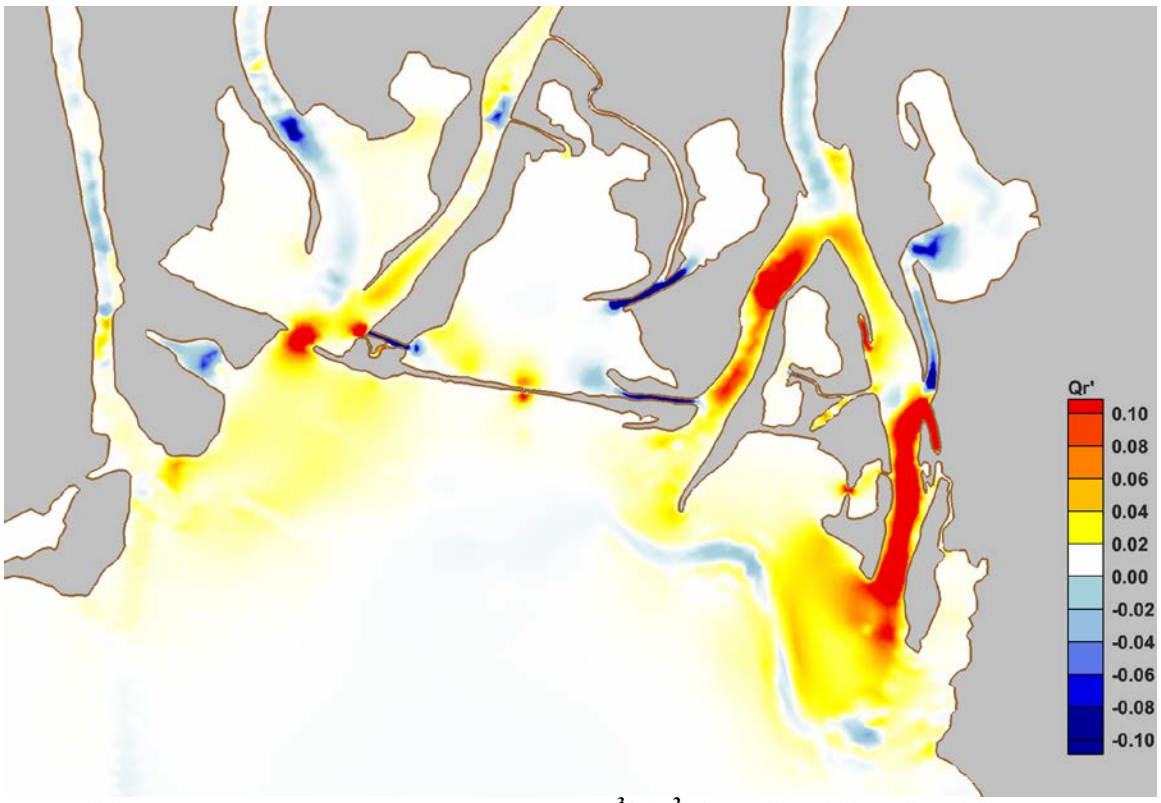

Figure 106. Potential changes in resuspension rates ($m^3/s/m^2$) from Case 002 to Case 012.

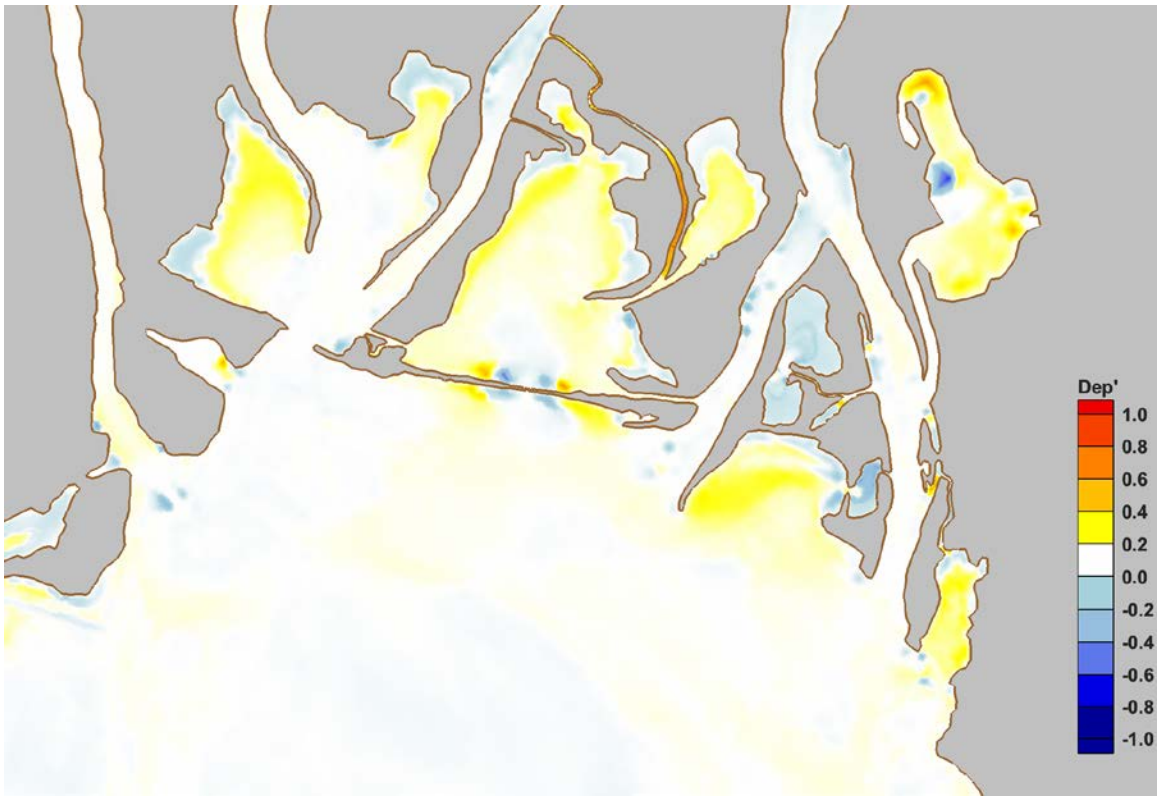

Figure 107. Changes in potential sediment depositional patterns and areas between Case 012 and Case 002.

Flushing

With few exceptions, the flushing capacity was reduced under elevated sea levels, which is consistent with previous observations of reductions in tide ranges, tidal exchange, and velocities. Relative to Case 002, increased residence times and exposure times were noted for individual particles as well as for the entire system. Moreover, 25% fewer particles were flushed from Choccolatta Bay in this scenario as compared to Case 002. Justin's Bay was found to have 40% fewer particles flushed from the system as compared to present-day sea levels. The predicted changes in particle residence times within Choccolatta and Justin's Bays are shown in Figure 108, and their system-wide characteristics are listed in Table 31.

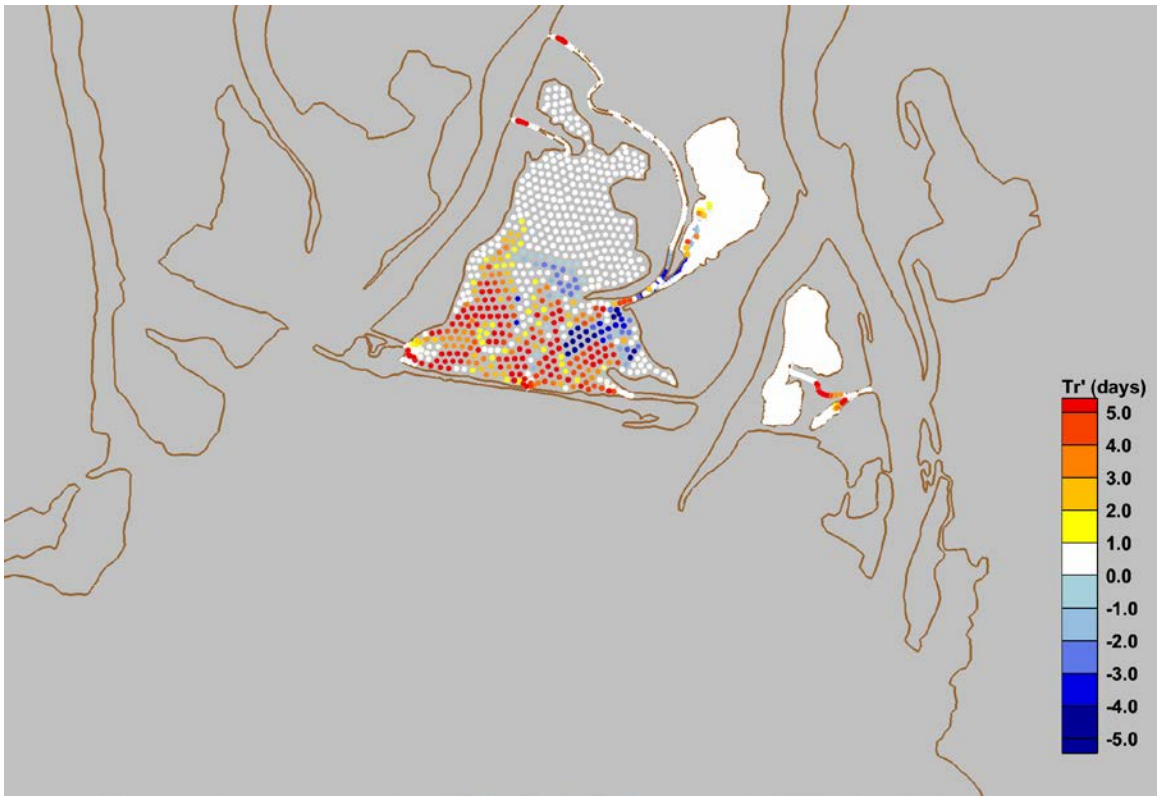

Figure 108. Predicted change in residence time (Tr') relative to particle initial position in Choccolatta and Justin's Bays from Case 002 to Case 012.

Table 31. System-wide average residence and exposure times and percentage of particles removed from the systems for Case 012.

Value	Choccolatta Bay	Justin's Bay
Average Residence Time (days)	8.3	8.6
Average Exposure Time (days)	8.6	8.7
Percentage of Particles Removed	14.8	5.0

Choccolatta Bay - Case 112

This hypothetical restoration scenario considers a constructed opening through the Causeway at Choccolatta Bay only. The forcing conditions consist of representative tides and average summer river discharge under future, elevated sea levels. Simulation results presented for Case 112 are shown as differences relative to existing conditions (Case 002).

Water Levels

The predicted changes in maximum water levels, relative to existing conditions (Case 002), with Choccolatta Bay open, and under elevated sea levels, are shown in Figure 109 (Case 112). The figure shows that the maximum water levels in Chocolatta Bay increased by approximately 4 to 6 cm, with

slightly larger values within Big Bateau. Water level changes in other parts of the system may be attributed to the elevated sea levels as described previously. Similar to the predicted water levels for Case 012, Choccolatta Bay experienced a roughly 25% amplification of maximum water levels due to sea level rise. However, these results were not substantially unique from those of Case 012 without the constructed opening for Choccolatta Bay.

A time-series comparison of water levels in Choccolatta Bay for Case 002 and Case 112 is provided in Figure 111. This figure clearly shows the +0.3 m sea level offset of the tidal signal above what was predicted under existing conditions (Case 002), a larger tide range, and an earlier arrival time for high water relative to existing conditions.

The model predicted a ~10% increase in the tide range for Choccolatta Bay and a ~4% increase in the tide range in Mobile Bay just south of the constructed opening for Choccolatta Bay. Note that in this scenario, the combined effect of the opening and sea level rise was to increase the tide range to a value larger than what was predicted to occur under present day sea levels. Other increases and decreases in tide range throughout the study area, listed in Table 32, may be attributed to elevated sea levels.

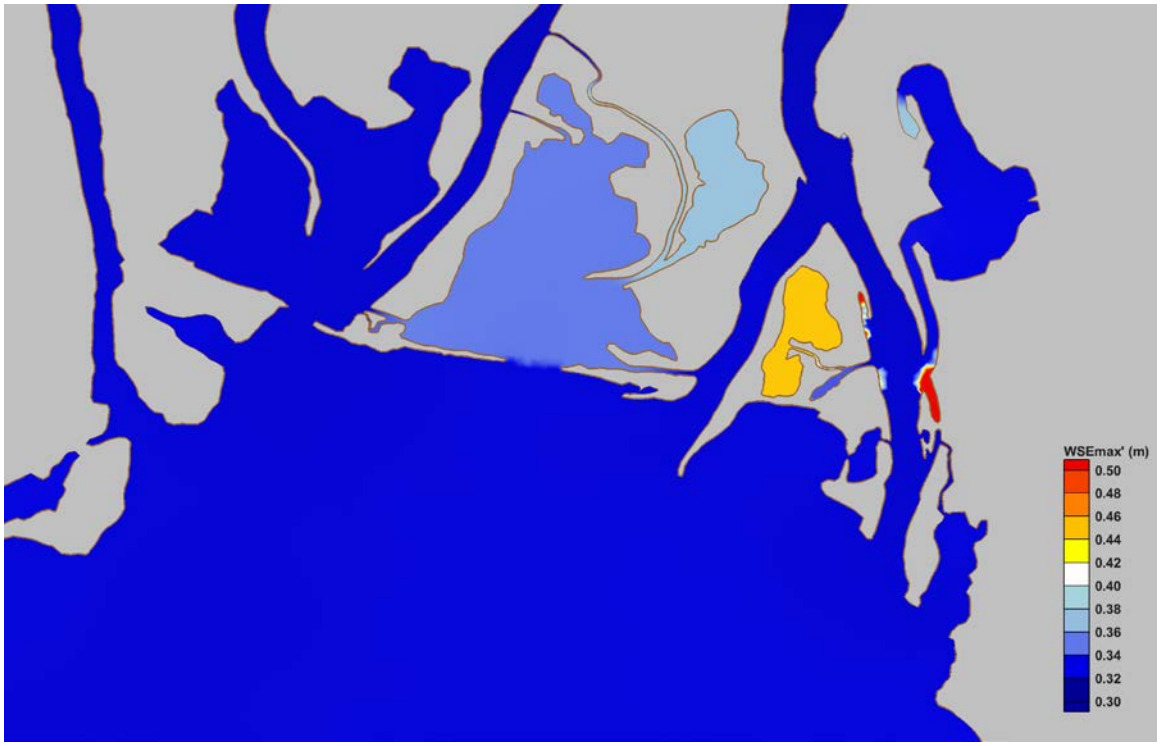

Figure 109. Predicted change in maximum water levels (WSEmax') from Case 002 to Case 112.

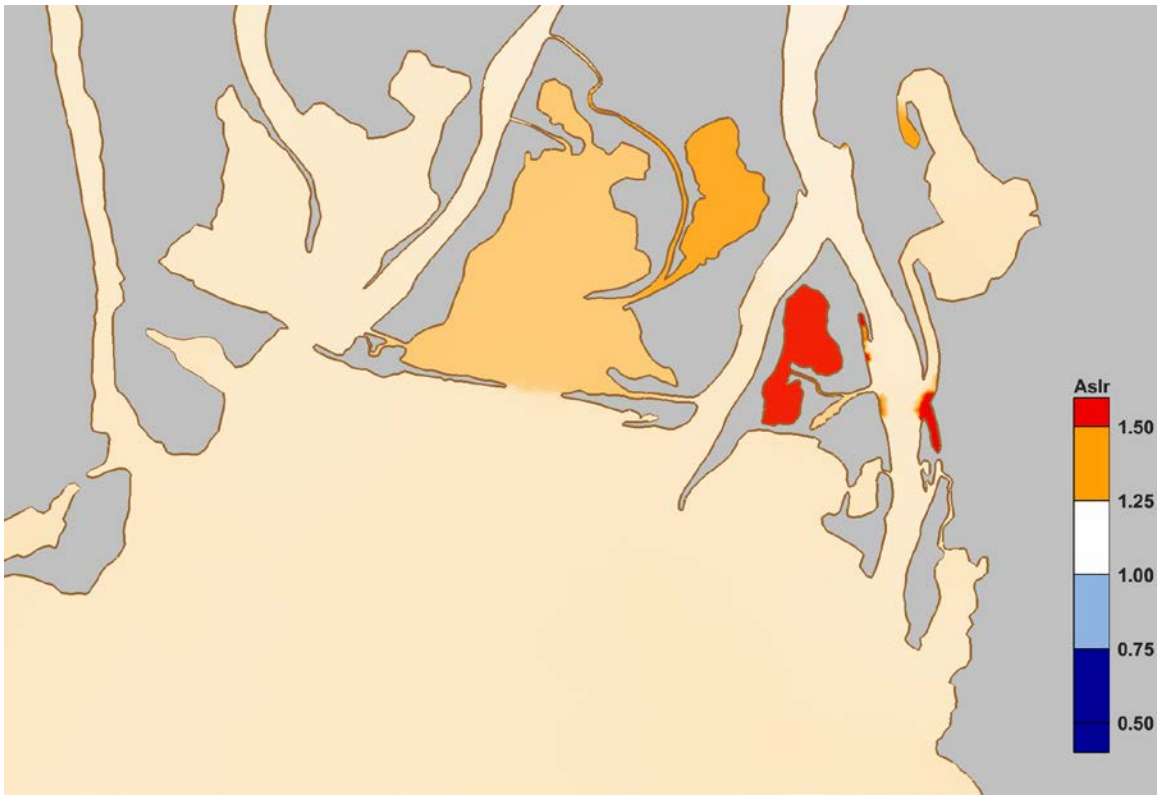

Figure 110. Amplification of maximum water levels due to sea level rise from Case 002 to Case 012.

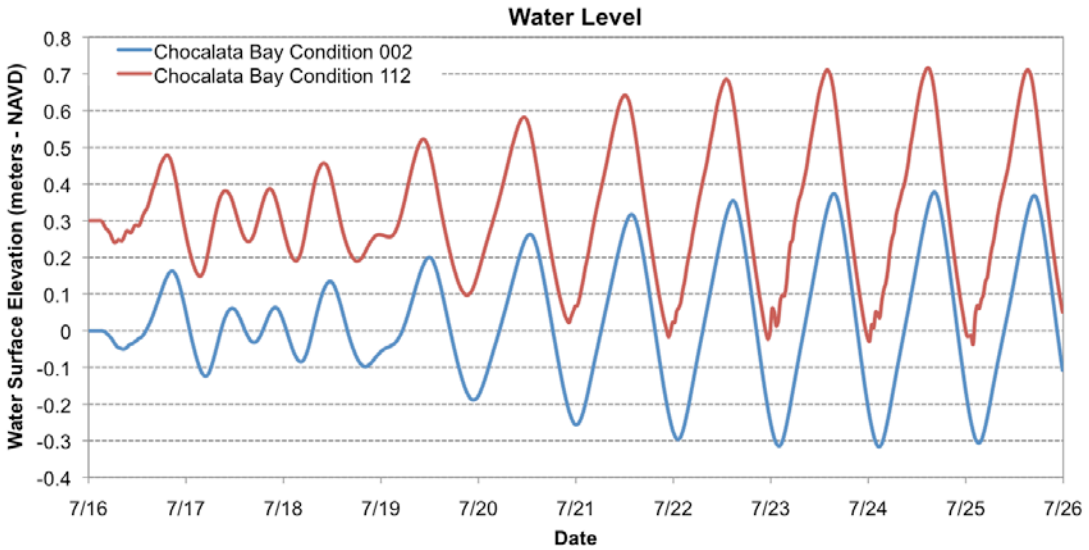

Figure 111. Comparison of predicted water level time-series in Choccolatta Bay for Case 002 and Case 012.

Table 32. Predicted maximum tide ranges for Case 112 and their relative changes from Case 002.

Location	Tide Range (m)	% Change, 002
Choccolatta Bay	0.747	+10.7
North Mobile Bay	0.751	+4.3
Justin's Bay	0.630	+42.9
Ducker Bay	0.706	-1.7
Shellbank River North	0.697	-3.3
Shellbank River South	0.708	-1.5

Flows

The model mostly predicted a more than 30 cm/s increase in maximum depth-averaged velocity throughout the study area, but some reductions of a similar magnitude were predicted to occur in lower Conway Creek, Pass Picada, and I-10 Cut. Recall that some of the demonstrated changes were attributed to the constructed opening, the effects of elevated sea levels, and also combinations of both acting simultaneously. These changes are shown in Figure 112.

Predicted changes in the subtidal flow magnitudes and directions, shown in Figure 113, are on the order of +1 to +3 cm/s in Choccolatta Bay. With the constructed opening in place, the model predicted a substantial seaward-directed subtidal flow throughout much of Choccolatta Bay. Model predictions revealed that the subtidal flow characteristics were such that, on average, flow entered through I-10 Cut and Pass Picada and left through the constructed opening. The model did, however, predict substantial changes in the behavior and magnitude of discharge through these two tidal channels: the discharge magnitudes were substantially reduced and became somewhat irregular.

The model predictions suggest that the effect of the constructed opening in Choccolatta Bay, as well as the influence of elevated sea levels, resulted in a greater than 55% increase in tidal exchange with surrounding water bodies as compared to existing conditions and present day sea levels. While considerable, the increase is substantially less than what was recorded for Case 102, which experienced a greater than 80% increase in tidal volume exchange by opening the Causeway. Therefore, the effect of sea level rise was to dampen, or reduce, tidal forcing and subsequent tidal exchange in this system. A summary of tidal volume exchanges for Choccolatta and Justin's Bays is provided in Table 33.

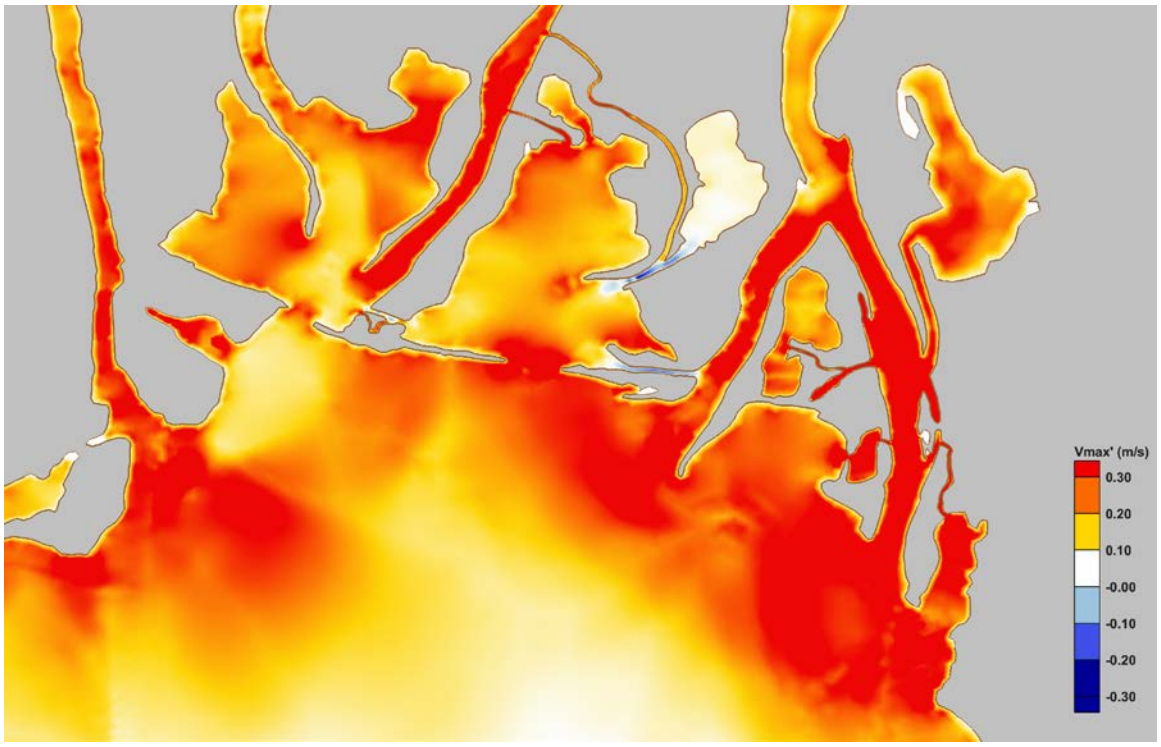

Figure 112. Predicted change in maximum depth-averaged water velocity (Vmax') from Case 002 to Case 112.

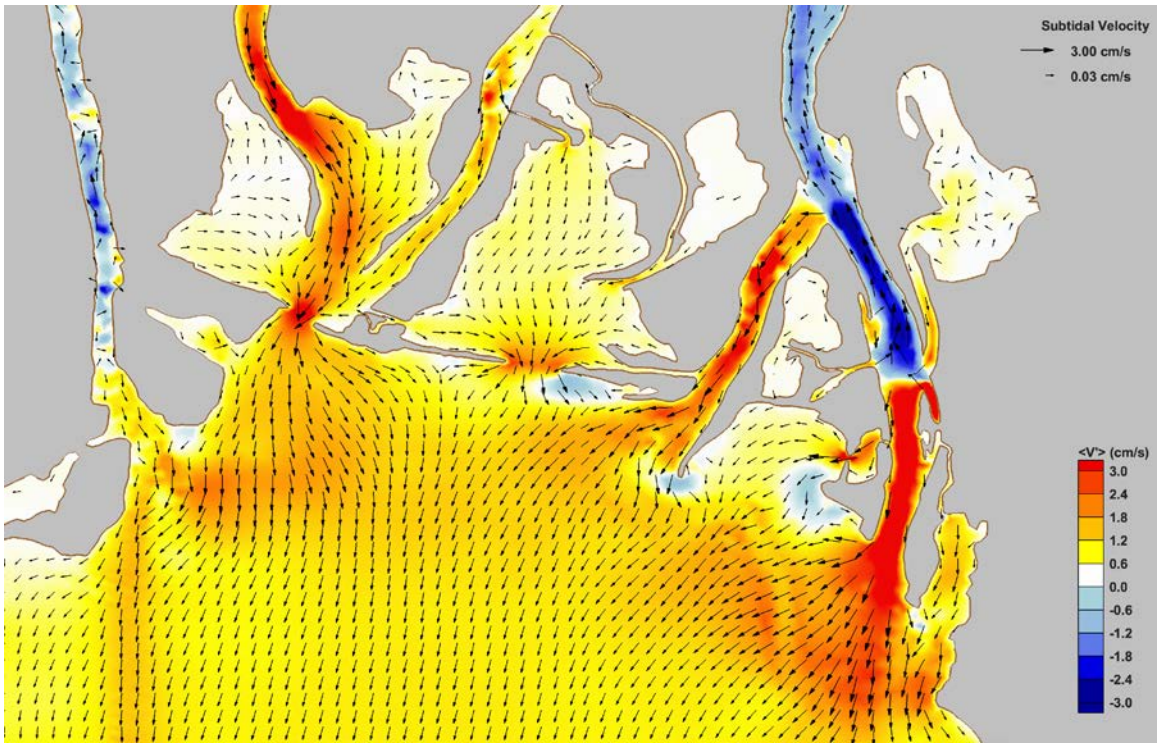

Figure 113. Predicted change in subtidal velocity (<V'>) from Case 002 to Case 112.

Table 33. Maximum tidal volume exchanged (in cubic meters) between successive low and high water of a maximum tide for Case 112, and the percent change relative to existing conditions (Case 002).

Location		Tidal Volume Exchange (m^3)	% Change, 002
Choccolatta Bay	I-10 Cut	218,185	-90.1
	Little Creek	39,260	+500
	Conway Creek	634,705	-31.6
	"Pass Choccolatta"	6,527,542	+7526.8
	Pass Picada	19,307	-99.2
	Total (net)	**5,654,698**	**+55.9**
Justin's Bay	Sardine Pass	220,084	-46.6

Sediment Transport Potential

Predicted increases in bedload sediment transport rates, on the order of ±0.05 $m^3/s/m^2$, were found in Choccolatta Bay with increases confined to the constructed opening. Decreases were noted in lower Conway Creek, I-10 Cut, and Pass Picada. Under this scenario, the reductions in transport rates were of a larger magnitude, on average, than corresponding increases. For example, the increased transport rates near the constructed opening were roughly 10% of the values predicted under existing conditions, but the reductions found in tidal channels were approximately 50% smaller than values predicted under existing conditions. Similar statements regarding the resuspension rates apply, with modest increases near the constructed opening and substantial reductions in tidal channels. These predicted changes in bedload sediment transport and resuspension rates are shown in Figure 114 and Figure 115, respectively.

As demonstrated in Figure 116, much of Choccolatta Bay was predicted to become slightly more depositional across the interior of the water body, whereas areas near I-10 Cut and Pass Picada became strongly depositional as a result of the constructed opening under elevated sea levels. There were reductions in the depositional nature of the system as well, and those were predicted to occur in and near the constructed opening.

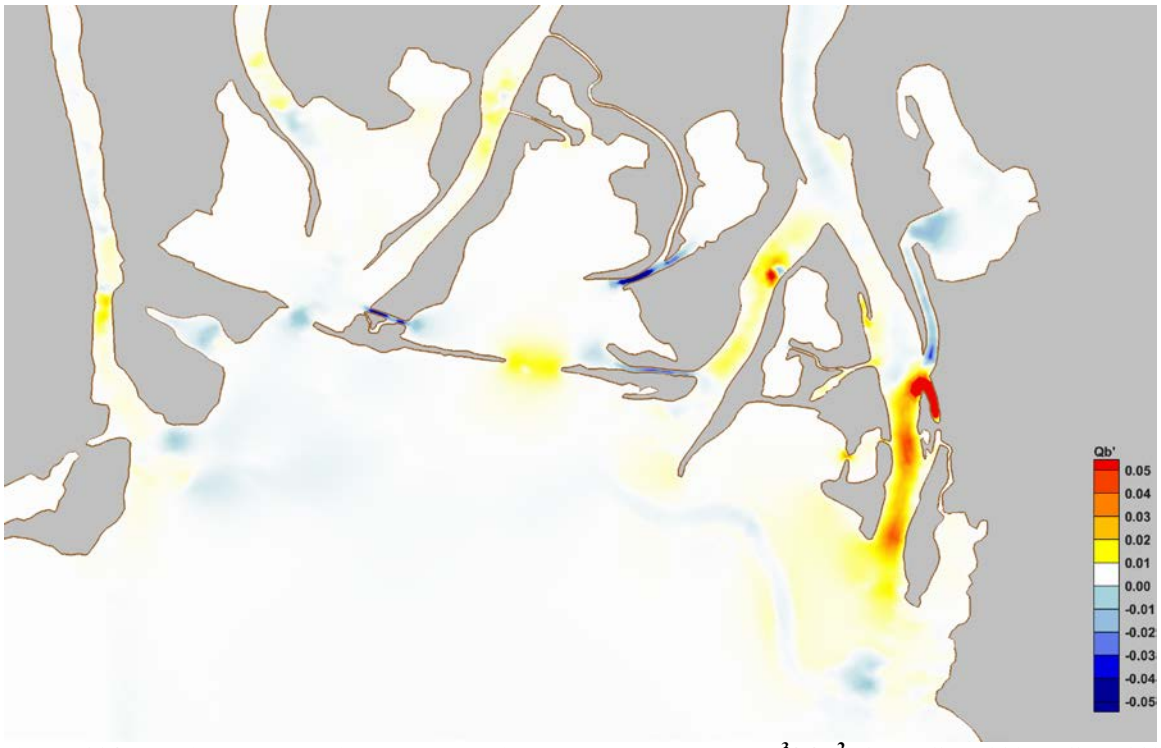

Figure 114. Predicted change in bedload sediment transport rates ($m^3/s/m^2$) from Case 002 to Case 112.

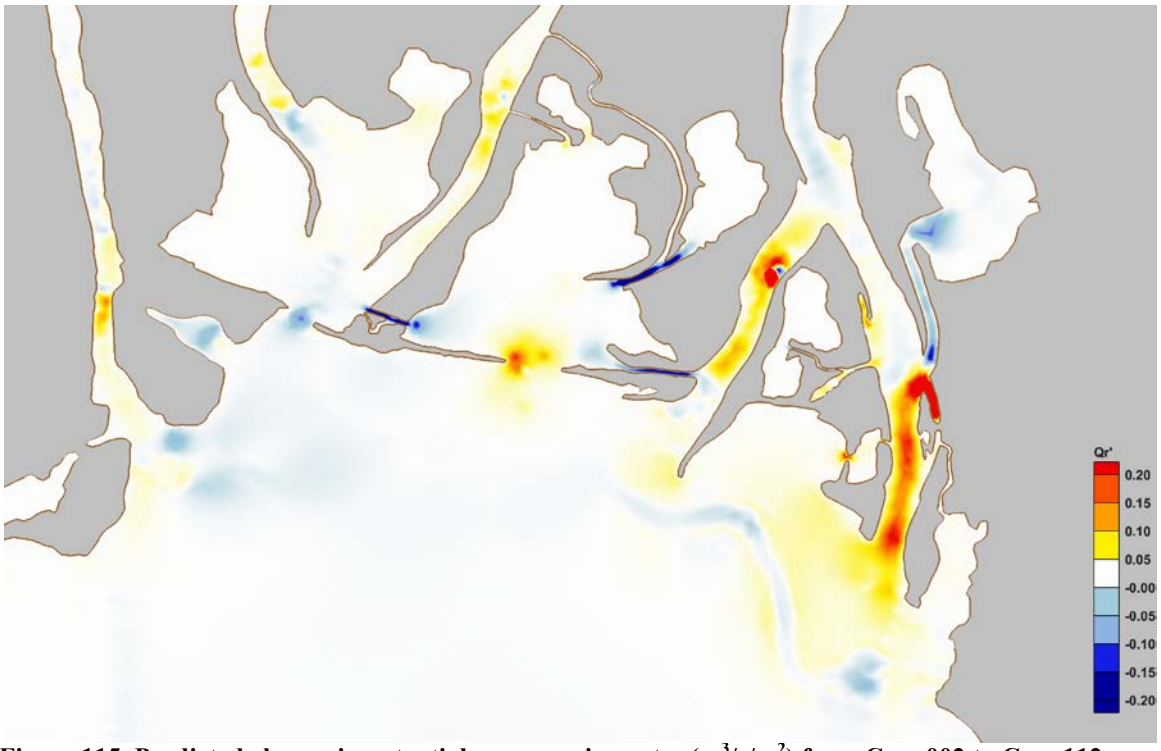

Figure 115. Predicted change in potential resuspension rates ($m^3/s/m^2$) from Case 002 to Case 112.

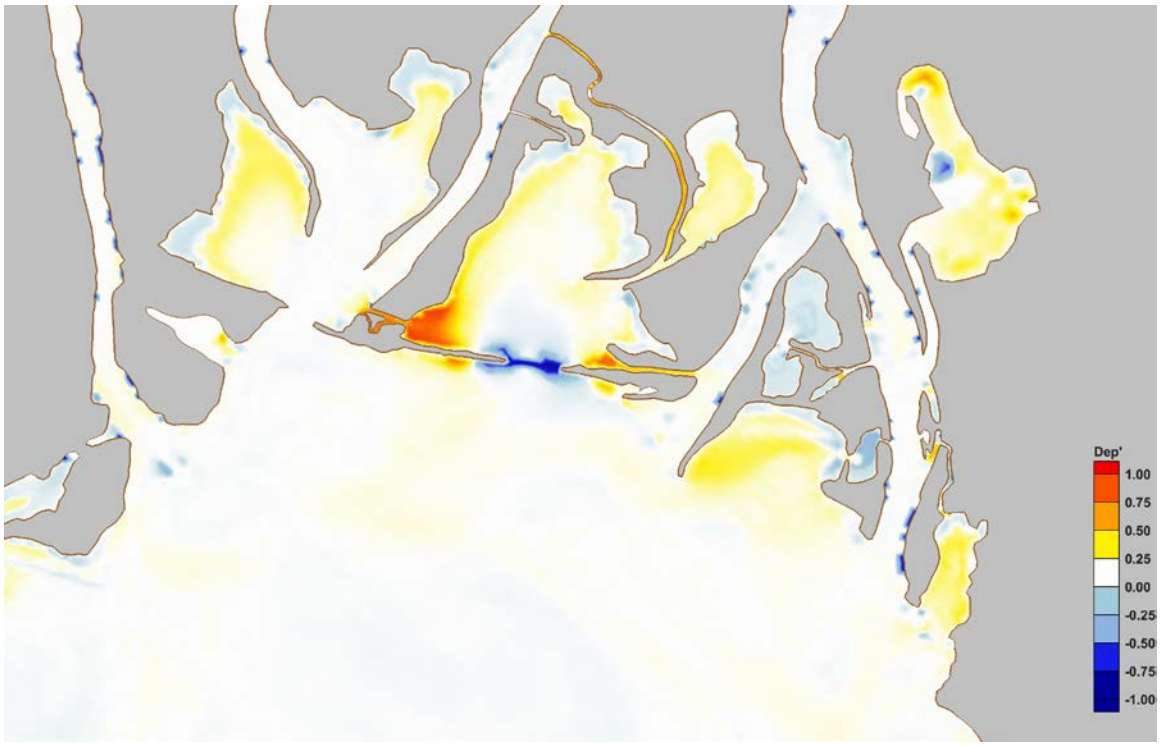

Figure 116. Predicted changes in potential sediment depositional patterns from Case 002 to Case 012.

Flushing

Simulation results showed 3-day increases in residence times near I-10 Cut and Pass Picada, and up to 3-day decreases in residence times adjacent to the constructed opening and through the central portion of the Bay extending northward. No change in particle residence time was predicted for areas in the northern part of the Bay, nor were there substantial changes to residence times in Big Bateau. However, there was an 85% increase in the flushing of particles from Choccolatta Bay as a result of the constructed opening. These results are shown in Figure 117, and a system-wide summary is provided in Table 34.

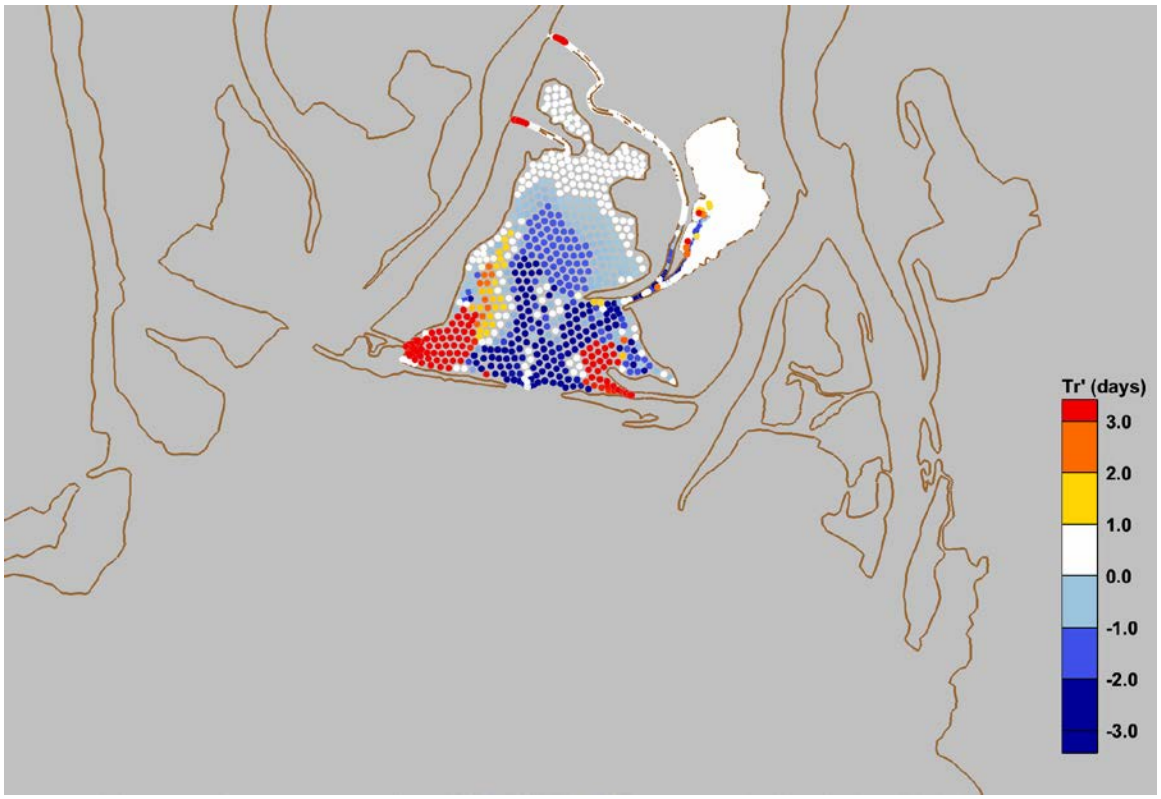

Figure 117. Predicted change in particle residence time (Tr') relative to initial position from Case 002 to Case 112.

Table 34. System-wide average residence and exposure times and percentage of particles removed for Case 112.

Location	Avg. Residence Time (days)		Avg. Exposure Time (days)		% Particles Removed	
	Case 002	Case 112	Case 002	Case 112	Case 002	Case 112
Choccolatta Bay	7.9	7.6	8.4	7.9	20.2	37.7
Justin's Bay	8.4	N/A	8.6	N/A	7.1	N/A

Justin's Bay - Case 212

This hypothetical restoration scenario considers a constructed opening through the Causeway at Justin's Bay only. The forcing conditions consist of representative tides and average summer river discharge under future, elevated sea levels. Simulation results presented for Case 212 are shown as differences relative to existing conditions (Case 002).

Water Levels

Predicted changes in maximum water levels between Case 212 and Case 002 are shown in Figure 118. The results show that Justin's Bay experienced maximum water levels that were between 44 and 46 cm higher than under existing conditions and present day sea levels. A portion of that change is explained by the +0.3 m sea level offset, while the remainder of the increase would be attributed to an increased tide range and amplification of the water levels due to sea level rise. As indicated in Figure 119, the

amplification of maximum water levels in Justin's Bay was over 1.5 times greater than the sea level increment included in the simulation.

With "Pass Justin" in place, the maximum tide range in Justin's Bay was predicted to increase by almost 63% relative to existing conditions and current sea levels. The tidal phase was also modified, eliminating the nearly three-hour tidal phase lag that defined the system under existing conditions and present day sea levels. The change in tide range and phase are demonstrated in the time-series comparison of water levels shown in Figure 120. The sea level offset of +0.3 m is clearly evident in the results. The maximum predicted tide ranges in Justin's Bay and other locations are provided in Table 35, as well as their changes relative to Case 002.

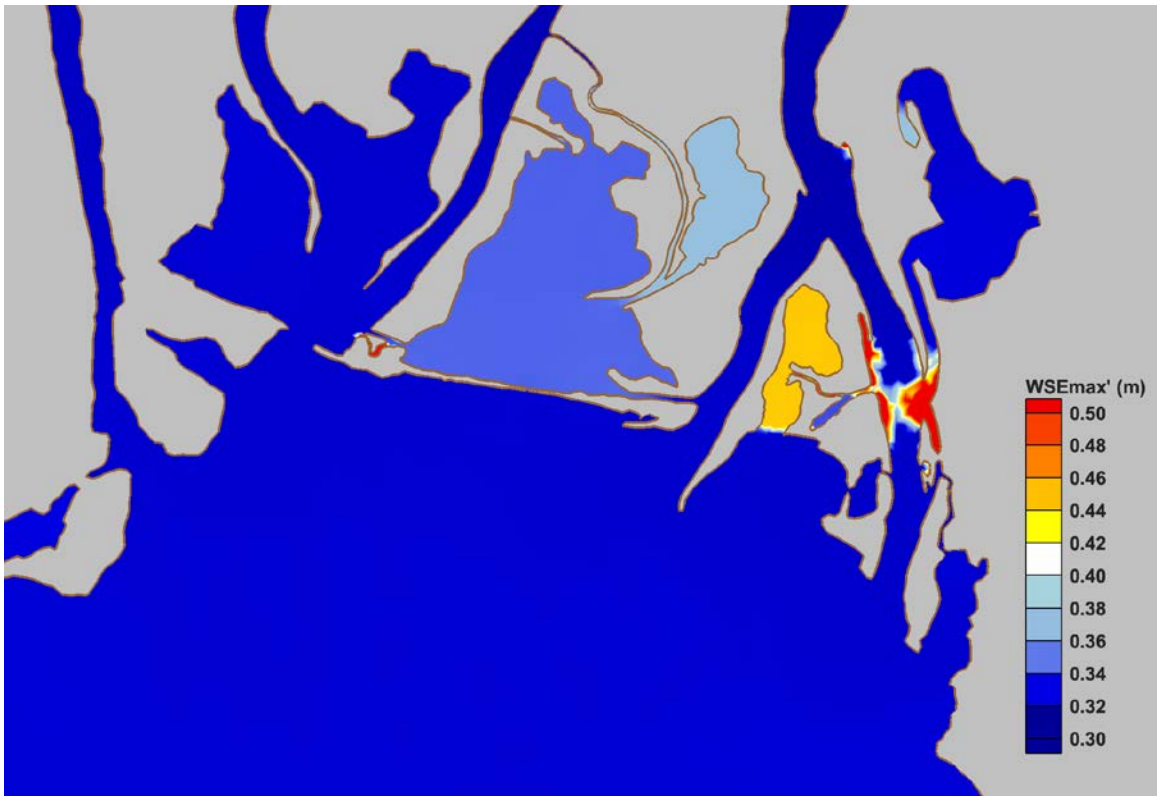

Figure 118. Predicted change in maximum water levels (WSEmax') from Case 002 to Case 212.

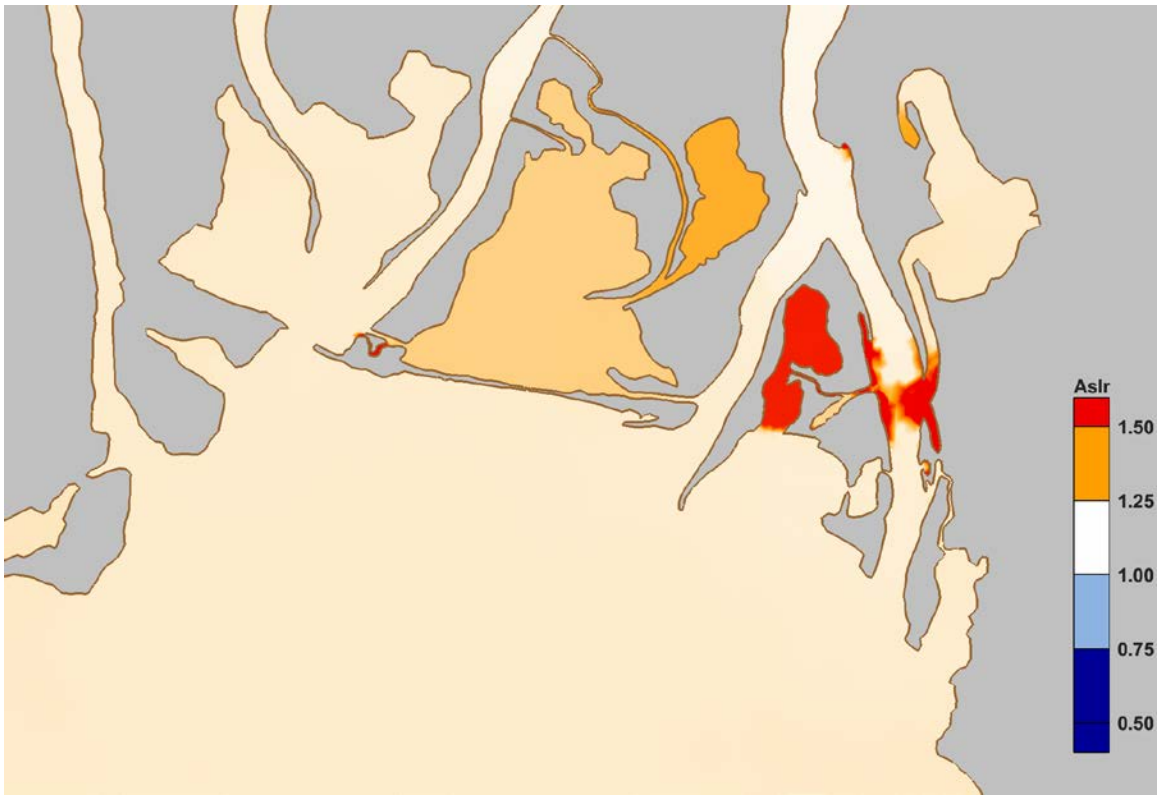

Figure 119. Predicted amplification of maximum water levels due to sea level rise for Case 212. Amplification is calculated as the difference in water levels between Case 212 and Case 002 divided by the sea level offset of 0.3 m.

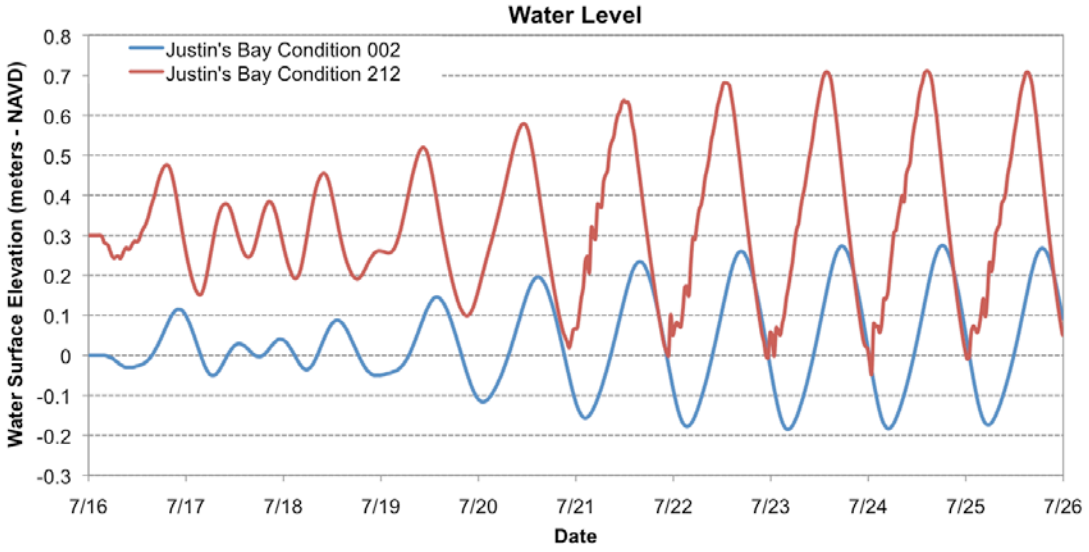

Figure 120. Predicted water level time-series in Justin's Bay for Case 002 and Case 212.

Table 35. Predicted maximum tide ranges for Case 212 and their relative changes from Case 002.

Location	Tide Range (m)	% Change, 002
Choccolatta Bay	0.719	+6.5
North Mobile Bay	0.724	<+1
Justin's Bay	0.717	+62.6
Ducker Bay	0.707	-1.5
Shellbank River North	0.675	-6.4
Shellbank River South	0.710	-1.3

Flows

Focusing specifically on Justin's Bay, the predicted changes in maximum velocity were on the order of +50 cm/s relative to existing conditions. Similar changes were also predicted for Sardine Pass and some areas of Choccolatta Bay. Overall, the maximum flows were predicted to increase considerably. These changes in maximum depth-averaged velocity are shown in Figure 121.

As shown in Figure 122, the predicted change in subtidal flow velocity magnitude and direction in and adjacent to Justin's Bay was an increase in southward flow on the order of +2 to +3 cm/s. These increases covered much of Justin's Bay, the constructed opening, and John's Bend to the south. Model results indicated a reduction in subtidal flow in Ducker Bay. However, the results indicated that there was considerably more subtidal flow directed to the south in much of northern Mobile Bay.

As described previously for Case 202, one implication of opening Justin's Bay through the Causeway was that the hydraulic efficiency of Duck Skiff Pass and Sardine Pass was substantially reduced. Under existing conditions Sardine Pass served as the only conduit for Justin's Bay. With the larger opening in place, the model predicted a five-fold decrease in the volume rate of discharge moving through Sardine Pass with a net exchange direction pointed into Justin's Bay.

The tidal exchange in Justin's Bay was predicted to increase by 11% relative to existing conditions. A summary of calculated tidal exchange volumes for Choccolatta Bay and Justin's bay is provided in Table 36.

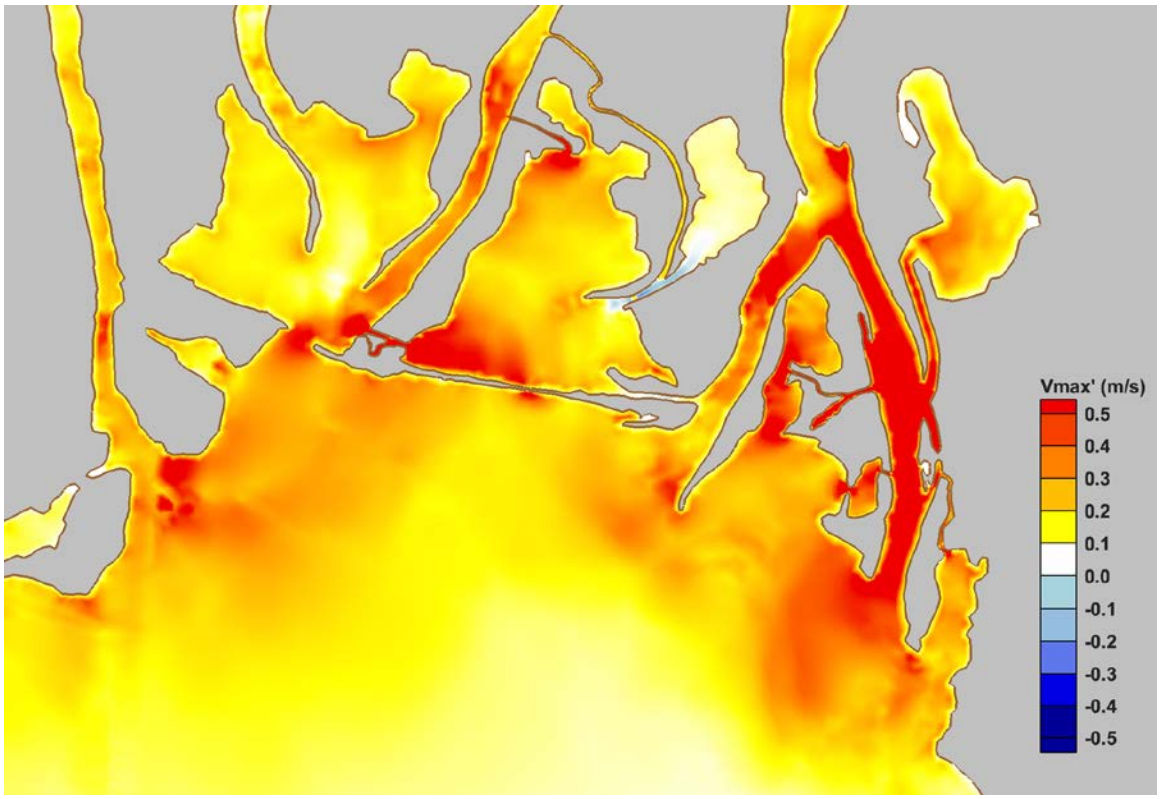

Figure 121. Predicted change in maximum depth-averaged velocity (Vmax') from Case 002 to Case 212.

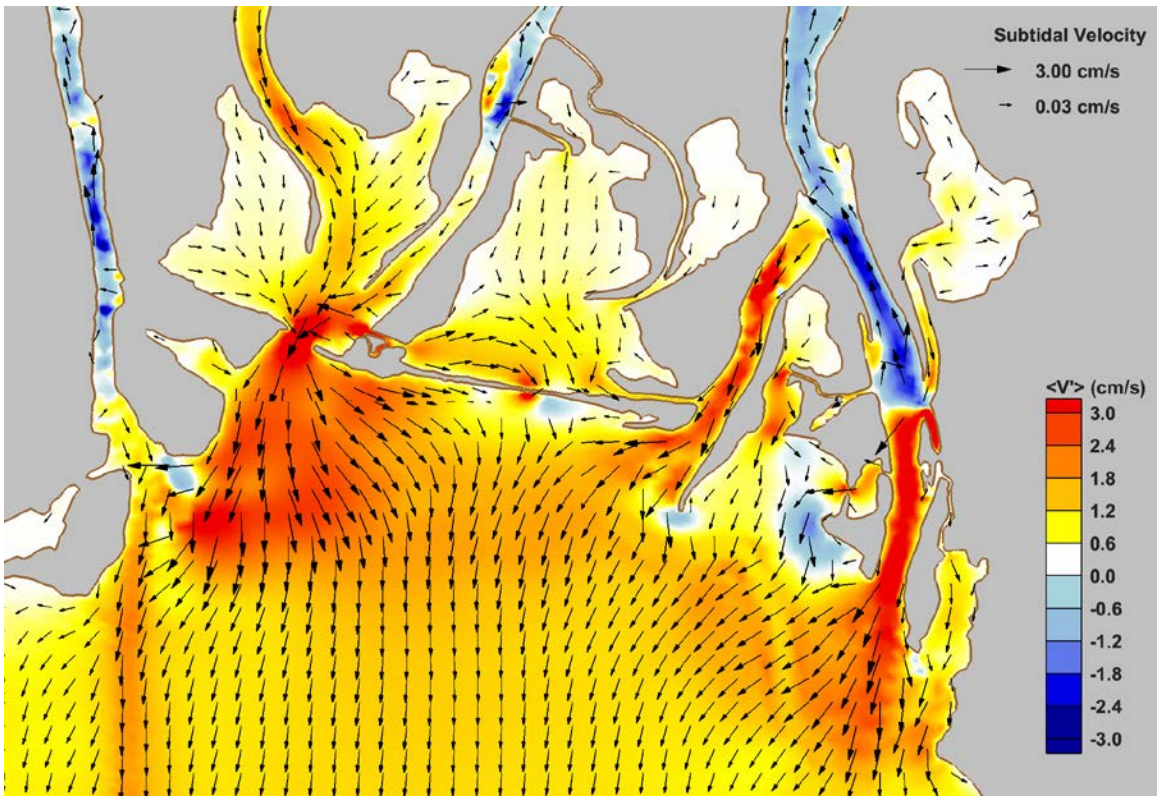

Figure 122. Predicted change in subtidal velocity (<V'>) from Case 002 to Case 212.

Table 36. Maximum tidal volume exchanged (in cubic meters) between successive low and high water of a maximum tide for Case 212, and the percent change relative to existing conditions (Case 002).

Location		Tidal Volume Exchange (m^3)	% Change, 002
Choccolatta Bay	I-10 Cut	985,068	-55.3
	Little Creek	11,545	+76.5
	Conway Creek	611,377	-34.1
	Culverts	28,280	-67
	Pass Picada	817,805	-64
	Total (net)	**1,208,230**	**-66.7**
Justin's Bay	Sardine Pass	198,430	-51.8
	"Pass Justin"	259,290	N/A
	Total (net)	**457,720**	**+11.2**

Sediment Transport Potential

Evaluating at the potential effects of the constructed opening on Justin's Bay and adjacent water bodies, the model results showed increased bedload transport and sediment resuspension in the Bay, as well as the lower portion of Sardine Pass. The magnitudes of the bedload and resuspension increases were approximately 8% and 10%, respectively. Most of these changes were confined to the middle and lower portions of Justin's Bay, with very little change predicted in the upper portions of the Bay. Predicted changes in bedload sediment transport rates and sediment resuspension rates are provided in Figure 123 and Figure 124, respectively.

Predicted changes in sediment deposition, shown in Figure 125, suggest that Justin's Bay would become much less depositional than it was under existing conditions, with perhaps no deposition potential at all in the area between Duck Skiff Pass and the Causeway. The results, however, do indicate some isolated areas that became more depositional and those were found in the portion of Sardine Pass closest to Blakeley River.

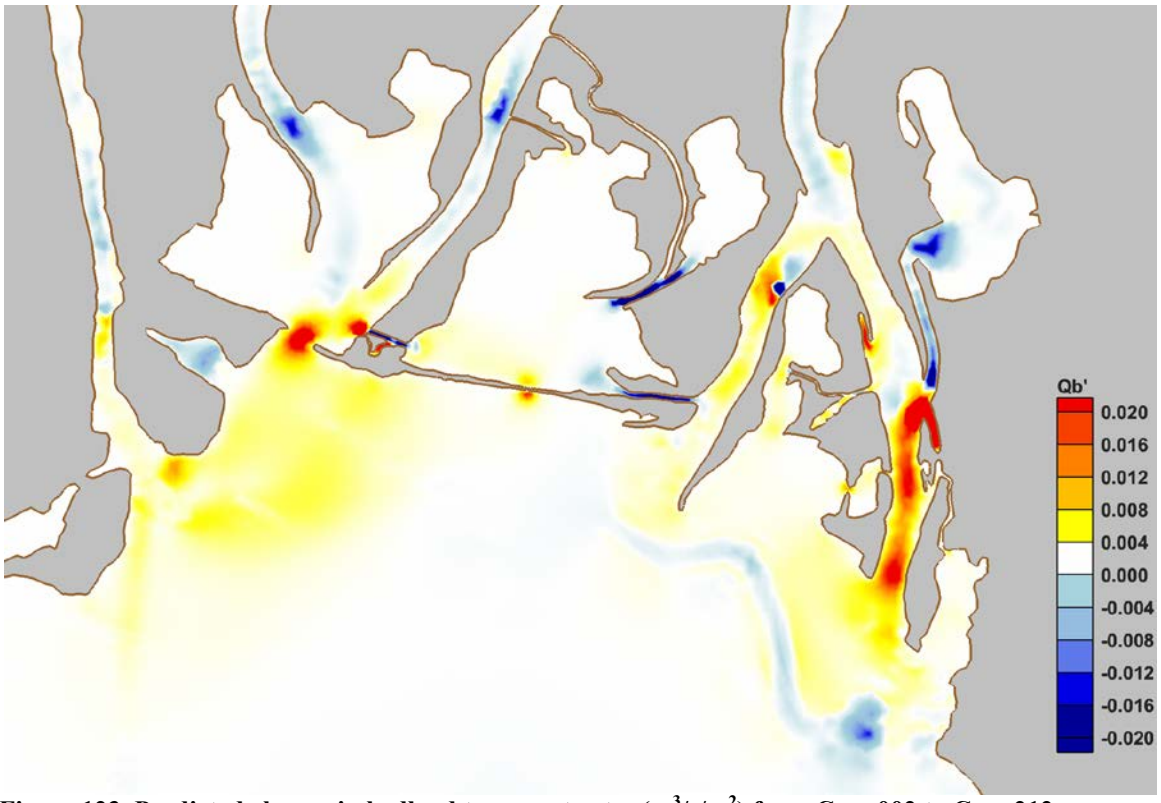

Figure 123. Predicted change in bedload transport rates ($m^3/s/m^2$) from Case 002 to Case 212.

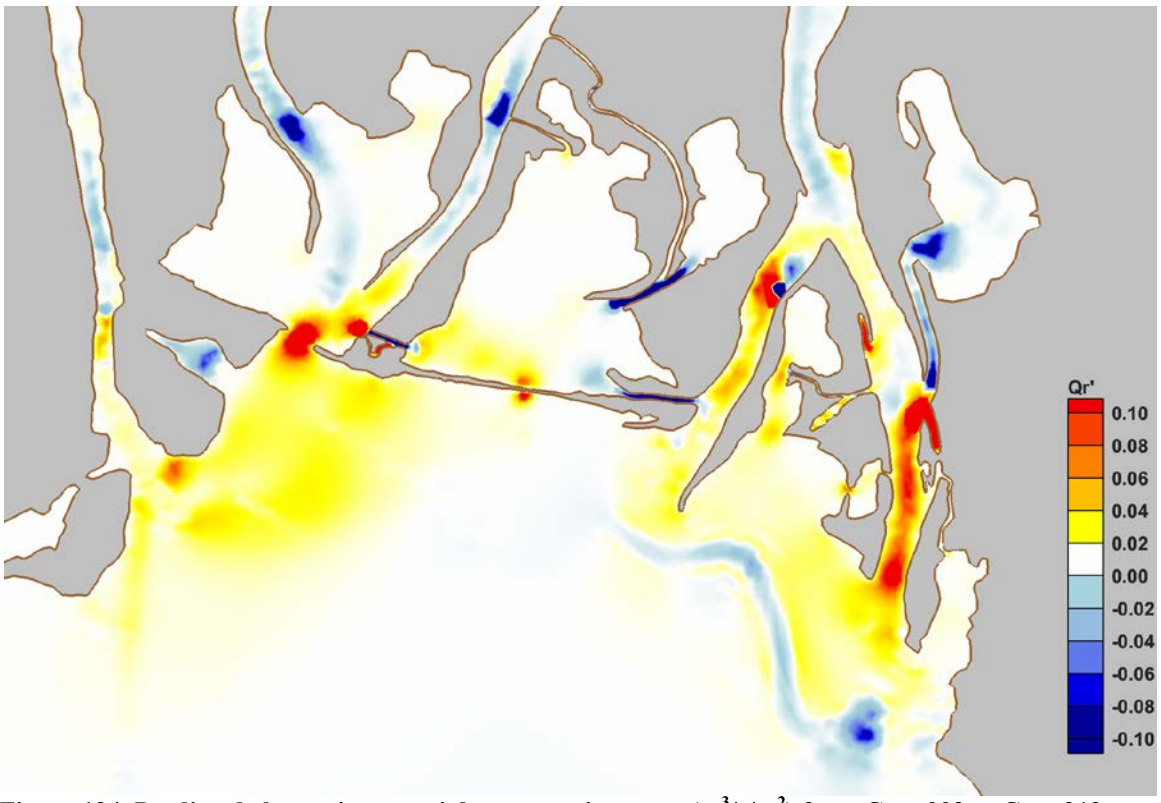

Figure 124. Predicted change in potential resuspension rates ($m^3/s/m^2$) from Case 002 to Case 212.

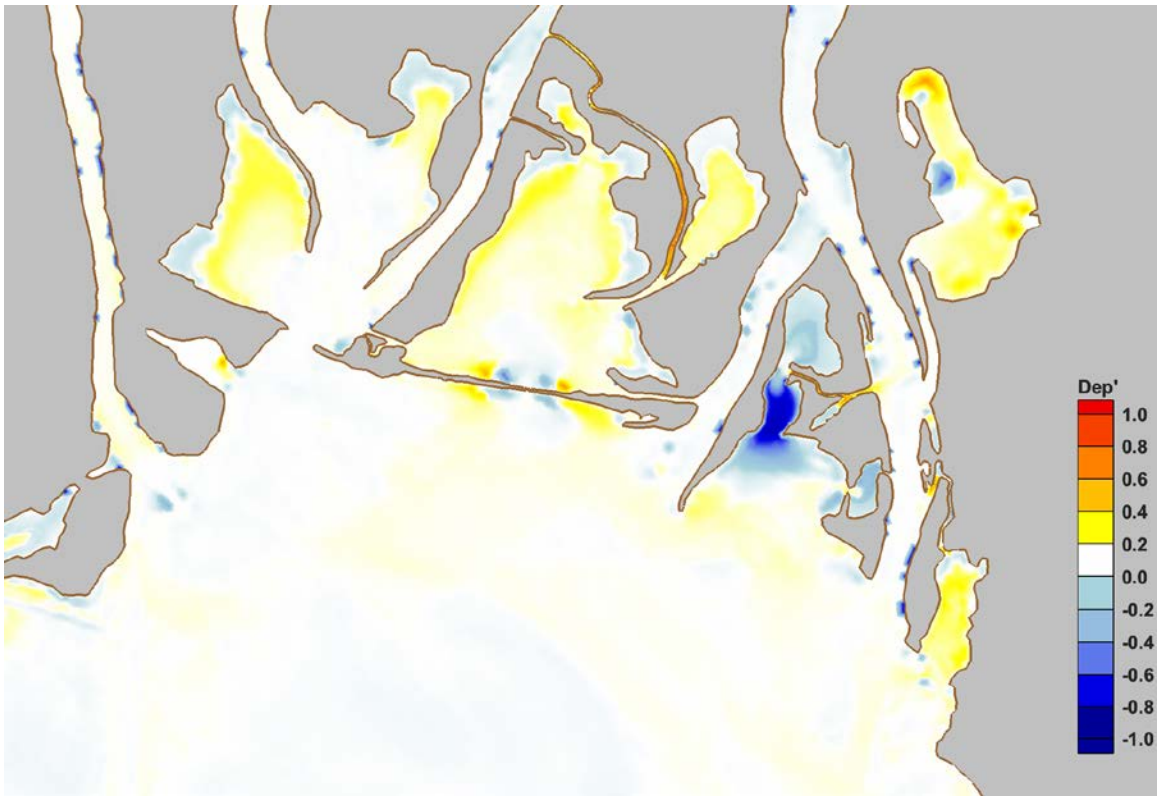

Figure 125. Predicted changes to sediment depositional patterns and areas from Case 002 to Case 212.

Flushing

The predicted impacts of "Pass Justin" on the flushing capacity of Justin's Bay was clearly to improve flushing south of Duck Skiff Pass, but reduce flushing potential through Duck Skiff Pass and portions of Sardine Pass. The model predicted an eight-fold increase in the number of particles flushed from the Justin's Bay system, with 100% of them leaving through "Pass Justin." Decreases in residence time were found to be on the order of 8 days, whereas some particle residence times in Sardine Pass increased by as much as 8 days, relative to existing conditions. These predicted changes in particle residence times in Justin's Bay are shown in Figure 126. The system-wide residence and exposure time values, shown in Table 37, indicate 2-day decreases in those times.

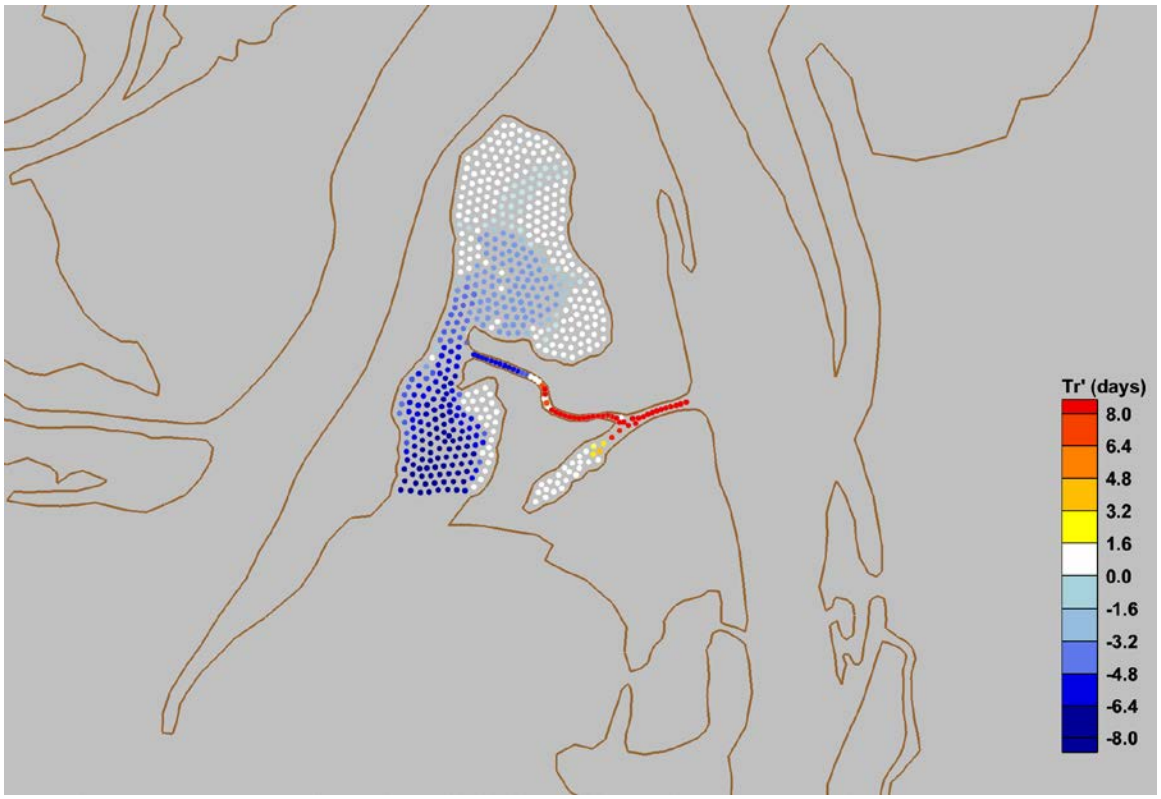

Figure 126. Predicted change in residence times (Tr') within Justin's Bay for Case 212 relative to Case 002.

Table 37. System-wide average residence and exposure times and percentage of particles removed for Case 212.

Location	Avg. Residence Time (days)		Avg. Exposure Time (days)		% Particles Removed	
	Case 002	Case 212	Case 002	Case 212	Case 002	Case 212
Choccolatta Bay	7.9	N/A	8.4	N/A	20.2	N/A
Justin's Bay	8.4	6.3	8.6	6.6	7.1	54.2

Shellbank River - Case 312

This hypothetical restoration scenario considers a constructed opening through the Causeway at Shellbank River only. The forcing conditions consist of representative tides and average summer river discharge under future, elevated sea levels. Simulation results presented for Case 312 are shown as differences relative to existing conditions (Case 002).

Water Levels

Since Shellbank River is mostly well connected to tidal influence, most of the predicted increase in maximum water levels (+32 cm) is attributed to the sea level offset considered in the simulation. Therefore, the model did not predict substantial changes in maximum water levels in Shellbank River as a result of its constructed opening through the Causeway. These predicted changes in maximum water levels for Shellbank River are shown in Figure 127. The corresponding amplification of water levels due to sea level rise was marginal in Shellbank River, as demonstrated in Figure 128.

The local effect of opening Shellbank River was to decrease the tide range by about 3% to 7%, which suggests that the opening through the Causeway would act like a relief valve, reducing water levels that may increase due to trapping in those areas. Model predictions of maximum tide ranges at selected locations in the study area, and their changes relative to existing conditions, are listed in Table 38.

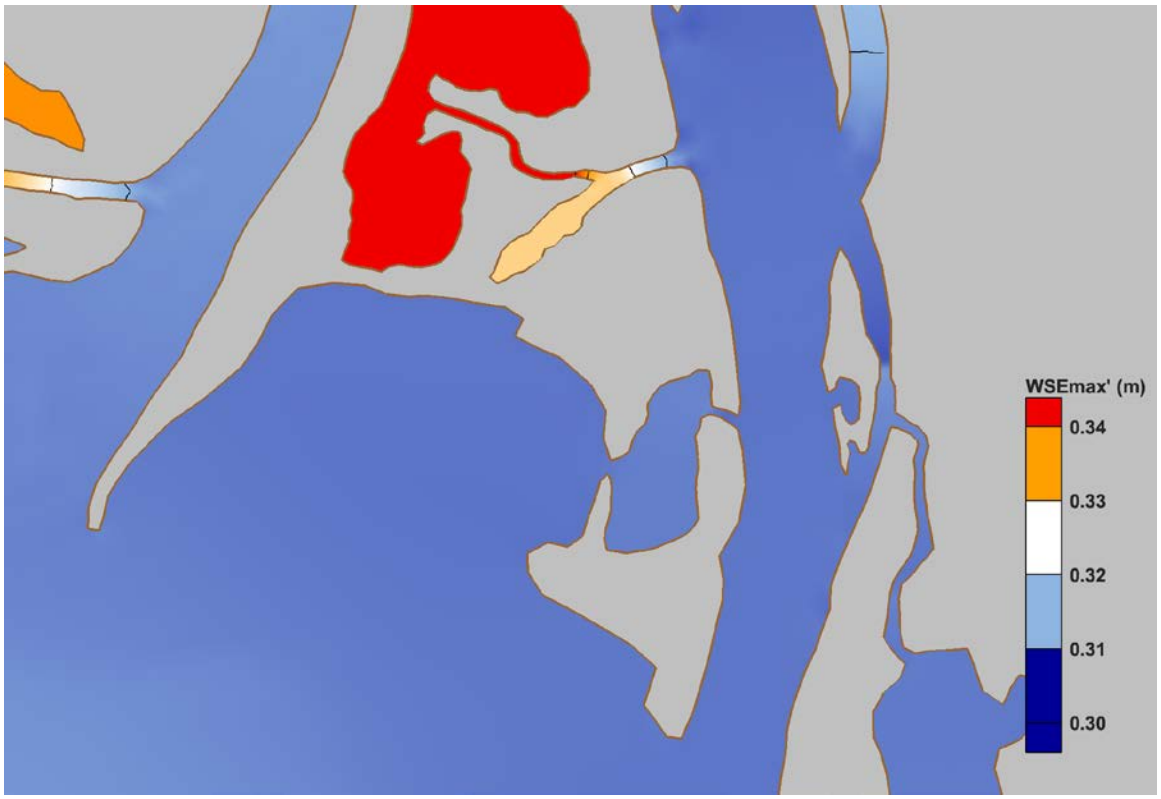

Figure 127. Predicted change in maximum water levels (WSEmax') from Case 002 to Case 312.

Figure 128. Amplification of maximum water levels due to sea level rise for Case 002 and Case 312.

Table 38. Predicted maximum tide ranges for Case 312 and their relative changes from Case 002.

Location	Tide Range (m)	% Change, 002
Choccolatta Bay	0.696	+3.1
North Mobile Bay	0.710	-1.4
Justin's Bay	0.618	+40.1
Ducker Bay	0.695	-3.2
Shellbank River North	0.670	-7.1
Shellbank River South	0.70	-2.6

Flows

Other than their magnitudes, the predicted changes in maximum depth-averaged velocity and subtidal velocity for the constructed opening on Shellbank River in Case 312 were very similar to those for Case 302. Here, the maximum velocity along Shellbank River was predicted to increase by nearly 1 m/s in some locations. These changes are shown in Figure 129.

The predicted subtidal flow patterns showed southward flow of 1 to 3 cm/s along Shellbank River and D'Olive Bay, and a decrease in southward flow along Blakeley River immediately to the west of Shellbank River. This may be explained by considering the requirement that under the case with the constructed opening on Shellbank River, some flow must split upstream of the confluence of Blakeley

and Shellbank Rivers, resulting in less southward flow along the Blakeley River relative to existing conditions. Predicted changes in subtidal flow patterns are demonstrated in Figure 130.

Whereas under existing conditions there was no net discharge through Shellbank River, the constructed opening allowed tidal forcing and river flows through the opening with a discharge of 1 m^3/s, on average, with the net direction being to the south.

When compared to predicted volume changes for Case 112 and Case 212, the constructed opening along Shellbank River had only a minor impact on tidal exchange values in Choccolatta and Justin's Bay. A summary of those tidal exchange volumes is provided in Table 39.

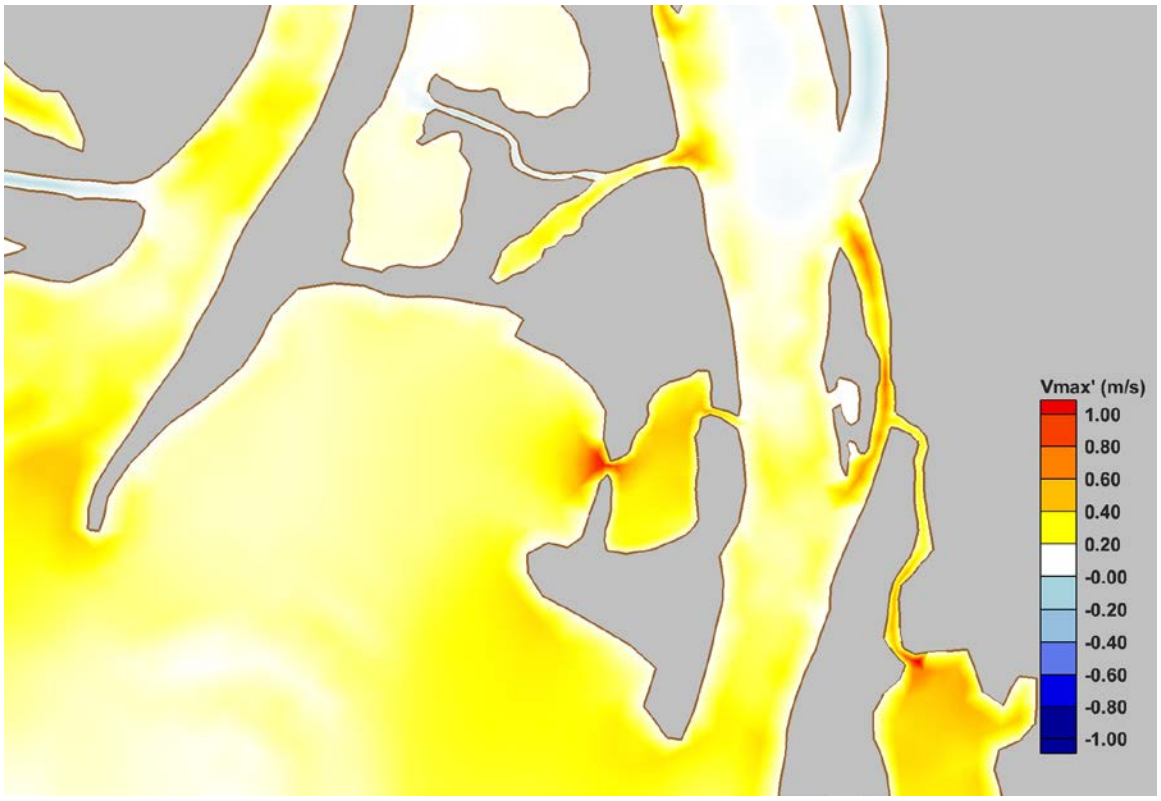

Figure 129. Predicted change in maximum depth-averaged velocity (Vmax') from Case 002 to Case 312.

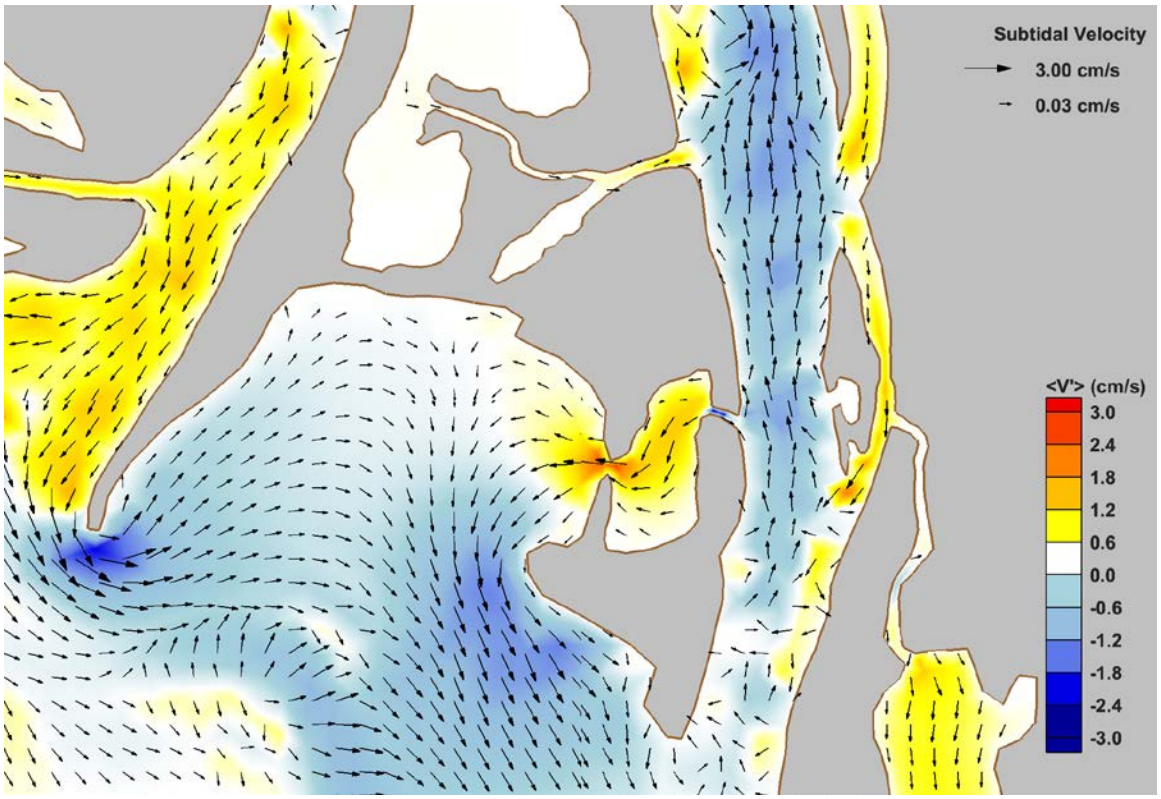

Figure 130. Predicted change in subtidal velocity (<V'>) from Case 002 to Case 312.

Table 39. Maximum tidal volume exchanged (in cubic meters) between successive low and high water of a maximum tide for Case 312, and the percent change relative to existing conditions (Case 002).

Location		Tidal Volume Exchange (m^3)	% Change, 002
Choccolatta Bay	I-10 Cut	763,249	-65.4
	Little Creek	20,164	+208.2
	Conway Creek	539,149	-41.9
	Culverts	24,070	-71.9
	Pass Picada	680,013	-70.1
	Total	**948,346**	**-73.9**
Justin's Bay	Sardine Pass	220,642	-46.4

Sediment Transport Potential

The predicted changes in bedload sediment transport and sediment resuspension rates are shown in Figure 131, and Figure 132, respectively. Most of the predicted changes shown were also predicted to occur in Case 012 without any restoration activities. Many of these changes are attributed to sea level rise and not the constructed opening along Shellbank River, where the model predicted almost no change in bedload transport or sediment resuspension.

Model predictions showed Shellbank River becoming less depositional relative to existing conditions. Some isolated areas of increased deposition were noted in D'Olive Bay and at each confluence of Shellbank River with Blakeley River. Changes in potential sediment deposition are shown in Figure 133.

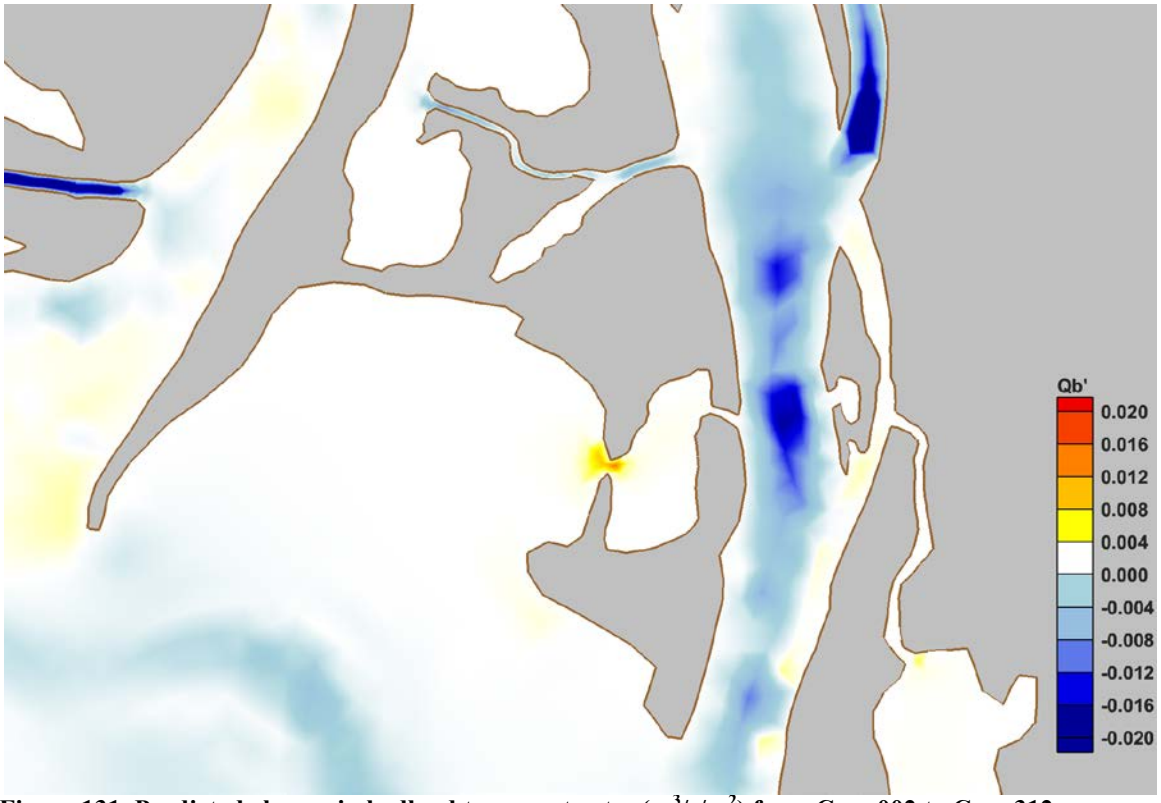

Figure 131. Predicted change in bedload transport rates ($m^3/s/m^2$) from Case 002 to Case 312.

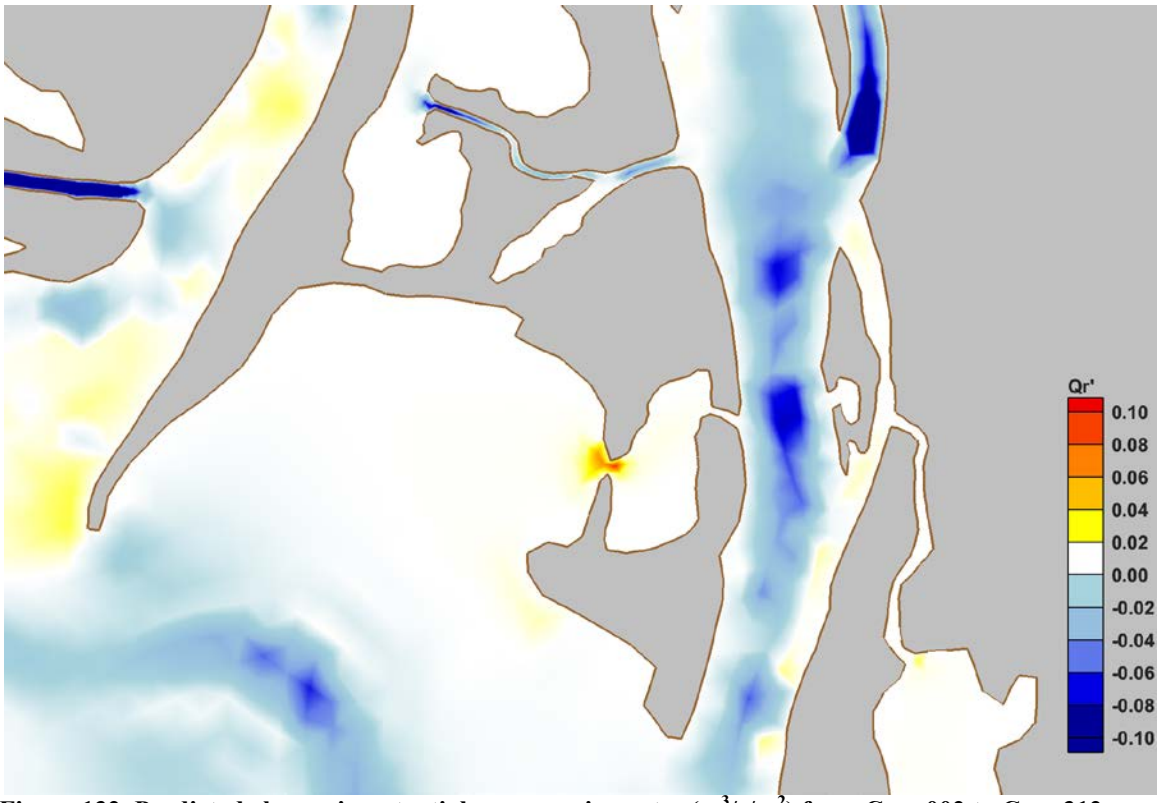

Figure 132. Predicted change in potential resuspension rates ($m^3/s/m^2$) from Case 002 to Case 312.

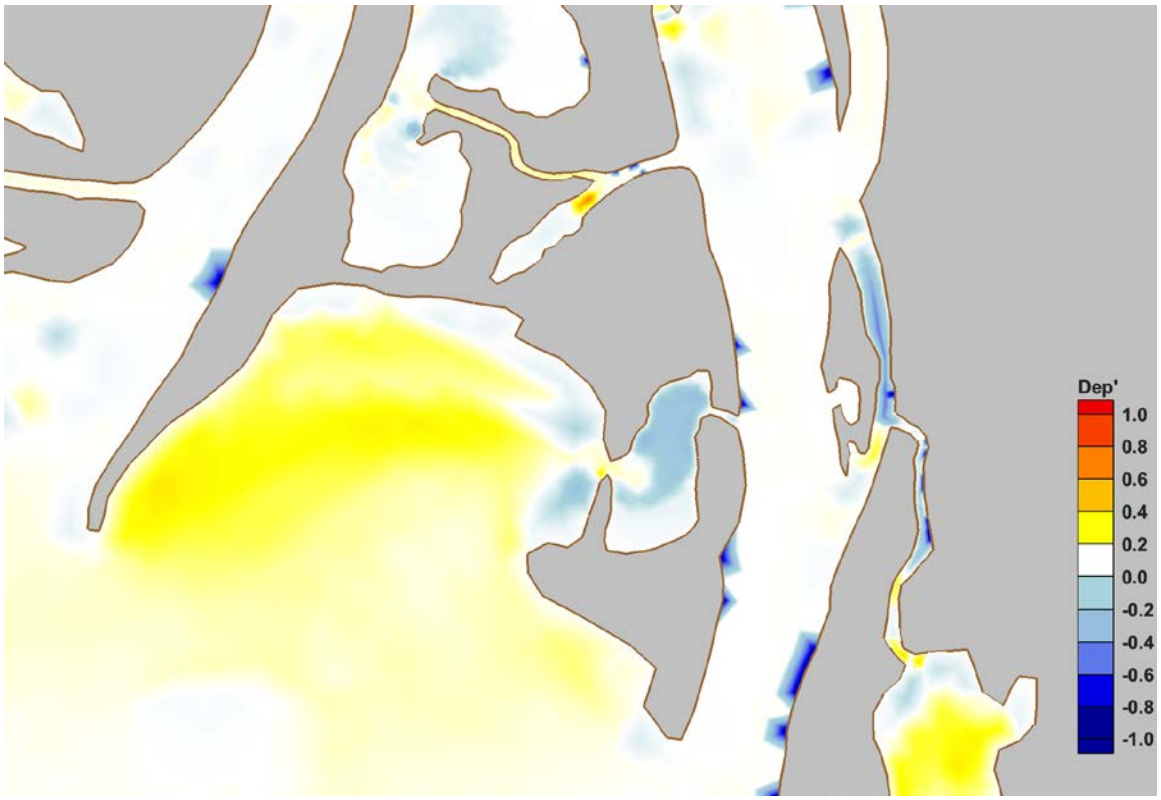

Figure 133. Predicted change in potential depositional patterns and areas from Case 002 to Case 312.

All Open - Case 412

This hypothetical restoration scenario considers all constructed openings through the Causeway at Choccolatta Bay, Justin's Bay, and Shellbank River. The forcing conditions consist of representative tides and average summer river discharge under future, elevated sea levels. Simulation results presented for Case 412 are shown as differences relative to existing conditions (Case 002).

Water Levels

Predicted changes in maximum water levels throughout the study area are shown in Figure 134 and represent the increase in water levels above those predicted under existing conditions and present day sea levels. Similar to the results of Case 012, Case 112, Case 212, and Case 312, the increase in maximum water levels throughout much of Mobile Bay was equal to the sea level offset applied in the simulation: +30 cm. Within the study area, there were localized changes that were considerably higher than the sea level offset (e.g., I-10 Cut, Choccolatta Bay, Big Bateau, and Justin's Bay). These predicted increases were attributed to both the constructed openings and the local amplification due to sea level rise, which are shown in Figure 135.

Predicted water levels over the duration of the simulation were recorded for Choccolatta Bay and Justin's Bay, and those time series are plotted in Figure 136 and Figure 137, respectively. Those figures show the sea level offset of +30 cm that increased the mean position of the tides, as well as the increased tide ranges and the earlier arrival times of low water and high water for each tidal cycle. With the constructed openings in place, the tidal phase lags in Choccolatta Bay and Justin's Bay were eliminated.

Under this restoration scenario where all constructed openings are simulated in the model, the maximum tide ranges in the study area increased by 6% and 56% in Choccolatta Bay and Justin's Bay, respectively. However, the maximum tide range was attenuated by 2% to 3% in north Mobile Bay, Ducker Bay, and Shellbank River. The tidal attenuation in these open-water areas was likely attributed to increased local depth and a corresponding decrease in tidal amplification. The maximum predicted tide ranges, and their changes relative to existing conditions, at specific locations in the study area are listed in Table 40.

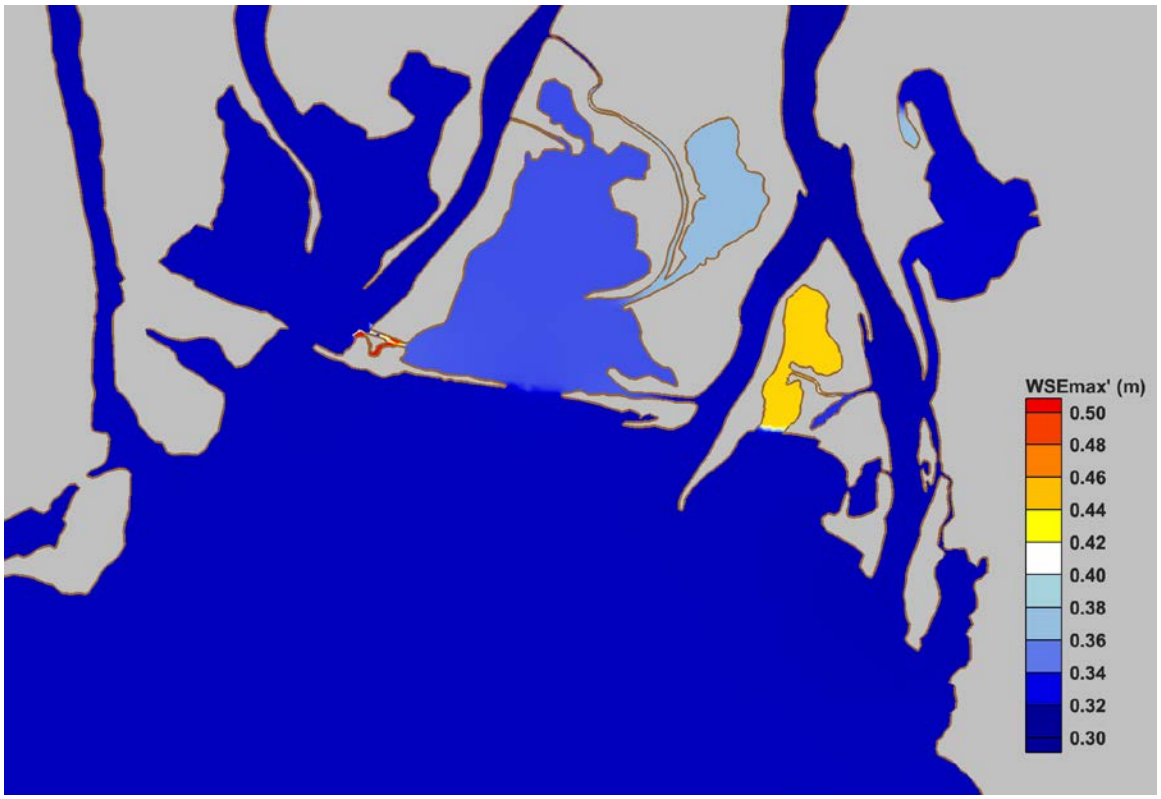

Figure 134. Predicted change in maximum water levels (WSEmax') from Case 002 to Case 412.

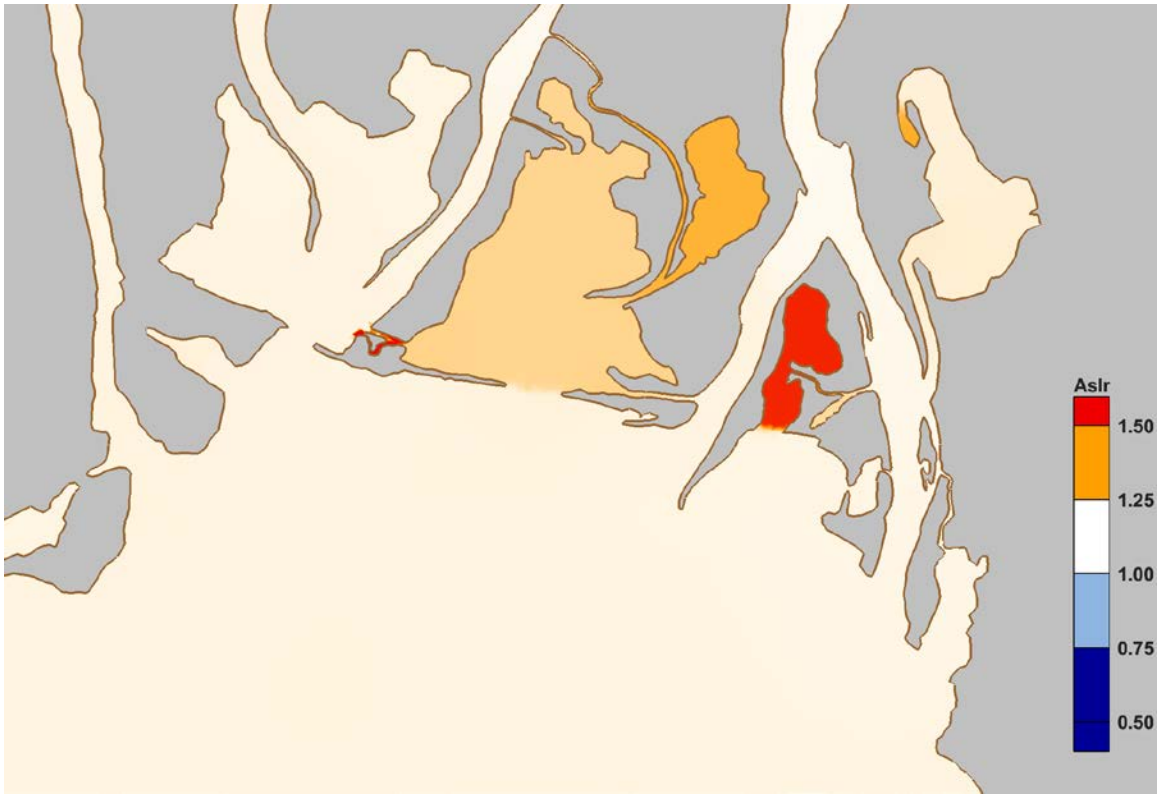

Figure 135. Amplification of maximum water levels due to sea level rise for Case 002 and Case 412.

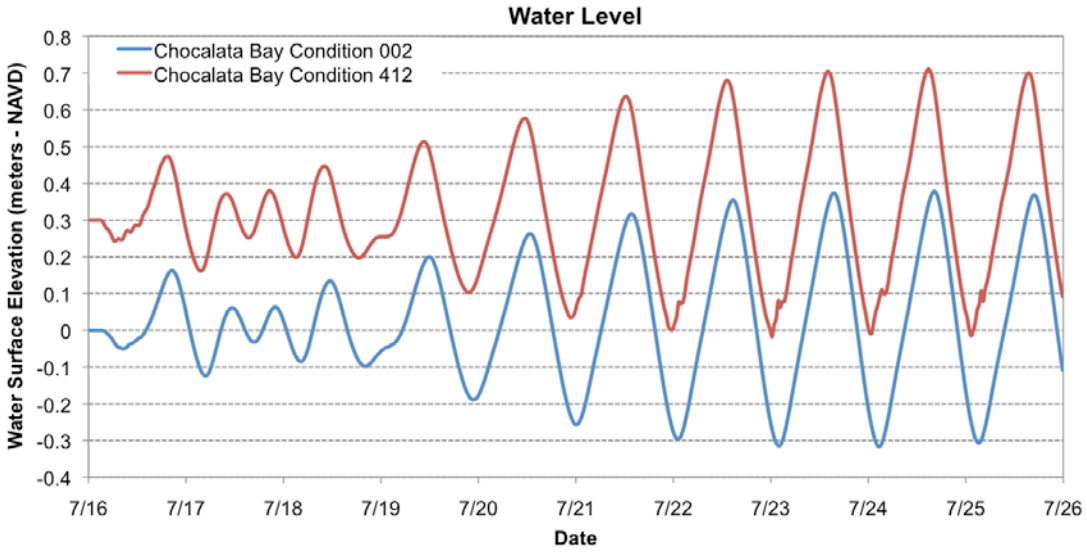

Figure 136. Predicted water level time-series in Choccolatta Bay for Case 002 and Case 412.

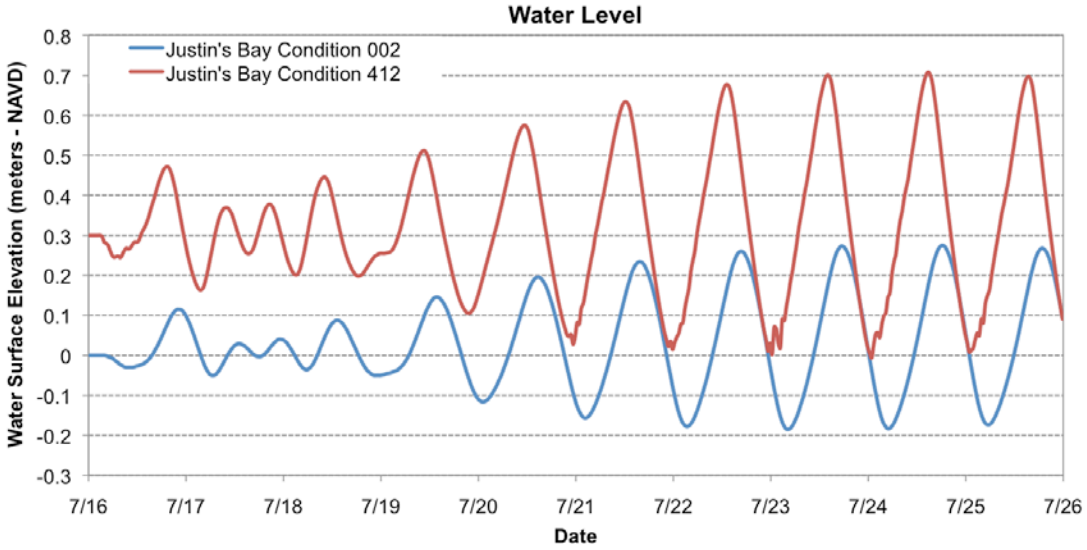

Figure 137. Predicted water level time-series in Justin's Bay for Case 002 and Case 412.

Table 40. Predicted maximum tide ranges for Case 412 and their corresponding changes from Case 002.

Location	Tide Range (m)	% Change, 002
Choccolatta Bay	0.715	+5.9
North Mobile Bay	0.707	-1.8
Justin's Bay	0.688	+56.0
Ducker Bay	0.696	-3.1
Shellbank River North	0.704	-2.4
Shellbank River South	0.70	-2.6

Flows

The predicted changes in maximum depth-averaged velocity throughout the study area are shown in Figure 138. As they are compared to maximum velocities under existing conditions, the changes shown are due to the combined effect of the constructed openings and sea level rise. Relative to maximum predicted velocities under existing conditions and current sea levels, the maximum velocities for Case 412 were predicted to increase by 10 cm/s to 40 cm/s throughout much of the study area, with the exception of some portions of Blakeley and Apalachee Rivers, which experienced decreases of approximately 10 cm/s to 20 cm/s. Similar decreases were predicted to occur in lower Conway Creek.

Predicted changes in subtidal flow, relative to existing conditions, showed similar patterns to those described for the maximum velocities. As shown in Figure 139, the model predicted an increase in seaward-directed subtidal flow in Choccolatta Bay, Justin's Bay, and Shellbank River, as well as much of the Mobile Bay system. These increases were predicted to be on the order of +1 cm/s to +3 cm/s. Reductions of subtidal flow to the south of a similar magnitude were predicted to occur in the main river systems, and may be a result of the decreased hydraulic gradient between the upstream boundary conditions and the increased tidal stage in Mobile Bay.

Significant reductions in discharge, or tidal exchange, through existing tidal channels was predicted to occur, as in other simulations. The constructed openings, under elevated sea levels, resulted in decreased and irregular discharge through these channels, and the net discharge in each case was directed into the system instead of out of the system. Therefore, the constructed openings became the primary drivers of tidal exchange and would be responsible for exporting water and constituents from the bay systems.

Relative to existing conditions, the constructed openings for Case 412 resulted in a 52% increase in tidal exchange for Choccolatta Bay, and a 55% increase in tidal exchange for Justin's Bay. These increases, while substantial, are considerably smaller than those predicted for Case 402 under present day sea levels (79% and 121%). A summary of tidal volume exchanges for Choccolatta Bay and Justin's Bay are listed in Table 41.

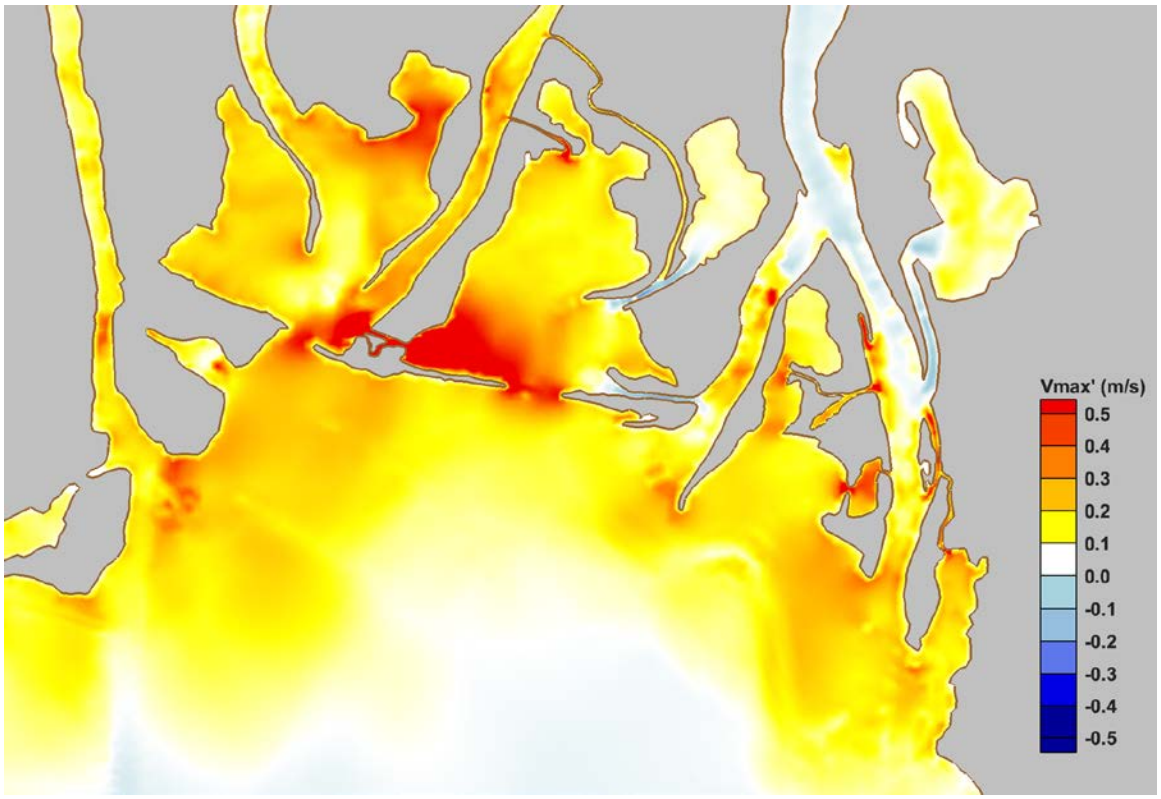

Figure 138. Predicted change in maximum depth-averaged water velocity (Vmax') from Case 002 to Case 412.

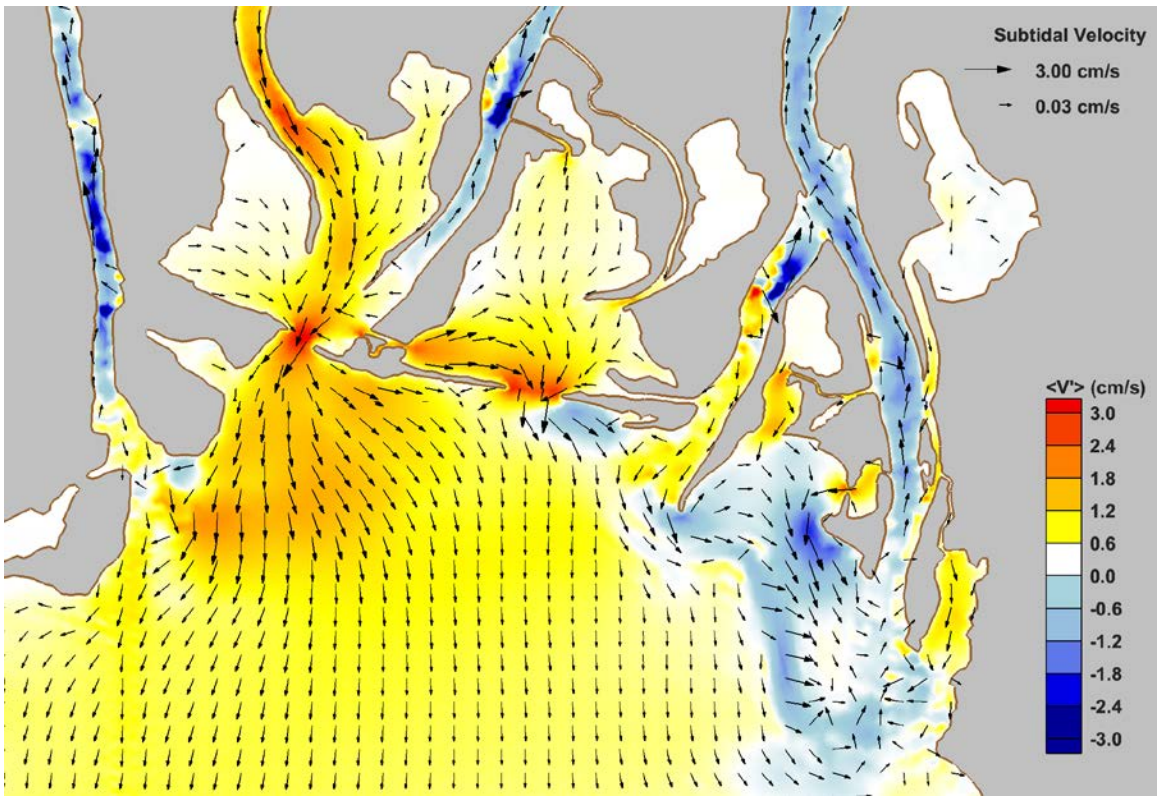

Figure 139. Predicted change in subtidal velocity patterns and magnitudes from Case 002 to Case 412.

Table 41. Maximum tidal volume exchanged (in cubic meters) between successive low and high water of a maximum tide for Case 412, and the percent change relative to existing conditions (Case 002).

Location		Tidal Volume Exchange (m^3)	% Change, 002
Choccolatta Bay	I-10 Cut	43,090	-98.1
	Little Creek	24,694	+277.4
	Conway Creek	607,961	-34.4
	"Pass Choccolatta"	6,132,087	+7064.8
	Pass Picada	61,036	-97.3
	Total (net)	**5,517,378**	**+52.1**
Justin's Bay	Sardine Pass	6,343	-98.5
	"Pass Justin"	633,114	N/A
	Total (net)	**639,457**	**+55.3**

Sediment Transport Potential

Predicted changes in bedload sediment transport rates and sediment resuspension rates within the study area are shown in Figure 140, and Figure 141, respectively. Qualitatively, the patterns of change are similar to other restoration scenarios, with increased transport rates near the constructed openings and decreased transport rates in many of the existing tidal channels. For example, the model predicted 10% and 25% increases in bedload transport and resuspension, respectively, near the constructed openings for Choccolatta and Justin's Bays, whereas transport and resuspension rates decreased by similar magnitudes in I-10 Cut, Pass Picada, Conway Creek, and Sardine Pass.

Similar to the results of other sea level rise scenarios, a modest increase in deposition potential was predicted to occur in the existing tidal channels and across much of Choccolatta Bay and Big Bateau. Large portions of Justin's Bay, Ducker Bay, John's Bend, and Shellbank River, however, became much less depositional by comparison. These changes are demonstrated in Figure 142.

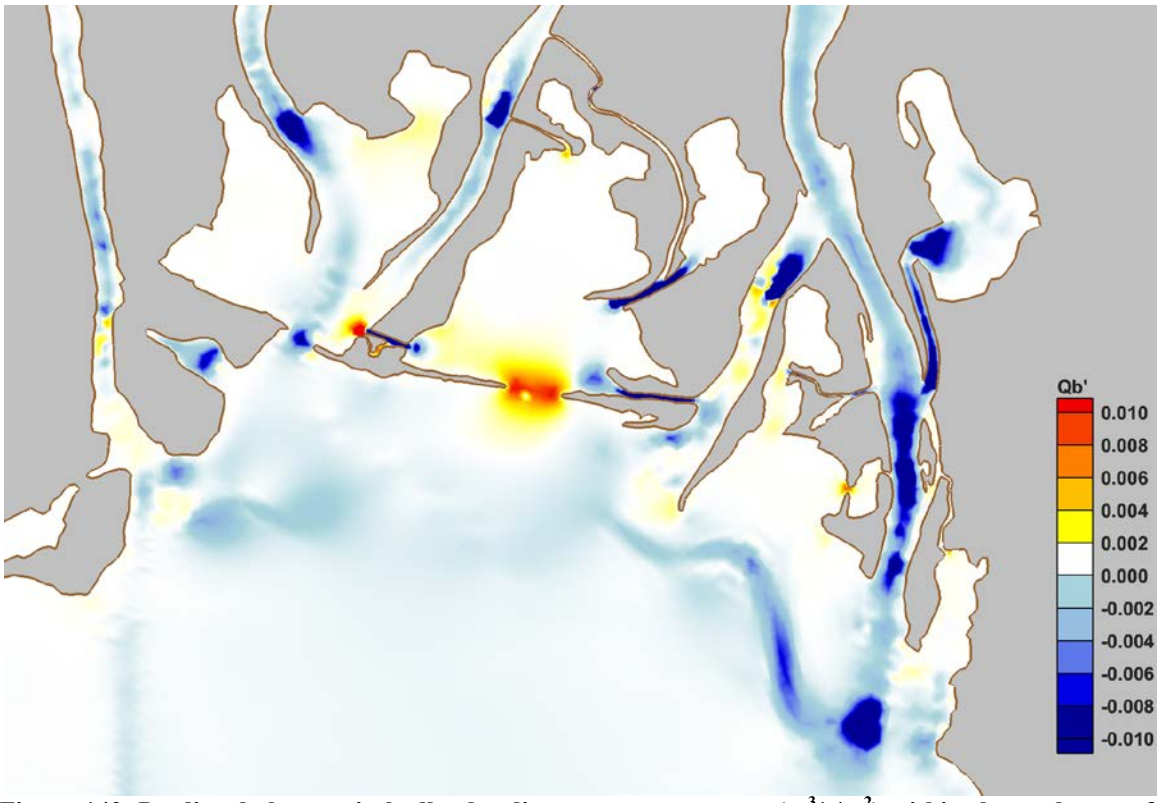

Figure 140. Predicted changes in bedload sediment transport rates ($m^3/s/m^2$) within the study area from Case 002 to Case 412.

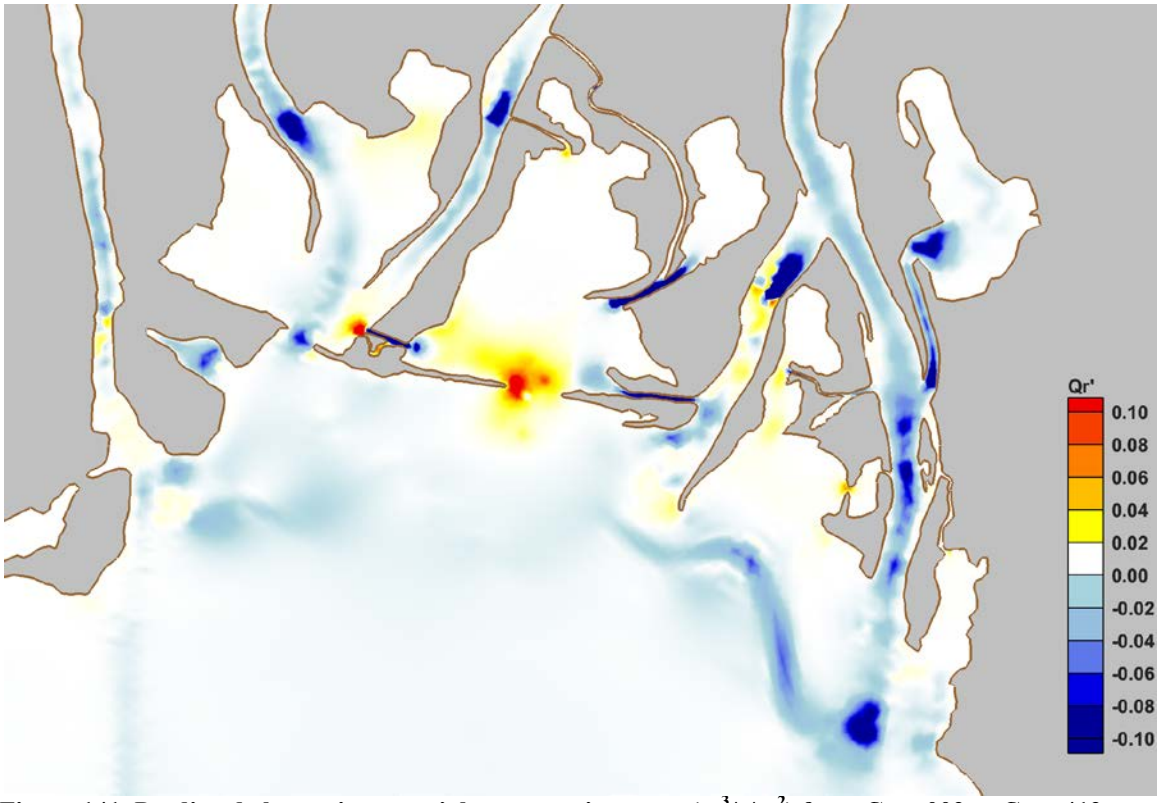

Figure 141. Predicted change in potential resuspension rates ($m^3/s/m^2$) from Case 002 to Case 412.

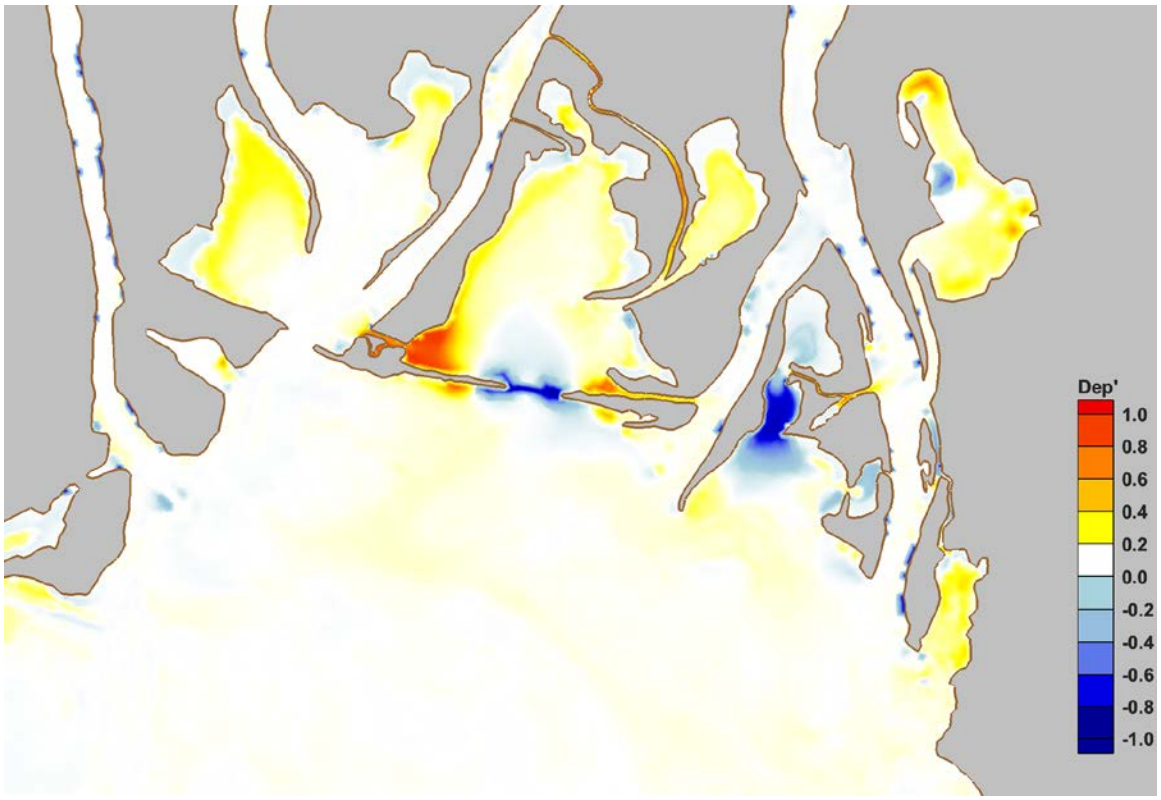

Figure 142. Predicted change in potential sediment depositional patterns and areas from Case 002 to Case 412.

Flushing

Model predictions reveal that much of Big Bateau and some portions of Choccolatta Bay, Justin's Bay, and Sardine Pass experienced no change in particle residence time. In those locations, the particles were likely not escaping and had residence time values beyond the limits of simulation duration. Some particle residence times near I-10 Cut and Pass Picada were predicted to increase by as much as 6 days, while particles nearest the constructed openings had residence times that were 6 days less compared to existing conditions. In Justin's Bay, similar increases and decreases were predicted, with the eastern portions of Duck Skiff Pass and Sardine Pass exhibiting increased residence times (~6 days) while much of Justin's Bay south of Duck Skiff Pass experienced substantial decreases in residence times due to the increased tidal exchange, flushing, and subtidal flow. These changes are shown in Figure 143, which shows the increase or decrease, in days, of particle residence times relative to existing conditions and present day sea levels.

Under this scenario, the flushing potential was predicted to increase by 70% in Choccolatta Bay, relative to existing conditions. In Justin's Bay, the number of particles flushed from the system increased by a factor of five (5). For each system, nearly 100% of particles escaped through the newly constructed openings. The calculated system-wide average residence and exposure times are provided in Table 42. For the case of constructed openings in both Bays, the average residence and exposure times decreased relative to existing conditions.

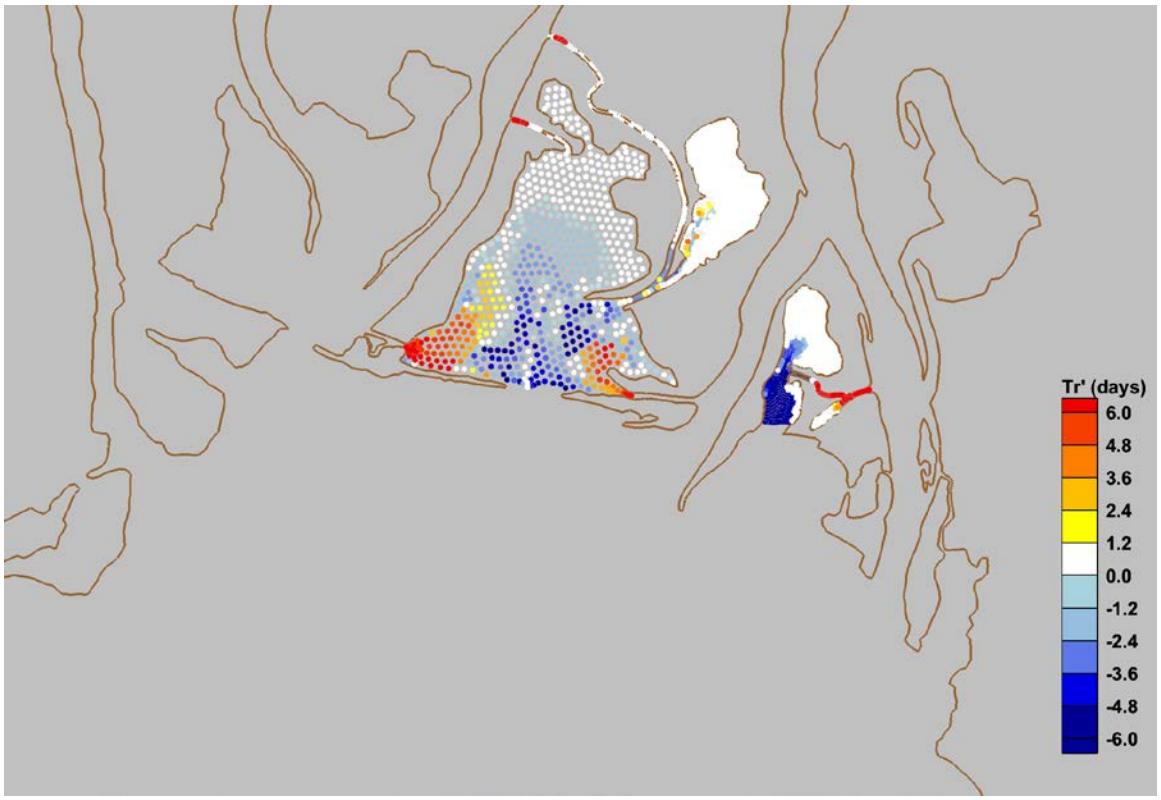

Figure 143. Predicted change in particle residence time (Tr') relative to initial position from Case 002 to Case 412.

Table 42. System-wide residence and exposure times and percentage of particles removed for Case 412.

Location	Avg. Residence Time (days)		Avg. Exposure Time (days)		% Particles Removed	
	Case 002	Case 412	Case 002	Case 412	Case 002	Case 412
Choccolatta Bay	7.9	7.6	8.4	7.9	20.2	33.9
Justin's Bay	8.4	6.8	8.6	7.1	7.1	35.4

Choccolatta + Justin's - Case 512

This hypothetical restoration scenario considers constructed openings through the Causeway at Choccolatta Bay and Justin's Bay only. The forcing conditions consist of representative tides and average summer river discharge under future, elevated sea levels. Simulation results presented for Case 512 are shown as differences relative to existing conditions (Case 002).

Water Levels

Predicted changes in the maximum water levels estimated during the simulation of Case 512 are shown in Figure 144. The magnitudes and patterns of those changes were similar to those predicted for Case 412, and for each of the restoration scenarios considered separately. As in other simulations, the maximum water levels increased in Choccolatta and Justin's Bay due to a combination of increased tide range and the sea level offset, as compared to existing conditions. There is one notable exception in water levels for this scenario, and it is found in Shellbank River. Without the constructed opening along Shellbank River, the model predicted an increase in maximum water levels well above existing

conditions, and beyond that which would be attributed to the sea level offset alone. This effect is also evident in the predicted amplification of water levels due to sea level rise shown in Figure 145. In that figure, the change in maximum water levels in Shellbank River are shown to be over 1.5 times larger than the sea level offset.

As described earlier for Case 402 and Case 502, the constructed opening at Shellbank River was predicted to have a modest effect on tides and water levels in Justin's Bay. When Shellbank River was open, the tide range in Justin's Bay was slightly smaller. Compared to the Case 412 results with Shellbank River open, the model predicted that the tide range in Justin's Bay would be 1.5% larger in this scenario. The differences, while minor, are shown in Figure 146, plotted as a time series of water levels in Justin's Bay corresponding to the largest tidal range.

The model predicted a 6% increase in the tide range within Choccolatta Bay, and a 57% increase in the tide range for Justin's Bay. Note that these increases were within 1% of those predicted for Case 412. Other locations in the study area had smaller tide ranges that were 1% to 3% lower than existing conditions, similar to the predictions for Case 412. A summary of tide ranges at specific locations in the study area, and their differences relative to existing conditions, are provided in Table 43.

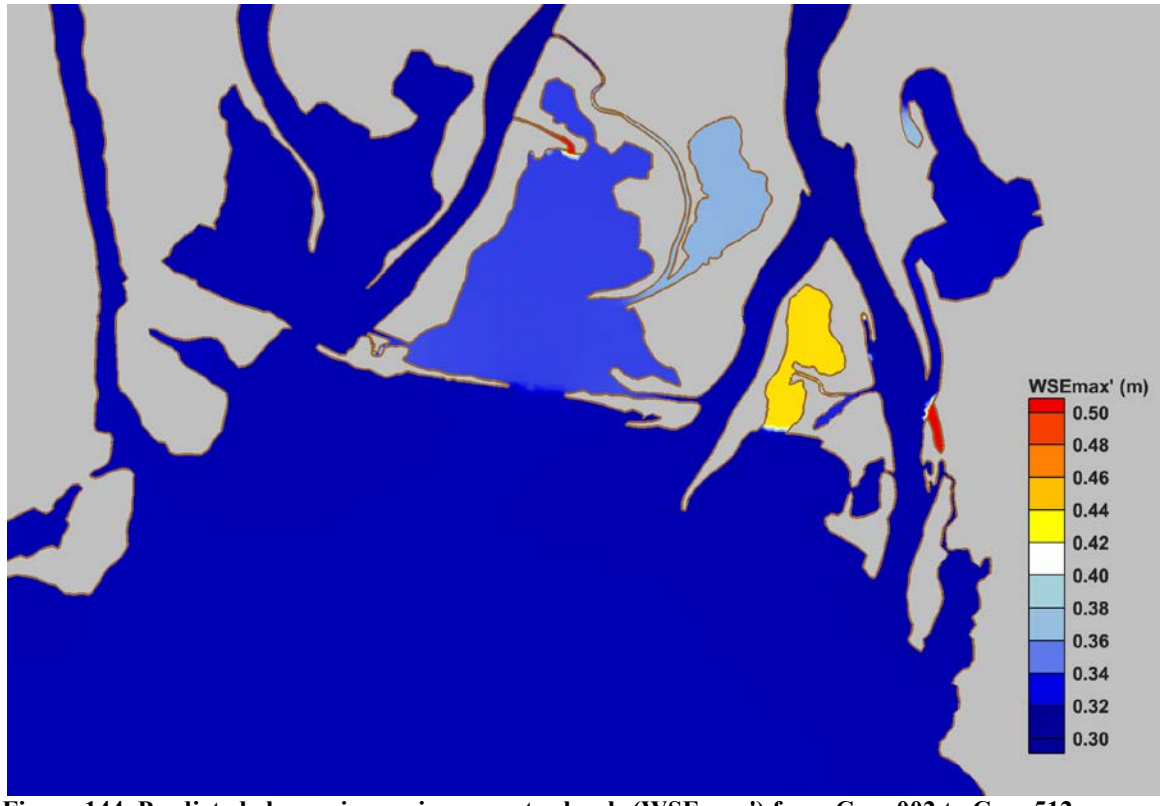

Figure 144. Predicted change in maximum water levels (WSEmax') from Case 002 to Case 512.

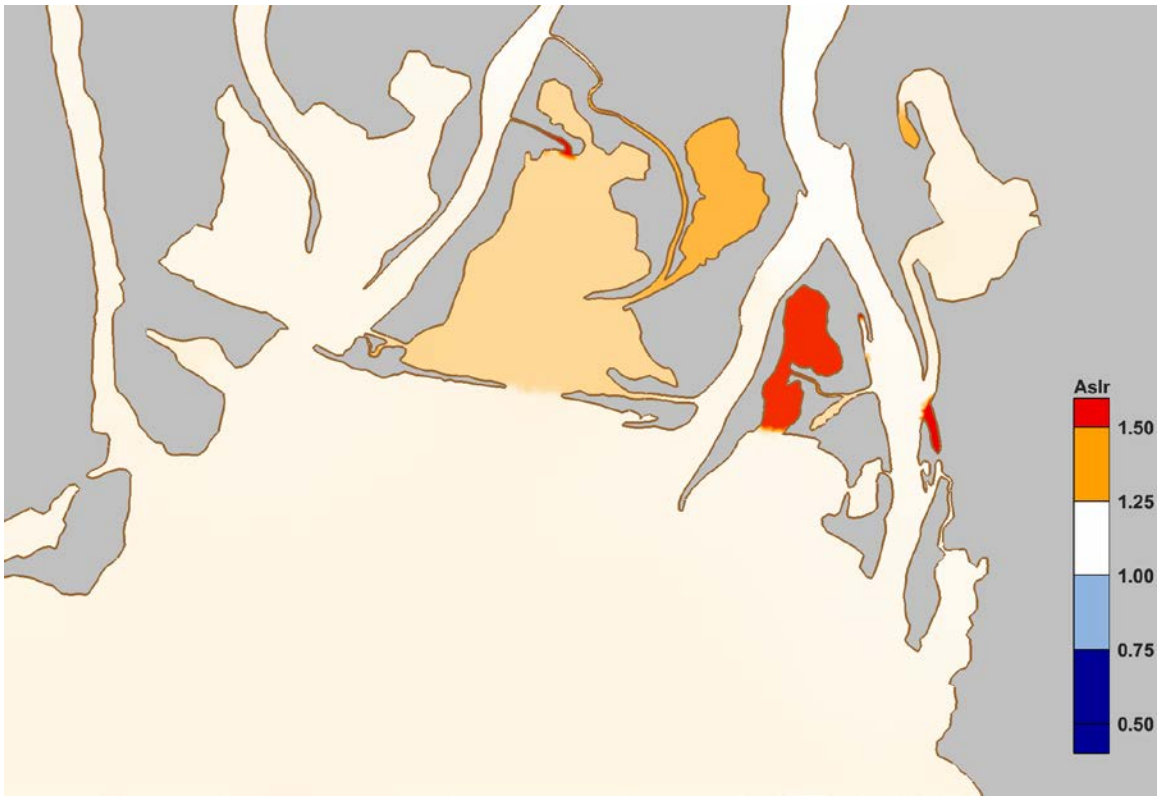

Figure 145. Potential amplification of maximum water levels due to sea level rise by 2100 for Case 002 and Case 512.

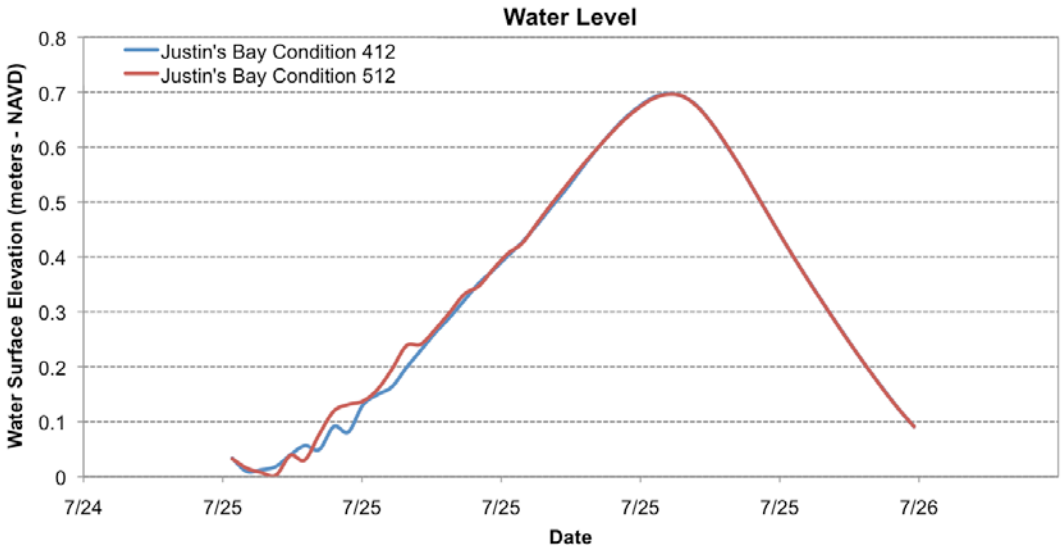

Figure 146. Time-series of water levels in Justin's Bay for Case 412 and Case 512 corresponding to the maximum tide range.

Table 43. Maximum recorded tide range for Case 512 and the corresponding change from Case 002.

Location	Tide Range (m)	% Change, 002
Choccolatta Bay	0.714	+5.8
North Mobile Bay	0.709	-1.5
Justin's Bay	0.694	+57.4
Ducker Bay	0.695	-3.2
Shellbank River North	0.70	-2.9
Shellbank River South	0.697	-3.1

Flows

Predicted changes in maximum depth-averaged velocity and subtidal velocity were consistent with changes predicted under Case 412: substantial increases in both flow velocity and subtidal velocity due to the combined effects of the constructed openings and sea level rise. The predicted changes in maximum velocity and subtidal velocity for Case 512 are shown in Figure 147 and Figure 148, respectively. Tidal volume exchanges for Choccolatta Bay and Justin's Bay for this scenario were similar to those of Case 412, with only minor changes (less than a few percent) noted for the potential impact of Shellbank River on Sardine Pass.

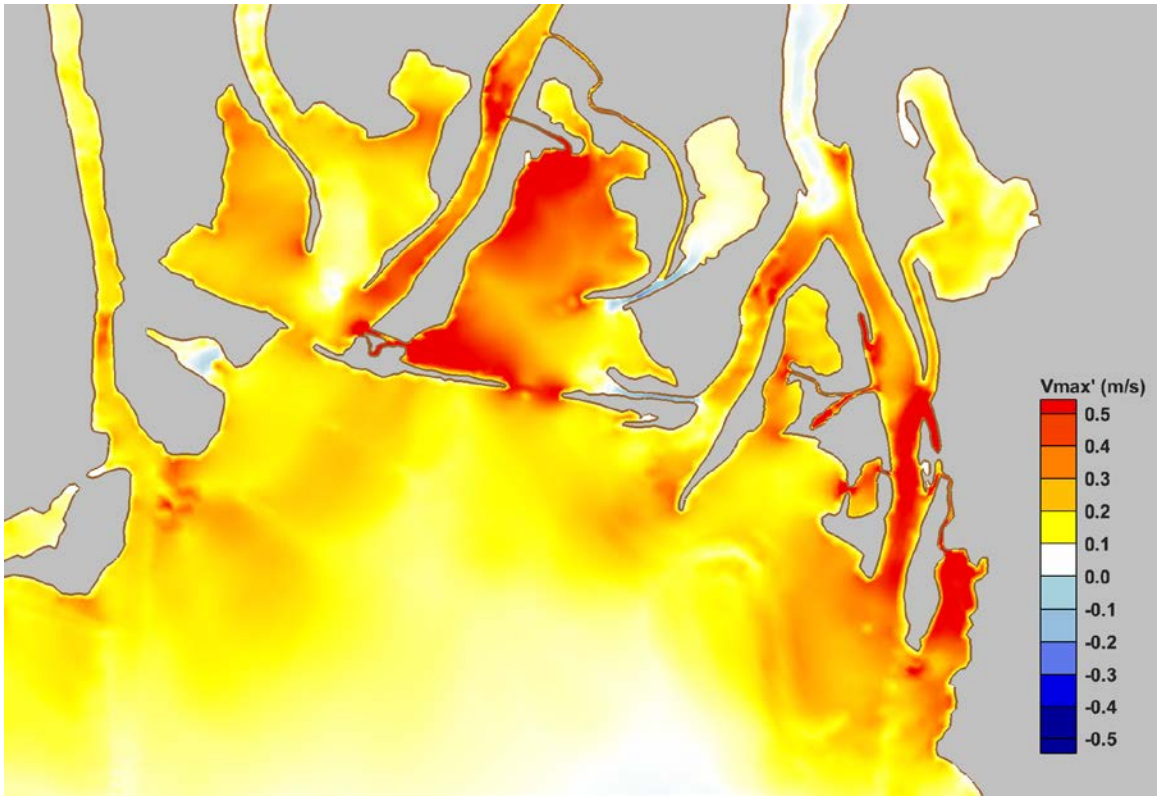

Figure 147. Predicted change in maximum depth-averaged velocity (Vmax') in the study area from Case 002 to Case 512.

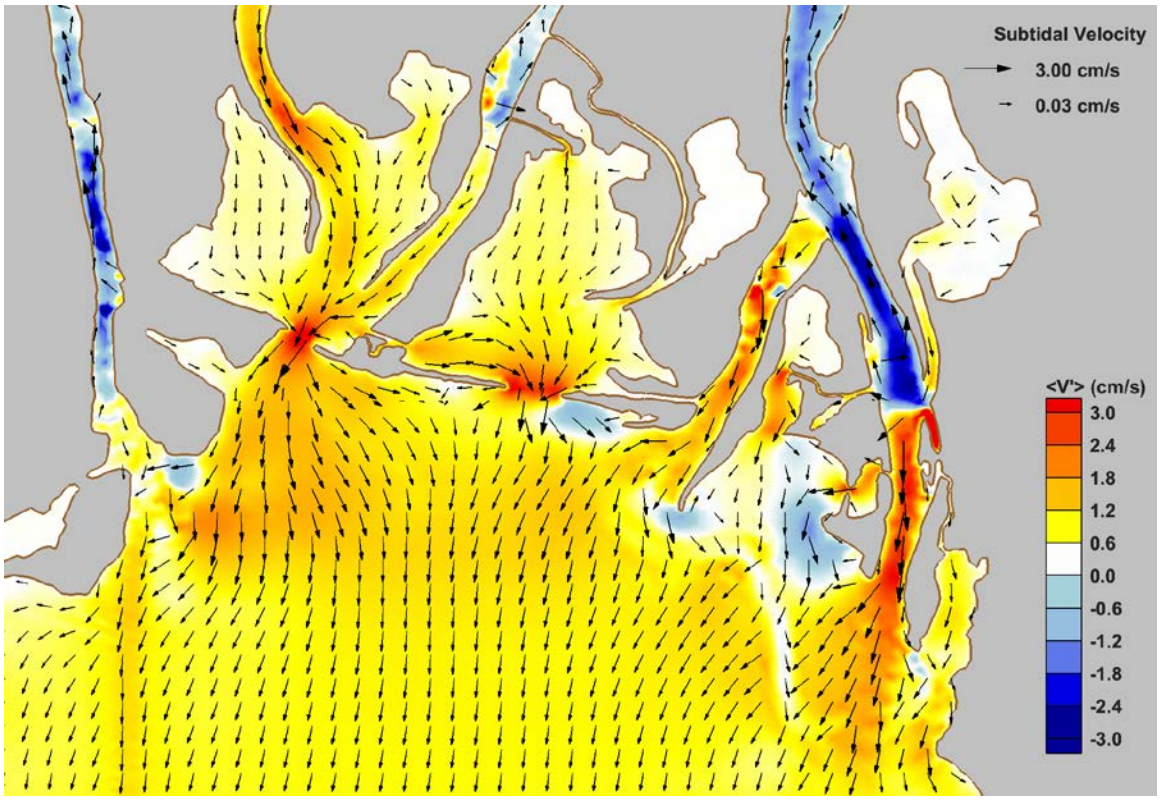

Figure 148. Predicted change in subtidal velocity (<V'>) from Case 002 to Case 512.

Sediment Transport Potential

Both the patterns and magnitudes of sediment transport and resuspension rates were similar to those described in Case 412, with the exception of Shellbank River. As in other simulations, the model predicted 10% increases in bedload transport rates in and adjacent to the constructed openings, and 10% decreases in bedload transport within existing tidal channels. Increased and decreased resuspension rates were predicted in similar areas having magnitudes 25% greater or less than those predicted under existing conditions and present day sea levels. These changes are shown in Figure 149 and Figure 150.

Similar to the results of Case 412, much of Choccolatta Bay was predicted to become marginally more depositional, with strong depositional tendencies in and adjacent to I-10 Cut and Pass Picada. Decreases in deposition potential were noted in and adjacent to both constructed openings as well as throughout much of Justin's Bay. The model predicted no substantial changes in the depositional tendencies of upper Justin's Bay and the lower portion of Sardine Pass. However, the portion of Sardine Pass closest to Blakeley River was predicted to become more depositional due to decreased flows and transport/resuspension in that area. Predicted changes in potential sediment deposition patterns and areas are shown in Figure 151.

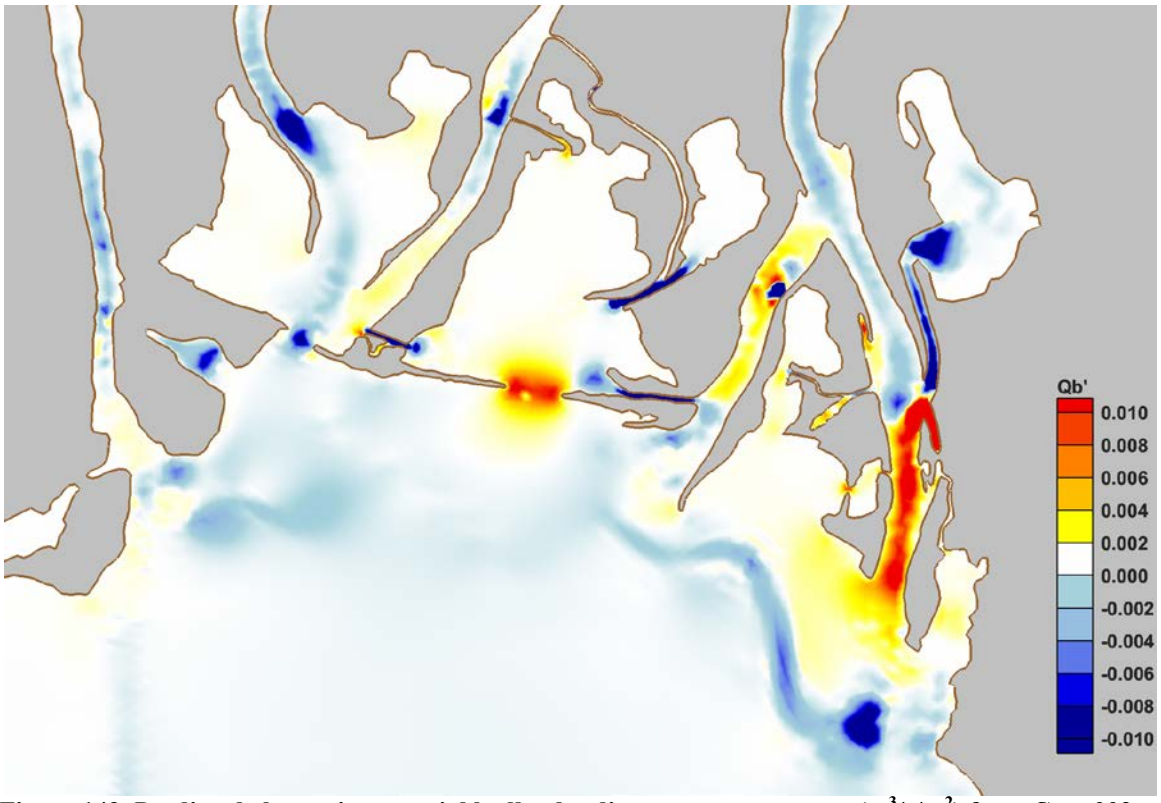

Figure 149. Predicted change in potential bedload sediment transport rates ($m^3/s/m^2$) from Case 002 to Case 512.

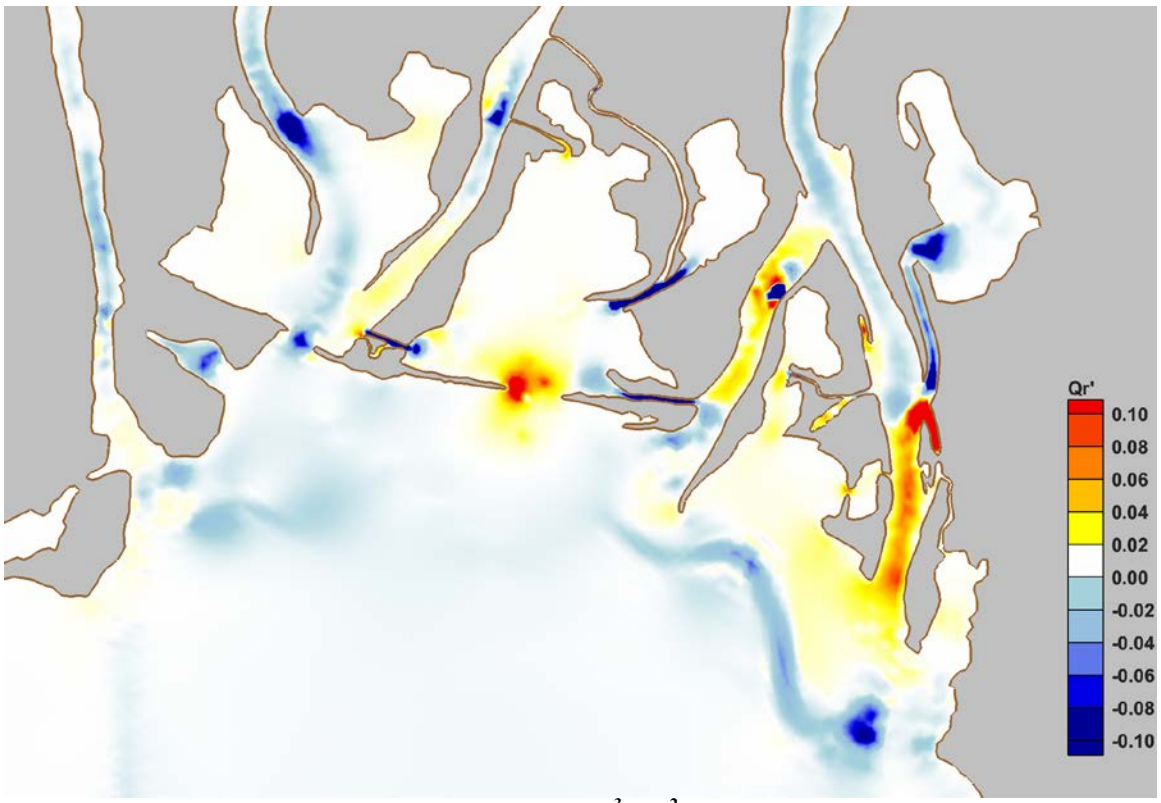

Figure 150. Predicted change in resuspension rates ($m^3/s/m^2$) from Case 002 to Case 512.

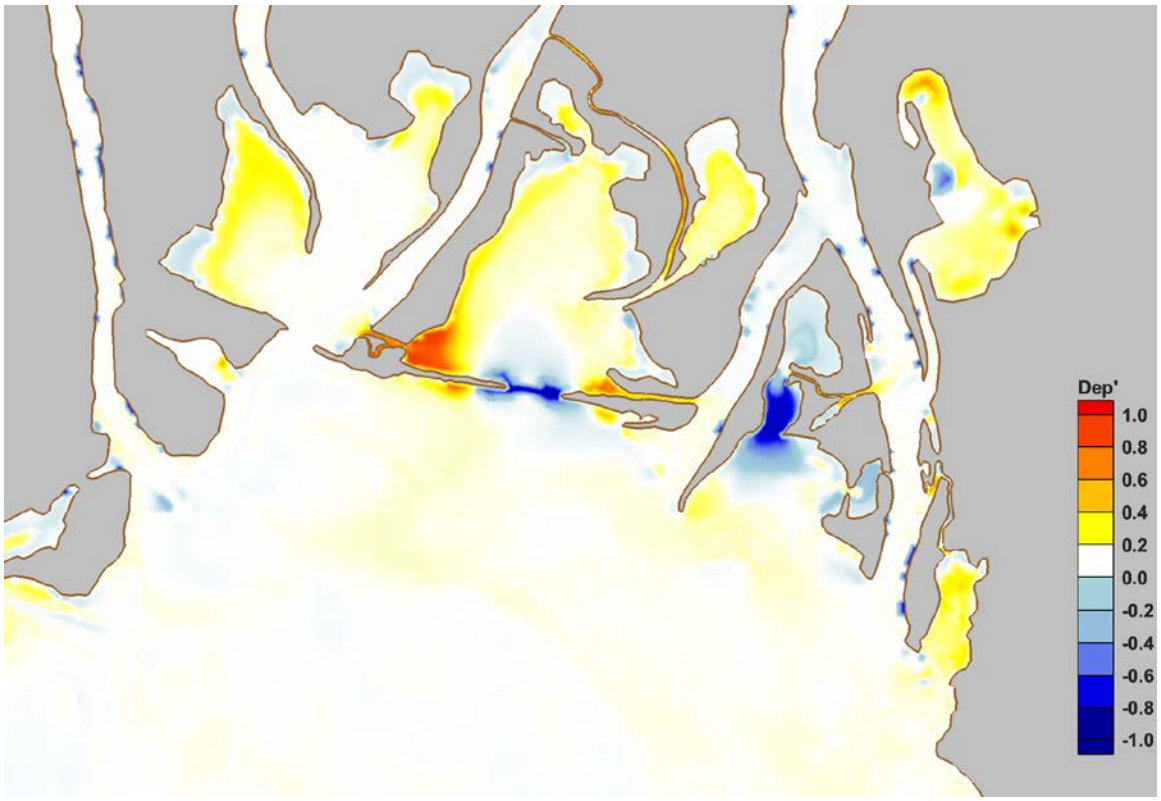

Figure 151. Predicted change in potential depositional patterns and areas from Case 002 to Case 512.

Flushing

With the constructed openings in place, flushing of Choccolatta was predicted to improve by 75%. A six-fold increase in flushing potential was noted for Justin's Bay. Similar to Case 412, the residence times of particles nearest the constructed openings were expected to have the largest decreases, on the order of 6 days or more. In some cases, particles in those locations under existing conditions never left the system. Case 512 suggested a broader improvement in residence times and flushing capacity over larger areas of each system as compared to other hypothetical scenarios. These predicted changes in particle residence times within Choccolatta and Justin's Bay are shown in Figure 152, and the system-wide assessments of residence and exposure times are listed in Table 44. The system-wide assessments showed anywhere from 0.5-day to 2-day decreases in average residence and exposure times.

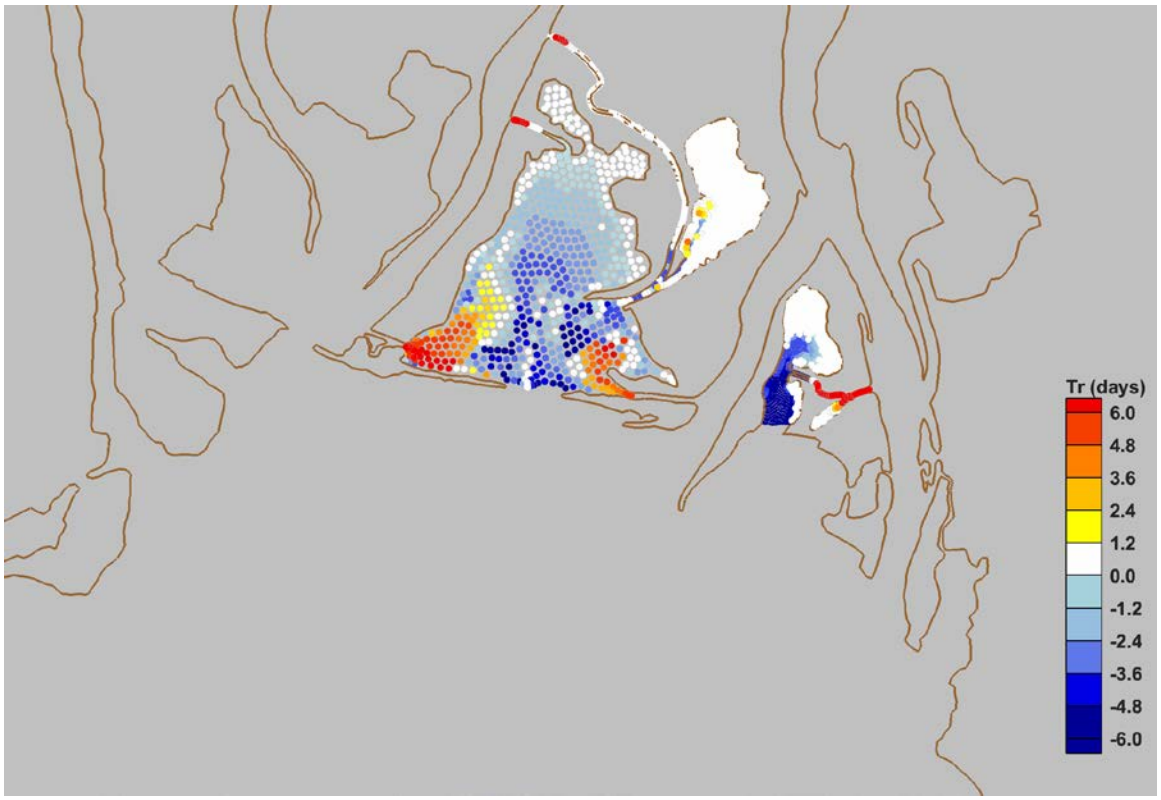

Figure 152. Predicted change in particle residence time (Tr') relative to initial position in Choccolatta and Justin's Bay from Case 002 to Case 512.

Table 44. System-wide residence and exposure times and percentage of particles removed from the system for Case 512.

Location	Avg. Residence Time (days)		Avg. Exposure Time (days)		% Particles Removed	
	Case 002	Case 512	Case 002	Case 512	Case 002	Case 512
Choccolatta Bay	7.9	7.4	8.4	7.7	20.2	35.6
Justin's Bay	8.4	6.5	8.6	6.8	7.1	45.4

Conclusions

Model Study Overview

The primary goal of this hydrodynamic model study was to evaluate the effects of hypothetical openings through the Mobile Causeway on tidal exchange between Mobile Bay and water bodies north of the Causeway. Specific areas of interest included Choccolatta Bay, Justin's Bay, Sardine Pass, John's Bend, Ducker Bay, and Shellbank River. This model study report a) described the field data collection procedures and data used to develop a hydrodynamic model of the study area; b) documented the model validation process and described those results; and c) presented the results of fourteen (14) unique hydrodynamic simulations of the study area under different forcing conditions. Model forcing conditions simulated representative tidal flows over a ten-day period, capturing some of the neap tidal cycle and most of a spring tidal cycle.

Model simulations of existing conditions and each of the five unique restoration alternative scenarios, identified by the project team in earlier tasks, were performed under representative river (Mobile and Tensaw Rivers) discharge values for the month of July (~470 m^3/s) and present day sea levels (6 total simulations). Another suite of simulations was conducted with the same river discharge values but with elevated sea levels representative of a possible condition in the year 2100 (6 total simulations). Two additional simulations were conducted with much higher river discharge (~1950 m^3/s), representative of an average of the wet season inflows to Mobile Bay, under present day sea levels.

The results of each simulation were evaluated for changes in water levels, tide ranges, subtidal velocity and circulation, tidal volume exchanges, sediment transport and deposition, and flushing capacity. With the exception of the high-flow simulations, the changes in the predicted hydrodynamic characteristics listed previously were evaluated as changes relative to existing conditions, July flows, and present day sea level. For the high-flow scenario, the results were assessed as changes relative to existing conditions, high flows, and present day sea level.

Summary of Objectives & Performance Measures

As part of the technical work plan formulation, the project team developed four main objectives that would be evaluated to support the stated project goal(s) of improving tidal exchange and water quality in the study area. A number of performance measures were linked to each objective with the purpose of providing specific, quantitative measures that could be used to assess each objective and potential outcomes of each restoration alternative. Conclusions drawn from the hydrodynamic model simulations are described below in terms of the project objectives and their performance measures.

Objective 1: Increase Tidal Communication

This objective specifically addresses the improvement in tidal communication between Mobile Bay and areas north of the Causeway that could occur as a result of constructed openings at Choccolatta Bay,

Justin's Bay, and/or Shellbank River. The objective was assessed by describing tidal volume fluxes; subtidal flows; tidal velocities; and sediment resuspension, transport and deposition potential throughout the study area. As a general statement, all restoration alternatives met the stated objective.

The constructed openings of each restoration alternative increased tidal volume exchange with Mobile Bay substantially. These increases were due to the improved tidal communication with Mobile Bay. A constructed opening to Choccolatta Bay was predicted to increase tidal exchange by over 80%. However, tidal exchanges through I-10 Cut and Pass Picada were predicted to decrease by 90%. Similarly, in Justin's Bay a constructed opening was predicted to increase tidal exchange with Mobile Bay by over 120%. A subsequent decrease in tidal exchange, by almost 90%, was predicted for Sardine Pass as a result of the constructed opening. These patterns, and relative magnitudes, were consistent for both the low and high river discharge scenarios. Similar effects on tidal exchange were noted for simulations incorporating sea level rise, but the magnitude of the changes was different.

The constructed openings were predicted to increase subtidal flows by 1 cm/s under typical conditions, 2 cm/s for high river discharge, and 3 cm/s in the sea level rise scenario. It is difficult to express these increases as percentages, since there is almost zero (1E-04 cm/s) subtidal flow in the water bodies of interest under existing conditions. The subtidal flow was directed toward the constructed opening in each of the water bodies, and then directed toward the central portion of Mobile Bay and seaward.

Maximum tidal velocities within the study area increased by ~30 cm/s under representative tidal forcing and both low and high river discharge scenarios. Increases were predicted to be greatest in and adjacent to the newly constructed openings. However, maximum predicted tidal velocities decreased by similar magnitudes in the existing tidal channels (e.g., I-10 Cut, Pass Picada, and Sardine Pass).

Sediment transport rates were predicted to increase as a result of the constructed openings, but decreases were also noted in areas experiencing reduced velocities and exchange. Bedload sediment transport rates increased by 10% to 25%, on average, in and adjacent to constructed openings. Decreases of similar magnitudes were noted in I-10 Cut, Pass Picada, and Sardine Pass. Predicted resuspension rates exhibited similar patterns, with increases or decreases on the order of 25% to 50% relative to rates under existing conditions.

Both the bedload transport and resuspension rates were predicted to have the largest magnitudes under existing conditions and typical river discharge, slightly smaller magnitudes for the case of high river discharge, and still smaller values under the sea level rise scenario. Note that this generalization applies mainly to Choccolatta Bay, Justin's Bay, and Shellbank River only. Substantially greater transport and resuspension rates were predicted in the main river channels under high river discharge.

With respect to potential changes in sediment deposition, Choccolatta Bay, Justin's Bay and Shellbank River became less depositional under typical and high flow scenarios. Their tidal channels, however, became strongly depositional due to the decreased flows and sediment transport potential in those areas. For the case of elevated sea levels, Choccolatta Bay was predicted to become more depositional while Justin's Bay and Shellbank River were expected to be less depositional in nature.

Objective 2: Increase Tidal Prism

This objective specifically addresses tidal prism increases in water bodies north of the Causeway that could occur as a result of constructed openings at Choccolatta Bay, Justin's Bay, and/or Shellbank River. The objective was assessed by describing changes in water levels, tide ranges, and tidal prisms in the study area. As a general statement, all restoration alternatives met the stated objective to varying degrees.

In terms of maximum predicted water levels throughout the study area, implementation of restoration alternatives resulted in increases of 2 cm to 4 cm in Choccolatta Bay (5% to 10% of existing values), more than 10 cm in Justin's Bay (30% more than existing values), and almost a negligible amount in Shellbank River (0.5 cm to 1 cm). Model predictions suggested that affected water levels would be limited to the water bodies directly connected to the constructed opening with negligible changes elsewhere in the study area.

In each of the model simulations the effect of constructed openings was to greatly increase the tide range, and therefore the tidal prism, in water bodies north of the Causeway. Tide ranges in Choccolatta and Justin's Bays were predicted to increase by 8% and 64%, respectively. Changes in tide ranges outside of the restoration areas were predicted to be less than 1%. Similar results were found during simulation of the hypothetical openings with elevated sea levels.

Objective 3: Decrease Tidal Phase Lag

This objective specifically addresses the degree to which tidal phase lags between Mobile Bay and areas north of the Causeway would be affected by selected restoration alternatives. The objective was assessed by describing the existing tidal phase lags in Choccolatta Bay, Justin's Bay, and Sardine Pass, and their predicted changes. As a general statement, all restoration alternatives met the stated objective to decrease tidal phase lags.

The tidal phase lags were completely eliminated under every restoration and forcing scenario with one exception. In the high flow scenario the tidal phase lag between Sardine Pass and John's Bend was reduced by 50% (from 1 hour to 0.5 hours), but not completely eliminated. Tidal phase lags in Choccolatta Bay, Justin's Bay, and Sardine Pass were on the order of 1 hour, 3 hours, and 0.5 hours, respectively, under representative tidal forcing and typical (low) river discharge. Under the high river discharge forcing, those tidal phase lags were predicted to be 1 hour, 3.5 hours, and 1 hour, respectively. In the sea level rise scenario they were noted as 1 hour, 1 hour, and 0.5 hours, respectively.

In the case of Choccolatta Bay, tidal phase lags were compared by noting the difference in high water times between a point in Choccolatta Bay and another located just south of the Causeway and the proposed opening. For Justin's Bay, the comparison was made between a point central to Justin's Bay and one immediately south of the Causeway in John's Bend. For Sardine Pass, the comparison was made between a point near Duck Skiff Pass and the point in John's Bend used to describe tidal phase lags in Justin's Bay.

Objective 4: Increase Flushing

This objective specifically addresses the flushing of water bodies in the study area and potential improvements due to restoration activities. The objective was assessed by describing changes in particle residence times, percentage of particles flushed from the system, and estimates of turnover time based on tidal prism methods. As a general statement, all restoration alternatives met the stated objective(s) of increasing flushing and decreasing residence times.

As a general conclusion, particle residence times fell by 5 to 8 days near constructed openings, but some increases of similar magnitude were noted near and in the existing tidal channels like I-10 Cut, Pass Picada, and Sardine Pass. Under some forcing scenarios substantial decreases in residence time were noted well north in Choccolatta and Justin's Bays; however, the upper portions of these bays remain poorly flushed with few to no particles escaping during the 9-day LPTM analysis.

Flushing of Choccolatta Bay and Justin's Bay was improved substantially when constructed openings were simulated. These changes were generally 75% to 85% improvements in the amount of flushing for Choccolatta Bay, and as much as a 500% improvement in flushing for Justin's Bay. Under every scenario the hypothetical opening was responsible for nearly all flushing with almost no particles leaving through existing tidal channels. This finding was supported by the substantial increases in particle residence time noted near existing tidal channels.

Since the LPTM analysis could only be considered over a nine-day simulation period, system-wide averages of residence time and exposure time are somewhat misleading: many (most) of the particles never leave the system in that short of a period. As demonstrated in Marr (2013), residence times were predicted to be well over 100 days for some values of river discharge. However, reductions in these system-wide averages were noted. In Choccolatta Bay the system-wide average residence and exposure times decreased by 0.5 days to 1.0 day. In Justin's Bay, those values decreased by 1.5 days to 2.5 days (relative to existing conditions).

A simple tidal prism method can be used to describe changes in system turnover time as well. The tidal prism method (see Sheldon & Alber, 2006) estimates the number of tidal periods required to "renew" system water by considering the ratio of system volume to the tide range volume. Here, the tide range volume refers to the product of the tide range and the bay surface area. Since both the system volume and tide range volume include an estimate of the bay surface area, they may be cancelled and the result is a ratio of average system depth to tide range.

Application of this simple tidal prism method suggests that under existing conditions Choccolatta and Justin's Bays would have turnover times of 1.5 days and 2.3 days, respectively. Based on the noted changes in tide range described earlier, turnover times in Choccolatta and Justin's Bays would decrease by 7% and 39%, respectively. These estimated values are consistent with the noted improvements in flushing determined through the LPTM analysis.

Suggestions for Future Work

The purpose of this hydrodynamic model study was to evaluate potential changes in tidal circulation as a result of hypothetical openings through the Causeway at Choccolatta Bay, Justin's Bay, and Shellbank River. Potential changes in water quality and the effects of waves throughout the study area were not considered here, but should be in future studies. Also, future studies could explore optimizations of the hypothetical opening widths that would lead to improvements in tidal communication without causing substantial reductions in tidal exchange through existing channels.

Works Cited

Dietrich, J.C., Trahan, C.J., Howard, M.T., Fleming, J.G., ... 2012. Surface trajectories of oil transport along the Northern Coastline of the Gulf of Mexico. *Continental Shelf Research* **41**, 17-47.

Luettich, R.A., Westerink, J.J., and Scheffner, N.W. 1992. ADCIRC: An Advanced Three-Dimensional Circulation Model for Shelves, Coasts, and Estuaries. Theory and Methodology of ADCIRC-2DDI and ADCIRC-3DL, Report 1. *Technical Report DRP-92-6*, US Army Corps of Engineers, Washington, D.C.

Marr, C.D. 2013. Hydrodynamic modeling of residence, exposure, and flushing time response to riverine discharge in Mobile Bay, Alabama. M.S. thesis, University of South Alabama, Dept. Civil Engineering.

Meyer-Peter, E., Müller, R., 1948. Formulas for bed-load transport. In: *Proceedings of the 2nd International Association of Hydraulic Research*. Stockholm, Sweden, pp. 39–64.

Nielsen, P., 1992. Coastal Bottom Boundary Layers and Sediment Transport. World Scientific, River Edge, NJ.

Sheldon, J.E., and Alber, M. 2006. The calculation of estuarine turnover times using freshwater fraction and tidal prism models: a critical evaluation. *Estuaries and Coasts* **29**(1), 133-146.

van Rijn, L.C., 1984. Sediment pick-up functions. *Journal of Hydraulic Engineering* **110**(10), 1494–1502.

van Rijn, L.C., 1993. Principles of Sediment Transport in Rivers, Estuaries, and Coastal Seas. Aqua Publications, Amsterdam, The Netherlands.

Webb, B.M. 2008. Small-scale sediment transport processes and bedform dynamics. Ph.D. thesis, University of Florida, Dept. Civil & Coastal Engineering, May. 304 pp.

Webb, B.M., Slinn, D.N. 2008. Phase-resolving sediment transport and morphology model, In: *Proceedings of the 31st International Conference on Coastal Engineering*, Hamburg, Germany.

Webb, B.M., Slinn, D.N. 2006. Modeling bed morphology under waves and currents, In: *Proceedings of the 30th International Conference on Coastal Engineering*, Vol. 4, 3254-3261. San Diego, CA.

Westerink, J.J., Bain, C.A., Luettich, Jr. R.A., and Scheffner, N.W. 1994. ADCIRC: An Advanced Three-Dimensional Circulation Model for Shelves, Coasts, and Estuaries. User's Manual for ADCIRC-2DDI: Report 2. *Technical Report DRP-92-6*, US Army Corps of Engineers, Washington, D.C.

Zedler, E.A., Street, R.L., 2001. Large-eddy simulation of sediment transport: currents over ripples. Journal of Hydraulic Engineering **127**(6), 444–452.